

The identity of *Argyria lacteella* (Fabricius, 1794) (Lepidoptera, Pyraloidea, Crambinae), synonyms, and related species revealed by morphology and DNA capture in type specimens

Bernard Landry¹, Julia Bilat¹, James Hayden², M. Alma Solis³,
David C. Lees⁴, Nadir Alvarez^{1,5,6}, Théo Léger⁷, Jérémy Gauthier^{1,5}

1 Muséum d'histoire naturelle de Genève, C.P. 6434, CH-1211, Geneva 6, Switzerland **2** Florida Department of Agriculture and Consumer Services, Division of Plant Industry, Entomology Section, 1911 SW 34th Street, Gainesville, Florida, 32608, USA **3** Systematic Entomology Laboratory, Beltsville Agriculture Research Center, Agricultural Research Service, U.S. Department of Agriculture, c/o National Museum Natural History, MRC 168, Smithsonian Institution, P.O. Box 37012, Washington, District of Columbia, 20013-7012, USA **4** Natural History Museum, Cromwell Road, London, SW7 5BD, UK **5** Département de Génétique et Evolution, Université de Genève, 30 quai Ernest Ansermet, 1205, Geneva, Switzerland **6** Muséum cantonal des sciences naturelles, Palais de Rumine, Place de la Riponne 6, 1005, Lausanne, Switzerland **7** Museum für Naturkunde, Leibniz-Institut für Evolutions- und Biodiversitätsforschung, Invalidenstr. 43, 10115, Berlin, Germany

Corresponding author: Bernard Landry (bernard.landry@ville-ge.ch)

Academic editor: Richard Mally | Received 7 October 2022 | Accepted 3 January 2023 | Published 7 February 2023

<https://zoobank.org/F9860399-D281-42A6-B703-C4115E01DDA1>

Citation: Landry B, Bilat J, Hayden J, Solis MA, Lees DC, Alvarez N, Léger T, Gauthier J (2023) The identity of *Argyria lacteella* (Fabricius, 1794) (Lepidoptera, Pyraloidea, Crambinae), synonyms, and related species revealed by morphology and DNA capture in type specimens. ZooKeys 1146: 1–42. <https://doi.org/10.3897/zookeys.1146.96099>

Abstract

In this study the aim was to resolve the taxonomy of several species of *Argyria* Hübner (Pyraloidea, Crambinae) with previously unrecognised morphological variation. By analysing the DNA barcode (COI-5P) in numerous specimens, the aim was to reconstruct phylogenetic relationships between species, to provide better evidence for synonymies, and to circumscribe their geographical distribution. Using an innovative DNA hybridisation capture protocol, the DNA barcode of the lectotype of *Argyria lacteella* (Fabricius, 1794) was partially recovered for comparison with the 229 DNA barcode sequences of *Argyria* specimens available in the Barcode of Life Datasystems, and this firmly establishes the identity of the species. The same protocol was used for the following type specimens: the *Argyria abronalis* (Walker, 1859) holo-

type, thus confirming the synonymy of this name with *A. lacteella*, the holotype of *A. lusella* (Zeller, 1863), **syn. rev.**, the holotype of *A. multifacta* Dyar, 1914, **syn. nov.** newly synonymised with *A. lacteella*, and a specimen of *Argyria diplomochalis* Dyar, 1913, collected in 1992. In addition, nine specimens of *A. lacteella*, *A. diplomochalis*, *A. centrifugens* Dyar, 1914 and *A. gonogramma* Dyar, 1915, from North to South America were sampled using classical COI amplification and Sanger sequencing. *Argyria gonogramma* Dyar, described from Bermuda, is the name to be applied to the more widespread North American species formerly identified as *A. lacteella*. Following morphological study of its holotype, *Argyria vestalis* Butler, 1878, **syn. nov.** is also synonymised with *A. lacteella*. The name *A. pusillalis* Hübner, 1818, is considered a nomen dubium associated with *A. gonogramma*. The adult morphology is diagnosed and illustrated, and distributions are plotted for *A. lacteella*, *A. diplomochalis*, *A. centrifugens*, and *A. gonogramma* based on slightly more than 800 specimens. For the first time, DNA barcode sequences are provided for the Antillean *A. diplomochalis*. This work provides a modified, improved protocol for the efficient hybrid capture enrichment of DNA barcodes from 18th and 19th century type specimens in order to solve taxonomic issues in Lepidoptera.

Keywords

Argyria centrifugens Dyar, *Argyria diplomochalis* Dyar, *Argyria gonogramma* Dyar, COI barcodes, Crambidae, historical DNA, hybrid enrichment, species delimitation

Introduction

The name *Tinea lacteella* Fabricius, 1794, and its synonyms, have been applied to small white moths of the genus *Argyria* Hübner collected in the New World since Fernald (1896) synonymised five species with it: *Argyria albana* (Fabricius), *Argyria pusillalis* Hübner, *Argyria lusella* (Zeller), *Argyria rufisignella* Zeller, and *Argyria pontiella* Zeller. Dyar (1903) then added *Argyria abronalis* Walker as another synonym in a North American checklist. During the subsequent decades of the 20th century, *A. rufisignella* and *A. pontiella* were removed from the list of synonyms of *A. lacteella* while *Argyria gonogramma* Dyar, 1914 was added to it as summarised by Munroe (1995). More recently, the name *A. lacteella* has been used, for example, in Moth Photographers Group (2022), BOLD (Ratnasingham and Hebert 2007), Scholtens and Solis (2015), and Landry et al. (2020). At the inception of this study, the BOLD database contained three widely separate lineages with specimens named *Argyria lacteella* and four with specimens identified as *Argyria centrifugens* Dyar, 1914. Among the latter group, one lineage contained specimens collected in Florida, USA, and morphological examination of the holotype proved that their identification was erroneous.

Thus, because morphological and DNA barcode variation was observed in *Argyria* specimens that otherwise share a similar (ca. 11 mm) wingspan and previously unrecognised external diagnostic characters, we found it necessary to try to fix the identity of *A. lacteella* and the species similar to it, and to better understand their synonymy and geographical distribution. We aimed to do that by integrating both the COI barcode data available in BOLD and the type specimens of the species as well as those pertaining to synonymised names.

Until recently it has been impossible to recover genetic information from old museum specimens because the DNA they contain is degraded and occurs in very low quantities compared to contaminant DNA from other organisms (Card et al. 2021). It has sometimes been possible to recover short DNA barcodes at the cost of laborious multiple PCRs (Hernández-Triana et al. 2014), but recent developments in both the ability to recover historic DNA, improved extractions and capture approaches, and the advent of high-throughput sequencing have opened the access to the genetic information of these specimens, allowing many new studies and the emergence of museomics (Raxworthy and Smith 2021). Among the various approaches developed to recover DNA from collection specimens, hybrid enrichment methods seem to be the most efficient (Raxworthy and Smith 2021). These capture approaches can target different regions of the genome such as mitochondria (Zhang et al. 2020), exons (Bi et al. 2012), and conserved regions via conserved anchored hybrid enrichment (Espeland et al. 2018), ultraconserved elements (UCE) (Faircloth et al. 2012; Blaimer et al. 2016), and randomly distributed loci using the ddRAD approach (Suchan et al. 2016; Gauthier et al. 2020; Toussaint et al. 2021). These new methods make it possible to integrate old samples into modern genetic studies.

In this study, we adapted hybrid enrichment methods to target the COI barcode in old museum specimens. We designed probes along the entire nucleotide sequence of the COI barcode and synthesised our own RNA probes. We extracted historical DNA from four type specimens dating back to the 18th, 19th, and early 20th centuries and an additional specimen collected in 1992. To successfully recover the COI barcode from this degraded, fragmented and contaminant-rich DNA, we combined hybrid enrichment capture and next-generation sequencing. We performed this sophisticated approach for these precious specimens because classic PCR amplification attempts were unsuccessful. In parallel, we amplified the DNA barcode for nine additional samples and integrated them with all available *Argyria* sequences in the BOLD database. Combining phylogenetic inferences, species delimitation approaches based on sequence data and morphology, we propose a new classification of several *Argyria* species. This study shows that innovative methods of museomics can solve complex taxonomic questions still debated. More generally, it reconciles the modernity of innovative molecular approaches with the biological heritage that museums have been preserving for centuries.

Materials and methods

Sources of information

The original description of *A. lacteella* and subsequent citation of the name by Fabricius (1794, 1798) were investigated, along with the original descriptions and subsequent citations of all other taxa/names treated here. The specimens examined came from the following institutions, in alphabetical order of acronyms:

CMNH	Carnegie Museum of Natural History, Pittsburgh, USA;
CUIC	Cornell University Insect Collection, Ithaca, New York, USA;
FSCA	Florida State Collection of Arthropods, Gainesville, Florida, USA (curated with the MGCL);
MFNB	Museum für Naturkunde, Berlin, Germany;
MGCL	McGuire Center for Lepidoptera and Biodiversity, Gainesville, Florida, USA;
MHNG	Muséum d'histoire naturelle, Geneva, Switzerland;
NHMUK	Natural History Museum, London, UK;
NMNH	(= USNM) National Museum of Natural History, Washington, D.C., USA;
OUMNH	Oxford University Museum of Natural History, Oxford, UK;
UCB	Essig Museum of Entomology, University of California, Berkeley, USA;
VOB	V. O. Becker collection, Camacan, Bahia, Brazil;
ZMUC	Zoological Museum of the University of Copenhagen, Denmark.

Dissection

Specimens from which DNA was not extracted were dissected following Robinson (1976): abdomens were macerated in hot 10% aqueous KOH, cleaned, stained variously with Orange G, Chlorazol black, or eosin Y, and slide-mounted in Euparal.

Illustrations

Photographs were taken with a variety of devices in five institutions (FSCA, MHNG, NMNH, NHMUK, ZMUC), including, at the MHNG (Figs 11–14, 20, 23–26), a Leica M205 binocular scope, a Leica DFC425 camera, and the Leica imaging software. The Visionary Digital imaging system was used at the NMNH. At the MHNG the photos were stacked using Zerene Stacker of Zerene Systems LLC and modified for better presentation using Adobe Photoshop Elements. At the FSCA, photographs were taken with a JVC digital camera KY-F75U 3-CCD with Leica Z16 Apo and Planapo 1.0× lenses, operated and stacked with Auto-Montage Pro v. 5.01.0005 (Syn-croscopy, Synoptics, 2004). High-resolution genitalic photographs (Figs 17, 18, 27, 28) were taken at the MGCL with a Leica DM6B compound microscope with a Leica DMC6200 camera, and photographs were stacked and processed with Leica Application Suite X v. 3.7.0. Postprocessing was done with Adobe Photoshop Elements 11.

Sampling

To ascertain the identity of *Argyria lacteella*, the DNA of its unique (as far as known) type specimen housed in the ZMUC was sampled from two legs. The DNA was sampled from the abdomen of the holotype of *Argyria abronalis* (Walker, 1859), recorded as a synonym of *A. lacteella* (e.g., Munroe 1995) and deposited in the OUMNH. DNA was also sampled from one leg of the holotype of *A. lusella* (Zeller, 1863), which had

been placed as a synonym of *A. lacteella* in the NHMUK, and from one leg and part of another for the holotype of *Argyria multifacta* Dyar, 1914 deposited in the NMNH. In addition, the DNA of a specimen identified (by BL) as *Argyria diplomochalis* Dyar, 1913 from the island of Anguilla, collected in 1992 and deposited in the CMNH, was also sampled in the same manner as the old holotypes just mentioned, and the DNA of two specimens of *A. diplomochalis* collected in 2021 on Saint Croix Island, US Virgin Islands, deposited in the MHNG, was sampled from one leg each using a Sanger protocol. The four specimens used here that were sequenced at the MFNB, but deposited in the MHNG, were sampled also from one leg each with a Sanger protocol. Additional specimens from the CMNH, CUIC, FSCA, MGCL, NMNH, UCB, and VOB were studied morphologically.

DNA extraction and capture

In the MHNG, the DNA barcode sequence from specimen *Argyria "centrifugens"* DHJ02 (BOLD sample ID BIOUG27552-D08; JEH20210604A) (in reality, *Argyria lacteella*) captured at Gainesville (Florida, USA; deposited in FSCA) (29.6922°N, 82.3650°W) was used as reference for molecular work. Probes were designed using the 648 bp reference sequence via a sliding window of 108 pb with steps of 27 bp, providing an overlap of 83 bp. Using this approach, 21 probes were designed for the forward and 21 for the reverse direction. T7 promoters were added to each probe sequence. Final probe sets were ordered from Integrated DNA Technologies (IDT). The T7 reverse-complement sequence was annealed to the probe sets to allow transcription into RNA and biotinylation in a single reaction using HiScribe T7 High Yield RNA Synthesis Kit (New England Biolabs) followed by a Dnase treatment to avoid sample contamination by probe DNA during the capture, a purification using RNeasy kit (Qiagen) and Rnase inhibition using SUPERase-IN (Invitrogen). Concentrations of RNA probes were measured in a Qubit RNA HS assay (Thermo Fisher Scientific).

DNA extraction on historical samples were performed using PCR & DNA Cleanup Kit (Monarch). The protocol was adapted from Patzold et al. (2020) and aims to improve the recovery of small DNA fragments on the column with the addition of ethanol. In the non-destructive protocol, after a night in the Monarch gDNA Tissue lysis buffer with proteinase K (2 mg/ml final concentration), the abdomen of specimen CRA01 was treated with KOH, the genitalia were separated, and both genitalia and abdomen pelt were cleaned and mounted on slide following procedures mentioned in Landry and Becker (2021); the leg of specimen CRA02 was retrieved from the buffer and returned to the NHMUK where it is preserved in a vial underneath the specimen. In the destructive protocol the tissues were crushed (Table 1). The quality and concentration of purified DNA was assessed using a Qubit dsDNA HS assay (Thermo Fisher Scientific) and/or with Fragment Analyzer. Due to their low DNA concentration (Table 1), the samples were not diluted prior to the preparation of shotgun libraries, except for sample CRA01 (abdomen), which was diluted to ~ 27 ng/μL.

A modified version of the protocol from Suchan et al. (2016) used in Toussaint et al. (2021) was applied for the preparation of shotgun libraries (detailed protocol in Suppl. material 1). Libraries were quantified using a Qubit dsDNA HS (Thermo Fisher Scientific) and pooled in equimolar quantities based upon their respective concentrations. For each probe set, forward and reverse, hybridisation capture for enrichment of shotgun libraries was performed following the protocol described in Toussaint et al. (2021). Sequencing was performed on Illumina Miseq Nano using a paired-end 150 protocol (Lausanne Genomic Technologies Facility, Switzerland).

For additional samples, the DNA barcode was amplified by PCR. For CRA05 and CRA06 (Table 1), destructive DNA extraction was performed using QIAamp DNA Micro Kit (QIAGEN) and the DNA barcode was amplified by PCR using H02198 and COImod primers (Landry and Andriollo 2020) and sequenced using Sanger sequencing (Microsynth AG, Balgach, Switzerland). Samples BLDNA 65, 137, 138, and 141 (Table 1) were processed at the MfN: DNA was extracted using the Macherey-Nagel DNA extraction kit (Dürren, Germany), and molecular work followed the protocol described in Mey et al. (2021). Sequencing was done by Macrogen (The Netherlands) in both directions. Sequences were eye-checked and aligned using Phyde 0.9971 (Müller et al. 2005). The COI barcode region of samples JEH20210604A, -C, and -D was sequenced using standard barcoding primers and protocols (Hebert et al. 2004) by the FDACS-DPI Molecular Diagnostics Laboratory, in Florida, USA.

COI locus reconstruction and phylogeny with existing data

Raw reads were cleaned using Cutadapt (Martin 2011) to remove barcodes, adapters and bases with a low quality, and quality was first checked using FastQC (Babraham Institute). Corresponding reads were first identified by BLASTn (Camacho et al. 2009) on the reference sequence and mapped using Geneious 6.0.3 Read Mapper (Kearse et al. 2012). Consensus sequences were generated keeping the most frequent bases and a minimum coverage of 3.

Phylogenetic inferences

To investigate the phylogeny of *Argyria* species, the sequences from all the samples including the keyword “Argyria” were retrieved from the Barcode of Life Data System (**BOLD**) (Suppl. material 2). Newly generated and retrieved sequences were aligned using MAFFT (Kato et al. 2002). The most likely nucleotide substitution model, i.e., GTR+G+I, has been identified using ModelFinder (Kalyaanamoorthy et al. 2017) implemented in IQ-TREE 2.0.5 (Minh et al. 2020). Phylogenetic inferences were performed in IQ-TREE 2.0.5 (Minh et al. 2020) and branch support were estimated using 1,000 ultrafast bootstraps along with 1,000 SH-aLRT tests (Guindon et al. 2010; Hoang et al. 2018). To avoid local optima, we performed 100 independent tree searches using IQ-TREE and selected the run showing the best likelihood score.

Table 1. Data pertaining to specimens sampled with hyRAD and Sanger protocols at MHNG (CRA01-07), MFNB (BLDNA 065, 137, 138, 141), and MGCL (JEH20210604A-C).

ID	Sample	Year of collect	Extraction method	Tissue	DNA conc. (ng/ul)	#_reads	#_fragments	Mean fragment size (bp)	% COI barcode
COI capture									
CRA01	OUMNH Holotype <i>Argyria abronalis</i> (Walker, 1859)	before 1859	non-destructive	abdomen	53.60	3,100,910	1,559,505	83.25	99.8
CRA02	NHMUK013696753 NHMUK Holotype <i>Argyria lasella</i> (Zeller, 1863)	before 1863	non-destructive	leg	0.40	8,889	1,583	81.88	96.3
CRA03	ZMUC Holotype <i>Argyria lacteella</i> (Fabricius, 1794)	1784–1789	destructive	leg	0.50	3,101	60	77.00	51.4
CRA04	GMNH <i>Argyria diplomochalis</i> (Dyar, 1913)	1992	destructive	leg	2.94	862,323	183,175	103.51	100
CRA07	USNM <i>Argyria multifacta</i> (Dyar, 1914)	1911	destructive	2 legs	0.17	14,538	10,686	49.40	93.1
PCR amplification									
CRA05	MHNG-ENTO-91928 MHNG <i>Argyria diplomochalis</i> (Dyar, 1913)	2021	destructive	leg	0.81				100
CRA06	MHNG-ENTO-91929 MHNG <i>Argyria diplomochalis</i> (Dyar, 1913)	2021	destructive	leg	0.79				100
BLDNA137	MHNG-ENTO-102922 <i>Argyria lacteella</i> (Fabricius, 1794)	2018	destructive	leg					100
BLDNA138	MHNG-ENTO-102923 <i>Argyria lacteella</i> (Fabricius, 1794)	2018	destructive	leg					100
BLDNA141	MHNG-ENTO-97427 <i>Argyria centrifugens</i> (Dyar, 1914)	2018	destructive	leg					100
BLDNA065	MHNG-ENTO-85677 <i>Argyria lacteella</i> (Fabricius, 1794)	2004	destructive	leg					100
JEH20210604A	FSCA UF-FLMNH-MGCL 1112885 <i>Argyria lacteella</i> (Fabricius, 1794)	2021	destructive	leg					100
JEH20210604C	FSCA UF-FLMNH-MGCL 1112830 <i>Argyria gonogramma</i> (Dyar, 1915)	2020	destructive	leg					100
JEH20210604D	FSCA UF-FLMNH-MGCL 1112845 <i>Argyria gonogramma</i> (Dyar, 1915)	2015	destructive	leg					100

Species delimitation and genetic distance

Three different methods were used to investigate species delimitation: Automatic Barcode Gap Discovery (ABGD) (Puillandre et al. 2012), Poisson Tree Processes (PTP) (Zhang et al. 2013) and General Mixed Yule-coalescent method (GMYC) (Pons et al. 2006). First, distance-based analysis ABGD was calculated using the K80 Kimura distance model and default parameters on the online platform (<https://bioinfo.mnhn.fr/abi/public/abgd/abgdweb.html>). Second, the single-locus species delimitation PTP method (Kapli et al. 2017) was used on the phylogeny excluding the outgroups *A. rufisignella* and *A. nummulalis*. Analyses were performed on the bPTP web server (<https://species.h-its.org>). The confidence of delimitation schemes was assessed using an MCMC chain of 10 million generations, a thinning of 100 and burn-in of 10%, and the partition with the best likelihood was kept. Third, the single threshold GMYC method was applied using the splits R package. The ultrametric tree required was generated using BEAST 1.10.4 (Suchard et al. 2018) with a GTR+G+I model as identified by ModelFinder (Kalyaanamoorthy et al. 2017), an uncorrelated relaxed clock with a lognormal distribution and an mtDNA COI substitution rate estimate of 0.0115 (Brower 1994). The species delimitation based on morphology has been compared to the delimitations based on molecular data. From the species described, the genetic p-distance was estimated between all pairs of samples using MEGA (Tamura et al. 2021) and summarised by species.

Data availability

The sequence dataset is available on BOLD (DS-ARGYRIA). Raw reads are available on the NCBI SRA BioProject PRJNA914237.

Results

DNA recovery from historical samples

Historical DNA extraction showed different yields mainly related to the age of the specimens but also to the type of tissue and the extraction method, i.e., destructive or non-destructive (Table 1). Indeed, for the oldest sample, i.e., CRA03, captured between 1784–1789, it has been possible to extract DNA using a destructive approach on only one leg. For the two 19th century samples, i.e., CRA01 and CRA02, a non-destructive approach was attempted. The sample with the lowest concentration of DNA is the CRA07 sample which was captured in 1911 and for which two legs were used destructively. Smaller fragments have been observed for the sample captured during the 18th century, CRA03, and larger fragments for the sample CRA04 captured in 1992. Sample CRA07 is a special case since it was captured in 1911 but

has small DNA fragments. For the more recent samples, captured after 2000, it was possible to extract enough DNA to perform a classical COI barcode amplification and Sanger sequencing (PCR amplification in Table 1). For the older samples, it has been necessary to develop a barcode capture approach because the amount of endogenous DNA was too low and initial trials at PCR amplification proved unsuccessful. This capture approach using probes designed along the COI barcode allowed NGS sequencing of 3.99 million reads in total with high heterogeneity between samples (Table 1). The number of reads seems correlated with the amount of DNA initially extracted. This heterogeneity in the amount of sequence recovered is then found throughout the bioinformatics analysis process until it impacts the percentage of barcode finally recovered. However, the capture approach was effective since it allowed the recovery of a sufficient proportion of the barcode to perform phylogenetic inferences for each of the samples, including the oldest sample, CRA03, and the particularly degraded CRA07 for which respectively more than 50% and 93.1% of the barcode was recovered.

Phylogenetic inference and species delimitation

Phylogenetic inference has been performed on the whole COI barcode alignment including BOLD sequences, barcodes amplified for this study and sequences recovered using our historical DNA capture approach. The samples corresponding to the two species *A. rufisignella* and *A. nummulalis* have been used as outgroups, and their common node is well supported (Fig. 1). Then a well-supported node separates two clades, one includes the species *A. diplomochalis*, *A. insons* C. Felder, R. Felder & Rogenhofer, 1875, and *A. centrifugens* on one side and the species *A. gonogramma* and *A. lacteella* on the other (Fig. 1). Overall, the nodes separating the five species are also well supported. The three species delimitation analyses are consistent with each other and with morphology. The five species described and identified morphologically are almost all found by the species delimitation approaches, only the separation between *A. gonogramma* and *A. lacteella* has not been found in the ABGD approach based on the levels of divergence between sequences. However, the node separating the two species is well supported. Analysis of genetic divergence (p-distance) between each pair of individuals within and between species shows contrasting levels of divergence (Fig. 2). Within species, genetic divergence is low between 0.43% for *A. centrifugens* and 2.47% for *A. diplomochalis* for which we have only three samples. The distribution of genetic divergence then shows a gap with much higher values between samples belonging to different species and a percentage of divergence ranging from 5.17% to 11.90%. These results support the species identified using morphology and species delimitation approaches. Within each species the species delimitation approaches also identified additional separations mainly related to geographic divergences. The details of the divergences within species will be discussed next in the “Molecular diagnosis” section of each species.

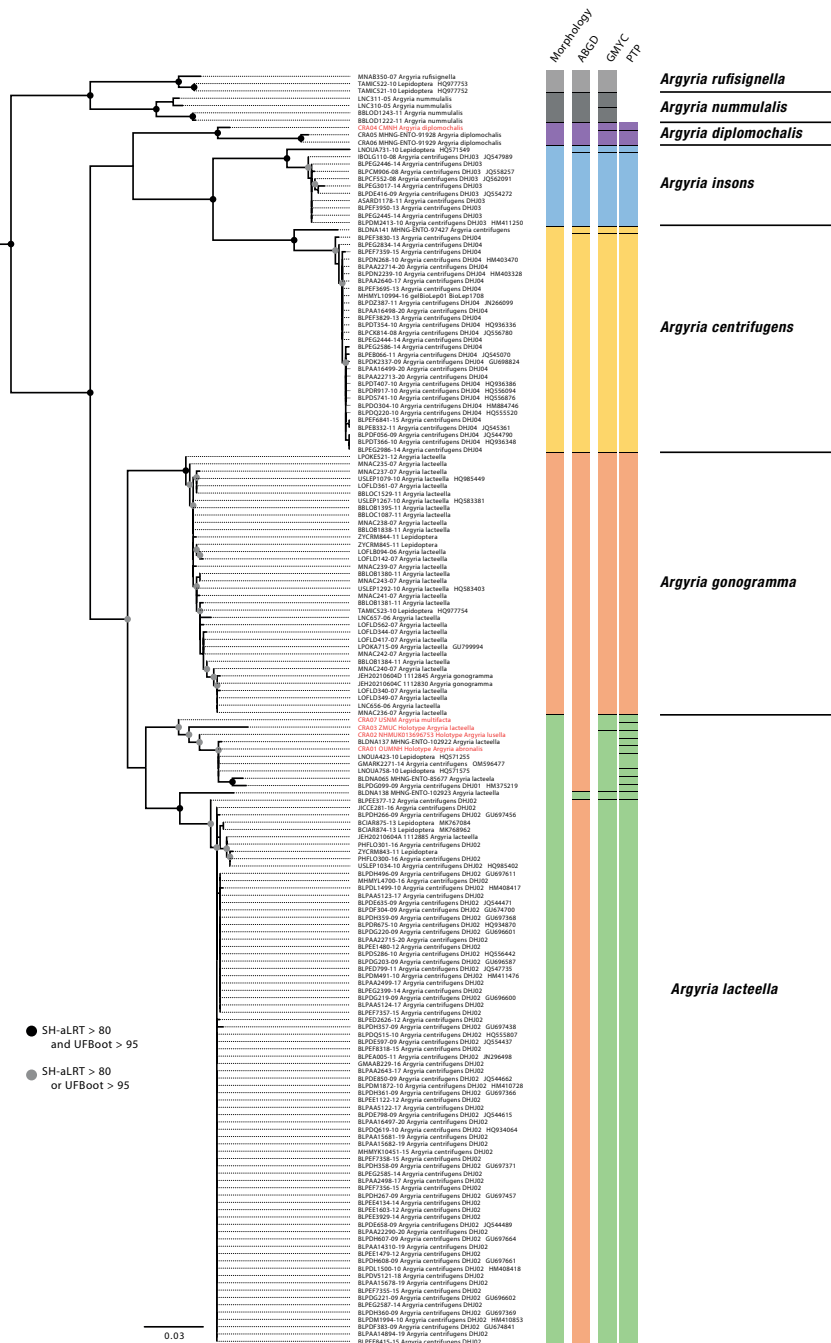


Figure 1. Phylogenetic inferences including 174 *Argyria* COI barcode sequences, i.e., 160 barcodes from BOLD, 9 COI sequences amplified by PCR (in bold), and 5 COI sequences obtained using capture from historical specimens (in red). Nodal support expressed in SH-aLRT and ultrafast bootstrap (UFBoot) is given as indicated in the caption except for nodes when SH-aLRT < 80 and/or UFBoot < 95. Species delimitation results including morphology, ABGD, GMYC, and PTP are indicated by different colours to represent the species proposed.

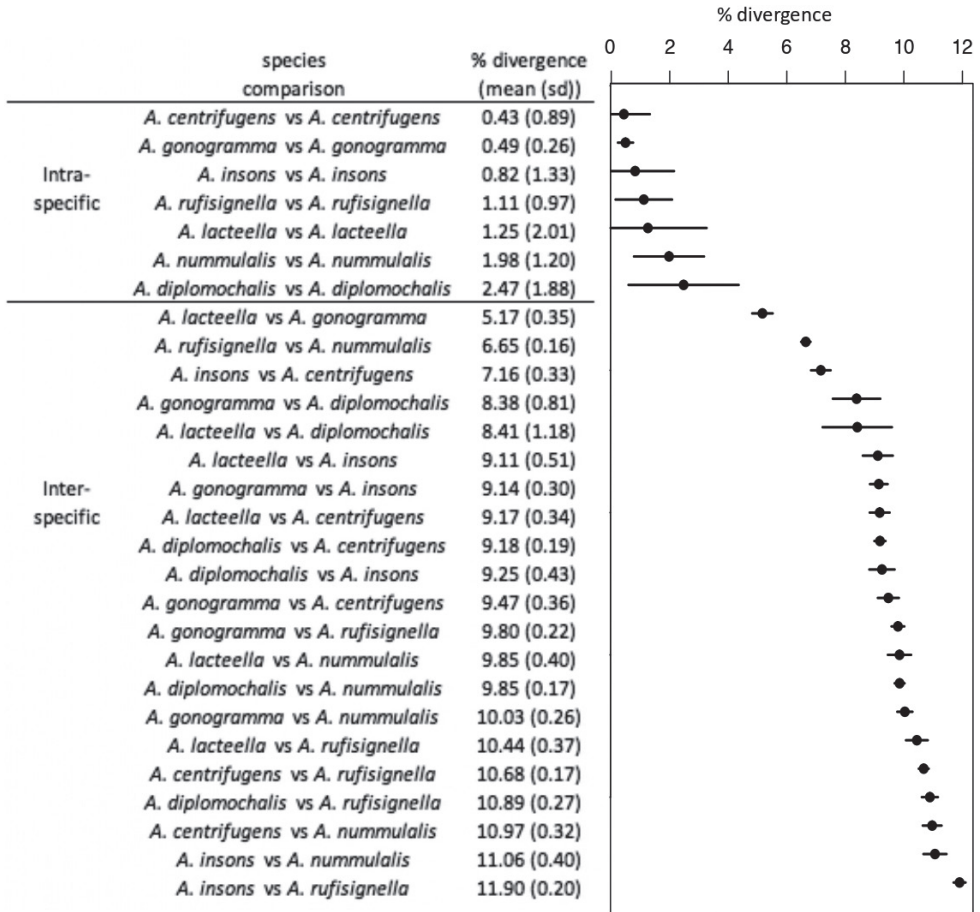


Figure 2. Mean genetic divergence (p-distance) between all samples from each species.

Taxonomic account

Argyria lacteella (Fabricius, 1794)

Figs 3–7, 11, 17, 24, 27, 29, 33

Tinea lacteella Fabricius, 1794: 313. Type locality: “*Americae insulis*” (USA Virgin Island of Saint Croix; see Remarks). Fernald 1896: 72, plate V figs 4, 6; Dyar 1903: 411; Grossbeck 1917: 126, probably referable to *A. gonogramma*, see Remarks; Schaus 1940: 400; Amsel 1956: 31, pl. 69 fig. 6, part of records, misspelled ‘lactella’; Munroe 1956: 127; Błeszyński and Collins 1962: 214; Zimsen 1964: 579, misspelled ‘lactella’; Kimball 1965: 234, part of records; Błeszyński 1967: 96; Jaume 1967: 2; De la Torre y Callejas 1967: 20; Alayo and Valdés 1982: 61; Tan 1984: 96 et seq., misidentification; Ferguson et al. 1991: 40, misidentification; Munroe 1995a: 35; Heppner 2003: 288, part of the records; Martinez and Brown 2007: 81, fig. 9, referable to *A. gonogramma*; Roque-Albelo and Landry

2010; Scholtens and Solis 2015: 54; Landry et al. 2020: 101, fig. 6B; Gibson et al. 2021: 29.

= *albana* (Fabricius, 1798 (*Pyralis*). Unnecessary replacement name.

= *abronalis* Walker, 1859: 969 (*Zebronia*?). Type locality: Brazil, Rio de Janeiro.

= *lusella* (Zeller, 1863: 51) (*Catharylla*). Type locality: St. Thomas Island [USA Virgin Islands]. Syn. rev.

= *vestalis* Butler, 1878: 494, 495. Type locality: Jamaica. Syn. nov.

= *multifacta* Dyar, 1914: 317. Type locality: Panama, Porto Bello. Syn. nov.

Type material examined. *Lectotype* of *Tinea lacteella* (Fig. 3), here designated, with label data as follows: 1- “P. albana | ex Ins: Amer: | ?Schmud?”, 2- “Mus[eum]. S[ehested] & T[oender] L[und], 3- “LECTOTYPE | *Tinea lacteella* | Fabricius, 1794 | Des[ignated] by B. Landry, 2021”; deposited in ZMUC.

Holotype of *Zebronia? abronalis* (Figs 4, 24), with label data as follows: 1- “Type”, 2- “Rio”, 3- “91”, 4- “Zebronia | Abronalis”, 5- “TYPE LEP: No 1195 | Zebronia ? | abronalis | Walker | HOPE DEP[ARTMEN]T.OXFORD”; deposited in OUMNH.

Holotype of *Catharylla lusella* (Fig. 5), with label data as follows: 1- “Type”, 2- Lusella | Zell[er]. Mon[ograph]. p.51.”, 3- Zell[er]. Coll[ection]. | 1884.”, 4- “♂ | Pyralidae | Brit.Mus. | Slide No. | 7092” | DNA voucher Lepidoptera B. Landry, n° 00158 | NHMUK013696754 | MOLECULAR 215427977; deposited in the NHMUK.

Holotype of *Argyria vestalis* (Fig. 6), with label data as follows: 1- “Type”, 2- “Jamaica | 78. 19”, 3- ♂ | Pyralidae | Brit.Mus. | Slide No. | 7093 | NHMUK013696753”; deposited in the NHMUK.

Holotype of *Argyria pusillalis* variety *multifacta* (Fig. 7) with label data as follows: 1- “PortoBello | Pan[ama]. Febr[uary]. [19]11 | AugustBusck”, 2- “Type | No.16316 | U.S.N.M.”, 3- “Platytes | multifacta | Type Dyar”, 4- “♀ genitalia | slide 3826 | R W Hodges”, 5- “Genitalia Slide | By RWH ♀ | USNM 10,709”; deposited in the NMNH. *Paratypes* of *Argyria pusillalis* variety *multifacta* with label data as follows: 1 ♂: 1- “PortoBello | Pan[ama]. Febr[uary]. [19]11 | AugustBusck”, 2- “♂ genitalia | slide, 29 Apr. ’32 | C.H. #29 | Genitalia slide | By ME ♂ | USNM 99,668”; 1 ♀: same data; 5 ♀♀, 2 ♂♂: same data except “Mar[ch]”; 2 ♀♀: 1- “RioTrinidad | Mar[ch]. [19]12 Pan[ama] | ABusck | coll”; 1 ♂: 1- “CorazolC[anal]Z[one] | Pan[ama] 3/24 [19]11 | AugBusck”, 2- “♂ genitalia | slide, 9 June. ’32 | C.H. #83” [slide not found]; deposited in the NMNH. [Note: the Tabernilla (Busck) and Corazol (Crafts) specimens were not found at NMNH]

Other specimens examined. 238 specimens (see Suppl. material 2).

Morphological diagnosis. This is a small satiny white moth of 9.5–14 mm in wingspan. The forewing brown markings are median triangles on the costa and dorsal margin usually linked by a thin straight line sometimes slightly thicker on the discal cell as a spot, but sometimes inconspicuous, another triangle subapically on costa, usually separated by a thin white line from a short oblique dash anteriorly, and a wavy terminal line (Figs 3–6, 11). There are also specimens of *A. lacteella* with a com-

plete median fascia (Fig. 7) in the South of the distribution of the species, in Panama (holotype of synonym *A. multifacta*), French Guiana, Bolivia, and Brazil. In forewing markings *A. lacteella* differs from *A. gonogramma* (Figs 8, 12), which usually has a well-marked darker, blackish-brown spot on the discal cell, linked by a thin, curved line to a short diagonal bar on costa and a thin triangle on the dorsal margin, and without a clear costal triangle subapically. In forewing markings *A. lacteella* is most similar to *A. centrifugens* (Fig. 10), which is generally bigger (14–19 mm in wingspan) and which has the line anterior to the subapical costal triangle curved to reach the costa at right angle whereas that line in *A. lacteella* runs obliquely into the costa. In male genitalia (Fig. 17) this species differs from the most similar *A. gonogramma* by the basal projection of the valva that is slightly longer and bent mesad at right angle whereas it is just barely curved in *A. gonogramma* (Figs 16, 18). The cornuti on the vesica also are smaller and thinner in *A. lacteella* compared to those of *A. gonogramma*. In female genitalia *A. lacteella* (Figs 24, 27) is also most similar to *A. gonogramma* (Fig. 28), but *A. lacteella* has two “pockets” anterolateral of the ostium bursae, whereas *A. gonogramma* has one continuous pocket anterior of the ostium.

Molecular results. Phylogenetic inference based on COI barcode alignment reveals a large clade grouping the *A. lacteella* samples. This clade is relatively homogeneous since the percentage of divergence within this species remains low with an average of 1.25% (Fig. 2). It is then divided into two clades also identified by the species delimitation approaches. The first one is mainly composed of samples from South America, i.e., Brazil, French Guiana, Argentina, Colombia, but also from the Galapagos Islands. The different intraspecific delimitations identified by the species delimitation approaches within this clade are therefore certainly related to geographical divergence. The historical samples originating from Panama and the United States Virgin Islands belong to this clade as well. The barcodes of these samples are not complete (Table 1), the missing may induce phylogenetic artefacts due to long-branch attraction. A molecular analysis focused on this species including more localities but especially more loci could clarify this situation. The second cluster is composed of a clade of samples from the US on one side and a very large clade of samples from Costa Rica on the other. The latter shows a very low level of variation.

Distribution. Widespread in the Western Hemisphere from the US State of Florida north to Alachua County in the north, across Central America and the Antilles, in South America to Argentina in the south, as well as on the Galápagos Islands (Fig. 33).

Remarks. Fabricius (1798) changed the name of his *lacteella* (1794) with another (*albana*). The reason for this is unrecorded and remains unclear, but this is possibly because Fabricius (1798: 476, spelling it “*lactella*”) incorrectly considered *lacteella* to be a homonym of *Tinea lactella* Denis & Schiffermüller, 1775 (a synonym of *Endrosis sarcitrella* (Linnaeus)). Also, he may have corrected ‘improper’ names as in his treatments of *Tinea compositella* Fabricius, 1794 and *T. tapetzella* Linnaeus, 1758, both without putative ‘homonyms’ and respectively renamed *Pyralis composana* and *P. tapezana* (Fabricius, 1798: 480), or he felt that the exact orthography of any name was not so important.



Figure 3. Lectotype of *Tinea lacteella* Fabricius, 1794 (copyright of Natural History Museum of Denmark, ZMUC). Scale bar: 1 mm.



Figure 4. Holotype of *Argyria lacteella* synonym. *Zebronia?? abronalis* Walker, 1859 (Oxford University Museum of Natural History; OUMNH). Scale bar: 10 mm.

The first label associated with the lectotype of *A. lacteella* (Fig. 3) reads “P[ylalis]. albana | ex Ins. Amer: | Schmidt”. The second line of this label means “from the American Islands” while the name of the third line refers to the collector of the specimen, who, according to Zimsen (1964) was either Adam Levin Smidt, a custom-house officer, or Johan Christian Schmidt, a surgeon. Both lived on the island of St Croix, which was at that time a Danish possession (T. Pape, pers. comm. to BL, 18 August 2022). The second label associated with this type specimen refers to the collection of Ove Ramel Sehested and Niels Tønder Lund who lived in Copenhagen and were pupils and friends of Fabricius (Baixeras and Karsholt 2011).



Figure 5. Holotype of *Argyria lacteella* synonym. *Catharylla lusella* Zeller, 1863 (NHMUK Trustees of the Natural History Museum).



Figure 6. Holotype of *Argyria lacteella* synonym. *Argyria vestalis* Butler, 1878 (NHMUK Trustees of the Natural History Museum).



Figure 7. Holotype of *Argyria lacteella* synonym. *Argyria pusillalis* variety *multifacta* Dyar, 1914 (NMNH; wingspan: 12 mm).

The locality of origin is an additional complication associated with *A. lacteella*. The locality of Fabricius' *Pyrallis albana* (1798) is mentioned as “*Americae insulis*” [American islands] whereas that of *A. lacteella* (1794) is “*Americae meridionalis arboretis*” [South American arboretum]. Given that “Dr. Pflug” is mentioned in the original description of *A. lacteella*, it is reasonable to conclude that “*Americae insulis*” was a correction for “*Americae meridionalis arboretis*”. This is because Paul Gottfrid Pflug (1741–1789), a medical doctor, lived in the Caribbean island of Saint Croix (United States Virgin Islands) during the last five years of his life, where he collected insects that he sent to Denmark. He is mentioned often by Fabricius as a specimen collector (O. Karsholt, pers. comm. to BL, 3 June 2021). Therefore, *A. lacteella albana* is from an American island (*Americae insulis*) that is probably Saint Croix.

As confirmed by Copenhagen Museum former curator Ole Karsholt and present curator Thomas Pape, only one type specimen presently exists for *lacteella albana* (Fig. 1) and because *albana* is best considered as an unjustified replacement name, the

type of *Pyralis albana* Fabricius, 1798 is the same as that of *Tinea lacteella* Fabricius, 1794. This specimen is without an abdomen and is designated as the lectotype upon the recommendation of curator T. Pape, who wrote (pers. comm. to BL, 7 June 2021): “As Fabricius does not indicate the number of specimens, I would consider a lectotype designation as appropriate, unless this has already been done by referring to this specimen as “the type” or something similar.” Such a designation also serves to stabilise the identity of the species name laden with confusion caused by Fabricius himself.

The type specimen of *A. lacteella* (Fig. 3) is badly rubbed, lacking most scales on the head, and some on the thorax and forewings as shown by the denuded anal vein on the right forewing. It also lacks most of the diagnostic brown markings of the forewing, notably the subapical triangle on the costa, but the terminal zigzagging brown line is almost complete and there are a few brown scales in the position of the median spot and fewer brown scales still on the dorsal margin medially.

Munroe (1995: 35) stated that *Argyria abronalis* is a nomen dubium, but this is incorrect as a female type (Figs 4, 24) is in the Oxford University Museum of Natural History (also figured at <https://www.oumnh.ox.ac.uk/collections-online#/item/oum-catalogue-3393>). The forewing markings, female genitalia morphology and DNA barcode all concur to validate the synonymy of *A. abronalis* with *A. lacteella*. The species was described from the female sex, without indication or indirect evidence of more than one specimen; therefore, the OUMNH specimen is considered the holotype.

The original description of *Catharylla lusella* Zeller (1863) explicitly mentioned one female only, described from the island of Saint Thomas, US Virgin Islands. Thus, the male sign on this holotype's slide number label is incorrect (Fig. 5). The specimen was dissected and although the genitalia dissection was not thoroughly cleaned, the visible morphological characters agree with those of *A. lacteella*. The forewing markings lack the median triangle of the dorsal margin and any indication of a median transverse line, as in the holotype of *A. lacteella*, but the subapical triangle on the costa and especially the COI barcode obtained clearly show that *C. lusella* syn. rev., should be considered a synonym of *A. lacteella*. The name had been synonymised by Fernald (1896), considered a synonym also by Schaus (1940), but considered valid again by Błeszyński and Collins (1962) and Munroe (1995; misspelled “*lusalla*”).

The original description of *Argyria vestalis* does not mention more than one specimen and the NHMUK does not hold additional specimens with these label data; therefore, this specimen is considered the unique holotype. It is a lightly marked, damaged, dissected male (Fig. 6); the dissection clearly shows the curved projection at the base of the valva that is diagnostic for *A. lacteella*; therefore, the name *A. vestalis* syn. nov. is considered a synonym of *A. lacteella*.

Argyria multifacta was described as a variety of *A. pusillalis* for which “All the specimens have the median band continuous across the wing” (Dyar 1914: 317). Among a series of specimens mentioned from several localities in the Panama Canal zone, one is recorded as Type with the type number and label data mentioned above (Fig. 7). Although this holotype shows a conspicuous and almost continuous median band on the forewing, thus revealing strong variation in that respect in the species, other wing characters, size, and the COI barcode data point to the synonymy of *A. multifacta* syn. nov. with *A. lacteella*.

This species evidently became established in Florida, USA in the 1970s and consequently, earlier records from Florida (Grossbeck 1917; Kimball 1965) are believed to be wrong and referable to *A. gonogramma*. The earliest specimen known to us was collected in Miami-Dade County, Fuchs Hammock near Homestead, by T.S. Dickel on 31 August 1979 (MGCL catalogue no. 1112898, slide 6219, deposited in FSCA). The species rapidly spread across the state, as shown by first collection years in other vouchered counties: 1983: Highlands, Monroe, Orange; 1986: Collier, Manatee; 1987: Volusia; 1988: Lee; 1990: Pinellas; 1991: Hernando; 2000: Brevard; 2003: Marion; 2005: Alachua; 2012: Indian River; 2013: Levy (FSCA, MGCL). The collection of *A. gonogramma* in Florida decades before *A. lacteella* strongly suggests that the latter species is non-native and that it invaded in the given time frame (see Remarks for *A. gonogramma*).

Amsel (1956: 31, pl. 69 fig. 6) mentions the species from specimens sporting a wingspan of 12–18 mm, and although his illustration probably represents *A. lacteella*, no specimens examined of that species were found to reach a wingspan of more than 14 mm.

The vesica of a male specimen from Florida, USA (not illustrated here) was successfully everted by J. Baixeras, who wrote the following to BL on 17 October 2022: “After a lot of manipulation I was able to evert what seems like a rather tubular vesica bearing a single row of non-deciduous cornuti tightly arranged like in a “gun charger” mode. The vesica seems to be somewhat convoluted at the base (I do not think it an artefact), then straight. The cornuti are extended all over the length of the vesica except in the terminal part, close to the genital opening. The basal convolution is interesting and, if my surmise is correct, should be correlated with some structure in the female, either a pocket, broadening sclerotisation or, in some cases, some corrugated area allowing expansion during insertion.” The basal convoluted bend at the base of the vesica reflects the shape of the basal section of the female ductus bursae, which is indeed corrugated (Figs 24, 27).

Argyria gonogramma Dyar, 1915

Figs 8, 12, 13, 15, 16, 18, 28, 30, 34

Argyria gonogramma Dyar, 1915: 87–88. Type locality: Bermuda. Błeszyński and Collins (1962: 213).

= *pussillalis* Hübner, 1818: 30, [36], [38], figs 167, 168. Type locality: [USA, Maryland] Baltimore. Nomen dubium.

= *pussillalis* [sic] Hübner, 1818: 28; original misspelling.

Argyria lacteella (Fabricius, 1794): Fernald 1896: 72, plate V fig. 5; Grossbeck 1917: 126; Kimball 1965: 233; Tan 1984: 96 et seq.; Ferguson et al. 1991: 40; Munroe 1995: 35 (in part); Martinez and Brown 2007: 81, fig. 9.

Type material examined. *Holotype* ♂ (Figs 8, 15, 16), with label data as follows: 1- “Bermuda, | 11.3.BWI | F.M. Jones”, 2- “V-3 | D”, 3- “Type No. | 18244 | U.S.N.M.”, 4- “Argyria | gonogramma | Type Dyar”, 5- “♂ genitalia | slide, 29Apr[il].’32 | C.H. #27”, 6- “Genitalia Slide | By 107,454 | USNM”; deposited in the NMNH.

Other specimens examined. 411 specimens (see Suppl. material 2).

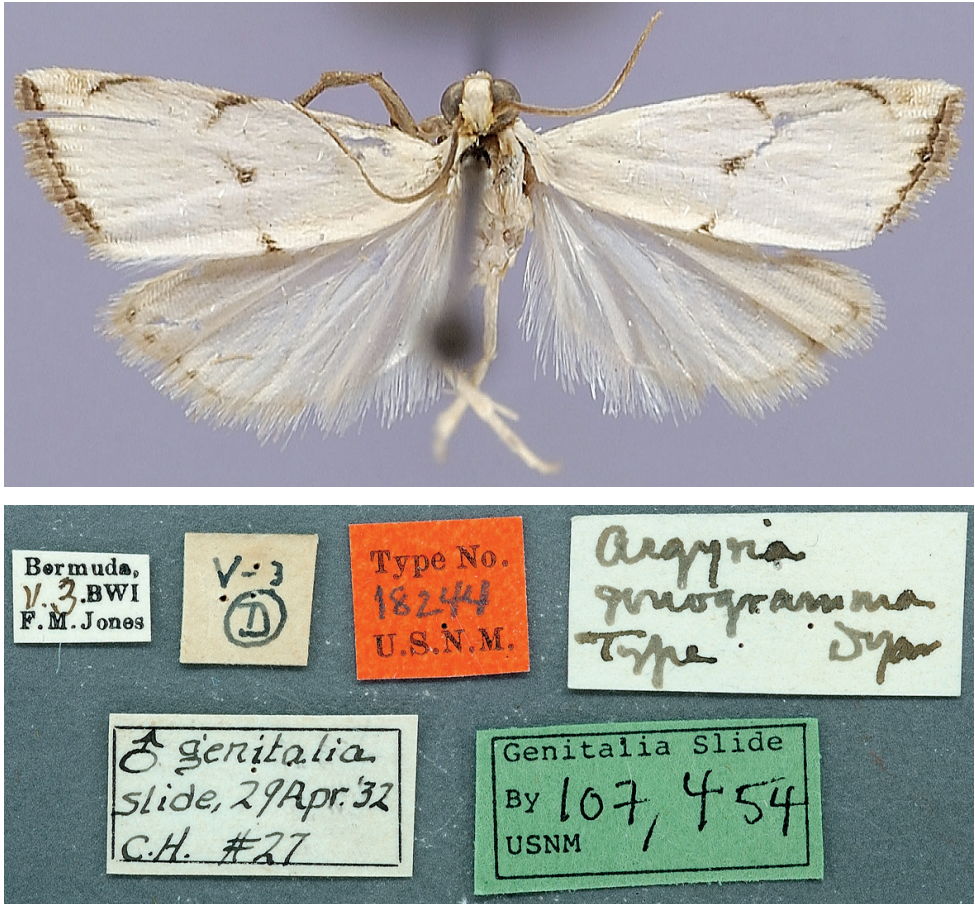


Figure 8. Habitus of *Argyria* type specimen (in NMNH) with labels underneath; holotype of *Argyria gonogramma* Dyar, 1915 (wingspan: 11 mm).

Morphological diagnosis. In this small satiny-white moth measuring between 10.5 and 13.5 mm in wingspan, the median markings of the forewing (Figs 8, 12) usually include a well-marked blackish-brown spot on the discal cell that is connected by curved lines to an oblique bar on the costa and a thin triangle on the dorsal margin. On the forewing costa, subapically, a thin curving bar is not followed by a triangle, but usually by 1–3 horizontal lines reaching the terminal margin below the apex. Relatively dark brown forms, with less contrasting markings (Fig. 13) have been collected in Alabama, Florida, and Louisiana (CUIC, FSCA, MHNG, NMNH) from December to April. In forewing markings this species is closest to *A. lacteella* (Fig. 11) in which there usually is a clear subapical triangle on the costa and for which the median spot, if present, is paler brown and usually smaller than the costal and dorsal triangles. In the absence of a subapical triangle on the forewing costa *A. gonogramma* is also similar to *A. diplomochalis* (Figs 9, 14), which, however, doesn't have any indication of a median spot or of any line between the median spot of the dorsal margin and the costa.

In the male genitalia *Argyria gonogramma* (Figs 15, 16, 18) has the basal projection of the valva shorter than that of *A. lacteella* (Fig. 17) and just barely curving (Fig. 16); the cornuti on the vesica are also longer and thicker than those of *A. lacteella*. In the female genitalia (Fig. 28) only one wide, sclerotised pocket can be found anterior of the ostium bursae, whereas *A. lacteella* (Figs 24, 27) has two pockets in the same area.

Molecular results. Phylogenetic inference reveals that *Argyria gonogramma* constitutes a homogeneous clade. The monophyletic clade is identified in both GMYC and PTP species delimitation approaches, but it is not found in the ABGD approach and is grouped with *A. lacteella* (Fig. 1). This clade shows very low genetic variability within the COI barcode with an average intraspecific divergence of only 0.49% (Fig. 2). This low genetic diversity may be the result of different evolutionary processes,



Figure 9. Habitus of *Argyria* type specimen (in NMNH) with labels underneath; lectotype of *Argyria diplomochalis* Dyar, 1913 (wingspan: 11 mm).



Figure 10. Habitus of *Argyria* type specimen (in NMNH) with labels underneath; holotype of *Argyria centrifugens* Dyar, 1914 (wingspan: 16 mm).

including recent colonisation. This species is mainly present in the US where it overlaps with *A. lacteella* in Florida (Figs 33, 34).

Distribution. Bermuda, Bahamas, widespread in the Eastern USA, from North Carolina in the North to the south of Florida, west to eastern Texas (Fig. 34).

Remarks. The specimen of *A. gonogramma* labelled 'Type' in the NMNH is considered the unique holotype; the species' description (Dyar 1915) doesn't indicate multiple specimens.



Figure 11. Habitus of additional *Argyria* specimen. *Argyria lacteella* (Florida, Putnam Co., FSCA). Scale bar: 2.5 mm.



Figure 12. Habitus of additional *Argyria* specimen. *Argyria gonogramma* (Florida, Seminole Co., MHNG). Scale bar: 2.5 mm.

Argyria pusillalis Hübner is associated here with *A. gonogramma* and not with *A. lacteella* as in Munroe (1995) because at the latitude of Baltimore, Maryland, U.S.A., the type locality of *A. pusillalis*, only the superficially similar *A. gonogramma* or *A. rufisignella* (Zeller, 1872) could occur. *Argyria nummulalis* Hübner, 1818 is also known to occur in the eastern USA at the latitude of Baltimore, but this species lacks any median markings across the forewing, unlike the illustration of *A. pusillalis*.



Figure 13. Habitus of additional *Argyria* specimen. *Argyria gonogramma* (dark form, Louisiana, Calcasieu Co., MHNG). Scale bar: 2.5 mm.



Figure 14. Habitus of additional *Argyria* specimen. *Argyria diplomochalis* (St Croix Island, MHNG). Scale bar: 2.5 mm.

The name *A. pusillalis* is considered a *nomen dubium* because the original description and illustration associated with it do not allow a conclusive determination. Hübner's collection was deposited in the Naturhistorisches Museum Wien, Vienna, Austria, which was destroyed by fire in 1835 (Horn et al. 1990). However, although type specimens of some of Hübner's Noctuidae species have recently been discovered in this museum (Gabor and László Ronkay, pers. comm. to BL, 11 April 2022), a search for a type specimen of *A. pusillalis* was not successful (S. Gaal, pers. comm. to BL, 10 August 2022).



Figure 15. Male genitalia of *Argyria gonogramma* holotype (NMNH). Whole genitalia.



Figure 16. Male genitalia of *Argyria gonogramma* holotype (NMNH). Close-up of bases of valvae with tip of phallus in middle.

This issue could be settled by the designation of a neotype, but we refrain from doing that in order to avoid more instability in the nomenclature of this group. Also, we believe that it should be done in conjunction with a taxonomic revision of *A. rufisignella*, at the least.

Argyria pusillalis was originally named “*pussillalis*” (Hübner 1818: 28), then mentioned as “*pusillalis*” on page 30 and on two indices (pages [36] and [38]), and finally as “*pussillalis*” again on the plate with the illustrations. Given that “*pusillus*” is Latin for small, it seems reasonable to believe that the original spelling “*pussillalis*” was in error.

Argyria gonogramma is a North American native species that was previously misidentified as *A. lacteella* and that has been collected in the United States since the late 1800’s. The earliest specimens in the NMNH were collected by C.V. Riley from Ar[t] elier, FL, 1882 and N.[orth]C.[arolina] (undated). Another specimen collected by Boll in Texas (collection date unknown) was identified by “Rag[onot] \[18]86”, and then by “CVR[iley]at the B. Mus. \[18]87”.

That this species is native to the Southeastern U.S., or at least was established long before *A. lacteella*, is shown by earlier collecting dates for specimens in the FSCA and MGCL. For example: Florida, Sarasota Co.: 1951, Alachua Co.: 1960, Volusia Co.: 1962, Okaloosa Co.: 1963, Texas: 1978, Louisiana: 1979.

The earliest record of *A. lacteella* in 1979 in the USA (Florida) supports the conclusion that Tan (1984), although referring to *A. lacteella*, was in fact dealing with *A. gonogramma*. Tan’s (1984) unpublished MSc thesis provided a description of larvae, with setal maps, which were reared from egg to adult on St. Augustine grass (*Stenotaphrum secundatum* (Walt.) Kuntze; Poaceae). Tan (1984) further mentions that the early instar larvae eat the upper epidermis only and when not feeding, larvae hide in shelters made of leaves attached with silk, wherein moulting occurs. Tan (1984) also records the construction by the mature larva of a “small, compact silken case covered with frass and tiny pieces of chewed grass for pupation.”

Based on collected series of specimens both *Argyria gonogramma* and *A. lacteella* now occur in sympatry and fly on the same dates in Florida, for example at Archbold Biological Station in Highlands County or in Pinellas County.

Fernald (1896) treated this species under *A. lacteella* (pl. V fig. 5), whereas his other illustrations on the same plate (Figs 4, 6) represent the true *A. lacteella*. Grossbeck (1917), Kimball (most or all records, 1965), and Martinez and Brown (2007) all treated this species under *A. lacteella*. Melanic specimens collected in winter months account for the specimens of “*A. diplomochalis*” cited by Kimball (1965). This colouration variant may represent an adaptation for hiding in dry grass during the winter months and/or to obtain extra calories from the sun to allow biological activity.

The single moth at the basis of the Vermont record has been dissected and is correctly determined, but it is far outside the range since we know of no other record of *A. gonogramma* north of North Carolina. It was collected in sandplain habitat (M. Sabourin, pers. comm. to JH, 29 August 2022), which is consistent with the species’ habitat preference in Florida.



Figure 17. Male genitalia of *Argyria* species. *Argyria lacteella* (Florida, Alachua Co.). In FSCA. Scale bar: 500 μ m.



Figure 18. Male genitalia of *Argyria* species. *A. gonogramma* (Florida, Wakulla Co.). In FSCA. Scale bar: 500 μ m.

***Argyria diplomochalis* Dyar, 1913**

Figs 9, 14, 19, 20, 25, 31, 35

Argyria diplomochalis Dyar, 1913: 113. Type locality: [USA] Culebra Island, Puerto Rico. Błeszyński and Collins 1962: 213; Kimball 1965: 234, US specimens misidentified; Błeszyński 1967: 96; De la Torre y Callejas 1967: 20; Alayo and Valdés 1982: 61; Munroe 1995: 35.

Argyria diplamachalis [sic]: Schaus, 1940: 400.

Type material examined. **Lectotype** ♂ (Fig. 9), here designated, with label data as follows: 1- “Culebra I[sland] | Feb[ruary]1899”, 2- “Porto Rico | Aug[ust.] Busck”, 3- “Type | No.16245” | U.S.N.M.”, 4- “Argyria | diplomochalis | Type Dyar”, 5- “♂ genitalia | slide, 27 Apr[il]. [19]’32 | C.H. #11.”, 6- “Genitalia Slide | By CH | 107,449 | USNM”, 7- “Lectotype | Argyria | diplomochalis Dyar, 1913 | Des[ignated] by M.A. Solis, 2022”, deposited in the NMNH. **Paralectotypes** (8 ♂, 1 ♀), here designated with label data as follows: 3 ♂♂: 1- “Culebra I[sland] | Feb[ruary]1899”, 2- “Porto Rico | Aug[ust] Busck”; 3 ♂♂: 1- “Bayamon | Jan[uary]1899”; 2- “Porto Rico | Aug[ust] Busck”; 1 ♀: 1- “Bayamon | Jan[uary]1899”, 2- “Porto Rico | Aug[ust] Busck”, 3- “GS-5620-SB | Argyria ♀ | lusella Z[eller] | det. Błeszyński, 19”, 4- “Genitalia slide | By SB ♀ | USNM 52861”; deposited in NMNH. 1 ♂ [abdomen in vial]: 1- “SYN-TYPE”, 2- “Bayamon | Jan 1899”, 3- “Porto Rico | Aug[ust] Busck”, 4- “Błeszyński | Collection | B.M. 1974-309”, 5- “Argyria | lusella Z[eller]. | ♂ | det. Błeszyński”, 6- “SYNTYPE | Argyria | diplomochalis | Dyar | det. M. Shaffer, 1975”, 7- “NHMUK013697137”; 1 ♂: 1- “SYN-TYPE”, 2- “Culebra I[sland]. | Feb 1899”, 3- “Porto Rico | Aug[ust] Busck”, 4- “Błeszyński | Collection | B.M. 1974-309”, 5- “SYN-TYPE” | Argyria | diplomochalis | Dyar | det. M. Shaffer, 1975”, 6- “NHMUK013697138”; deposited in the NHMUK.

Other specimens examined. 41 (see Suppl. material 2).

Morphological diagnosis. Measuring 10–13 mm in wingspan this species (Figs 9, 14) is quite similar in size and forewing markings to *A. gonogramma* (Figs 8, 12), but it lacks a median line on the forewing and the median marginal markings are reduced to a faint brown bar on costa and a small dark-brown spot on the dorsal margin; the forewing costa and the head also appear more strongly marked (Fig. 31), notably more thickly dark brown at the base of the costa, on the frons laterally and on the labial and maxillary palpi; the costa of the forewing is also gold yellow to the apex, following the dark brown base. In male genitalia (Figs 19, 20), this species differs most noticeably from the others treated here in the thicker and less strongly bent apical section of the gnathos and in the short valva with a prominent sickle-shaped projection at its base. In female genitalia (Fig. 25), *A. diplomochalis* differs from the others treated here more noticeably by the long and narrow ductus bursae without sclerotised section as well as in the large, circular corpus bursae; the ostium region also lacks any sclerotised ‘pockets’.

Molecular results. The phylogenetic clade corresponding to the species *A. diplomochalis* comprises only three samples sequenced for this study. It appears that



Figure 19. Male genitalia of *Argyria diplomochalis*. Holotype (NMNH).

no sequence available in the BOLD database corresponds to this species. All three species delimitation approaches identify this clade (Fig. 1) and the average genetic divergence with the two closest species, *A. insons* and *A. centrifugens*, are respectively 9.25% and 7.16%, which confirms the high divergence of this clade and its specific status. Within this species, the GMYC and PTP approaches separate CRA04 on one hand and CRA05 and CRA06 on the other; and a mean divergence of 2.87% is observed between the samples of this clade. But this divergence may be related to a geographical divergence since CRA04 comes from the island of Anguilla and CRA05–CRA06 come from the US Virgin Island of Saint Croix. The integration of a larger number of samples in a genetic study could allow a finer molecular characterisation of this species.

Distribution. Antilles, from Cuba in the West to Dominica in the Lesser Antilles in the east (Fig. 35).

Remarks. Described from 12 cotypes from Culebra Island and Bayamon, Puerto Rico, a lectotype is designated here to ensure that the name continues to refer to this species exclusively. Dyar (1913) stated “Cotypes, 12 specimens”, but only seven specimens were found at the NMNH while two others (now paralectotypes) are in the NHMUK.

Examination of specimens of “*A. diplomochalis*” cited by Kimball (1965), including ones in the FSCA labelled “5958,1” (Kimball’s number for that species), are



Figure 20. Male genitalia of *Argyria diplomochalis*. Specimen from St Croix Island (MHNG-ENTO-91929) (A) with phallus detached (B).

A. gonogramma with scattered honey-brown scales on the forewings. This may be melanism caused by pupation during cold weather; all the specimens have been collected in winter or early spring.

***Argyria centrifugens* Dyar, 1914**

Figs 10, 21–23, 26, 32, 35

Argyria centrifugens Dyar, 1914: 318. Type locality: Panama, Canal Zone, Paraiso. Błeszyński and Collins 1962: 212; Błeszyński 1967: 96; Munroe 1995: 35; Miller et al. 2012: 11; Landry et al. 2020: 101, fig. 6A.

Type material examined. *Holotype* ♂ (Figs 10, 21, 22), with label data as follows: 1- “ParaisoC[anal]Z[one] | Pan[ama]. Febr[uary].10.[19]11 | AugustBusck”, 2- “Type | No.16318 | U.S.N.M.”, 3- “Platytes | centrifugens| Type Dyar”, 4- “♂ genitalia | slide, 29Apr[il].[19]’32| C[arl].H[einrich]. #28”, 5- “Genitalia Slide | By 107,465 | USNM”; deposited in the NMNH.

Other specimens examined. 87 specimens (see Suppl. material 2).

Morphological diagnosis. *Argyria centrifugens* (Fig. 10) is very similar in wing markings to *A. lacteella* (Fig. 11), with which it can occur in sympatry in Central and South America, although the median line is always thin and not more pronounced in the middle or wide as in some South American specimens of *A. lacteella* (Fig. 7). It is also a bigger species, sporting a wingspan of 16 (male holotype) –17 mm in males and 16–19 mm in females, compared to 9.5–12.0 mm in males and 11.0–14.0 mm in females of *A. lacteella*. Apart from size these two species differ in the colouration of their labial palpi as those of *A. lacteella* (Fig. 29) and *A. gonogramma* (Fig. 30) are pale greyish brown and yellowish gold with the apex satiny white whereas those of *Argyria centrifugens* (Fig. 32) are mostly dark brown with paler scales on the first palpomere but with the third palpomere dark brown to slightly paler brown. Both species are also very different in genitalia. The male genitalia of *A. centrifugens* (Figs 21–23) differ most notably in the three-pronged gnathos, the wider valva with a widely rounded apex and without a short hook-like projection at base but with a large membranous structure sporting a thin and pointed rod about half as long as the valva, directed toward the base of the valva and apparently articulated. The entire female genitalia are about twice as long in *A. centrifugens* (Fig. 26) than in *A. lacteella* (Fig. 24), the ostium is surrounded by a broad chamber with sclerotised wrinkles on the ventral wall, and the ductus bursae at the base is a medium-sized, thickly sclerotised tube in *A. centrifugens* whereas in *A. lacteella* the antrum consists of two lateral pockets of medium size and the base of the ductus bursae is a lightly sclerotised and corrugated round pocket.

Molecular results. Phylogenetic inference reveals that the species *A. gonogramma* constitutes a distinct lineage separate from the species *A. insons*. The three species delimitation methods identified this species but also identified a subcluster separating the sample BLDNA141. This specimen originates from Colombia while all the other specimens come from Costa Rica. The observed genetic divergence is certainly related to a geographical divergence. A genetic study including samples from more distant localities such as Brazil would better characterise the genetic variability of this species.

Distribution. Central and South America, from Honduras to Colombia and Brazil. Records from the central west coast of Florida are possibly recent introductions (Fig. 35).



Figure 21. Male genitalia of *Argyria centrifugens* (NMNH) holotype.

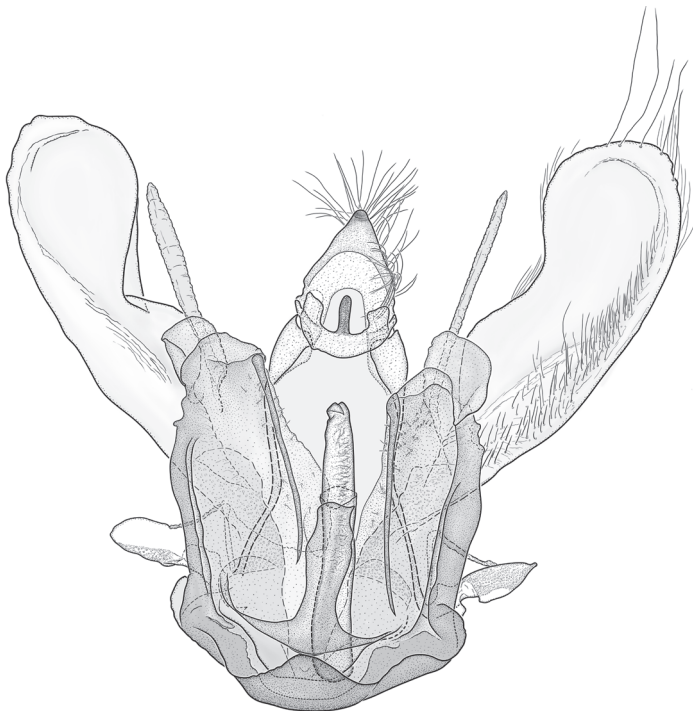


Figure 22. Male genitalia of *Argyria centrifugens* holotype (NMNH); drawing without pheromone scales.

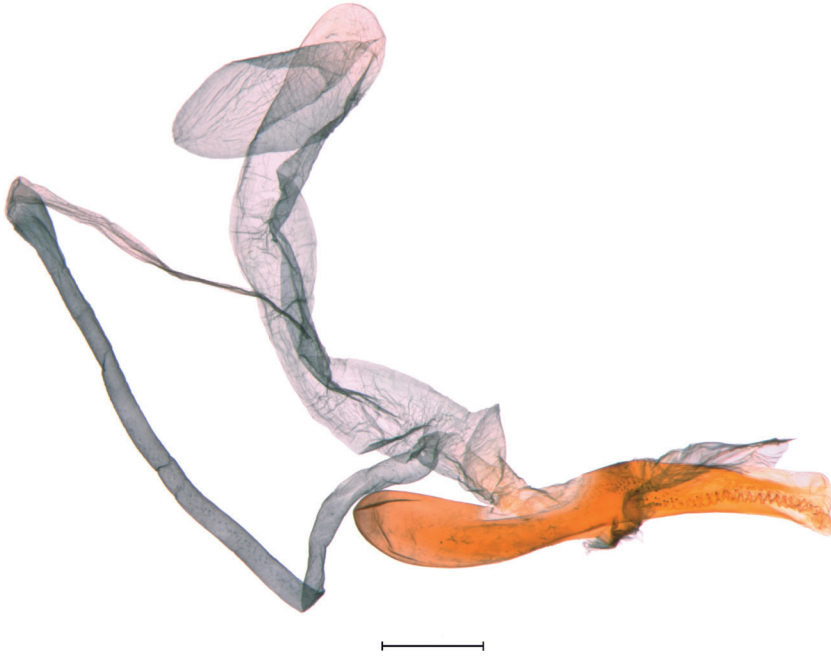
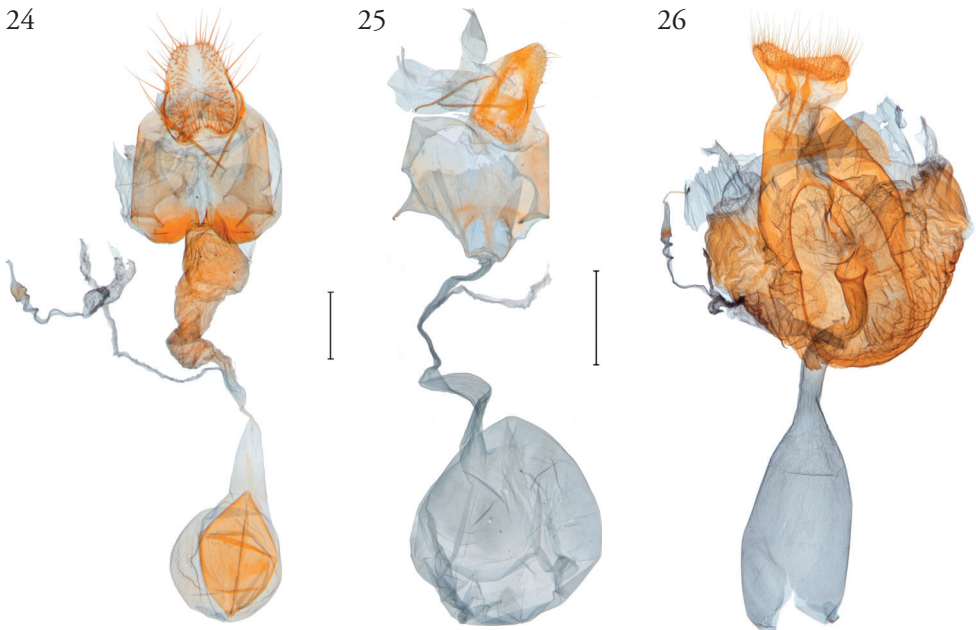
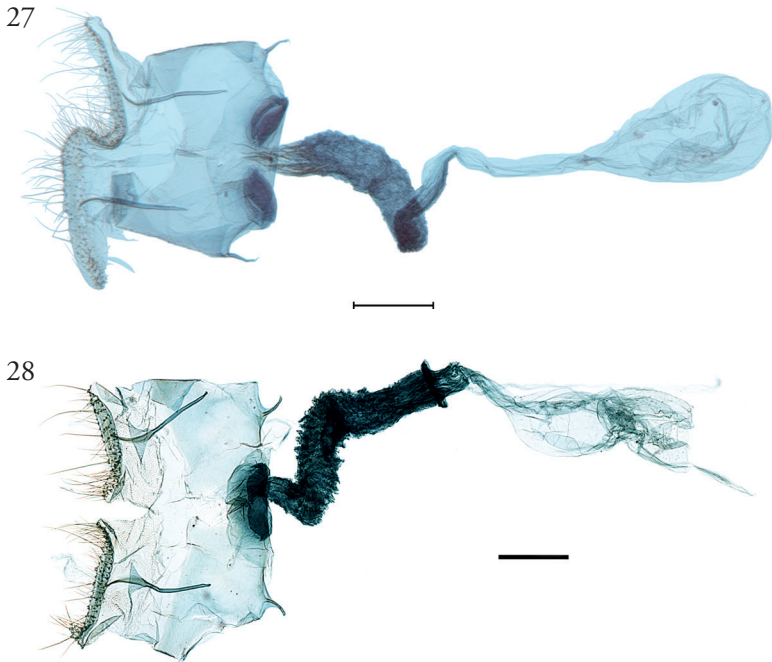


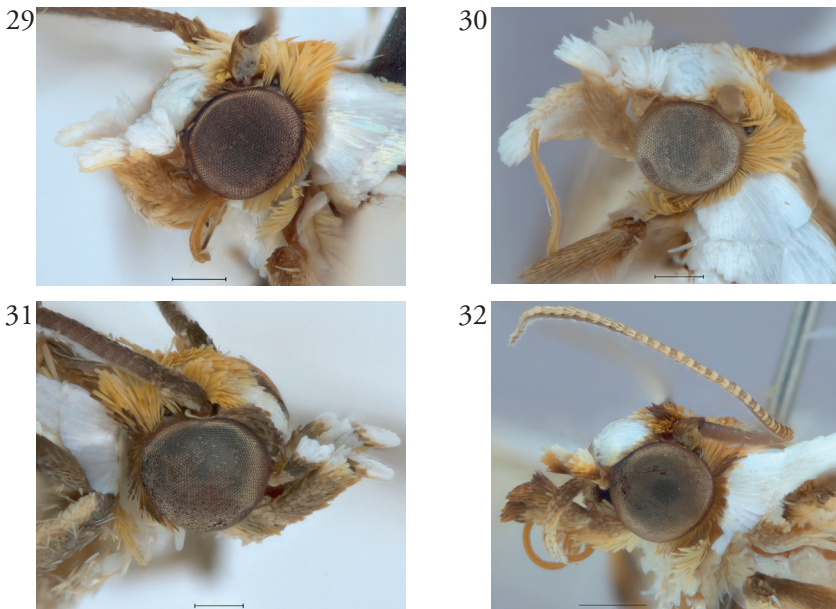
Figure 23. Male genitalia of *Argyria centrifugens* (NMNH). Phallus in lateral view (Nicaragua, Selva Negra Ecodge, MHNG-ENTO-13299). Scale bar: 250 μm .



Figures 24–26. Female genitalia of *Argyria* species **24** *Argyria lacteella* (holotype of *A. abronalis*, with spermatophore inside corpus bursae; OUMNH) **25** *A. diplomochalis* (Anguilla Island, BL 1889, CMNH) **26** *A. centrifugens* (Colombia, Amazonas, Leticia, MHNG-ENTO-97427). Scale bars: 250 μm (**24**), 500 μm (**25, 26**).



Figures 27, 28. Female genitalia of *Argyria* species with ultimate segments cut dorsomedially from base to apex **27** *Argyria lacteella* (USA, Florida, Glades Co.) **28** *A. gonogramma* (USA, Florida, Orange Co.). Both in FSCA. Scale bar: 250 µm.



Figures 29–32. Heads of *Argyria* specimens **29** *A. lacteella* (USA, Florida, Pinellas Co.) **30** *A. gonogramma* (USA, Florida, Levy Co.) **31** *A. diplomochalis* (US Virgin Islands, St Croix) **32** *A. centrifugens* (Colombia, Amazonas, Leticia). All in MHNG. Scale bars: 250 µm (**29–31**), 500 µm (**32**).

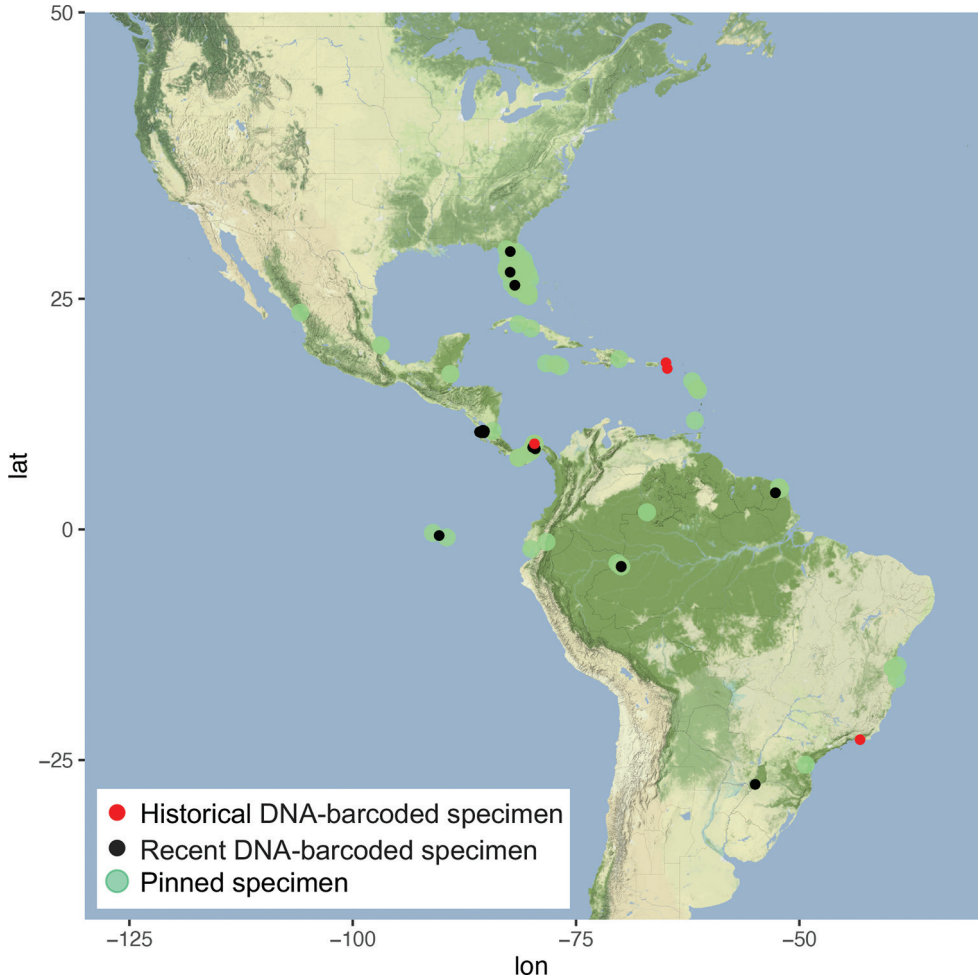


Figure 33. Distribution of *Argyria lacteella* (Fabricius).

Remarks. The species was described from a specimen labelled “Type” of an unspecified sex and two other specimens, “Also two others, Cabima, May, 1911 (Busck).” (Dyar 1914). This “Type” is here considered the holotype. There is some variation observed in the male genitalia, especially noticeably in the length of the median process of the gnathos and in the length of the thin pointed rod at the base of the valva.

One female specimen identifiable as *A. centrifugens* was collected in Florida (Largo, Pinellas County), 1 Feb. 1995, by J.-G. Filiatrault, deposited in the FSCA (MGCL #1112910). It differs from typical specimens in that the labial palpi are mostly yellowish brown with a few dark brown scales on the first and second palpomeres. However, the maculation is otherwise typical, and the genitalia have the same rugose circumstrial chamber as described above.

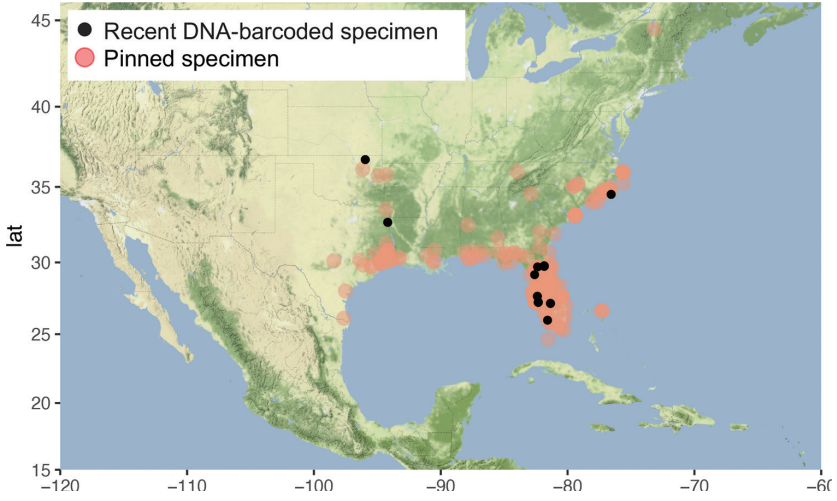


Figure 34. Distribution of *Argyria gonogramma* Dyar.

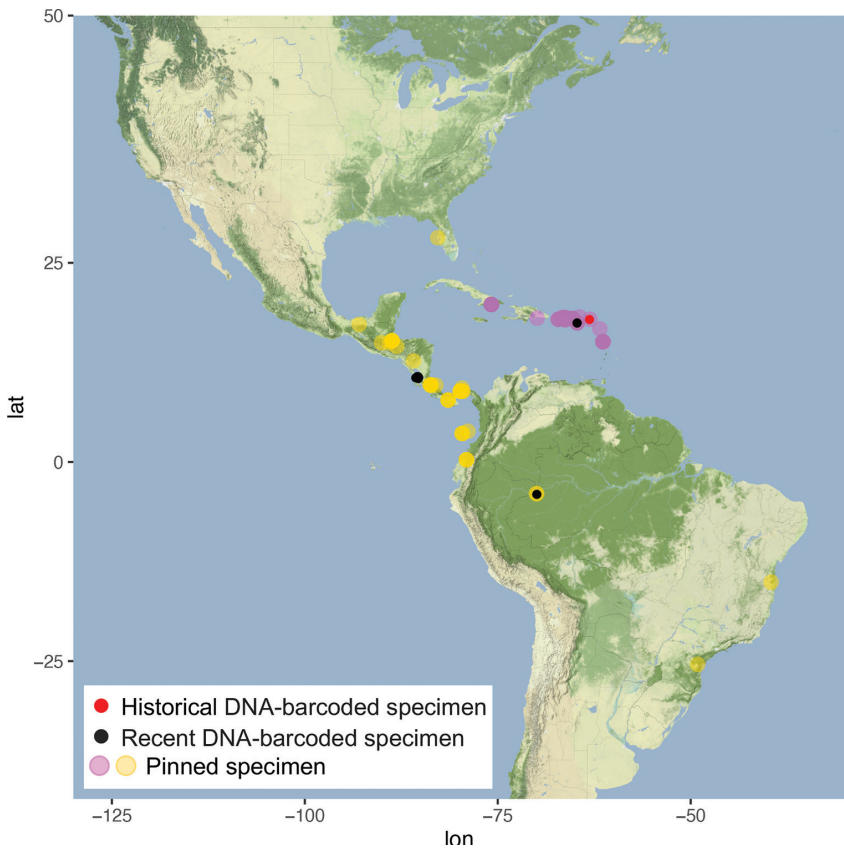


Figure 35. Distributions of *A. centrifugens* Dyar (yellow) and *A. diplomochalis* Dyar (pink).

Discussion

We were able to resolve complex taxonomic questions for *Argyria* using an innovative DNA hybridisation capture protocol to recover high percentages of the DNA barcode of 18th–20th century type specimens. Thus, we were able to solve taxonomic problems regarding synonymies of multiple names applied to the same species. Furthermore, we compiled distribution maps based on refined identities and specimens from multiple museums, leading to other questions regarding responses to environmental change through time. For example, we provided evidence to refine the type locality of *Argyria lacteella* as St Croix Island, whereas the three recent (2021) specimens we examined from that island belong to *A. diplomochalis* (see Suppl. material 2). The possible absence of *A. lacteella* on St Croix currently would not necessarily reflect the environmental situation of 235 years or so ago when the holotype was collected. Various reasons could explain why *A. diplomochalis* was recently collected on St Croix, instead of *A. lacteella*, including habitat change and/or destruction. A thorough moth collecting effort on the island may resolve the question of whether *A. lacteella* still occurs there. Much remains to be learned about this group of *Argyria* moths, especially about their biology and immature stages. Their distribution is also incompletely known and some specimen records, for example those of *A. gonogramma* in Vermont and of *A. centrifugens* in Florida, need further validation. Finally, many more taxonomic situations such as those dealt with in this paper occur in other insect groups that could be resolved using the innovative DNA hybridisation capture protocol presented here.

Acknowledgements

James Hogan (OUMNH) and Thomas Pape (ZMUC) provided two of the type specimens or parts thereof for sequencing and also provided images of these type specimens. John Rawlins (deceased) and James W. Fetzner Jr. (CMNH) provided on loan several hundred specimens of *Argyria* for identification. Ben Proshok (SEL, USDA) provided images of the NMNH type specimens and Floyd Shockley (Collection Manager, Entomology, NMNH) approved the loan of *A. multifacta* to B. Landry during the 2020–2022 covid pandemic that was critical to this study. Carlos Lopez-Vaamonde (INRAE Orléans & IRBI Tours, France) provided sequenced specimens on loan. Paul Hebert and colleagues (Centre for Biodiversity Genomics at the University of Guelph, Ontario, Canada) provided access to BOLD data. John W. Brown (Smithsonian Research Associate, NMNH) sent a gift of two specimens of *Argyria diplomochalis* from St Croix Island to BL along with several other specimens of *Argyria* from the USA. Ole Karsholt (ZMUC) and Thomas Pape provided information on Fabricius and his work and collection. Steve Nanz provided information on North American species of *Argyria*, and his inquiry about *A. "centrifugens"* in Florida motivated in part the present study. Christina Lehmann-Graber (MHNG) inked and improved the drawing originally made by BL of the holotype of *A. centrifugens*; she

also improved the images taken by BL at the MHNG. In the MFNB Robert Schreiber performed the lab work. Sabine Gaal, Lepidoptera Curator (Naturhistorisches Museum Wien, Vienna, Austria), searched for a potential type specimen of *Argyria pusillalis* Hübner. Charles V. Covell, Jr. sorted *Argyria* specimens in the FSCA and MGCL; collecting work in the Bahamas was supported in part by National Geographic Scientific Research Grant # 9439-14, with Principal Investigator Jacqueline Y. Miller. Jean-François Landry (curator of microlepidoptera) and Lisa Bartels opened the Canadian National Collection of Insects, Arachnids, and Nematodes (Ottawa, Ontario) to BL and sent photographs of *Argyria* moths. Steven C. Passoa (USDA/APHIS/PPQ, U.S. Forest Service Northern Research Station and The Ohio State University, Columbus, Ohio, U.S.A.) provided crucial information. Last but not least, Joaquín Baixeras Almela (Institut Cavanilles de Biodiversitat i Biologia Evolutiva, Universitat de València, Paterna, Spain) performed the difficult task of everting the vesica of a specimen of *A. lacteella* and sent its photo to BL. We thank them all deeply for their interest and kind support.

References

- Alayo DP, Valdés AE (1982) Lista Anotada de los Microlepidópteros de Cuba. Academia de ciencias de Cuba, La Habana, 122 pp.
- Amsel HG (1956) Microlepidoptera Venezolana I. Boletín de Entomología Venezolana. Maracay 10(1–2): 1–336.
- Baixeras J, Karsholt O (2011) The Tortricidae described by J. C. Fabricius (Lepidoptera). Zootaxa 3127(1): 1–37. <https://doi.org/10.11646/zootaxa.3127.1.1>
- Bi K, Vanderpool D, Singhal S, Linderoth T, Moritz C, Good JM (2012) Transcriptome-based exon capture enables highly cost-effective comparative genomic data collection at moderate evolutionary scales. BMC Genomics 13(1): e403. <https://doi.org/10.1186/1471-2164-13-403>
- Blaimer BB, Lloyd MW, Guillory WX, Brady SG (2016) Sequence capture and phylogenetic utility of genomic ultraconserved elements obtained from pinned insect specimens. PLoS ONE 11(8): e0161531. <https://doi.org/10.1371/journal.pone.0161531>
- Błeszyński S (1967) Studies on the Crambinae (Lepidoptera). Part 44. New Neotropical genera and species. Preliminary check-list of Neotropical Crambinae. Acta zoologica cracoviensia 12(5): 39–110. [pls. 11–14]
- Błeszyński S, Collins RJ (1962) A short catalogue of the world species of the family Crambidae (Lepidoptera). Acta zoologica cracoviensia 7(12): 197–389.
- Brower AVZ (1994) Rapid morphological radiation and convergence among races of the butterfly *Heliconius erato* inferred from patterns of mitochondrial DNA evolution. Proceedings of the National Academy of Sciences of the United States of America 91(14): 6491–6495. <https://doi.org/10.1073/pnas.91.14.6491>
- Butler AG (1878) On a small collection of Lepidoptera from Jamaica. Proceedings of the General Meetings for Scientific Business of the Zoological Society of London 1878(3): 480–495. <https://doi.org/10.1111/j.1469-7998.1878.tb07985.x>

- Camacho C, Coulouris G, Avagyan V, Ma N, Papadopoulos J, Bealer K, Madden TL (2009) BLAST+: Architecture and applications. *BMC Bioinformatics* 10(1): e421. <https://doi.org/10.1186/1471-2105-10-421>
- Card DC, Shapiro B, Giribet G, Moritz C, Edwards SV (2021) Museum Genomics. *Annual Review of Genetics* 55(1): 633–659. <https://doi.org/10.1146/annurev-genet-071719-020506>
- De la Torre y Callejas SL (1967) Pirálidos (Lepidoptera, Pyralidae) de Cuba en la Colección del Museo Nacional de los Estados Unidos. *Poeyana Ser. A, N° 33*, 27 pp.
- Dyar HG (1903) A list of North American Lepidoptera. *Bulletin of the United States National Museum, Washington* 52: 1–723. <https://doi.org/10.5479/si.03629236.52.i>
- Dyar HG (1913) Note on the American silvery species of *Argyria* (Lepidoptera, Pyralidae). *Insector Inscitiae Menstruus, Washington* 1: 111–114.
- Dyar HG (1914) Report on the Lepidoptera of the Smithsonian Biological Survey of the Panama Canal Zone. *Proceedings of the United States National Museum, Washington* 47(2050): 139–350. <https://doi.org/10.5479/si.00963801.47-2050.139>
- Dyar HG (1915) Pyralidae of Bermuda. *Insector Inscitiae Menstruus, Washington* 3(5–7): 86–89.
- Espeland M, Breinholt J, Willmott KR, Warren AD, Vila R, Toussaint EFA, Maunsell SC, Aduse-Poku K, Talavera G, Eastwood R, Jarzyna MA, Guralnick R, Lohman DJ, Pierce NE, Kawahara AY (2018) A comprehensive and dated phylogenomic analysis of butterflies. *Current Biology* 28(5): 770–778. <https://doi.org/10.1016/j.cub.2018.01.061>
- Fabricius JC (1794) *Entomologica Systematica Emendata et Aucta. Secundum Classes, Ordines, Genera, Species Adiectis Synonymis, Locis, Observationibus, Descriptionibus*. C. G. Proft et C. F. Mohr, Hafniae et Kiliae, 349 pp.
- Fabricius JC (1798) *Supplementum Entomologiae Systematicae*. Proft et Storch, Hafniae, [i]–[iv], 572 pp. [1–52, emendanda.]
- Faircloth BC, McCormack JE, Crawford NG, Harvey MG, Brumfield RT, Glenn TC (2012) Ultraconserved elements anchor thousands of genetic markers spanning multiple evolutionary timescales. *Systematic Biology* 61(5): 717–726. <https://doi.org/10.1093/sysbio/sys004>
- Ferguson DC, Hilburn DJ, Wright B (1991) The Lepidoptera of Bermuda: Their food plants, biogeography, and means of dispersal. *Memoirs of the Entomological Society of Canada, Ottawa* 123(158): 1–105. <https://doi.org/10.4039/entm123158fv>
- Fernald CH (1896) *The Crambidae of North America*. Massachusetts Agricultural College, 93 pp. [pls a–c, pls I–V] <https://doi.org/10.5962/t.173040>
- Gauthier J, Pajkovic M, Neuenschwander S, Kaila L, Schmid S, Orlando L, Alvarez N (2020) Museomics identifies genetic erosion in two butterfly species across the 20th century in Finland. *Molecular Ecology Resources* 20(5): 1191–1205. <https://doi.org/10.1111/1755-0998.13167>
- Gibson LD, Covell Jr CV, Laudermilk EL (2021) Additions, deletions and corrections to the Kentucky list of Lepidoptera. *News of the Lepidopterists' Society* 63(1): 24–32.
- Grossbeck JA (1917) *Insects of Florida IV: Lepidoptera*. *Bulletin of the American Museum of Natural History* 37: 1–147.
- Guindon S, Dufayard J-F, Lefort V, Anisimova M, Hordijk W, Gascuel O (2010) New algorithms and methods to estimate maximum-likelihood phylogenies: Assessing the per-

- formance of PhyML 3.0. *Systematic Biology* 59(3): 307–321. <https://doi.org/10.1093/sysbio/syq010>
- Hebert PDN, Penton EH, Burns JM, Janzen DH, Hallwachs W (2004) Ten species in one: DNA barcoding reveals cryptic species in the neotropical skipper butterfly *Astraptes fulgerator*. *Proceedings of the National Academy of Sciences of the United States of America* 101(41): 14812–14817. <https://doi.org/10.1073/pnas.0406166101>
- Heppner JB (2003) *Lepidoptera of Florida. Part 1. Introduction and catalog. Arthropods of Florida and neighbouring land areas* 17: 1–670.
- Hernández-Triana LM, Prosser SW, Rodríguez-Perez MA, Chaverri LG, Hebert PDN, Gregory TR (2014) Recovery of DNA barcodes from blackfly museum specimens (Diptera: Simuliidae) using primer sets that target a variety of sequence lengths. *Molecular Ecology Resources* 14(3): 508–518. <https://doi.org/10.1111/1755-0998.12208>
- Hoang DT, Chernomor O, Von Haeseler A, Minh BQ, Vinh LS (2018) UFBoot2: Improving the ultrafast bootstrap approximation. *Molecular Biology and Evolution* 35(2): 518–522. <https://doi.org/10.1093/molbev/msx281>
- Horn W, Kahle I, Friese G, Gaedike R (1990) *Collectiones Entomologicae. Ein Komendium über den Verbleib Entomologischer Sammlungen der Welt bis 1960. Teil I: A bis K. Teil II: L bis Z. Akademie der Landwirtschaftswissenschaften der DDR, Berlin*, 573 pp.
- Hübner J (1808–1818 [imprint “1818”]) *Zuträge zur Sammlung exotischer Schmettlinge [sic], bestehend in Bekundigung einzelner Fliegmuster neuer oder rarer nichteuropäischer Gattungen. Augsburg. [1]–[3]–4–6–[7]–8–32–[33]–[40], pls [1]–[35]*.
- Jaume ML (1967) *Catalogo de la fauna de Cuba XXIII. Catalogo de la familia Crambidae (Lepidoptera) en las Antillas. Museo Felipe Poey de la Academia de Ciencias de Cuba Trabajos de Divulgación* (51): 1–21.
- Kalyaanamoorthy S, Minh BQ, Wong TK, von Haeseler A, Jermin LS (2017) ModelFinder: Fast model selection for accurate phylogenetic estimates. *Nature Methods* 14(6): 587–589. <https://doi.org/10.1038/nmeth.4285>
- Kapli P, Lutteropp S, Zhang J, Kobert K, Pavlidis P, Stamatakis A, Flouri T (2017) Multi-rate Poisson tree processes for single-locus species delimitation under maximum likelihood and Markov chain Monte Carlo. *Bioinformatics* 33(11): 1630–1638. <https://doi.org/10.1093/bioinformatics/btx025>
- Katoh K, Misawa K, Kuma K-I, Miyata T (2002) MAFFT: A novel method for rapid multiple sequence alignment based on fast Fourier transform. *Nucleic Acids Research* 30(14): 3059–3066. <https://doi.org/10.1093/nar/gkf436>
- Kearse M, Moir R, Wilson A, Stones-Havas S, Cheung M, Sturrock S, Buxton S, Cooper A, Markowitz S, Duran C, Thierer T, Ashton B, Meintjes P, Drummond A (2012) Geneious Basic: An integrated and extendable desktop software platform for the organization and analysis of sequence data. *Bioinformatics* 28(12): 1647–1649. <https://doi.org/10.1093/bioinformatics/bts199>
- Kimball CP (1965) *The Lepidoptera of Florida: an annotated checklist. Arthropods of Florida and neighbouring land areas* 1: 1–363. [26 pls]
- Landry B, Andriollo T (2020) A review of the genus *Microcrambus* Bleszyński, 1963 (Lepidoptera, Pyraloidea, Crambinae) in Colombia, with descriptions of two new species. *Revista Udca*

- Actualidad & Divulgacion Cientifica 23(2): e1628. <https://doi.org/10.31910/rudca.v23.n2.2020.1628>
- Landry B, Becker VO (2021) A taxonomic review of the genus *Diptychophora* Zeller (Lepidoptera, Pyralidae *sensu lato*, Crambinae) in Brazil, with descriptions of three new species. *Revue Suisse de Zoologie* 128(1): 73–84. <https://doi.org/10.35929/RSZ.0036>
- Landry B, Basset Y, Hebert PDN, Maes J-M (2020) On the Pyraloidea fauna of Nicaragua. *Tropical Lepidoptera Research* 30(2): 93–102. <https://doi.org/10.5281/zenodo.4317575>
- Martin M (2011) Cutadapt removes adapter sequences from high throughput sequencing reads. *EMBnet.Journal* 17(1): 10–12. <https://doi.org/10.14806/ej.17.1.200>
- Martinez EL, Brown RL (2007) *Argyriini* (Lepidoptera: Crambidae) of Mississippi and Alabama with a redescription of *Argyria rufisignella* (Zeller). *Journal of the Lepidopterists Society* 61(2): 78–83.
- Mey W, Léger T, Van Lien V (2021) New taxa of extant and fossil primitive moths in South-East Asia and their biogeographic significance (Lepidoptera, Micropterigidae, Agathiphaagidae, Lophocoronidae). *Nota Lepidopterologica* 44: 29–56. <https://doi.org/10.3897/nl.44.52350>
- Miller JY, Matthews DL, Warren AD, Solis MA, Harvey DJ, Gentili-Poole P, Lehman R, Emmel TC, Covell Jr CV (2012) An annotated list of the Lepidoptera of Honduras. *Insecta Mundi*, Gainesville, Florida 205: 1–72.
- Minh BQ, Schmidt HA, Chernomor O, Schrempf D, Woodhams MD, von Haeseler A, Lanfear R (2020) IQ-TREE 2: New models and efficient methods for phylogenetic inference in the genomic era. *Molecular Biology and Evolution* 37(5): 1530–1534. <https://doi.org/10.1093/molbev/msaa015>
- Moth Photographers Group (2022) Moth Photographers Group. <http://mothphotographers-group.msstate.edu> [accessed 25 August 2022]
- Müller J, Müller K, Neinhuis C, Quandt D (2005) PhyDE-Phylogenetic Data Editor.
- Munroe EG (1956) Pyralides récoltés à l'île de la Guadeloupe par M. L. Berland, [Lepid.]. *Revue française d'entomologie*, Paris 23: 121–127.
- Munroe EG (1995) Crambidae (Crambinae, Schoenobiinae, Cybalomiinae, Linostinae, Glaphyriinae, Dichogaminae, Scopariinae, Musotiminae, Midilinae, Nymphulinae, Odontiinae, Evergestinae, Pyraustinae). In: Heppner JB (Ed.) *Atlas of Neotropical Lepidoptera. Checklist: Part 2. Hyblaeoidea - Pyraloidea - Tortricoidea* 3. Association for Tropical Lepidoptera & Scientific Publishers, Gainesville, 34–79.
- Patzold F, Zilli A, Hundsdoerfer AK (2020) Advantages of an easy-to-use DNA extraction method for minimal-destructive analysis of collection specimens. *PLoS ONE* 15(7): e0235222. <https://doi.org/10.1371/journal.pone.0235222>
- Pons J, Barraclough T, Gomez-Zurita J, Cardoso A, Duran D, Hazell S, Kamoun S, Sumlin W, Vogler A (2006) Sequence-based species delimitation for the DNA taxonomy of undescribed insects. *Systematic Biology* 55(4): 595–610. <https://doi.org/10.1080/10635150600852011>
- Puillandre N, Lambert A, Brouillet S, Achaz G (2012) ABGD, Automatic Barcode Gap Discovery for primary species delimitation. *Molecular Ecology* 21(8): 1864–1877. <https://doi.org/10.1111/j.1365-294X.2011.05239.x>

- Ratnasingham S, Hebert PDN (2007) BOLD: The Barcode of Life Data System (www.barcodinglife.org). *Molecular Ecology Notes* 7(3): 355–364. <https://doi.org/10.1111/j.1471-8286.2007.01678.x>
- Raxworthy CJ, Smith BT (2021) Mining museums for historical DNA: Advances and challenges in museomics. *Trends in Ecology & Evolution* 36(11): 1049–1060. <https://doi.org/10.1016/j.tree.2021.07.009>
- Robinson GS (1976) The preparation of slides of Lepidoptera genitalia with special reference to the Microlepidoptera. *Entomologist's Gazette* 27: 127–132.
- Roque-Albelo L, Landry B (2010) List of known butterflies and moths species from the Galapagos Islands - Lista de especies de mariposas y polillas conocidos de las Islas Galápagos. In: Bungartz F, Herrera H, Jaramillo P, Tirado N, Jiménez-Uzategui G, Ruiz D, Guézou A, Ziemmeck F (Eds) List of all known species from the Galapagos Islands - Lista de todas las especies conocidas de las Islas Galápagos. Online repository of the Charles Darwin Foundation / Fundación Charles Darwin, Puerto Ayora, Galapago. <http://www.darwinfoundation.org/datazone/checklists/terrestrial-invertebrates/lepidoptera/> [accessed on 3 August 2022]
- Schaus W (1940) Insects of Porto Rico and the Virgin Islands. Moths of the families Geometridae and Pyralidae [sic]. *New York Academy of Sciences, Scientific Survey of Porto Rico and the Virgin Islands* 12(3): 289–417.
- Scholtens BG, Solis MA (2015) Annotated checklist of the Pyraloidea (Lepidoptera) of America North of Mexico. *ZooKeys* 535: 1–136. <https://doi.org/10.3897/zookeys.535.6086>
- Suchan T, Pitteloud C, Gerasimova NS, Kostikova A, Schmid S, Arrigo N, Pajkovic M, Ronikier M, Alvarez N (2016) Hybridization capture using RAD probes (hyRAD), a new tool for performing genomic analyses on collection specimens. *PLoS ONE* 11(3): e0151651. <https://doi.org/10.1371/journal.pone.0151651>
- Suchard MA, Lemey P, Baele G, Ayres DL, Drummond AJ, Rambaut A (2018) Bayesian phylogenetic and phylodynamic data integration using BEAST 1.10. *Virus Evolution* 4(1): vey016. <https://doi.org/10.1093/ve/vey016>
- Tamura K, Stecher G, Kumar S (2021) MEGA11: Molecular Evolutionary Genetics Analysis version 11. *Molecular Biology and Evolution* 38(7): 3022–3027. <https://doi.org/10.1093/molbev/msab120>
- Tan C-L (1984) Biology and taxonomy of sod webworms (Lepidoptera: Pyralidae) destructive to turfgrasses in Florida. M.Sc. Thesis, University of Florida.
- Toussaint EF, Gauthier J, Bilat J, Gillett CP, Gough HM, Lundkvist H, Blanc M, Muñoz-Ramírez CP, Alvarez N (2021) HyRAD-X exome capture museomics unravels giant ground beetle evolution. *Genome Biology and Evolution* 13(7): evab112. <https://doi.org/10.1093/gbe/evab112>
- Walker F (1859) Part XIX. Pyralides. List of the Specimens of Lepidopterous Insects in the Collection of the British Museum, London 19: 799–1036.
- Zeller PC (1863) Chilonidarum et Crambidarum genera et species. Wiegandt & Hempel, Meseritz & Berlin, 1–56. <https://doi.org/10.5962/bhl.title.66009>
- Zhang J, Kapli P, Pavlidis P, Stamatakis A (2013) A general species delimitation method with applications to phylogenetic placements. *Bioinformatics* 29(22): 2869–2876. <https://doi.org/10.1093/bioinformatics/btt499>

- Zhang J, Lees DC, Shen J, Cong Q, Huertas B, Martin G, Grishin NV (2020) The mitogenome of a Malagasy butterfly *Malaza fastuosus* (Mabille, 1884) recovered from the holotype collected over 140 years ago adds support for a new subfamily of HesperIIDae (Lepidoptera). *Genome* 63(4): 195–202. <https://doi.org/10.1139/gen-2019-0189>
- Zimsen E (1964) *The Type Material of I. C. Fabricius*. Munksgaard, Copenhagen, 606 pp.

Supplementary material 1

Identity of *Argyria lacteella* (Fabricius) revised

Authors: Bernard Landry, Julia Bilat, James Hayden, M. Alma Solis, David C. Lees, Nadir Alvarez, Théo Léger, Jérémy Gauthier

Data type: word document

Copyright notice: This dataset is made available under the Open Database License (<http://opendatacommons.org/licenses/odbl/1.0/>). The Open Database License (ODbL) is a license agreement intended to allow users to freely share, modify, and use this Dataset while maintaining this same freedom for others, provided that the original source and author(s) are credited.

Link: <https://doi.org/10.3897/zookeys.1146.96099.suppl1>

Supplementary material 2

Species names, code numbers and collecting data

Authors: Bernard Landry, James Hayden, M. Alma Solis, David C. Lees, Théo Léger, Jérémy Gauthier

Data type: specimens names and collecting data

Explanation note: This table contains the species names, code numbers, and collecting data of all of the specimens examined in this study and that were used to generate the distribution maps.

Copyright notice: This dataset is made available under the Open Database License (<http://opendatacommons.org/licenses/odbl/1.0/>). The Open Database License (ODbL) is a license agreement intended to allow users to freely share, modify, and use this Dataset while maintaining this same freedom for others, provided that the original source and author(s) are credited.

Link: <https://doi.org/10.3897/zookeys.1146.96099.suppl2>

A survey of the spider genus *Dysdera* Latreille, 1804 (Araneae, Dysderidae) in Iran, with fourteen new species and notes on two fossil genera

Alireza Zamani¹, Yuri M. Marusik², Tamás Szűts³

1 Zoological Museum, Biodiversity Unit, FI-20014 University of Turku, Turku, Finland **2** Department of Zoology & Entomology, University of the Free State, Bloemfontein 9300, South Africa **3** Department of Ecology, University of Veterinary Medicine Budapest, Rottenbiller u. 50, Budapest, 1077, Hungary

Corresponding author: Alireza Zamani (zamani.alireza5@gmail.com)

Academic editor: G. Blagoev | Received 13 November 2022 | Accepted 19 December 2022 | Published 7 February 2023

<https://zoobank.org/01E76F6A-B991-4F33-9BD6-991090F07E80>

Citation: Zamani A, Marusik YM, Szűts T (2023) A survey of the spider genus *Dysdera* Latreille, 1804 (Araneae, Dysderidae) in Iran, with fourteen new species and notes on two fossil genera. ZooKeys 1146: 43–86. <https://doi.org/10.3897/zookeys.1146.97517>

Abstract

The taxonomy of the Iranian species of the dysderid spider genus *Dysdera* Latreille, 1804 is revised. Currently, the only species of this genus known from Iran is *D. pococki* Dunin, 1985, albeit on the basis of a doubtful record. The following 14 species are described as new to science in this paper: *D. achaemenes* sp. nov. (♀; Fars), *D. bakhtiari* sp. nov. (♂; Chaharmahal & Bakhtiari), *D. damavandica* sp. nov. (♂; Mazandaran), *D. genoensis* sp. nov. (♂♀; Hormozgan), *D. hormuzensis* sp. nov. (♀; Hormozgan), *D. iranica* sp. nov. (♂♀; Fars, Hormozgan), *D. isfahanica* sp. nov. (♂♀; Isfahan), *D. mazeruni* sp. nov. (♀; Mazandaran), *D. medes* sp. nov. (♂; Tehran), *D. persica* sp. nov. (♂♀; Golestan, Mazandaran), *D. sargartia* sp. nov. (♂♀; Tehran), *D. tapuria* sp. nov. (♂♀; Mazandaran), *D. verkana* sp. nov. (♂; Golestan), and *D. xerxesi* sp. nov. (♂; Bushehr). Distribution records of all species are mapped. Also, the taxonomy of *Mistura* Petrunkevitch, 1971 and *Segistriites* Straus, 1967, two fossil genera currently considered in Dysderidae, is discussed and the latter is transferred to Segestriidae.

Keywords

Aranei, Middle East, *Mistura*, red devil spiders, *Segistriites*, woodlouse hunters

Introduction

The spider family Dysderidae C.L. Koch, 1837 comprises 591 extant species in 25 genera distributed in the West Palaearctic (WSC 2022). Most species have limited dispersal abilities and very small ranges; one exception is *Dysdera crocata* C.L. Koch, 1838 which has a cosmopolitan distribution due to anthropogenic transportations (Jocqué and Dippenaar-Schoeman 2006).

Although the first record of this family in Iran dates back to late 19th century (Pocock 1889), the dysderid fauna of this country remains almost completely unknown. Currently, there are only three species of Dysderidae known from Iran: *Dysdera pococki* Dunin, 1985, *Dysderella transcaspica* (Dunin & Fet, 1985), and *Harpactea parthica* Brignoli, 1980 (Zamani et al. 2022a). The Iranian records of several species (i.e., *Dysdera aculeata* Kroneberg, 1875, *D. asiatica* Nosek, 1905, *D. erythrina* (Walckenaer, 1802), *Harpactea babori* (Nosek, 1905), *H. dohati* Alicata, 1974, and *Tedia oxygnatha* Simon, 1882) were recently considered as misidentifications and subsequently these species were rejected from the checklist of Iranian spiders (Zamani et al. 2017, 2022b). Recently, we had the opportunity to examine a collection of Iranian specimens of *Dysdera* Latreille, 1804, in which 14 species new to science were detected. In this paper, all species of this genus occurring in Iran are surveyed, their distributions are mapped, and those new to science are described and illustrated. Additionally, the taxonomy of two fossil genera currently considered in Dysderidae is discussed, and one of them is herein transferred to Segestriidae.

Materials and methods

Photographs of specimens and their copulatory organs were obtained using a Nikon D300S DSLR camera attached to a Nikon S800 stereomicroscope, a Tucsen TrueChrome Metrics microscope camera attached to a Nikon Eclipse E200 compound microscope, and an Olympus Camedia E-520 camera attached to an Olympus SZX16 stereomicroscope or to the eye piece of an Olympus BH2 transmission microscope. Digital images of different focal planes were stacked with Helicon Focus™ 8.1.1. Illustrations of internal genitalia were made after digesting tissues off with Neo PanPur commercial pancreatic enzyme cocktail pill, clearing the structures in wintergreen oil (methyl-salicylate), then mounting them on a temperate slide preparation (Coddington 1983). Body measurements exclude the chelicerae and spinnerets. Leg segments were measured on the dorsal side. Measurements of legs are listed as: total length (femur, patella, tibia, metatarsus, tarsus). All measurements are given in millimetres. Geographic coordinates of collection localities were obtained from the labels or georeferenced using Google Earth. Measurements and characters of the palp used in the diagnoses are based on the retrolateral view, unless otherwise indicated.

Abbreviations: Eyes: **AME** – anterior median eye, **PLE** – posterior lateral eye, **PME** – posterior median eye. Spination: **d** – dorsal, **Fe** – femur, **Mt** – metatarsus, **Pa** – patella, **pl** – prolateral, **rl** – retrolateral, **Ti** – tibia, **v** – ventral.

Depositories: **MHNG** – Muséum d'histoire naturelle, Genève, Switzerland (P.J. Schwendinger, L. Monod); **MMUE** – Manchester Museum of the University of Manchester, United Kingdom (D.V. Logunov); **SMF** – Senckenberg Museum, Frankfurt am Main, Germany (P. Jäger); **ZMUT** – Zoological Museum of the University of Turku, Finland (V. Vahtera).

Taxonomy

Family Dysderidae C.L. Koch, 1837

Comments. The family was divided into four tribes (i.e., Dysderini, Harpactini, Orsolobini and Rhodini) by Cooke (1965), of which three were elevated to subfamilies (i.e., Dysderinae, Harpacteinae and Rhodinae) by Deeleman-Reinhold and Deeleman (1988), and one was elevated to the family-level (i.e., Orsolobidae Cooke, 1965) by Forster and Platnick (1985).

Although Dysderidae appears to be a monophyletic family often considered restricted to the Palaearctic, it is in fact distributed only in the West Palaearctic (from Canary Islands to west Xinjiang) and polyphyletic with its current generic composition. Eleven species of five genera are known from fossils (Dunlop et al. 2020): *Dasumiana* Wunderlich, 2004 (3 spp.), *Dysdera* (1 sp.), *Harpactea* Bristowe, 1939 (5 spp.), *Segistriites* Straus, 1967 (1 sp.), and *Mistura* Petrunkevitch, 1971 (1 sp.). Judging by the position of the legs (i.e., legs I–III directed forwards) and the overall somatic features of *Segistriites cromei* Straus, 1967, this monotypic Neogene fossil genus is herein transferred to Segestriidae Simon, 1893. At the time of the description of *Segistriites*, Segestriidae was not a separate family but rather a subfamily (i.e., Segestriinae Simon, 1893) of Dysderidae. Furthermore, Strauss (1967) explicitly mentions the close affinity of this genus to *Segestria* Latreille, 1804, the type genus of Segestriidae. The monotypic Neogene fossil genus *Mistura* also appears to be misplaced in Dysderidae: the holotype specimen of *Mistura perplexa* Petrunkevitch, 1971 has an unknown arrangement of eyes and several characters different from Dysderidae, including a lack of claw tufts, the presence of an onychium, and long spinnerets (Petrunkevitch 1971).

Composition. More than 600 species in 26 genera (Dunlop et al. 2020; WSC 2022; current paper).

Subfamily Dysderinae C.L. Koch, 1837

Diagnosis. This subfamily can be diagnosed from other dysderids by the edge of sternum-labium joint ca. 2.5–3× longer than the edge of the maxilla-sternum joint,

all tarsi bearing claw tufts, posterior metatarsi bearing scopulae, and the spineless anterior tibiae and metatarsi. Furthermore, the bulb of dysderines does not bear a free embolus (with the exception of *Harpactocrates* Simon, 1914), and the posterior diverticulum of endogyne is large and wide (Deeleman-Reinhold and Deeleman 1988; Le Peru 2011; Kunt et al. 2019).

Composition. Around 360 species in 11 genera: *Cryptoparachtes* Dunin, 1992, *Dysdera* Latreille, 1804, *Dysderella* Dunin, 1992, *Dysderocrates* Deeleman-Reinhold & Deeleman, 1988, *Harpactocrates*, *Hygrocrates* Deeleman-Reinhold, 1988, *Kut* Kunt, Elverici, Yağmur & Özkütük, 2019, *Parachtes* Alicata, 1964, *Rhoderia* Deeleman-Reinhold, 1989, *Stalitochara* Simon, 1913, and *Tedia* Simon, 1882. The position of *Rhoderia* in Dysderinae is questionable (see Le Peru 2011).

Genus *Dysdera* Latreille, 1804

Type species. *Aranea erythrina* Walckenaer, 1802, from France.

Diagnosis. *Dysdera* can be diagnosed from other dysderine genera by the interdistance of PLE and PME less than half of their diameter, three or four cheliceral teeth in one series, punctiform (= highly reduced) fovea, and femur I at least twice as long as coxa I. The bulb is cylindrical, bearing a broad posterior apophysis and a distal psemبولus. The endogyne is composed by an anterior diverticulum bearing a dorsal arch and a ventral arch, a transverse receptacle and a posterior diverticulum bearing a transverse bar (Deeleman-Reinhold and Deeleman 1988; Le Peru 2011).

Comments. Deeleman-Reinhold and Deeleman (1988) proposed nine species groups within *Dysdera*: *aculeata*, *asiatica*, *crocata*, *erythrina*, *festai*, *lata*, *longirostris*, *ninnii*, and *punctata*. Charitonov (1956) and Fomichev and Marusik (2021) proposed an additional *cylindrica* group composed of Central Asian species considered within *asiatica* group by Deeleman-Reinhold and Deeleman (1988), mostly based on their disjunct distribution. Here, we tentatively treat these species within *aculeata* group, primarily on the basis of the conformation of male palp and considering that the discovery of similar species in Iran fills this distributional gap. Furthermore, characters based on spination used by Deeleman-Reinhold and Deeleman (1988) in definition of the species groups are not followed here as they appear to be variable; assignment of the species treated here to their respective groups is primarily based on the conformation of male palp.

Composition. More than 310 species (WSC 2022).

aculeata species group

Diagnosis. This group can be diagnosed by a combination of the following characters: the carapace elongated and hexagonal, and the psemبولus longer than the tegulum, with an anterior (= median) crest and an acuminate apex (Deeleman-Reinhold and Deeleman 1988).

Comments. Currently, there is no clear distinction between the *aculeata* and *asiatica* groups, both of which are in serious need of a thorough revision (see Dimitrov 2021).

***Dysdera achaemenes* sp. nov.**

<https://zoobank.org/83006184-7584-4AB0-9862-8C050A4A719C>

Figs 1A–C, 2A, B

Type material. *Holotype* ♀ (ZMUT), IRAN: Fars Province: Khanj, Khan Cave, 27°44'N, 53°20'E.

Etymology. The specific epithet is a noun in apposition, referring to the apical ancestor of the Achaemenid dynasty of rulers of Persia.

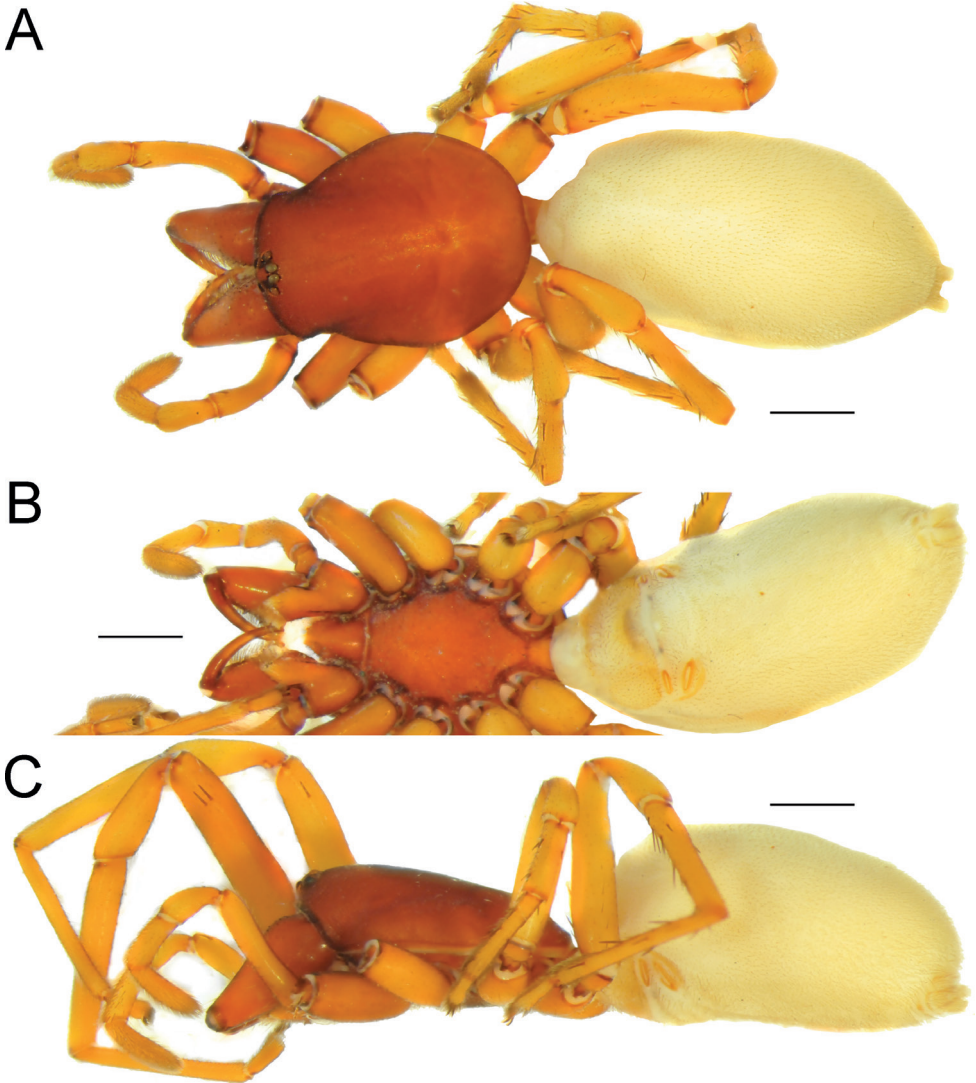


Figure 1. Female of *Dysdera achaemenes* sp. nov., habitus. **A** dorsal view **B** ventral view **C** lateral view. Scale bars: 1.0 mm.

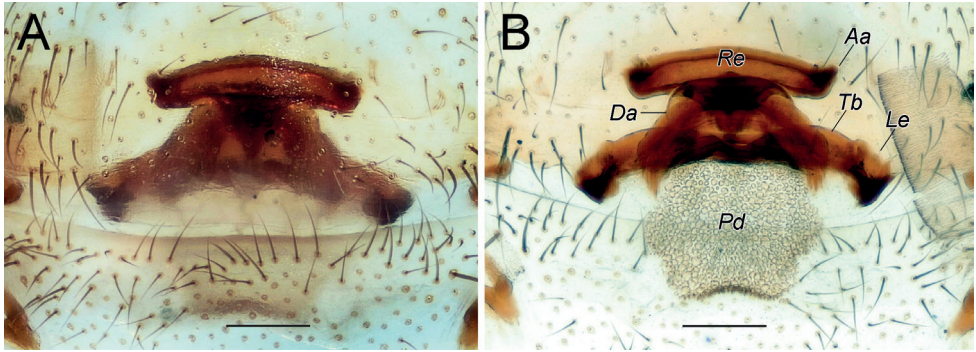


Figure 2. Female of *Dysdera achaemenes* sp. nov., endogyne. **A** ventral view **B** dorsal view. Scale bars: 0.25 mm. Abbreviations: *Aa* – anterior angle, *Da* – dorsal arch, *Le* – lateral edge, *Pd* – posterior diverticulum, *Re* – receptacle, *Tb* – transverse bar.

Diagnosis. The new species differs from its congeners occurring in the region by the very long receptacle (*Re*), longer than the posterior margin of the dorsal arch (*Da*) (vs. shorter).

Description. Female. Habitus as in Fig. 1A–C. Total length 8.13. Carapace 3.28 long, 2.58 wide. Eye diameters: AME 0.12, PME 0.12, PLE 0.14. Carapace, sternum, chelicerae, labium, and maxillae reddish. Legs pale orange. Abdomen pale cream-coloured, without any pattern. Spinnerets uniformly pale cream-coloured. Measurements of legs: I: 8.77 (2.64, 1.56, 2.21, 1.78, 0.58), II: 8.49 (2.42, 1.44, 2.02, 2.08, 0.53), III: 6.54 (1.87, 0.99, 1.30, 1.92, 0.46), IV: 8.99 (2.51, 1.32, 2.07, 2.47, 0.62). Spination: I: Fe: 3pl. II: Fe: 1pl. III: Fe: 1pl; Ti: 4pl, 1rl, 6v; Mt: 3pl, 2rl, 6v. IV: Fe: 9d, 1rl; Ti: 4pl, 6v; Mt: 3pl, 2rl, 5v.

Endogyne as in Fig. 2A, B; length/width ratio ca. 2.6; receptacle slightly arched, 5× longer than wide, anterior angles (*Aa*) rounded, not long; dorsal arch (*Da*) trapezoidal; transverse bar (*Tb*) as wide as receptacle, lateral edges (*Le*) directed posterolaterally; posterior diverticulum (*Pd*) hexagonal.

Male. Unknown.

Distribution. Known only from the type locality in Fars Province, southern Iran (Fig. 35).

***Dysdera bakhtiari* sp. nov.**

<https://zoobank.org/8B8C7362-DAA2-4167-ACE9-4BEB6528ACBE>

Figs 3, 4A–D

Type material. Holotype ♂ (MHNG), IRAN: Chaharmahal & Bakhtiari Province: Zard Kuh, 32°23'N, 50°07'E, 2700 m, 20.06.1974 (A. Senglet).

Etymology. The specific epithet is a noun in apposition, referring to an Iranian tribe primarily inhabiting Chaharmahal & Bakhtiari, Khuzestan, Lorestan, Bushehr, and Isfahan provinces.



Figure 3. Male of *Dysdera bakhtiari* sp. nov., habitus, dorsal view. Scale bar: 1.0 mm.

Diagnosis. This species can be distinguished from other species of the *aculeata* group occurring in the region by having a wider psembolus (i.e., 1.5× wider than the tegulum).

Description. Male. Habitus as in Fig. 3. Total length 5.97. Carapace 2.55 long, 1.97 wide. Eye diameters: AME 0.10, PME 0.08, PLE 0.11. Carapace, sternum, chelicerae, labium, and maxillae reddish brown. Legs orange. Abdomen cream-coloured, without any pattern. Spinnerets uniformly cream-coloured. Measurements of legs: I: 7.40 (2.07, 1.26, 1.80, 1.82, 0.45), II: 6.68 (1.83, 1.17, 1.61, 1.61, 0.46), III: 5.02 (1.42, 0.81, 0.98, 1.40, 0.41), IV: 6.51 (1.87, 0.97, 1.43, 1.77, 0.47). Spination: I: Fe: 4pl. II: Fe: 3pl. III: Fe: 3pl, 1rl; Ti: 4pl, 2rl, 5v; Mt: 6pl, 2rl, 2v. IV: Fe: 7d, 1pl; Ti: 5pl, 2rl, 5v; Mt: 5pl, 2rl, 5v.

Palp as in Fig. 4A–D; bulb ca. 2× longer than wide; tegulum bell-shaped, 1.2× longer than wide; psembolus 1.5× longer than tegulum; median crest (*Mc*) rounded, ca. 2.2× shorter than length of psembolus, ca. 4× wider than high; posterior apophysis (*Ap*) very large, rounded; incision between tegulum and psembolus absent; retrolateral crest (*Rc*) gradually rounded.

Female. Unknown.

Distribution. Known only from the type locality in Chaharmahal & Bakhtiari Province, southwestern Iran (Fig. 35).

***Dysdera hormuzensis* sp. nov.**

<https://zoobank.org/0AAED40A-FE9B-4302-A6FB-71C20654D745>

Figs 5A–C, 6A, B

Type material. Holotype ♀ (ZMUT), IRAN: Hormozgan Province: Hormuz Island, 27°02'N, 56°29'E, 01.2014 (A. Zamani).

Etymology. The specific epithet is an adjective referring to Hormuz Island, from where the holotype was collected.

Diagnosis. The new species differs from all *Dysdera* species occurring in the region by the receptacle divided into two chambers (vs. undivided), and the indistinct dorsal arch (vs. distinct).

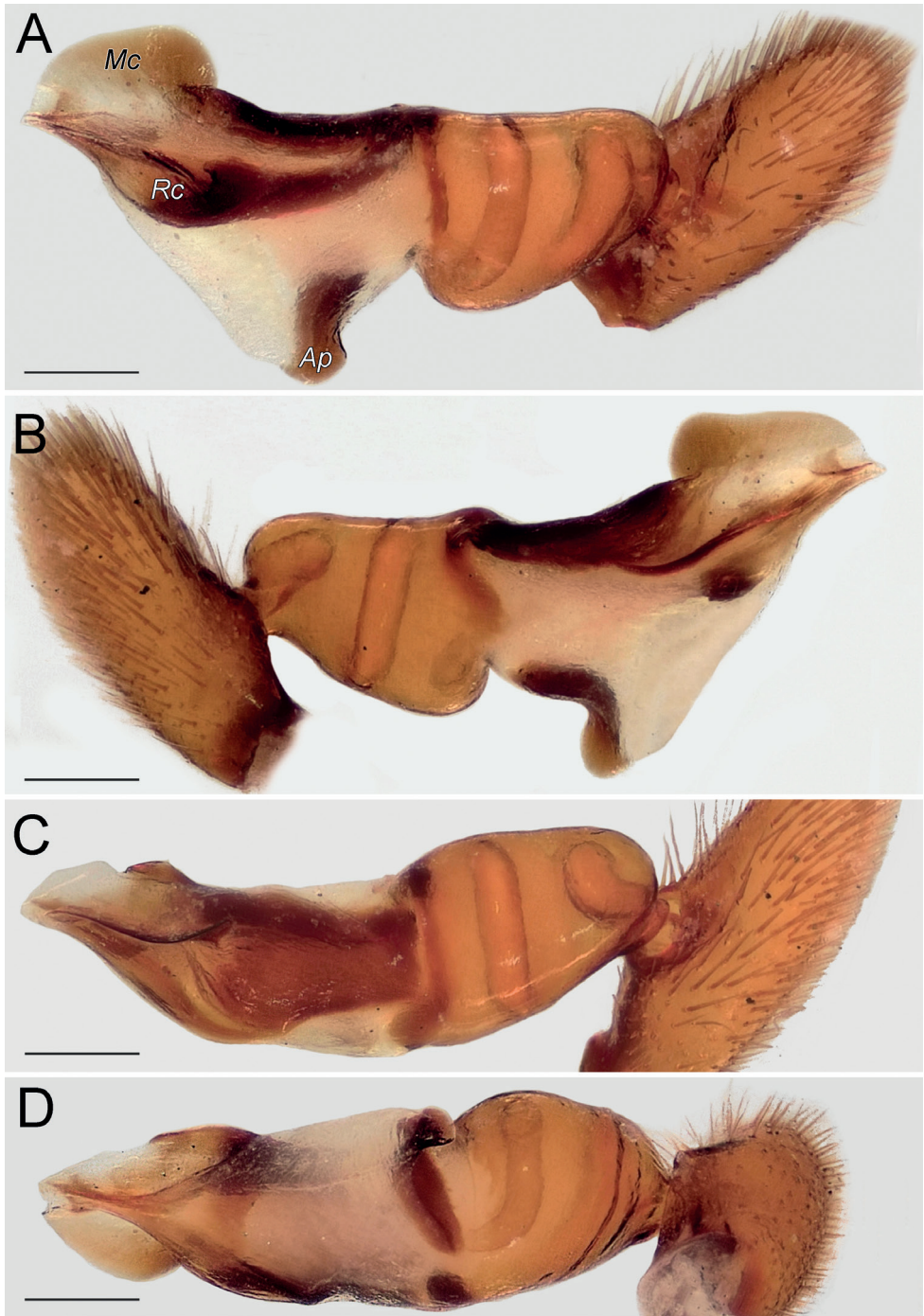


Figure 4. Male of *Dysdera bakhtiari* sp. nov., bulb **A** retrolateral view **B** prolateral view **C** anterior view **D** posterior view. Scale bars: 0.25 mm. Abbreviations: *Ap* – posterior apophysis, *Mc* – median crest, *Rc* – retrolateral crest.

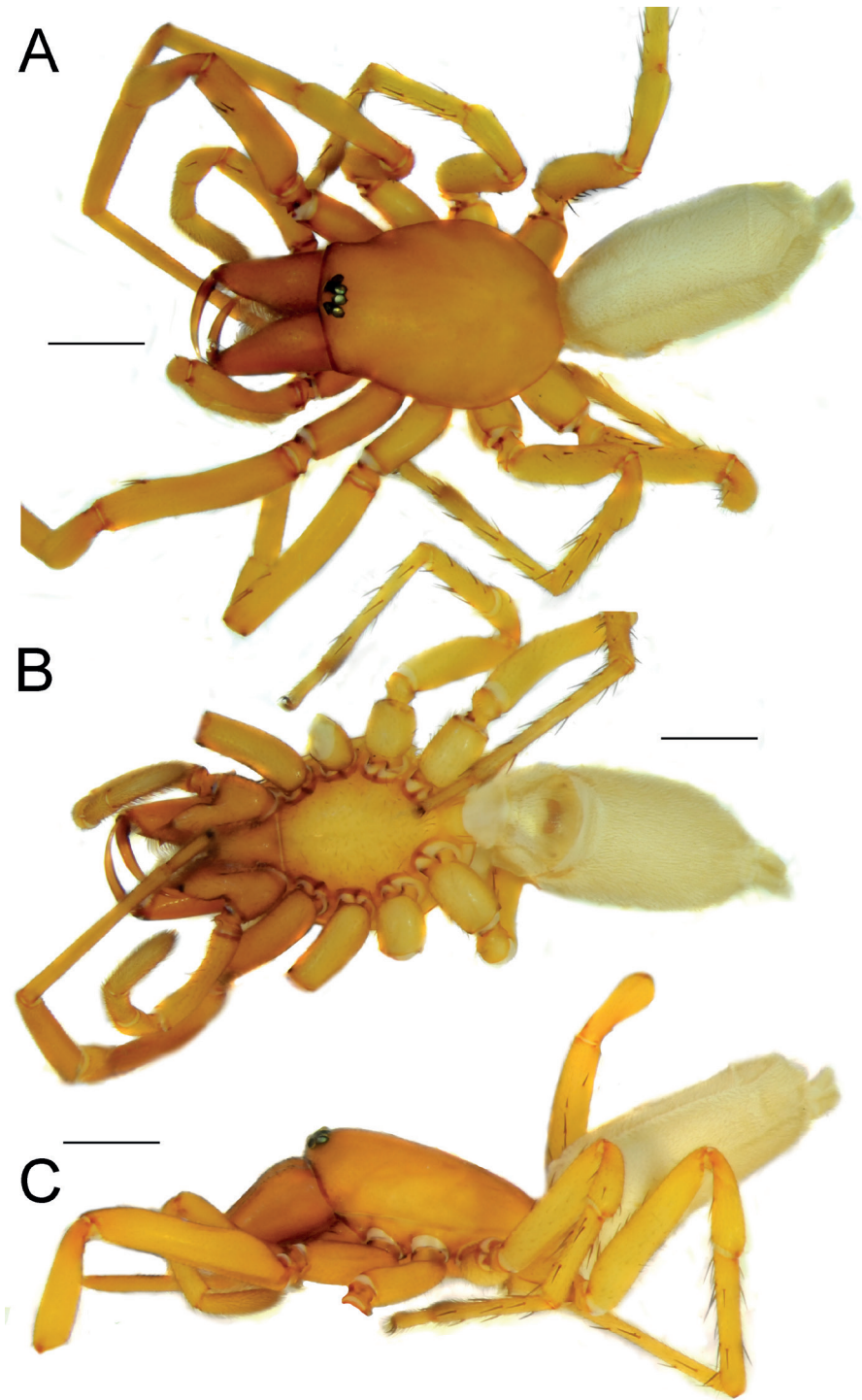


Figure 5. Female of *Dysdera hormuzensis* sp. nov., habitus **A** dorsal view **B** ventral view **C** lateral view. Scale bars: 1.0 mm.

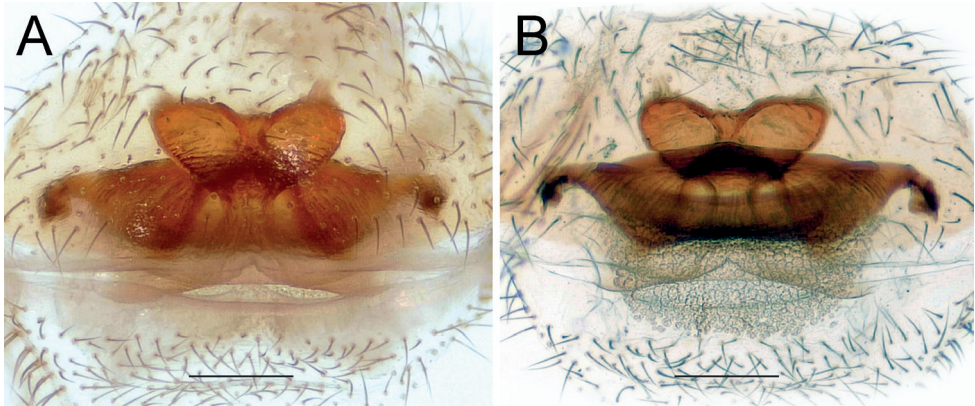


Figure 6. Female of *Dysdera hormuzensis* sp. nov., endogyne **A** ventral view **B** dorsal view. Scale bars: 0.25 mm.

Description. Female. Habitus as in Fig. 5A–C. Total length 8.11. Carapace 3.26 long, 2.56 wide. Eye diameters: AME 0.13, PME 0.13, PLE 0.14. Carapace, sternum, chelicerae, labium, and maxillae orangish. Legs pale orange. Abdomen pale cream-coloured, without any pattern. Spinnerets uniformly pale cream-coloured. Measurements of legs: I: 7.87 (2.19, 1.29, 2.01, 1.85, 0.53), II: 7.31 (1.99, 1.19, 1.77, 1.83, 0.53), III: 5.83 (1.61, 0.88, 1.13, 1.74, 0.47), IV: 7.27 (1.83, 1.05, 1.56, 2.22, 0.61). Spination: I: Fe: 2pl. II: Fe: 3pl. III: Fe: 3d; Pa: 1d, 1pl; Ti: 5pl, 2rl, 6v; Mt: 3d, 6pl, 2rl. IV: Fe: 8d; Pa: 1pl; Ti: 5pl, 3rl, 6v; Mt: 3pl, 4rl, 3v.

Endogyne as in Fig. 6A, B; length/width ratio ca. 2.6; receptacle 2× longer than wide, divided in two chambers, with an anterior median concavity; anterior angles located almost at mid-part of each chamber and directed anteriorly, approximately as long as wide; dorsal arch indistinct; transverse bar ca. 4.6× longer than wide, mid-part similar to an inverted trapezoid, anterior part 1.3× longer than posterior part; lateral edges directed postero-laterally, clearly separated from transverse bar by an incision; posterior diverticulum elongated horizontally.

Male. Unknown.

Comments. The species group (or even generic) assignment of this species is tentative pending the collection of the corresponding male.

Distribution. Known only from the type locality in Hormuz Island, the Persian Gulf (Fig. 35).

***Dysdera iranica* sp. nov.**

<https://zoobank.org/DB4E6E44-A312-424C-9AA5-BBE9E6A06FB5>

Figs 7A–F, 8A–D, 9A, B

Type material. Holotype ♂ (ZMUT), IRAN: Hormozgan Province: Siahu, 27°45'N, 56°20'E, 02.2018 (A. Zamani). **Paratypes:** 1 ♀ (ZMUT), same data as the holotype; 1 ♂

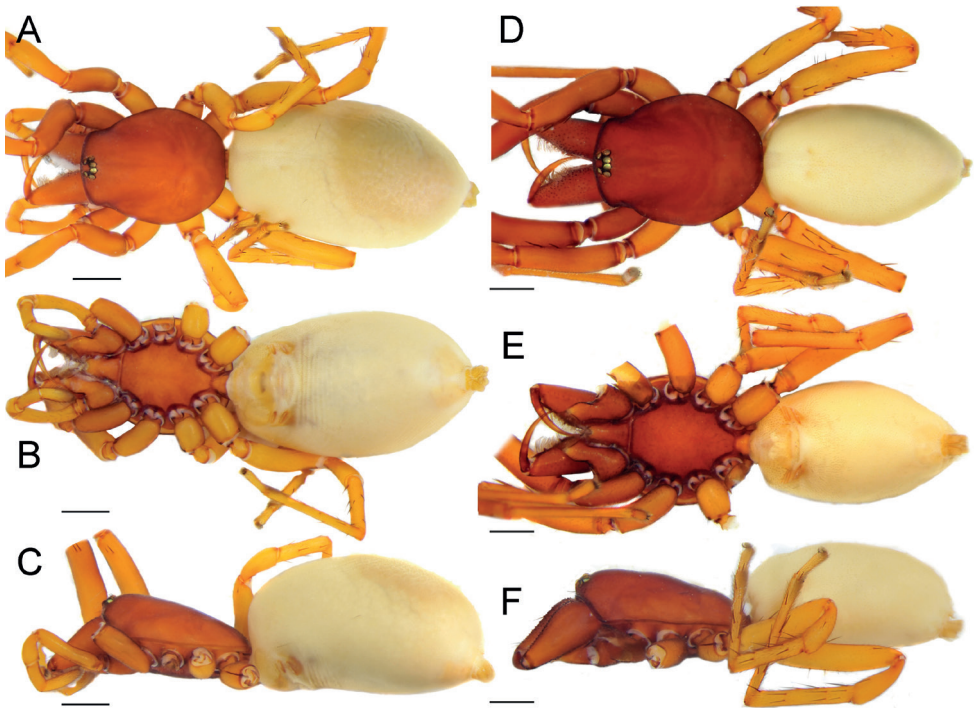


Figure 7. Female (A–C) and male (D–F) of *Dysdera iranica* sp. nov., habitus A, D dorsal view B, E ventral view C, F lateral view. Scale bars: 1.0 mm.

(MMUE), Fars Province: Shiraz, inside house, 29°37'N, 52°30'E, 6.05.1982 (P. Hassanzadeh); 1♂ (MMUE), Shiraz, garden, 29°37'N, 52°30'E, 04.1982 (P. Hassanzadeh); 1♂1♀ (MMUE), Shiraz, inside house, 29°37'N, 52°30'E, 06.1982 (P. Hassanzadeh); 1♀ (ZMUT), Hormozgan Province: Siahu, 27°45'N, 56°20'E, 02.2020 (A. Zamani); 1♀ (ZMUT), Siahu, palm orchards, 27°45'N, 56°20'E, 02.2020 (A. Zamani).

Etymology. The specific epithet is an adjective and refers to the country from where the specimens of the new species were collected.

Diagnosis. The male of the new species is somewhat similar to that of *D. arabica* Deeleman-Reinhold, 1988 from Oman (cf. Fig. 8A–D and Deeleman-Reinhold and Deeleman 1988: figs 309–310), but differs by the small, claw-like posterior apophysis (vs. broad and rounded) and keel-like median crest (vs. rounded). The male of *D. iranica* sp. nov. differs from those of its congeners occurring in Iran by the elongate keel-like median crest (vs. rounded or triangular). The female of *D. iranica* sp. nov. is most similar to that of *D. tapuria* sp. nov. by having a very wide receptacle (i.e., > 2× wider than the transverse bar), but differs by having a triangular extension (T_e) in the anterior margin of the receptacle (vs. absent).

Description. Male (Holotype). Habitus as in Fig. 7D–F. Total length 7.32. Carapace 3.35 long, 2.63 wide. Eye diameters: AME 0.15, PME 0.15, PLE 0.15. Carapace, sternum, chelicerae, labium, and maxillae reddish. Legs yellowish orange. Abdomen

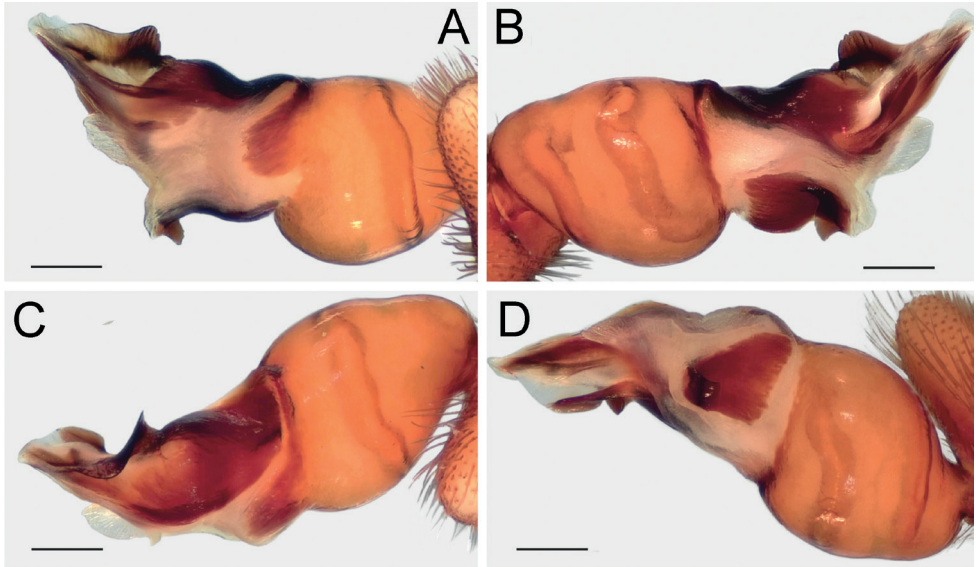


Figure 8. Male of *Dysdera iranica* sp. nov., bulb **A** retrolateral view **B** prolateral view **C** anterior view **D** posterior view. Scale bars: 0.25 mm.

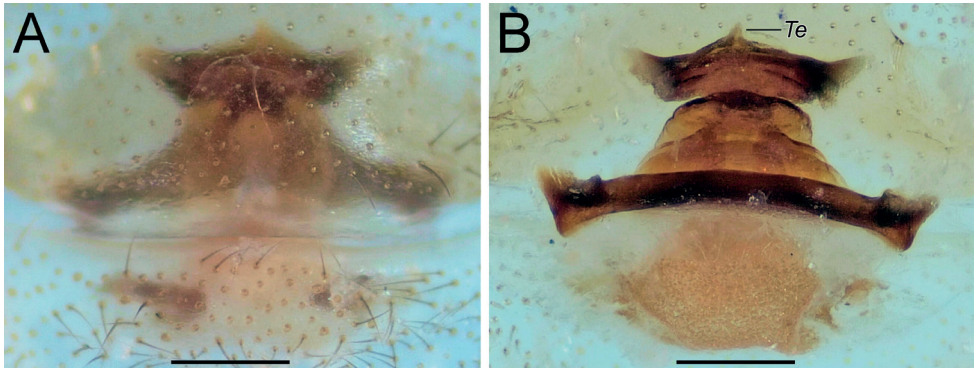


Figure 9. Female of *Dysdera iranica* sp. nov., endogyne **A** ventral view **B** dorsal view. Scale bars: 0.25 mm. Abbreviation: *Te* – triangular extension.

cream-coloured, without any pattern. Spinnerets uniformly dark yellowish. Measurements of legs: I: 11.4 (3.14, 1.92, 2.86, 2.84, 0.63), II: 10.26 (2.72, 1.78, 2.46, 2.68, 0.62), III: 7.61 (2.14, 1.17, 1.54, 2.13, 0.63), IV: 9.75 (2.69, 1.53, 2.12, 2.74, 0.67). Spination: I: Fe: 3pl. II: Fe: 3pl. III: Fe: 3pl, 1rl; Pa: 1pl; Ti: 5pl, 3rl, 5v; Mt: 6pl, 2rl, 2v. IV: Fe: 7d, 2pl, 1rl; Pa: 1pl; Ti: 6pl, 2rl, 6v; Mt: 3pl, 2rl, 5v.

Palp as in Fig. 8A–D; bulb ca. 2.5× longer than wide; tegulum bell-shaped, almost as long as wide; psembolus 1.4× longer than tegulum; median crest rounded, ca. 2.5× shorter than length of psembolus, ca. 2.5× wider than high; posterior apophysis

claw-shaped, 1.5× longer than wide; incision between tegulum and psembolus absent; retrolateral crest gradually rounded.

Female. Habitus as in Fig. 7A–C. Total length 8.20. Carapace 3.03 long, 2.45 wide. Eye diameters: AME 0.14, PME 0.13, PLE 0.14. Colouration as in male. Measurements of legs: I: 8.45 (2.48, 1.44, 1.94, 2.01, 0.58), II: 7.79 (2.17, 1.35, 1.88, 1.91, 0.48), III: 6.25 (1.77, 1.05, 1.16, 1.71, 0.56), IV: 7.88 (2.28, 1.29, 1.72, 2.01, 0.58). Spination: I: Fe: 3pl. II: Fe: 2pl. III: Fe: 2d, 3pl, 3rl; Ti: 4pl, 2rl, 5v; Mt: 5pl, 2rl, 3v. IV: Fe: 7d, 1rl; Ti: 3pl, 2rl, 6v; Mt: 3pl, 2rl, 3v.

Endogyne as in Fig. 9A, B; length/width ratio ca. 2.1; receptacle 4× longer than wide, almost inverted trapezoidal; anterior angle large and triangular, with its base as wide as receptacle, directed antero-laterally; receptacle with median triangular extension (*Te*); dorsal arch trapezoidal, anterior corners rounded, posterior margin 1.6× longer than anterior, anterior margin ca. 1.25× longer than width of dorsal arch; transverse bar slightly arched, 1.5× longer than receptacle; lateral edges with horizontal anterior margins; posterior diverticulum trapezoidal.

Distribution. Known from the listed localities in Fars and Hormozgan provinces, south-central and southern Iran (Fig. 35).

***Dysdera isfahanica* sp. nov.**

<https://zoobank.org/BDD33AFB-357C-4213-8EC6-2D30E261FE4B>
Figs 10A–D, 11A, B, 12A–D, 14A–D

Dysdera erythrina: Roewer 1955: 752 (in part, misidentification).

Type material. *Holotype* ♂ (SMF), IRAN: Isfahan Province: Pir Bakran, 150 km west of Isfahan, 32°28'N, 51°33'E (H. Löffler). *Paratype*: 1♀ (SMF), same data as the holotype.

Etymology. The specific epithet is an adjective, referring to the type locality of the species.

Diagnosis. The male of this species differs from those of the other species of the *aculeata* group occurring in the region by the very long psembolus (i.e., length of psembolus/length of tegulum = 1.85 in the new species, vs. 1.6 or less in most other species), rounded arch-like ridge (*Ar*), presence of the notch of posterior apophysis (vs. absent), and median position of the posterior apophysis on the psembolus (vs. close to tegulum). *Dysdera persica* sp. nov. also bears a long psembolus (i.e., length of psembolus/length of tegulum = 2), but differs from *D. isfahanica* sp. nov. in the shape of the posterior apophysis. The female of this species can be recognized by its long anterolaterally stretched angles of the receptacle.

Description. Male. Habitus as in Figs 10A, C, 11A, B. Total length 10.47. Carapace 4.15 long, 3.45 wide. Eye diameters: AME 0.17, PME 0.14, PLE 0.15. Carapace, sternum, chelicerae, labium, and maxillae orange. Legs yellowish. Abdomen pale beige, without any pattern. Spinnerets uniformly pale beige. Measurements of legs: I: 13.57

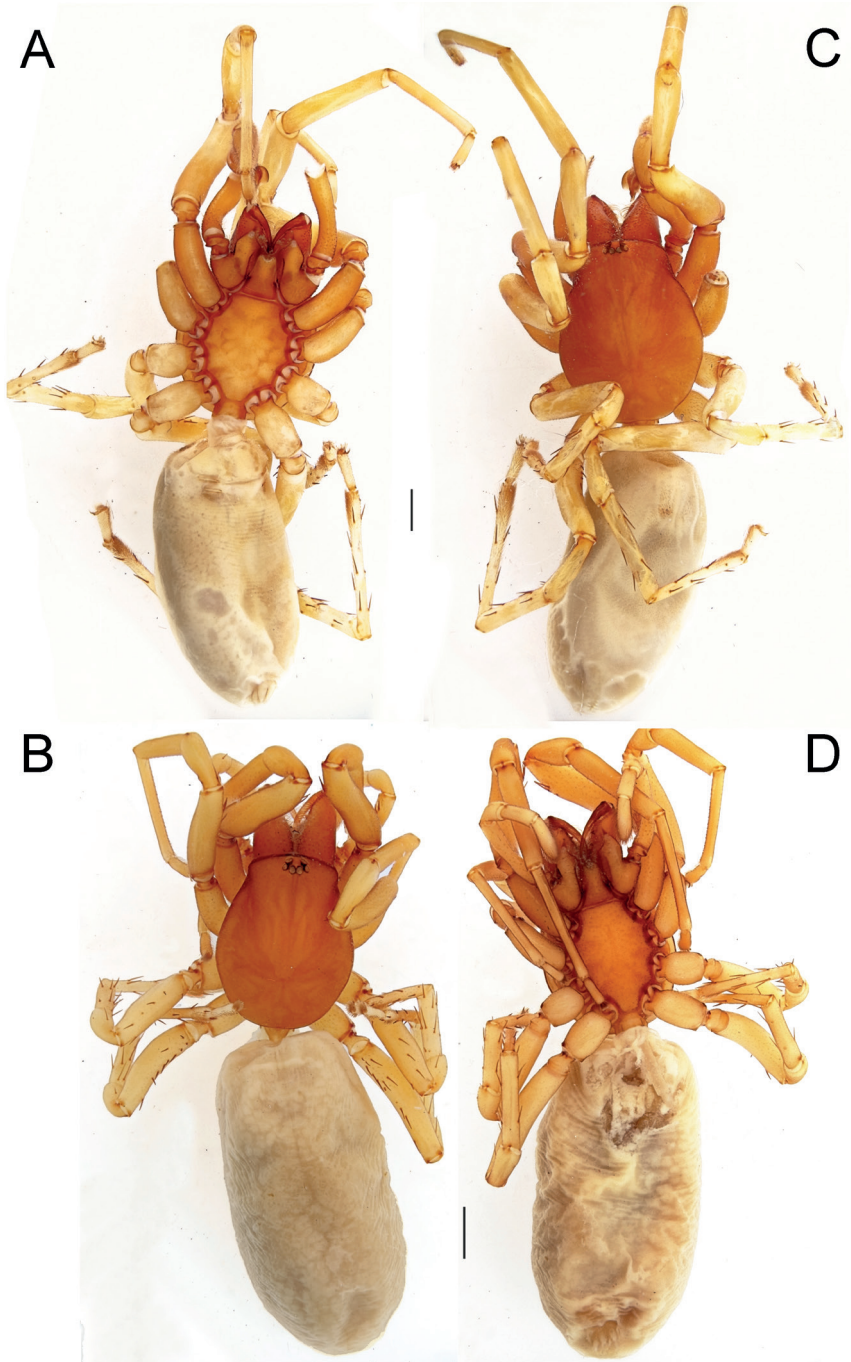


Figure 10. Male (**A, C**) and female (**B, D**) of *Dysdera isfahanica* sp. nov., habitus **A, D** ventral view **B, C** dorsal view. Scale bars: 1.0 mm.

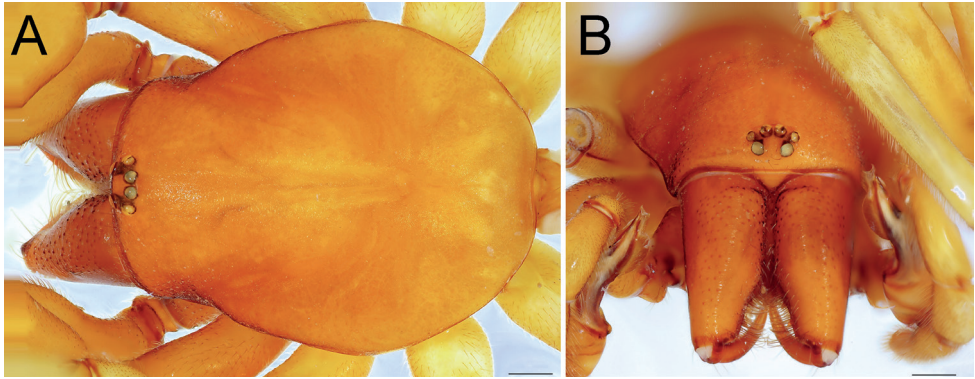


Figure 11. Male of *Dysdera isfahanica* sp. nov., prosoma **A** dorsal view **B** frontal view. Scale bars: 0.5 mm.

(3.77, 2.47, 3.23, 3.21, 0.89), II: 12.83 (3.47, 2.34, 2.96, 3.16, 0.90), III: 9.23 (2.60, 1.39, 1.95, 2.58, 0.71), IV: 12.28 (3.47, 1.91, 2.59, 3.43, 0.88). Spination: I: Fe: 1–2pl. II: no spines. III: Ti: 4pl, 2rl, 4v; Mt: 6pl, 6rl. IV: Fe: 6d; Ti: 2d, 2pl, 2rl, 2v; Mt: 6pl, 5rl.

Palp as in Fig. 12A–D; bulb ca. 2.5× longer than wide; tegulum bell-shaped, almost as long as wide; psembolus 1.8× longer than tegulum; median crest rounded, ca. 3.4× shorter than length of psembolus, ca. 2× wider than high; posterior apophysis claw-like, 2.3× longer than wide; incision between tegulum and psembolus absent; retrolateral crest forming right angle.

Female. Habitus as in Fig. 10B, D. Total length 9.45. Carapace 3.30 long, 2.55 wide. Eye diameters: AME 0.15, PME 0.14, PLE 0.12. Colouration as in male. Measurements of legs: I: 9.74 (2.76, 1.66, 2.31, 2.40, 0.61), II: 8.80 (2.52, 1.50, 2.08, 2.13, 0.57), III: 6.74 (1.94, 1.08, 1.28, 1.90, 0.54), IV: 8.68 (2.47, 1.31, 1.90, 2.46, 0.54). Spination: I: Fe: 3pl. II: Fe: 4pl. III: Fe: 5d, 1rl; Pa: 3pl; Ti: 4pl, 2rl, 6v; Mt: 3pl, 2rl, 6v. IV: Fe: 8–11d, 2pl; Pa: 1pl; Ti: 5pl, 4rl, 6v; Mt: 2pl, 3rl, 6v.

Endogyne as in Fig. 14A–D; length/width ratio ca. 2; receptacle ca. 5× longer than wide, with long anterior angles (i.e., longer than width of their bases), anterior margin almost straight; dorsal arch trapezoidal; transverse bar straight, 1.6× longer than receptacle; anterior margin of lateral edge inclined, lateral edge approximately as wide as receptacle; posterior diverticulum almost rectangular, its posterior edge rounded.

Comments. The material of this species and *D. mazeruni* sp. nov. (i.e., one male and two females in total) were reported by Roewer (1955); although he indicated that the females were collected in two different localities, they were found preserved in the same vial. The paratype female of *D. isfahanica* sp. nov. is matched with the holotype male due to their similar spination pattern and colouration.

Distribution. Known only from the type locality in Isfahan Province, central Iran (Fig. 35).

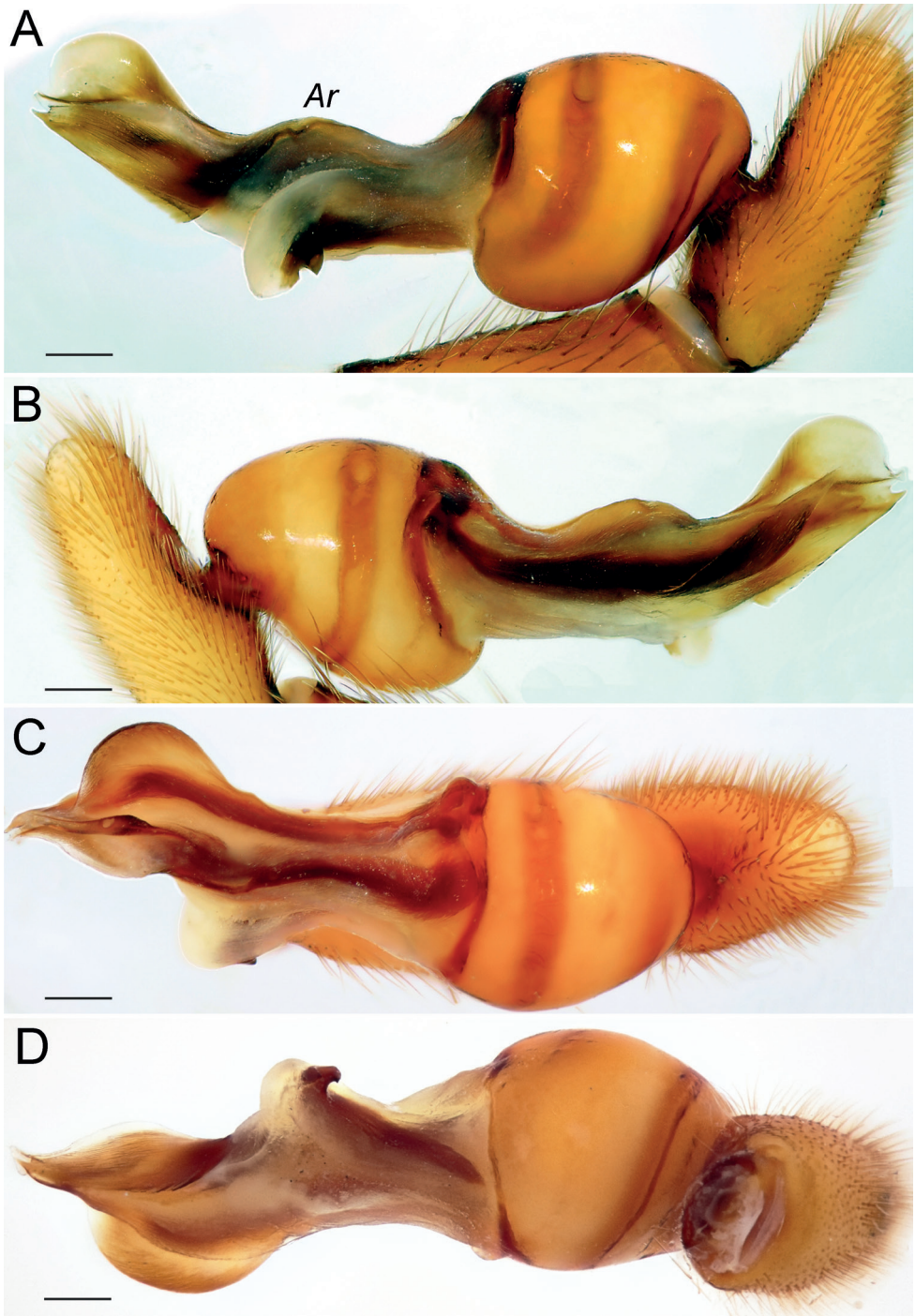


Figure 12. Male of *Dysdera isfahanica* sp. nov., bulb **A** retrolateral view **B** prolateral view **C** anterior view **D** posterior view. Scale bars: 0.25 mm. Abbreviation: *Ar* – arch-like ridge.

***Dysdera mazeruni* sp. nov.**

<https://zoobank.org/53699EB1-066B-405B-872C-84E69085B8F6>

Figs 13A, B, 14E–G

Dysdera erythrina: Roewer 1955: 752 (in part, misidentification).

Type material. *Holotype* ♀ (SMF), IRAN: Mazandaran Province: Caspian coast, forest in Chalus, 36°40'N, 51°25'E (F. Starmühlner). *Paratype*: 1♀ (MMUE), north of Javaher-Deh Vil., ~ 500 m down by elevation down from vil., 36°52'19.2"N, 50°28'01.2"E, 9.06.2000 (Y.M. Marusik).

Etymology. The specific epithet is a noun in apposition, named after an Iranian language of the northwestern branch spoken by the Mazandarani people.

Diagnosis. The new species is similar to *D. isfahanica* sp. nov., but differs by the arched anterior margin of receptacle (vs. almost straight), almost square-shaped dorsal arch (vs. distinctly trapezoidal), and shorter anterior angles (vs. longer, cf. Fig. 14A–D, E–G).

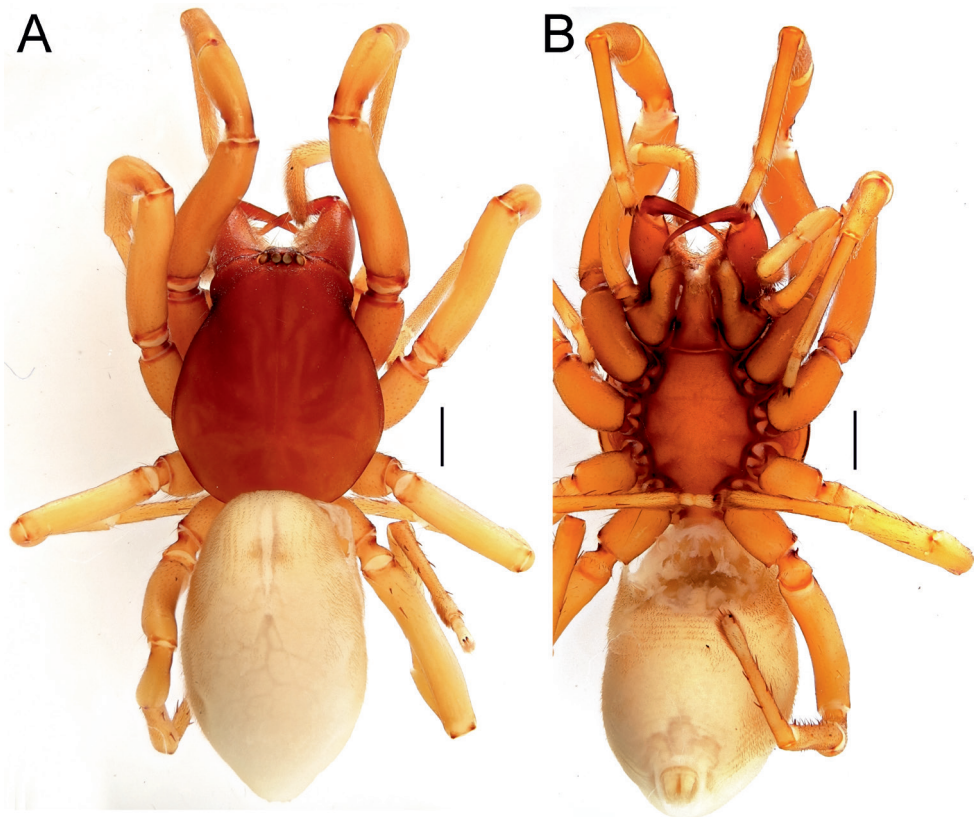


Figure 13. Female of *Dysdera mazeruni* sp. nov., habitus **A** dorsal view **B** ventral view. Scale bars: 1.0 mm.

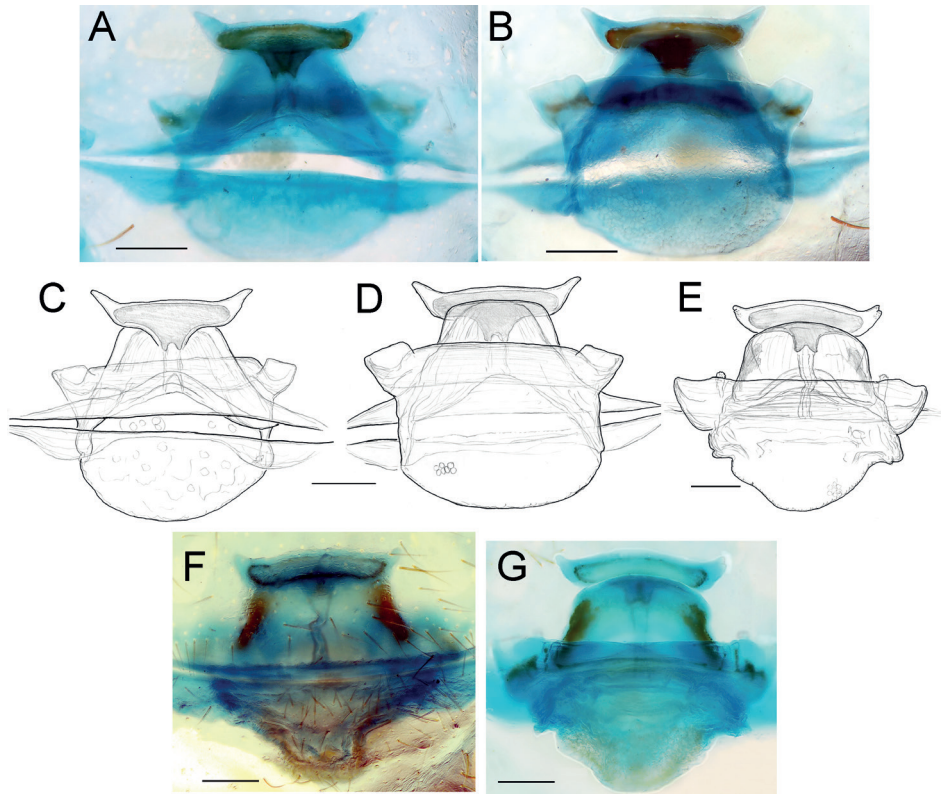


Figure 14. Females of *Dysdera isfahanica* sp. nov. (**A–D**) and *D. mazeruni* sp. nov. (**E–G**), endogyne **A, C, F** ventral view **B, D, E, G** dorsal view. Scale bars: 0.2 mm.

Description. Female (Holotype). Habitus as in Fig. 13A, B. Total length 8.90. Carapace 4.25 long, 3.37 wide. Eye diameters: AME 0.21, PME 0.19, PLE 0.22. Carapace, sternum, chelicerae, labium, and maxillae orange. Legs yellowish. Abdomen pale beige, without any pattern. Spinnerets uniformly pale beige. Measurements of legs: I: 10.93 (3.48, 2.02, 2.50, 2.25, 0.68), II: 10.00 (2.95, 1.86, 2.31, 2.25, 0.63), III: 7.46 (2.38, 1.08, 1.44, 1.91, 0.65), IV: 9.92 (2.71, 1.50, 2.12, 2.88, 0.71). Spination: I, II: no spines. III: Fe: 1d; Ti: 2pl, 2rl, numerous v spine-like setae; Mt: 2pl, 4rl, 5v. IV: Fe: 2d; Ti: 2pl, 2rl, numerous v spine-like setae; Mt: 3pl, 2rl, 6v.

Endogyne as in Fig. 14E–G; length/width ratio ca. 2.2; receptacle with slightly arched anterior margin, ca. 5× longer than wide, anterior angles slightly rounded; dorsal arch almost square-shaped, posterior margin 1.2× longer than anterior margin; transverse bar straight, 1.7× longer than receptacle; lateral edges broad, wider than receptacle; posterior diverticulum narrowing posteriorly.

Male. Unknown.

Comments. As for the previous species.

Distribution. Known only from the listed localities in Mazandaran Province, northern Iran (Fig. 35).

***Dysdera persica* sp. nov.**

<https://zoobank.org/5CCD54FC-78A6-4AA9-A521-C53C8C70F140>

Figs 15A–F, 16A–D, 17A, B

Type material. *Holotype* ♂ (ZMUT), IRAN: Golestan Province: Shast Kalateh, 36°45'N, 54°21'E, 2017 (R. Rafiei-Jahed). *Paratypes*: 7♂5♀ (ZMUT), same data as the holotype; 1♂ (ZMUT), Mazandaran Province: Polur, 35°50'N, 52°03'E, 10.2015 (A. Zamani); 1♂ (MHNG), Kiyasar, 36°14'N, 53°33'E, 1500 m, 11.07.1975 (A. Senglet).

Etymology. The specific epithet is an adjective, referring to the historical region of the Middle East, located in eastern Mesopotamia, which is now Iran.

Diagnosis. The male of this species differs from those of the other species of the *aculeata* group occurring in Iran by the extremely long bulb (especially psembolus, i.e., twice longer than tegulum), and by the tegulum with posterior margin 1.3× longer than anterior margin (vs. equal or shorter in length). The female of *D. persica* sp. nov. differs from those of its congeners by having the broadest dorsal arch, bearing almost angled anterior corners (vs. rounded).

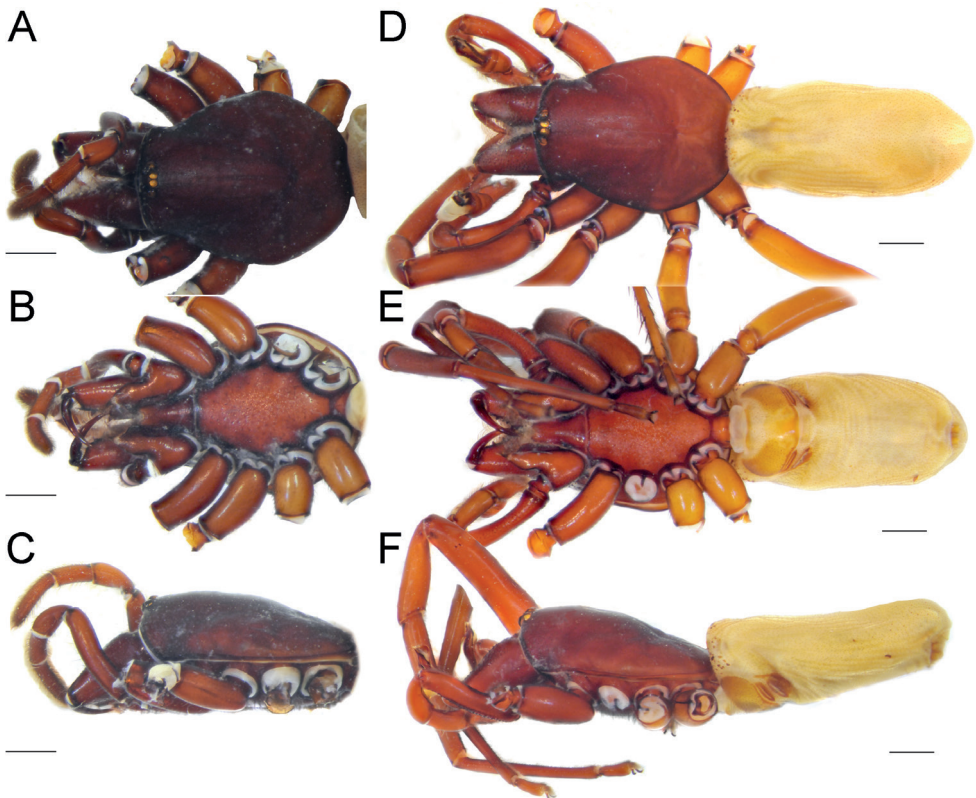


Figure 15. Female (A–C) and male (D–F) of *Dysdera persica* sp. nov., habitus **A, D** dorsal view **B, E** ventral view **C, F** lateral view. Scale bars: 1.0 mm.

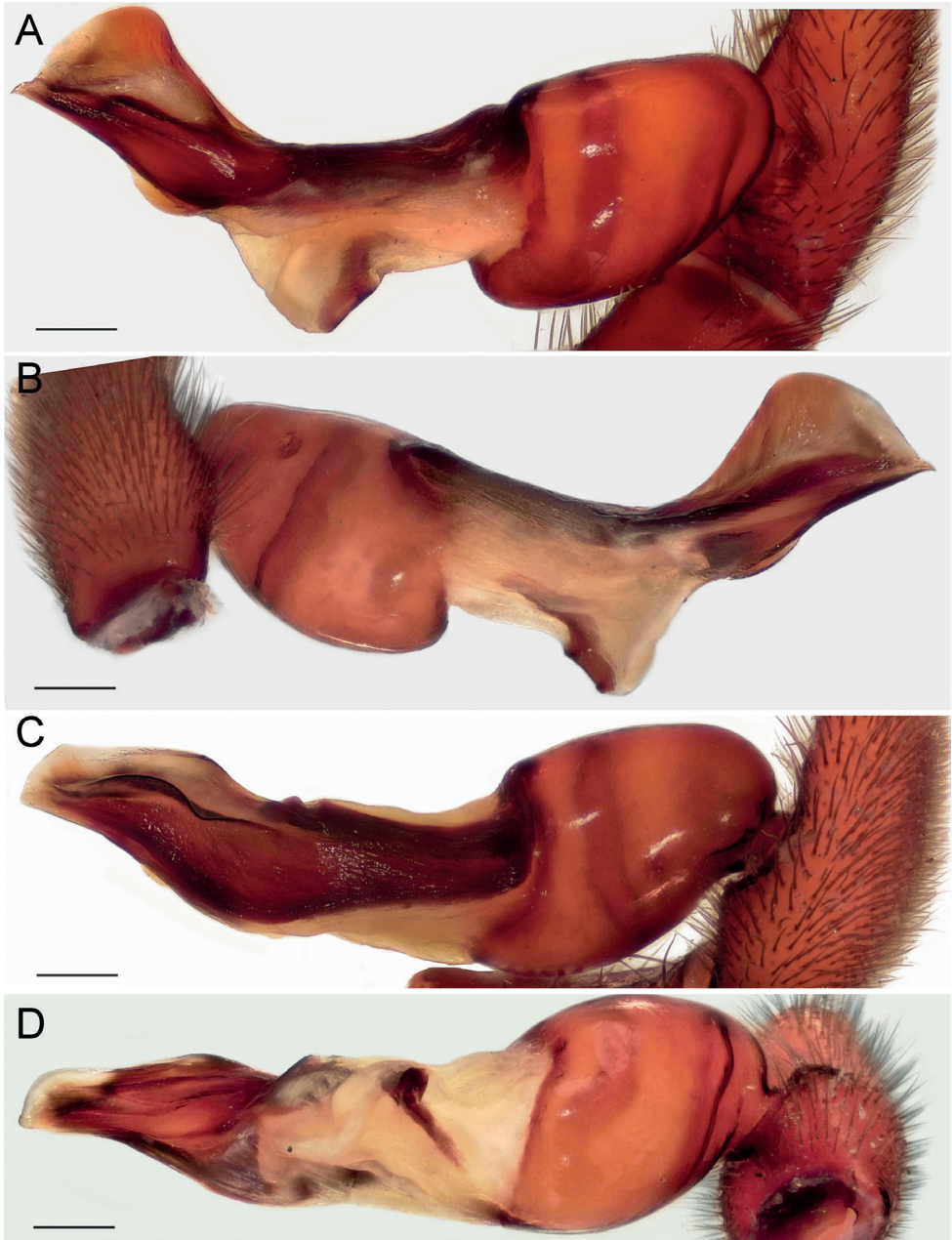


Figure 16. Male of *Dysdera persica* sp. nov., bulb **A** retrolateral view **B** prolateral view **C** anterior view **D** posterior view. Scale bars: 0.25 mm.

Description. Male (Holotype). Habitus as in Fig. 15D–F. Total length 9.06. Carapace 4.19 long, 3.20 wide. Eye diameters: AME 0.14, PME 0.16, PLE 0.17. Carapace, sternum, chelicerae, labium, and maxillae reddish brown. Legs orange. Abdomen greyish, without any pattern. Spinnerets uniformly dark yellowish. Measurements of

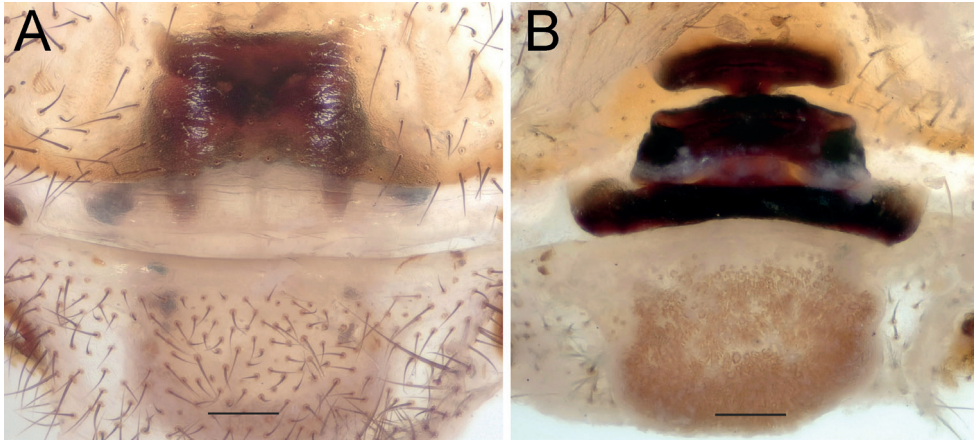


Figure 17. Female of *Dysdera persica* sp. nov., endogyne **A** ventral view **B** dorsal view. Scale bars: 0.25 mm.

legs: I: 13.98 (3.96, 2.36, 3.43, 3.52, 0.71), II: 12.87 (3.60, 2.11, 3.07, 3.27, 0.82), III: 9.38 (2.74, 1.51, 1.84, 2.70, 0.59), IV: 12.37 (3.54, 1.95, 2.66, 3.40, 0.82). Spination: I: Fe: 2pl. II: Fe: 1pl. III: Fe: 1pl; Ti: 5pl, 3rl, 4v; Mt: 5d, 9pl, 5rl, 3v. IV: Fe: 4d; Ti: 4pl, 6rl, 1v; Mt: 5d, 6pl, 7rl, 6v. Ti III–IV with a row of thin rigid ventral setae.

Palp as in Fig. 16A–D; bulb ca. 2.3× longer than wide; tegulum bell-shaped, almost as long as wide; psembolus 2× longer than tegulum; median crest triangular, ca. 2× shorter than length of psembolus, ca. 2.4× wider than high; posterior apophysis broad; incision between tegulum and psembolus present; retrolateral crest gradually rounded.

Female. Habitus as in Fig. 15A–C. Total length 11.0. Carapace 4.25 long, 3.16 wide. Eye diameters: AME 0.17, PME 0.18, PLE 0.15. Carapace and chelicerae dark reddish violet; sternum, labium, and maxillae reddish brown. Leg reddish brown. Abdomen greyish, without any pattern. Spinnerets uniformly greyish. Measurements of legs: I: 11.02 (3.15, 1.98, 2.59, 2.51, 0.79), II: 9.61 (2.72, 1.76, 2.32, 2.14, 0.67), III: 8.07 (2.27, 1.33, 1.62, 2.14, 0.71), IV: 10.54 (3.02, 1.66, 2.15, 2.89, 0.82). Spination: I: Fe: 3pl. II: Fe: 1pl. III: Fe: 1d; Ti: 4pl, 4rl; Mt: 12pl, 5rl, 4v. IV: Fe: 4d; Ti: 5pl, 4rl, 1v; Mt: 14pl, 9rl, 3v. Ti III–IV with a row of thin rigid ventral setae.

Endogyne as in Fig. 17A, B; length/width ratio ca. 1.9; receptacle 3.5× longer than wide, 1.2× wider than transverse bar; anterior angles rounded; dorsal arch trapezoidal; transverse bar straight, ca. 1.8× longer than receptacle; lateral edges with almost horizontal anterior margins, as long as width of receptacle; posterior diverticulum rectangular.

Distribution. Known only from listed localities in Golestan and Mazandaran provinces, northern Iran (Fig. 35).

Dysdera pococki Dunin, 1985

Dysdera concinna: Pocock 1889: 112 (misidentified as per Deeleman-Reinhold and Deeleman 1988: 236).

Dysdera pococki Dunin 1985: 114, figs 1, 2 (♂).

Comments. The Iranian record of this species is doubtful. Dunin (1985) described *D. pococki* on the basis of a male specimen from Turkmenistan, and the female of the species remains undescribed. Without providing any illustrations, Pocock (1889) reported a single female specimen from northeastern Iran which he tentatively identified as *D. concinna* L. Koch, 1878; this record was later attributed to *D. pococki* by Deeleman-Reinhold and Deeleman (1988), due to their close collection localities and without an examination of the Iranian material. This matter should be revisited once the female of *D. pococki* is described and the specimen reported by Pocock from Iran is studied and illustrated.

Records in Iran. Razavi Khorasan (Pocock 1889) (Fig. 35).

Distribution. Iran, Turkmenistan.

***Dysdera sagartia* sp. nov.**

<https://zoobank.org/FD19AF41-B7A5-4B99-A384-9FEB0D8B3E77>

Figs 18A–F, 19A–D, 20A, B

Type material. *Holotype* ♂ (ZMUT), IRAN: Tehran Province: Tehran, 35°45'N, 51°24'E, 04.2014 (A. Zamani). *Paratypes*: 1♂1♀ (ZMUT), Tehran, 35°42'N, 51°25'E, 03.2014 (A.H. Bakhtiari).

Etymology. The specific epithet is a noun in apposition, referring to an ancient tribe dwelling in the Iranian plateau.

Diagnosis. The male of this species differs from those of the other species of the *aculeata* group occurring in Iran by the strong dorsal incision between tegulum and

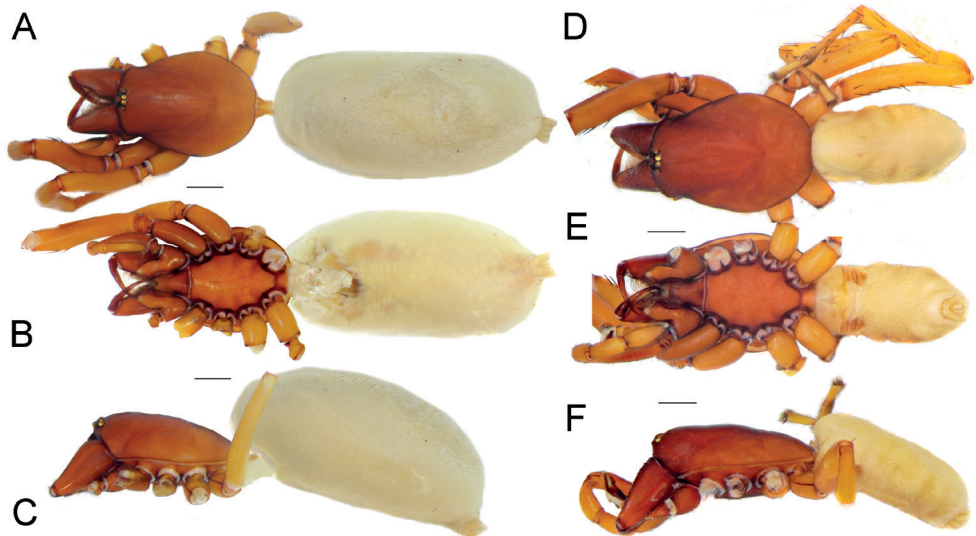


Figure 18. Female (A–C) and male (D–F) of *Dysdera sagartia* sp. nov., habitus A, D dorsal view B, E ventral view C, F lateral view. Scale bars: 1.0 mm.

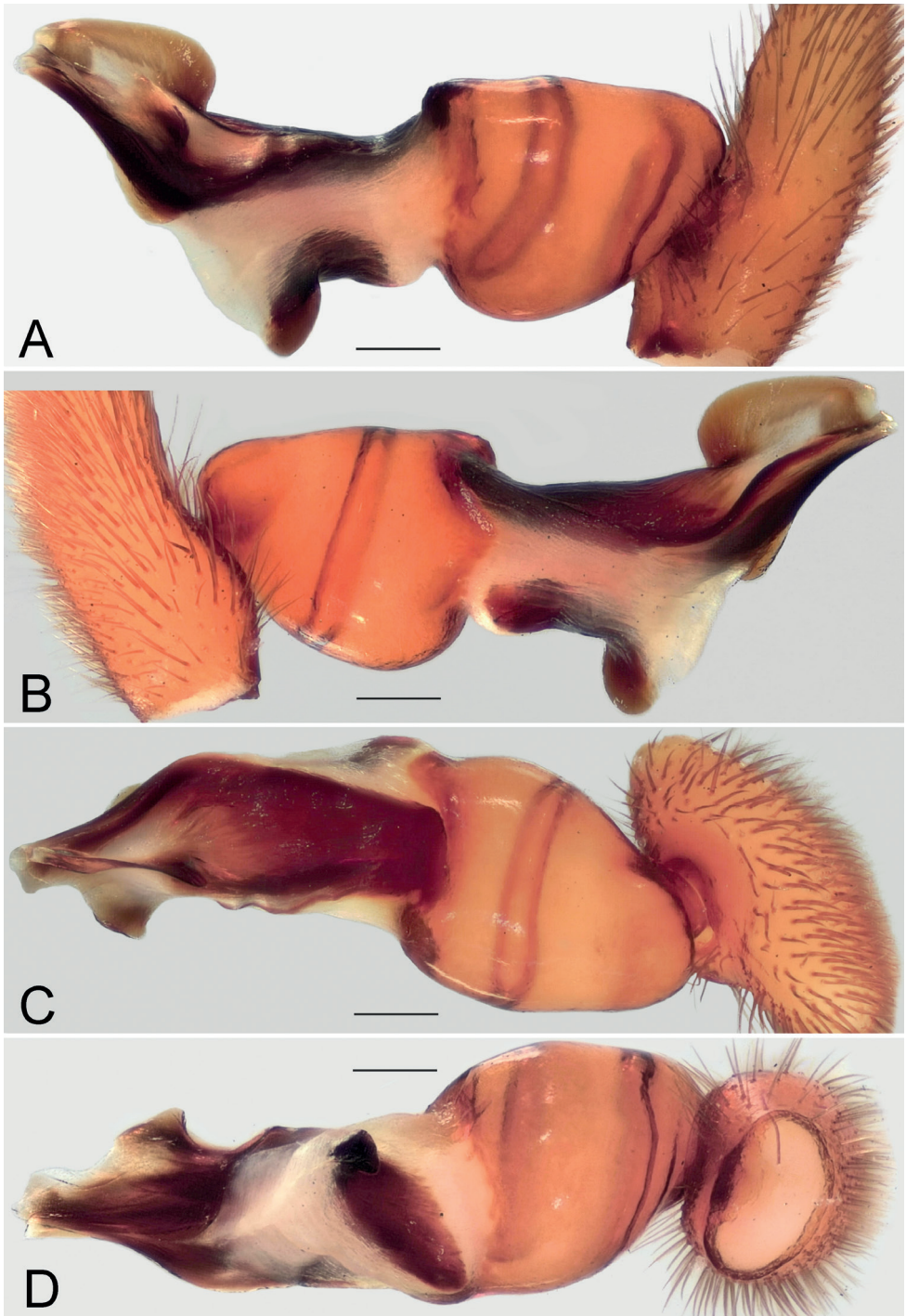


Figure 19. Male of *Dysdera sagartia* sp. nov., bulb **A** retrolateral view **B** prolateral view **C** anterior view **D** posterior view. Scale bars: 0.25 mm.

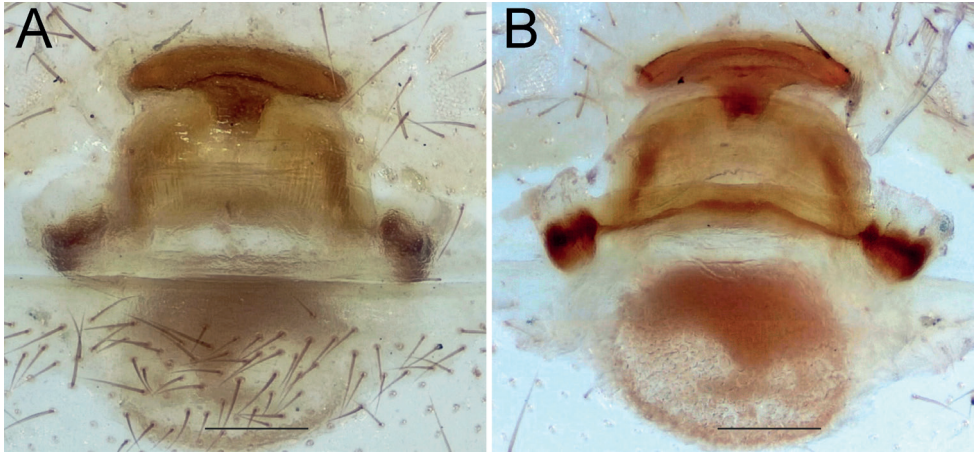


Figure 20. Female of *Dysdera sagartia* sp. nov., endogyne **A** ventral view **B** dorsal view. Scale bars: 0.25 mm.

psembolus, and the posterior apophysis bent on right angle (vs. no or small incision, and posterior apophysis not bent on right angle); the most similar species is *D. mikhailovi* Fomichev & Marusik, 2021 from Tajikistan, from which the new species differs by having a dorsal incision between tegulum and psembolus, the parallel dorsal sides of tegulum and psembolus (vs. dorsal margin of psembolus inclined), and smaller retrolateral crest angled at distal 1/3 of psembolus (vs. larger and angled at mid-part). The female of *D. sagartia* sp. nov. differs from those of its congeners occurring in Iran by having an arched anterior margin of receptacle in combination with a lack of anterior angles (vs. species with arched receptacle have anterior angles), and the almost semiround dorsal arch (vs. trapezoidal).

Description. Male (Holotype). Habitus as in Fig. 18D–F. Total length 8.38. Carapace 4.29 long, 3.17 wide. Eye diameters: AME 0.18, PME 0.15, PLE 0.15. Carapace, sternum, chelicerae, labium, and maxillae reddish. Legs yellowish orange. Abdomen cream-coloured, without any pattern. Spinnerets uniformly cream-coloured. Measurements of legs: I: 14.51 (3.99, 2.46, 3.61, 3.68, 0.77), II: 12.87 (3.41, 2.02, 3.19, 3.50, 0.75), III: 9.24 (2.75, 1.17, 2.04, 2.47, 0.81), IV: 11.84 (3.51, 1.62, 2.70, 3.13, 0.88). Spination: I: Fe: 3pl. II: Fe: 3pl. III: Fe: 1d, 3pl; Ti: 5pl, 2rl, 5v; Mt: 6pl, 4rl, 2v. IV: Fe: 8d, 1pl, 1rl; Ti: 6pl, 3rl, 7v; Mt: 6pl, 2rl, 5v.

Palp as in Fig. 19A–D; bulb ca. 2.1× longer than wide; tegulum bell-shaped, almost as long as wide; psembolus 1.44× longer than tegulum; median crest rounded, ca. 2.3× shorter than length of psembolus, ca. 3.1× wider than high; posterior apophysis broad; incision between tegulum and psembolus present; retrolateral crest bent on obtuse, almost right, angle.

Female. Habitus as in Fig. 18A–C. Total length 11.7. Carapace 3.85 long, 2.91 wide. Eye diameters: AME 0.16, PME 0.14, PLE 0.12. Colouration as in male. Meas-

measurements of legs: I: 10.60 (2.87, 1.75, 2.62, 2.73, 0.63), II: 11.38 (3.24, 1.86, 3.04, 2.81, 0.43), III: 8.27 (2.46, 1.27, 1.60, 2.32, 0.62), IV: 10.86 (3.07, 1.50, 2.36, 3.16, 0.77). Spination: I: Fe: 3pl. II: Fe: 3pl. III: Fe: 1d, 1pl; Ti: 6pl, 2rl, 5v; Mt: 2d, 4pl, 2rl, 3v. IV: Fe: 7d; Ti: 2pl, 2rl, 8v; Mt: 2d, 4pl, 5v.

Endogyne as in Fig. 20A, B; length/width ratio ca. 2; receptacle slightly arched, ca. 4.7× longer than wide, anterior angles indistinct; dorsal arch semi-oval, its posterior margin 1.5× longer than anterior; transverse bar 1.5× longer than receptacle and approximately as wide, slightly arched, lateral edges longer than wide; posterior diverticulum rounded.

Distribution. Known only from the listed localities in Tehran Province, northern Iran (Fig. 35).

Dysdera verkana sp. nov.

<https://zoobank.org/2E18F484-6E0E-4296-B253-285A0E98E268>

Figs 21A–C, 22A–D

Type material. *Holotype* ♂ (ZMUT), IRAN: Golestan Province: Azadshahr County, Khosh Yeylaq, 36°49'N, 55°20'E, 15.06.2016 (D. Kasatkin).

Etymology. The specific epithet is a noun in apposition, referring to an Old Persian word for the Gorgan region, meaning “land of wolves”.

Diagnosis. The male of the new species is most similar to that of *D. sagartia* sp. nov., but differs by the more rounded median crest, the posterior apophysis not bent on right angle (cf. Fig. 22A and Fig. 19A), and the relatively longer psembolus (i.e., length of psembolus/length of tegulum = 1.66 in *D. verkana* sp. nov., vs. 1.44 in *D. sagartia* sp. nov.).

Description. Male. Habitus as in Fig. 21A–C. Total length 10.8. Carapace 5.65 long, 4.26 wide. Eye diameters: AME 0.24, PME 0.23, PLE 0.21. Carapace, sternum, chelicerae, labium, and maxillae reddish brown. Legs orange. Abdomen cream-coloured, without any pattern. Spinnerets uniformly dark yellowish. Measurements of legs: I: 13.04 (3.90, 2.23, 3.10, 3.06, 0.75), II: 11.76 (3.39, 1.98, 2.91, 2.71, 0.77), III: 8.56 (2.64, 1.26, 1.69, 2.33, 0.64), IV: 11.46 (3.32, 1.76, 2.48, 3.20, 0.70). Spination: I: Fe: 2pl. II: Fe: 1pl. III: Fe: 1d, 2pl; Ti: 4pl, 2rl, 5v; Mt: 3pl, 2rl, 6v. IV: Fe: 6d, 1pl; Ti: 4pl, 4rl, 5v; Mt: 4pl, 2rl, 6v.

Palp as in Fig. 22A–D; bulb ca. 2.2× longer than wide; tegulum bell-shaped, almost as long as wide; psembolus 1.66× longer than tegulum; median crest rounded, ca. 2.3× shorter than length of psembolus, ca. 2.7× wider than high; posterior apophysis broad; incision between tegulum and psembolus present; retrolateral crest roundly bent, forming right angle.

Female. Unknown.

Distribution. Known only from the type locality in Golestan Province, northern Iran (Fig. 35).

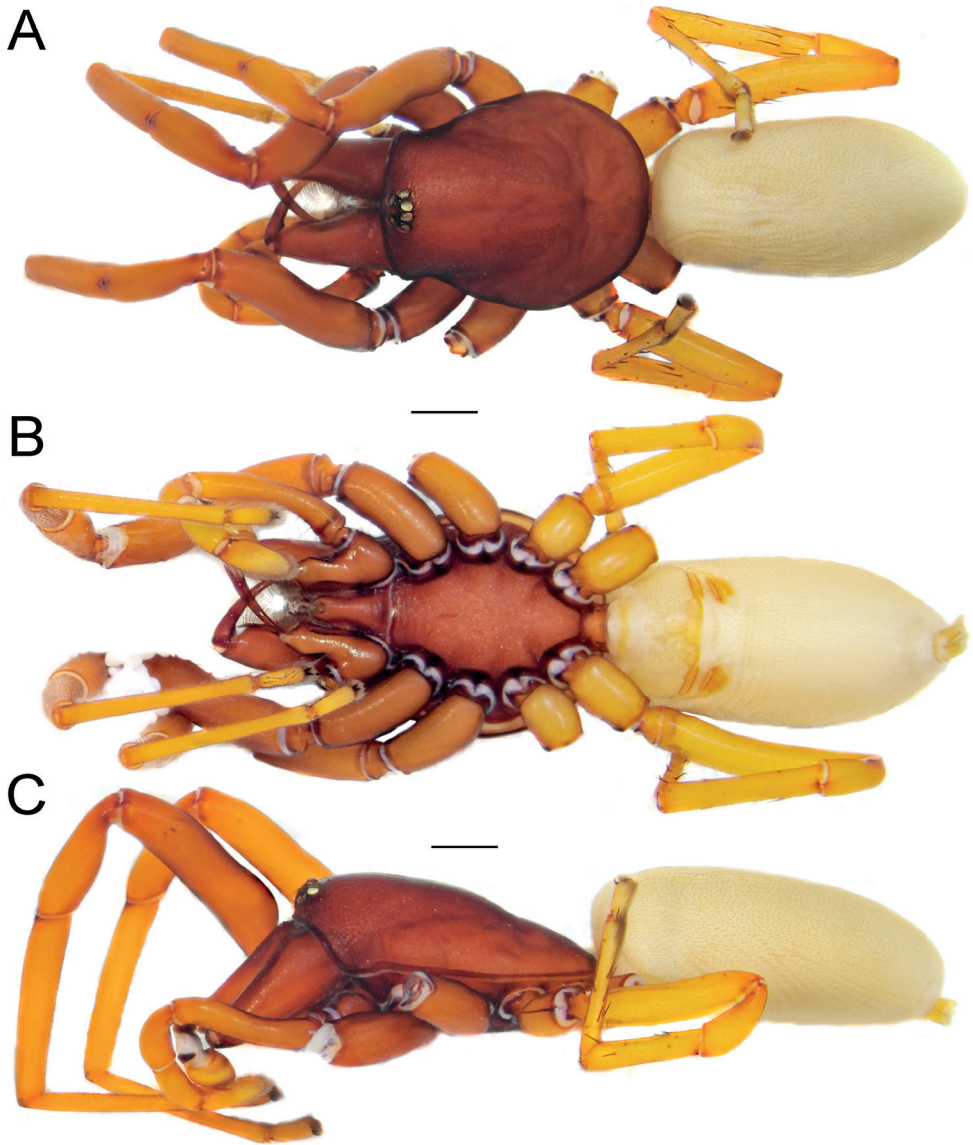


Figure 21. Male of *Dysdera verkana* sp. nov., habitus **A** dorsal view **B** ventral view **C** lateral view. Scale bars: 1.0 mm.

crocata species group

Diagnosis. This group can be diagnosed by a combination of the following characters: the chelicerae straight or anteriorly convergent and longer than half of the length of the carapace, carapace broad and flat, and bulb with small or no lateral projection (Deeleman-Reinhold and Deeleman 1988).

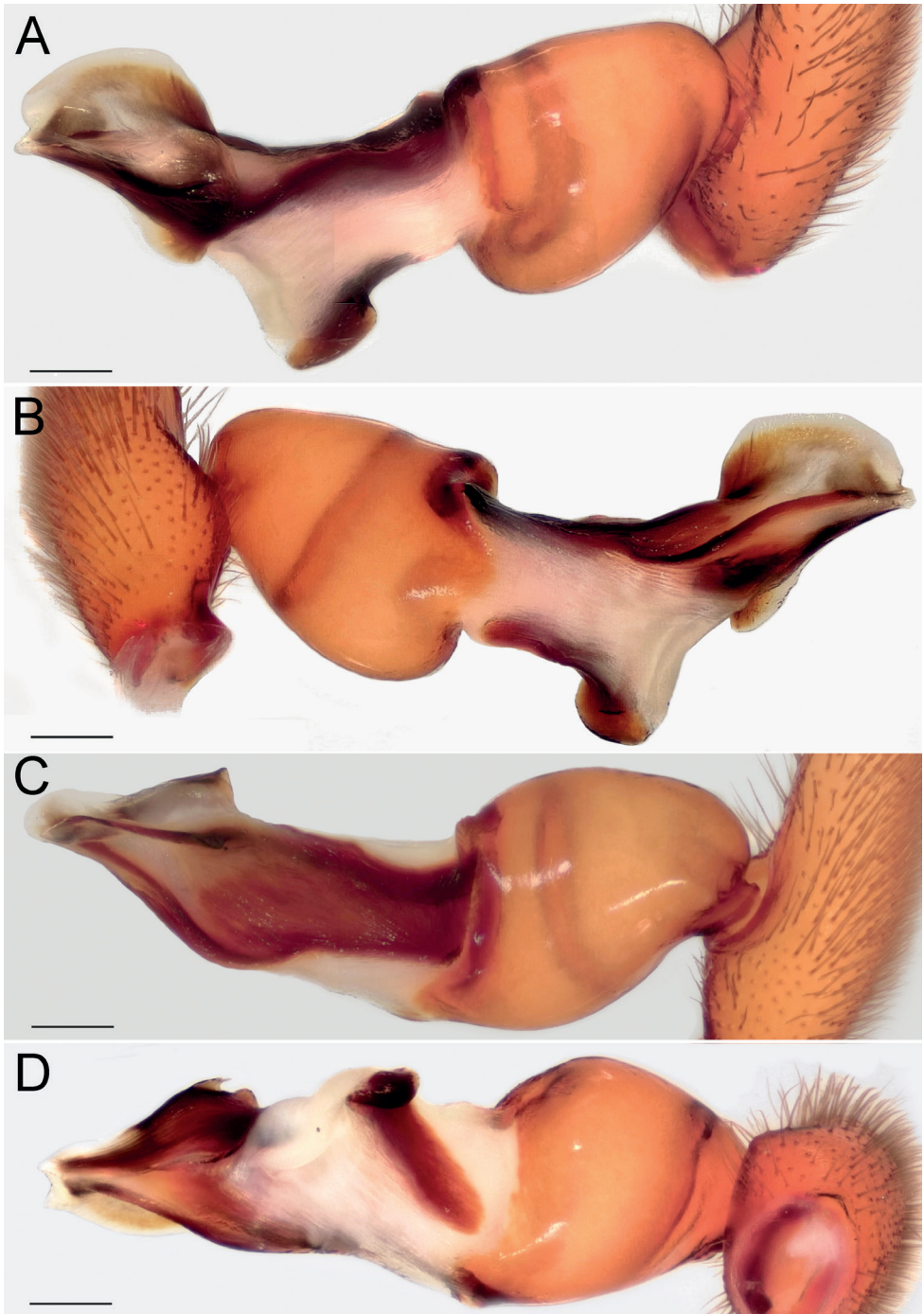


Figure 22. Male of *Dysdera verkana* sp. nov., bulb **A** retrolateral view **B** prolateral view **C** anterior view **D** posterior view. Scale bars: 0.25 mm.

***Dysdera xerxesi* sp. nov.**

<https://zoobank.org/84EDB4F0-007B-445B-A76D-C163B290ADFF>

Figs 23A–C, 24A–D

Type material. *Holotype* ♂ (ZMUT), IRAN: Bushehr Province: Asaluyeh, 27°20'N, 52°49'E, 27.01.2016 (A. Zamani).

Etymology. The new species is named after Xerxes I, the fourth King of Kings of the Achaemenid Empire, ruling from 486 to 465 BC; adjective.

Diagnosis. The new species differs from all of its congeners occurring in the region by having a stylus (*St*), rounded median crest (*Mc*) and wide posterior apophysis (*Ap*); none of the other species has a rounded median crest, and those with a stylus, have a small posterior apophysis.

Description. **Male.** Habitus as in Fig. 23A–C. Total length 4.02. Carapace 2.14 long, 1.60 wide. Eye diameters: AME 0.11, PME 0.09, PLE 0.08. Carapace, sternum, chelicerae, labium, and maxillae reddish brown. Legs missing. Abdomen cream-coloured, without any pattern. Spinnerets uniformly cream-coloured.

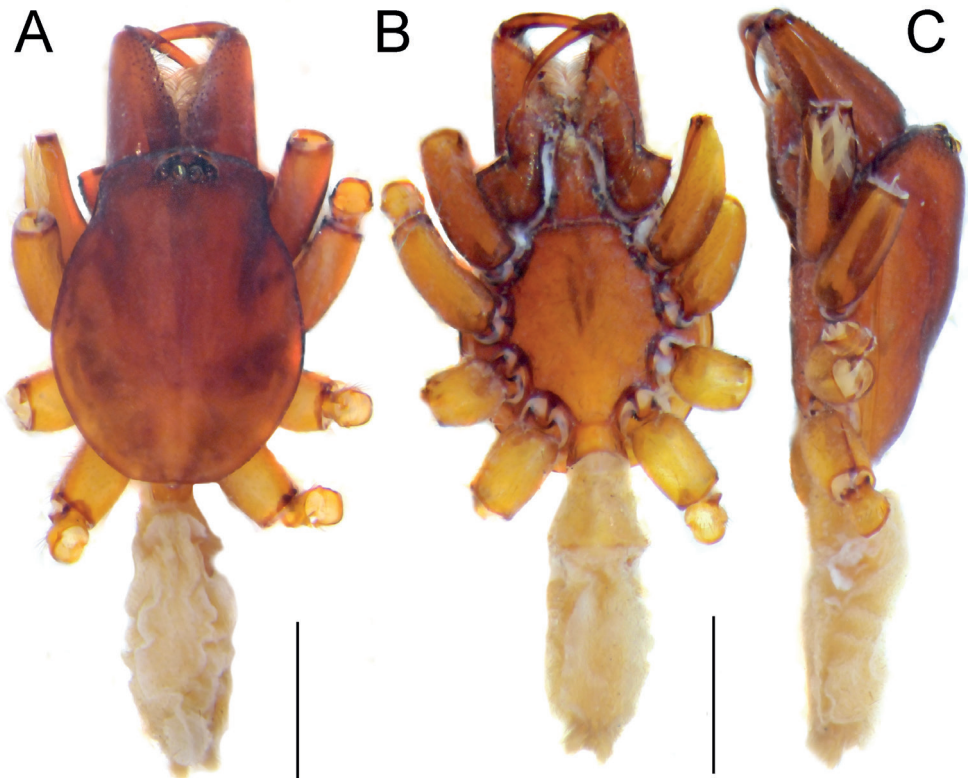


Figure 23. Male of *Dysdera xerxesi* sp. nov., habitus **A** dorsal view **B** ventral view **C** lateral view. Scale bars: 1.0 mm.

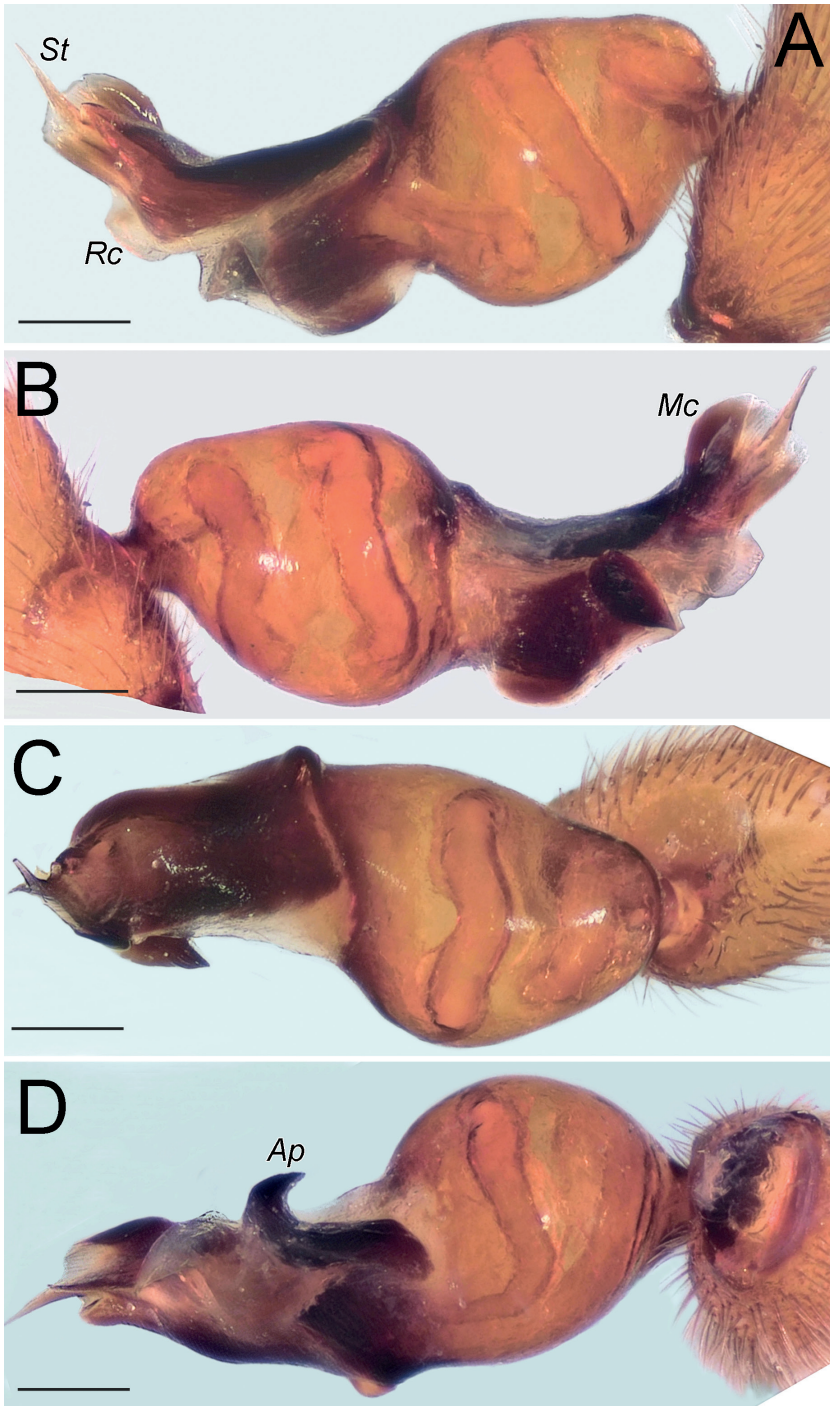


Figure 24. Male of *Dysdera xerxesi* sp. nov., bulb **A** retrolateral view **B** prolateral view **C** anterior view **D** posterior view. Scale bars: 0.25 mm. Abbreviations: *Ap* – posterior apophysis, *Mc* – median crest, *Rc* – retrolateral crest, *St* – stylus.

Palp as in Fig. 24A–D; bulb ca. 2.3× longer than wide; tegulum bell-shaped, almost as long as wide; psembolus 1.48× longer than tegulum; median crest (*Mc*) rounded, ca. 3.45× shorter than length of psembolus, ca. 2.3× wider than high; posterior apophysis (*Ap*) broad and hook-shaped; incision between tegulum and psembolus absent; retrolateral crest (*Rc*) gradually rounded; stylus (*St*) membranous and shorter than median crest.

Female. Unknown.

Distribution. Known only from the type locality in Bushehr Province, southern Iran (Fig. 35).

longirostris species group

Diagnosis. This group can be diagnosed by a combination of the following characters: cheliceral fang as long as the basal segment, carapace broad, flat and anteriorly convergent, and bulb with lateral projection smaller than the apex (Deeleman-Reinhold and Deeleman 1988).

Dysdera damavandica sp. nov.

<https://zoobank.org/4A417CC6-E9AD-4FA8-B3AD-750B3BB3184B>

Figs 25A–C, 26A–D

Type material. *Holotype* ♂ (ZMUT), IRAN: Mazandaran Province: Polur, surroundings of Mount Damavand, 35°50'N, 52°03'E, 10.2015 (A. Zamani).

Etymology. The specific epithet is an adjective, referring to the type locality of the species.

Diagnosis. The male of the new species is most similar to that of *D. concinna* L. Koch, 1878 from Azerbaijan, but differs by longer bulb (i.e., bulb length/tegulum width =3.1, vs. 2.7), relatively shorter median crest, and longer stylus (cf. Fig. 26A and Dunin 1982: fig. B). *Dysdera damavandica* sp. nov. is also similar to *D. tapuria* sp. nov. but differs by the median crest higher than wide (vs. wider than high), relatively longer stylus (cf. Fig. 26A and Fig. 30A) and posterior apophysis located at distal half of the bulb (vs. located at mid-part).

Description. Male. Habitus as in Fig. 25A–C. Total length 10.40. Carapace 5.53 long, 4.12 wide. Eye diameters: AME 0.18, PME 0.19, PLE 0.23. Carapace, sternum, chelicerae, labium, and maxillae reddish brown. Legs dark orange. Abdomen greyish, without any pattern. Spinnerets uniformly greyish. Measurements of legs: I: 15.64 (4.51, 2.54, 4.12, 3.56, 0.91), II: 15.12 (4.16, 2.67, 3.73, 3.69, 0.87), III: 10.91 (3.21, 1.73, 2.22, 3.01, 0.74), IV: 13.75 (3.82, 2.02, 3.13, 3.94, 0.84). Spination: I: Fe: 2pl. II: Fe: 2pl. III: Fe: 1pl; Ti: 4pl, 2rl, 5v; Mt: 3pl, 2rl, 3v. IV: Fe: 7d; Ti: 2pl, 3rl, 5v; Mt: 4pl, 3rl, 5v.

Palp as in Fig. 26A–D; bulb ca. 3.1× longer than wide; tegulum bell-shaped, almost as long as wide; psembolus 2.77× longer than tegulum; median crest (*Mc*) triangular,

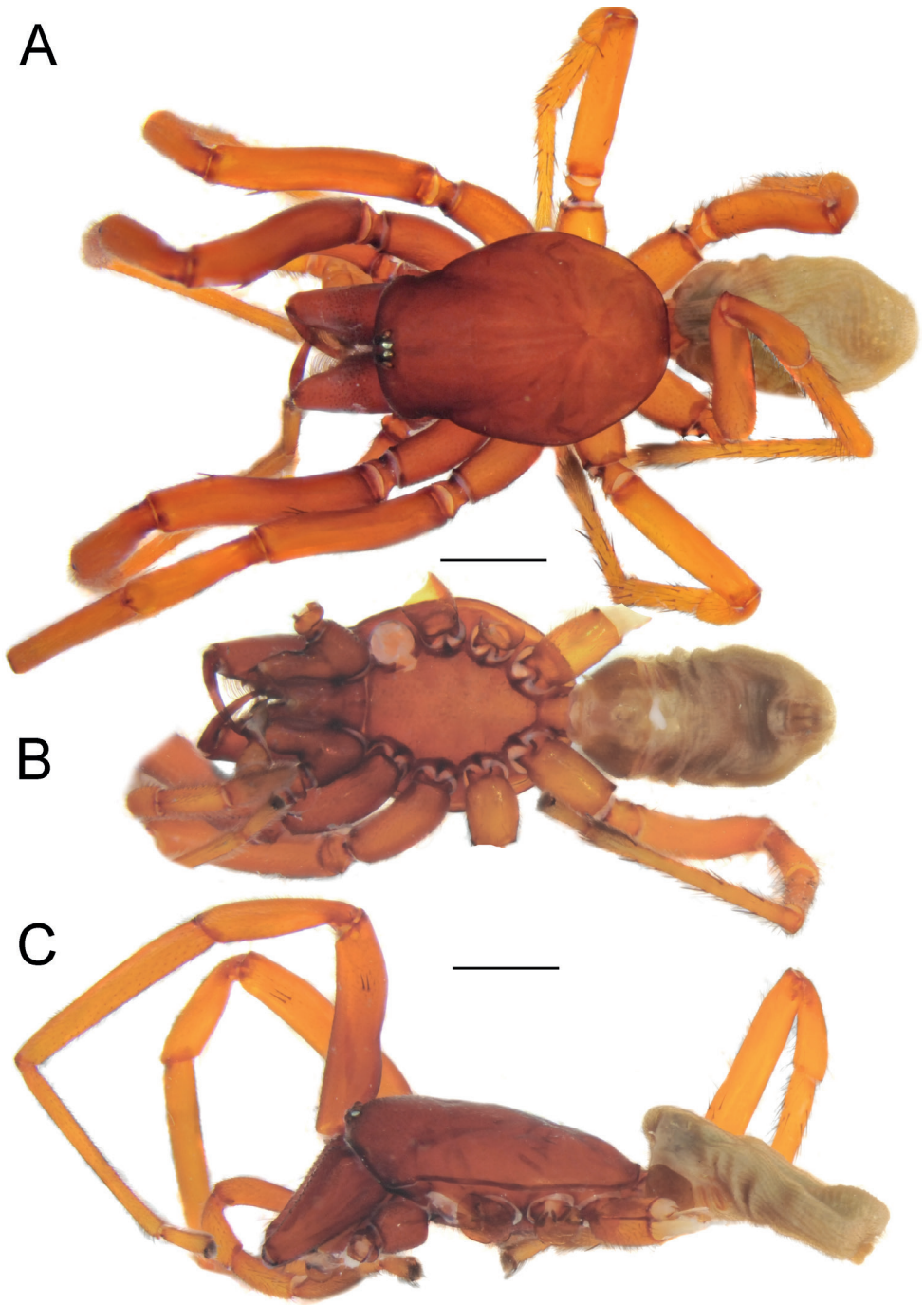


Figure 25. Male of *Dysdera damavandica* sp. nov., habitus **A** dorsal view **B** ventral view **C** lateral view. Scale bars: 1.0 mm.

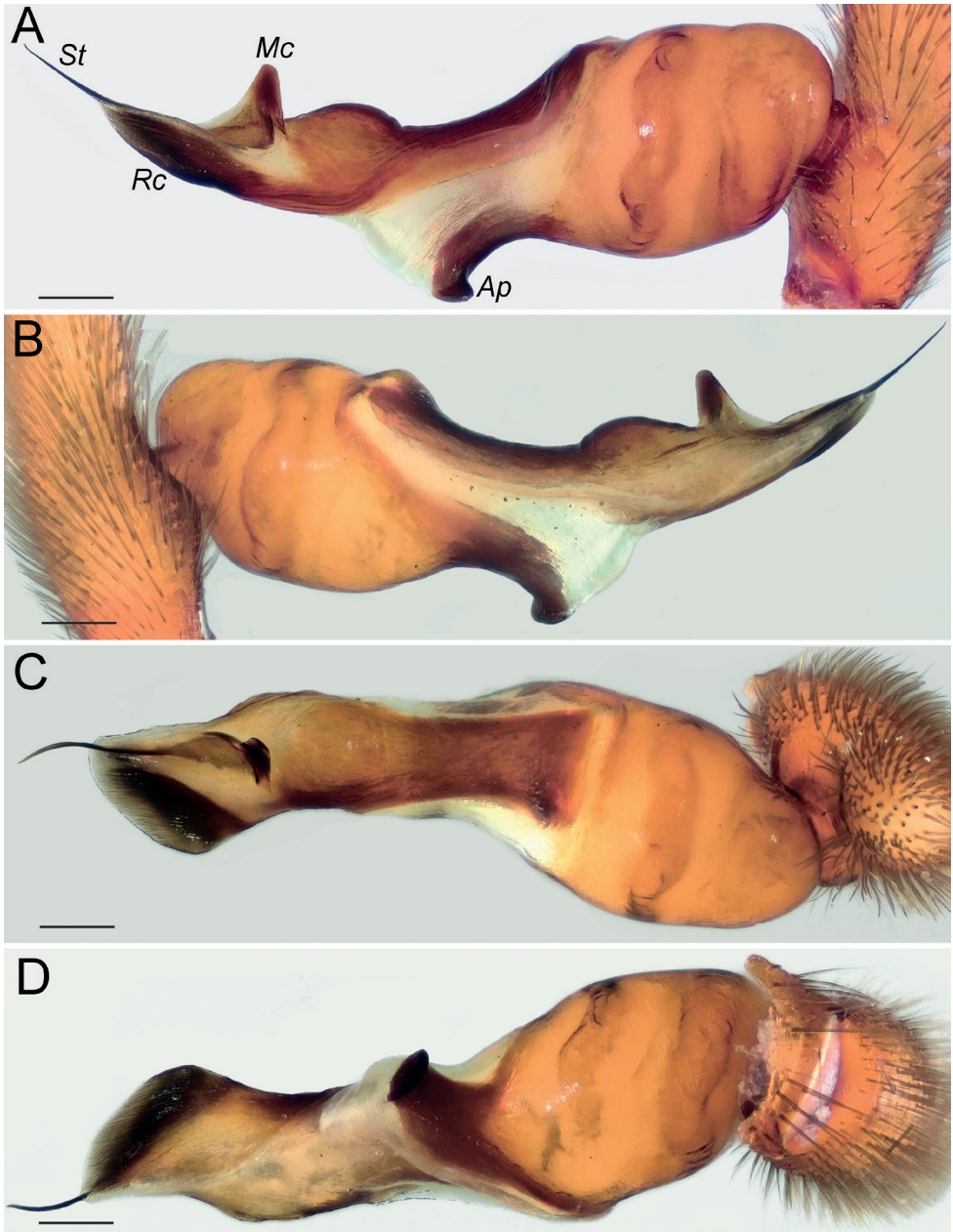


Figure 26. Male of *Dysdera damavandica* sp. nov., bulb **A** retrolateral view **B** prolateral view **C** anterior view **D** posterior view. Scale bars: 0.25 mm. Abbreviations: *Ap* – posterior apophysis, *Mc* – median crest, *Rc* – retrolateral crest, *St* – stylus.

ca. 6.65× shorter than length of psembolus, higher than wide; posterior apophysis (*Ap*) rounded; incision between tegulum and psembolus present; retrolateral crest almost straight; stylus (*St*) straight, longer than median crest.

Female. Unknown.

Distribution. Known only from the type locality in Mazandaran Province, northern Iran (Fig. 35).

***Dysdera medes* sp. nov.**

<https://zoobank.org/ED370972-D544-4411-A52E-4599D12E3850>

Figs 27A–C, 28A–D

Type material. *Holotype* ♂ (ZMUT), IRAN: Tehran Province: Tehran, 35°43'N, 51°24'E, 1994 (A. Savoji).

Etymology. The specific epithet is a noun in apposition, referring to an ancient Iranian people who inhabited an area known as Media between western and northern Iran.

Diagnosis. The male of the new species is similar to that of *D. granulata* Kulczyński, 1897 from Italy and the Balkan Peninsula, but differs by the shape of the tegulum (i.e., almost as wide as long, vs. 1.5× longer than wide), and by thinner psembolus (as wide as tegulum, vs. wider than tegulum). The male of *D. medes* sp. nov. differs from those of its congeners occurring in Iran by the very long median crest (i.e., longer than half of psembolus, vs. shorter), abrupt tip of psembolus in ventral and dorsal views (Fig. 28C, D) (vs. not abrupt), and posterior apophysis with two teeth (vs. one).

Description. Male. Habitus as in Fig. 27A–C. Total length 10.0. Carapace 4.19 long, 3.17 wide. Eye diameters: AME 0.14, PME 0.14, PLE 0.14. Carapace, sternum, chelicerae, labium, and maxillae reddish brown. Legs orange. Abdomen greyish, without any pattern. Spinnerets uniformly dark yellowish. Measurements of legs: I: 12.33 (3.54, 2.03, 2.89, 3.00, 0.87), II: 13.50 (3.80, 2.40, 3.12, 3.29, 0.89), III: 9.99 (2.95, 1.59, 1.86, 2.69, 0.90), IV: 12.31 (3.73, 1.80, 2.46, 3.30, 1.02). Spination: I, II: no spines. III: Ti: 4pl, 2rl, 5v; Mt: 6pl, 3rl, 2v. IV: Fe: 7d; Ti: 7pl, 4rl, 8v; Mt: 7pl, 3rl, 4v.

Palp as in Fig. 28A–D; bulb ca. 2.8× longer than wide; tegulum bell-shaped, almost as long as wide; psembolus 1.9× longer than tegulum; median crest rounded, ca. 2.42× shorter than length of psembolus, ca. 5.3× wider than high; posterior apophysis claw-shaped, with 2 teeth (Fig. 28B, D); incision between tegulum and psembolus absent; retrolateral crest almost straight.

Female. Unknown.

Distribution. Known only from the type locality in Tehran Province, northern Iran (Fig. 35).

***Dysdera tapuria* sp. nov.**

<https://zoobank.org/67653B32-6B9D-494E-8921-C4D8CEDBE70B>

Figs 29A–F, 30A–D, 31A–D

Type material. *Holotype* ♂ (MMUE), IRAN: Mazandaran Province: Tooban, Khorram-Abad, 36°43'N, 50°48'E, 8–10.06.2000 (Y.M. Marusik). *Paratypes*: 1♀ (MMUE), same data as the holotype; 1♂ (MHNG), Chorteh, 36°49'N, 50°38'E,

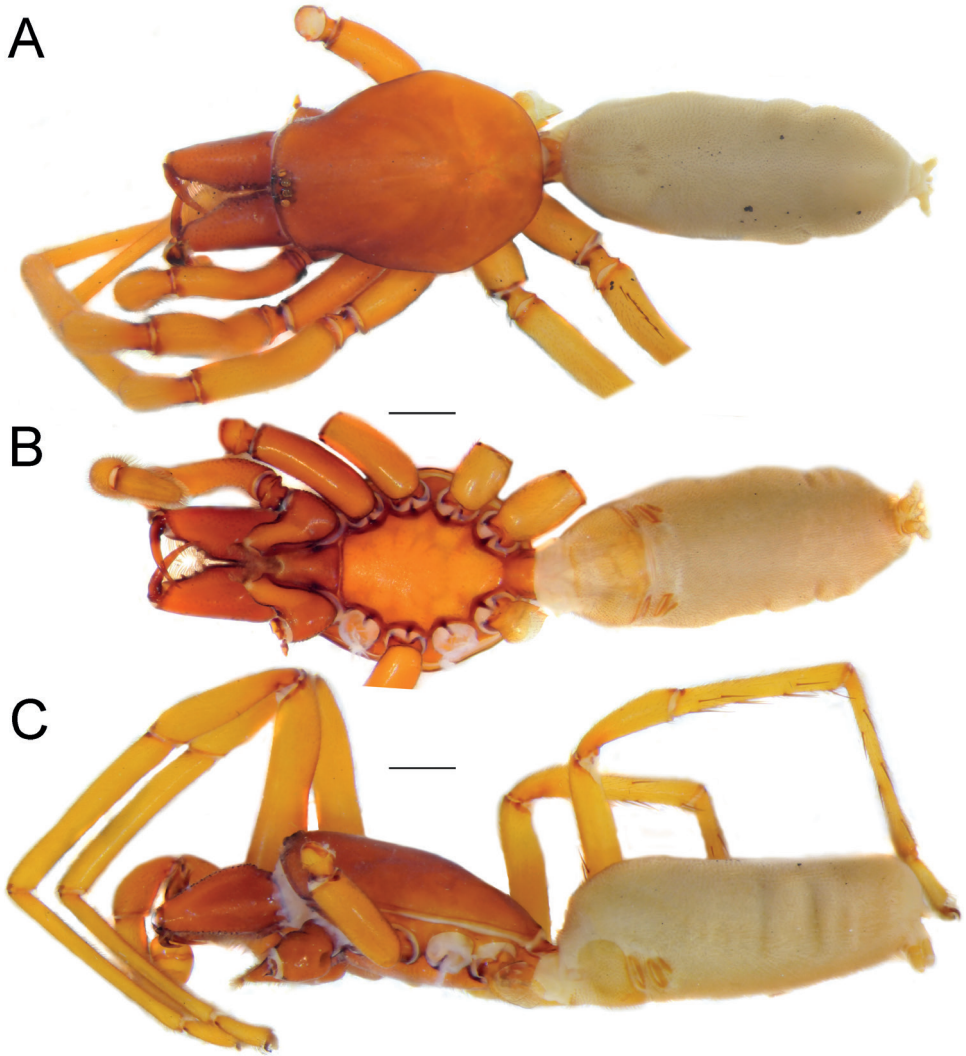


Figure 27. Male of *Dysdera medes* sp. nov., habitus **A** dorsal view **B** ventral view **C** lateral view. Scale bars: 1.0 mm.

1300 m, 5.08.1974 (A. Senglet); 1♂ (MHNG), Chorteh, 36°49'N, 50°38'E, 1300 m, 8.07.1973 (A. Senglet).

Etymology. The specific epithet is a noun in apposition, referring to the term applied to a mountainous region located in the Caspian coast of northern Iran.

Diagnosis. The male of the new species is most similar to that of *D. concinna*, but differs by longer bulb (i.e., bulb length/tegulum width = 3.1, vs. 2.7), median crest wider than high (vs. higher than wide), and shorter stylus (cf. Fig. 30B and

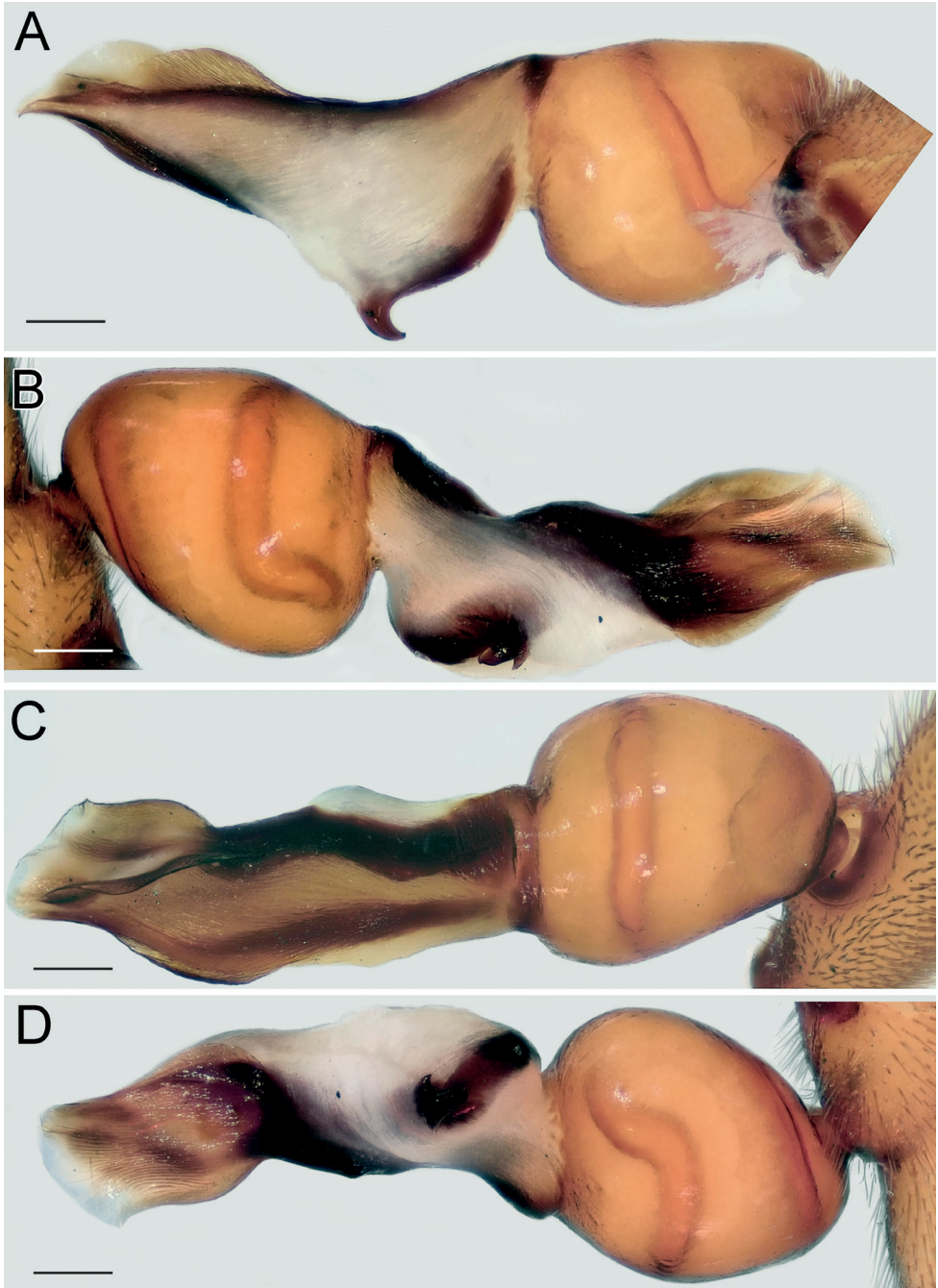


Figure 28. Male of *Dysdera medes* sp. nov., bulb **A** retrolateral view **B** prolateral view **C** anterior view **D** posterior view. Scale bars: 0.25 mm.

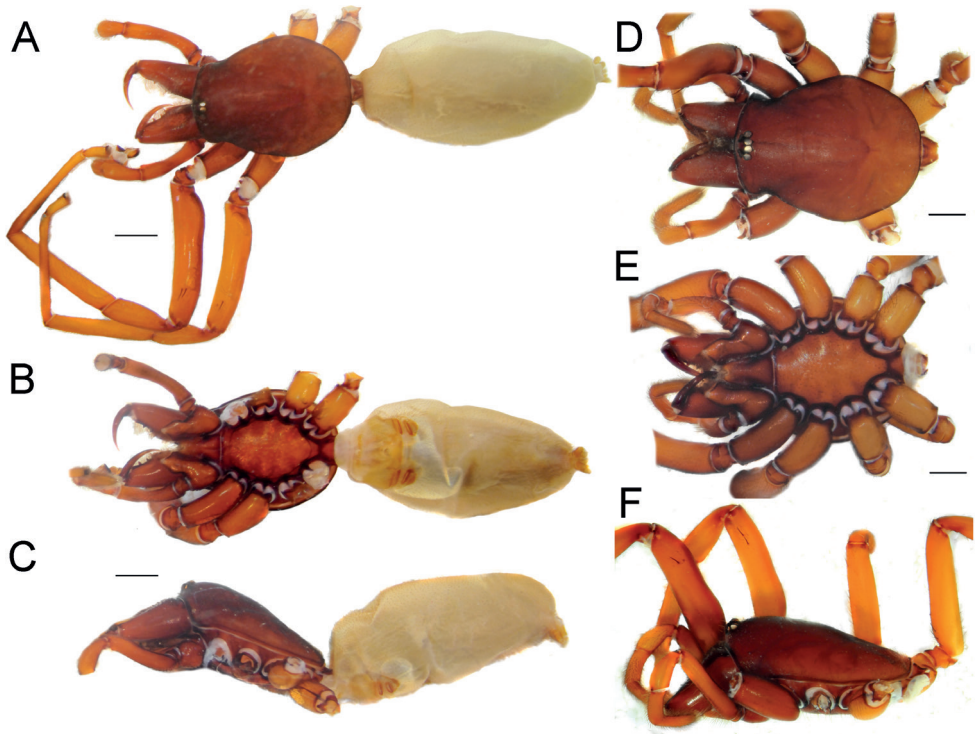


Figure 29. Male (A–C) and female (D–F) of *Dysdera tapuria* sp. nov., habitus A, D dorsal view B, E ventral view C, F lateral view. Scale bars: 1.0 mm.

Dunin 1982: fig. B). The male of *D. tapuria* sp. nov. is also similar to that of *D. damavandica* sp. nov., but differs by the median crest wider than high (vs. higher than wide) and relatively shorter stylus (cf. Fig. 30A and Fig. 26A). The female of this species differs from those of its congeners occurring in the region by the very wide lateral edges of the receptacle (i.e., approximately half of the receptacle’s width, vs. less than half).

Description. Male (Holotype). Habitus as in Fig. 29A–C. Total length 9.55. Carapace 3.76 long, 2.86 wide. Eye diameters: AME 0.14, PME 0.13, PLE 0.13. Carapace, sternum, chelicerae, labium, and maxillae reddish brown. Legs orange. Abdomen cream-coloured, without any pattern. Spinnerets uniformly dark yellowish. Measurements of legs: I: 14.04 (4.16, 2.14, 3.65, 3.24, 0.85), II: 12.72 (3.79, 2.08, 3.00, 3.11, 0.74), III: 10.01 (2.93, 1.44, 2.14, 2.77, 0.73), IV: 11.90 (3.72, 1.48, 2.73, 3.19, 0.78). Spination: I: Fe: 2pl. II: Fe: 1pl. III: Ti: 5pl, 3rl, 1v; Mt: 5pl, 2rl, 3v. IV: Fe: 8d, 1rl; Pa: 1pl; Ti: 5pl, 3rl, 6v; Mt: 6pl, 2rl, 5v.

Palp as in Fig. 30A–D; bulb ca. 3.1× longer than wide; tegulum bell-shaped, almost as long as wide; psembolus 1.8× longer than tegulum; median crest triangular, ca. 7× shorter than length of psembolus, ca. 2.5× wider than high; posterior apophysis claw-shaped; incision between tegulum and psembolus present; retrolateral crest roundly bent in proximal part and almost straight distally; stylus straight, as long as median crest.

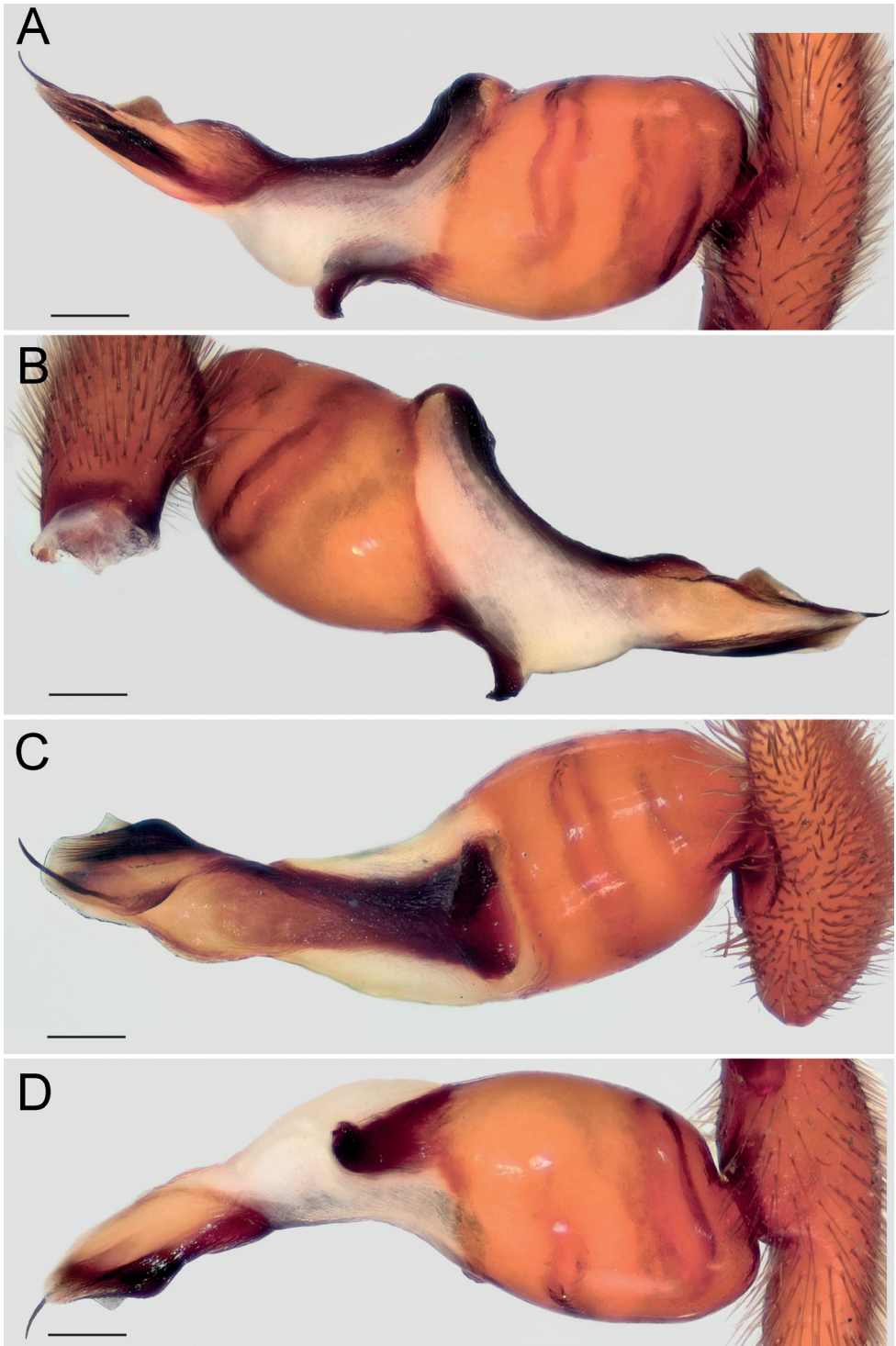


Figure 30. Male of *Dysdera tapuria* sp. nov., bulb **A** retrolateral view **B** prolateral view **C** anterior view **D** posterior view. Scale bars: 0.25 mm.

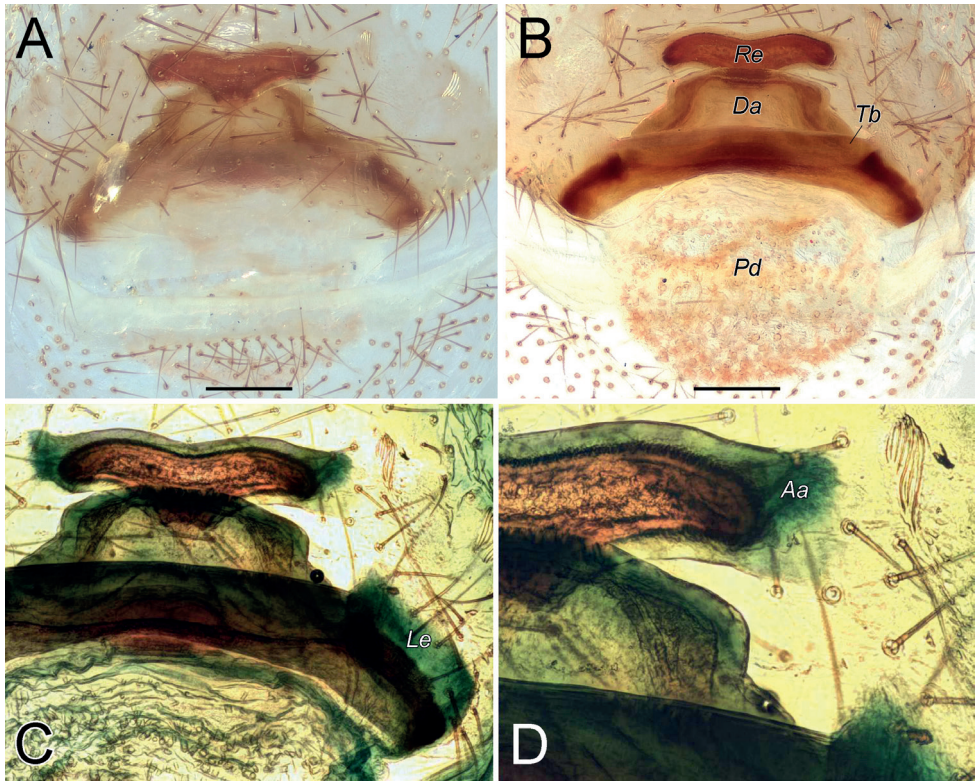


Figure 31. Female of *Dysdera tapuria* sp. nov., endogyne **A** ventral view **B–D** dorsal view. Scale bars: 0.25 mm. Abbreviations: *Aa* – anterior angle, *Da* – dorsal arch, *Le* – lateral edge, *Pd* – posterior diverticulum, *Re* – receptacle, *Tb* – transverse bar.

Female. Habitus as in Fig. 29D–F. Total length 18.1. Carapace 7.77 long, 6.01 wide. Eye diameters: AME 0.30, PME 0.30, PLE 0.34. Colouration as in male. Measurements of legs: I: 14.24 (3.99, 2.54, 3.62, 3.44, 0.65), II: 13.46 (4.31, 2.10, 3.22, 3.06, 0.77), III: 10.20 (2.96, 1.70, 1.97, 2.75, 0.82), IV: 13.08 (3.99, 1.72, 2.85, 3.62, 0.90). Spination: I: Fe: 2pl. II: Fe: 2pl. III: Fe: 1pl; Ti: 2pl, 2rl, 4v; Mt: 3pl, 4rl, 5v. IV: Fe: 3d; Ti: 2pl, 2rl, 6v; Mt: 5pl, 4rl, 5v.

Endogyne as in Fig. 31A–D; length/width ratio ca. 3; receptacle (*Re*) with shallow median concavity, ca. 4.5× longer than wide, anterior angles (*Aa*) indistinct; dorsal arch (*Da*) trapezoidal, posterior margin ca. 1.6× longer than anterior, anterior angles rounded; transverse bar (*Tb*) almost 2× longer and slightly wider than receptacle; transverse bar's anterior margin straight, posterior margin arched; lateral edges (*Le*) very wide, directed latero-posteriorly; posterior diverticulum (*Pd*) rounded.

Distribution. Known only from the listed localities in Mazandaran Province, northern Iran (Fig. 35).

ninnii species group

Diagnosis. This group can be diagnosed by a combination of the following characters: chelicerae shorter than the width of carapace, carapace relatively short with anteriorly converging lateral margins, and bulb with simple crest, simple apex bearing a long subapical tooth, and a crescent-shaped lateral projection (Deeleman-Reinhold and Deeleman 1988).

Dysdera genoensis sp. nov.

<https://zoobank.org/0B0CBC7E-F121-4D54-BC35-364827CB6ECC>

Figs 32A–F, 33A–F, 34A, B

Type material. *Holotype* ♂ (ZMUT), IRAN: Hormozgan Province: Geno Biosphere Reserve, 27°22'N, 56°07'E, 02.2020 (A. Zamani). *Paratypes*: 3♀ (ZMUT), same data as the holotype.

Etymology. The specific epithet is an adjective, referring to the type locality of the species.

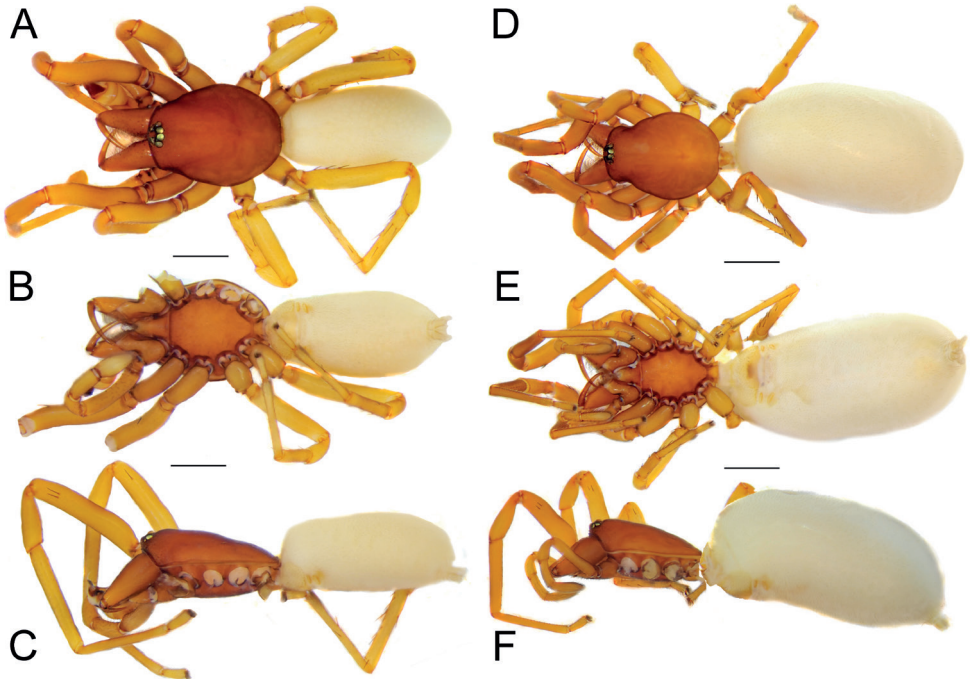


Figure 32. Male (A–C) and female (D–F) of *Dysdera genoensis* sp. nov., habitus A, D dorsal view B, E ventral view C, F lateral view. Scale bars: 1.0 mm.

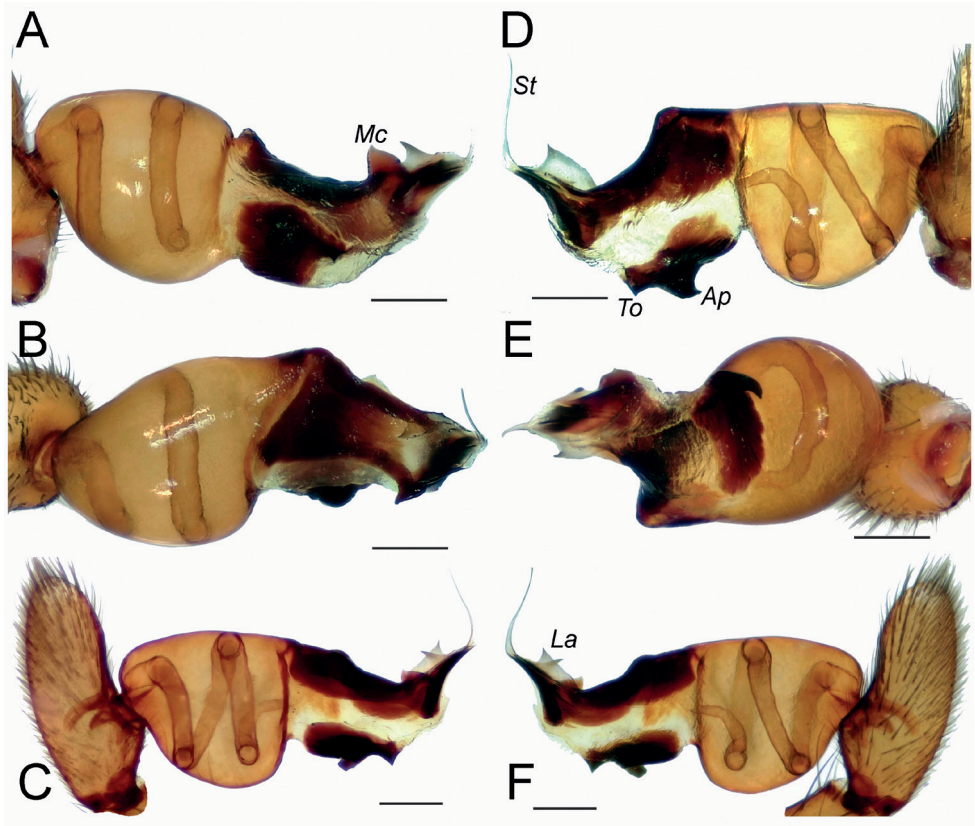


Figure 33. Male of *Dysdera genoensis* sp. nov., bulb **A** proanterior view **B** anterior view **C** prolateral view **D** retroposterior view **E** posterior view **F** retrolateral view. Scale bars: 0.25 mm. Abbreviations: *Ap* – posterior apophysis, *La* – laminae, *Mc* – median crest, *St* – stylus, *To* – triangular outgrowth.

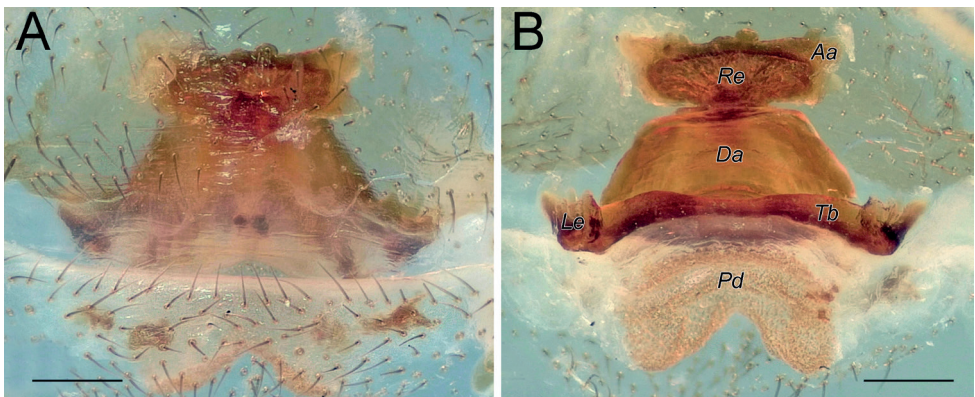


Figure 34. Female of *Dysdera genoensis* sp. nov., endogyne **A** ventral view **B** dorsal view. Scale bars: 0.25 mm. Abbreviations: *Aa* – anterior angle, *Da* – dorsal arch, *Le* – lateral edge, *Pd* – posterior diverticulum, *Re* – receptacle, *Tb* – transverse bar.

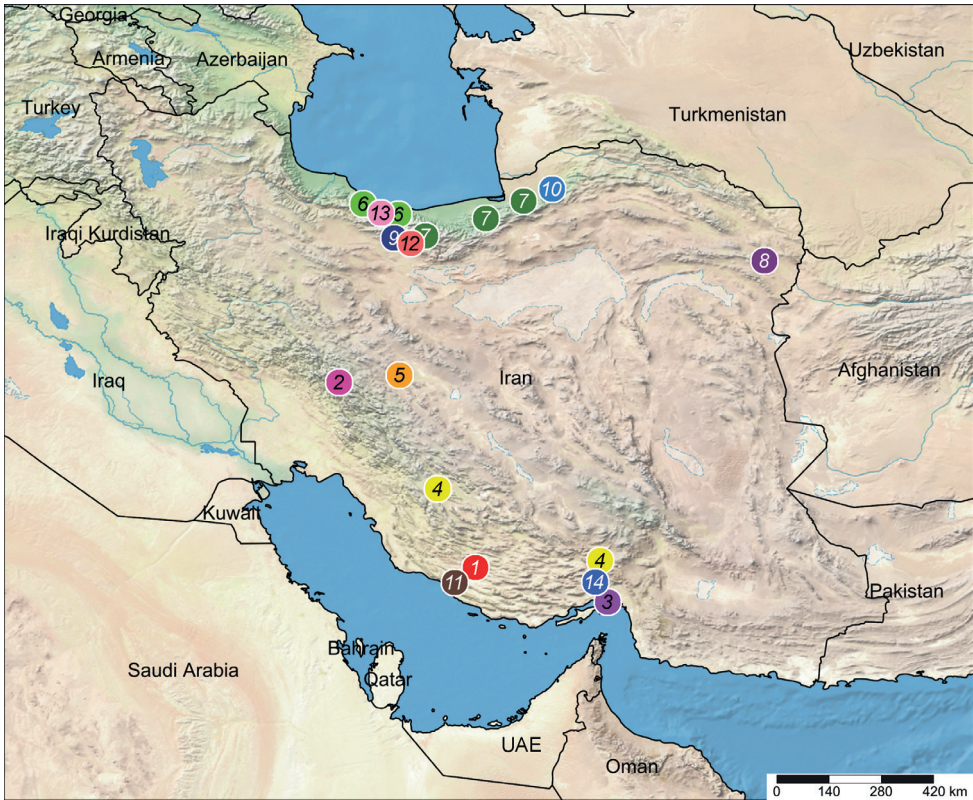


Figure 35. Distribution records of *Dysdera* spp. in Iran 1 *D. achaemenes* sp. nov. 2 *D. bakhtiari* sp. nov. 3 *D. hormuzensis* sp. nov. 4 *D. iranica* sp. nov. 5 *D. isfahanica* sp. nov. 6 *D. mazeruni* sp. nov. 7 *D. persica* sp. nov. 8 *D. pococki* 9 *D. sagartia* sp. nov. and *D. medes* sp. nov. 10 *D. verkana* sp. nov. 11 *D. xerxesi* sp. nov. 12 *D. damavandica* sp. nov. 13 *D. tapuria* sp. nov. 14 *D. genoensis* sp. nov.

Diagnosis. The male of the new species differs from those of its congeners by having weakly sclerotized bent stylus (*St*) (Fig. 32C, F) (vs. stylus, if present, not bent). The female of this species is very similar to that of *D. iranica* sp. nov. by having a wide receptacle (i.e., $> 2\times$ wider than transverse bar), but differs by the relatively wider receptacle lacking an anterior triangular projection, and the presence of a median concavity on the transverse bar (vs. receptacle with triangular projection, transverse bar without concavity).

Description. Male (Holotype). Habitus as in Fig. 32A–C. Total length 5.49. Carapace 2.42 long, 1.88 wide. Eye diameters: AME 0.15, PME 0.13, PLE 0.11. Carapace, sternum, chelicerae, labium, and maxillae pale reddish. Legs orange. Abdomen cream-coloured, without any pattern. Spinnerets uniformly cream-coloured. Measurements of legs: I: 11.78 (3.23, 1.90, 2.87, 3.02, 0.76), II: 10.21 (2.91, 1.60, 2.52, 2.45, 0.73), III: 7.98 (2.31, 1.15, 1.65, 2.29, 0.58), IV: 10.30 (2.89, 1.44, 2.28, 2.96, 0.73). Spination: I: Fe: 2pl. II: Fe: 1pl. III: Fe: 1pl; Ti: 3pl, 2v; Mt: 3pl, 4rl, 3v. IV: Fe: 4d; Pa: 1pl; Ti: 3pl, 1rl, 4v; Mt: 1pl, 1rl, 3v.

Palp as in Fig. 33A–F; bulb ca. 2.3× longer than wide; tegulum bell-shaped, almost as long as wide; psemبولus as long as tegulum, length/width ratio ca. 1.25; median crest (*Mc*) triangular; apex with two triangular laminae (*La*); posterior apophysis (*Ap*) claw-shaped, accompanied by a triangular outgrowth (*Tb*) anteriorly; incision between tegulum and psemبولus absent; stylus (*St*) bent, long, and weakly sclerotized.

Female. Habitus as in Fig. 32D–F. Total length 6.52. Carapace 2.06 long, 1.59 wide. Eye diameters: AME 0.11, PME 0.11, PLE 0.10. Colouration as in male. Measurements of legs: I: 7.71 (1.93, 1.37, 2.01, 1.88, 0.52), II: 7.31 (1.99, 1.26, 1.77, 1.74, 0.55), III: 5.84 (1.58, 0.92, 1.19, 1.65, 0.50), IV: 7.77 (2.19, 1.21, 1.79, 2.04, 0.54). Spination: I: Fe: 2pl. II: Fe: 2pl. III: Fe: 1pl; Ti: 2pl, 1rl, 5v; Mt: 5pl, 2rl. IV: Fe: 5d, 1rl; Pa: 1rl, 1v; Ti: 5pl, 1rl, 5v; Mt: 4pl, 2rl, 3v.

Endogyne as in Fig. 34A, B; length/width ratio ca. 2; receptacle (*Re*) inverted trapezoidal, anterior margin 1.4× longer than posterior; dorsal arch (*Da*) trapezoidal, posterior margin 1.6× longer than anterior margin, 1.25× longer than receptacle; anterior margin of transverse bar (*Tb*) with median concavity, posterior margin arched; lateral edges (*Le*) small, approximately as long as wide; posterior diverticulum (*Pa*) bilobed.

Distribution. Known only from the type locality in Hormozgan Province, southern Iran (Fig. 35).

Discussion

Considering the results of this paper, there are 17 species of three genera of Dysderidae known from Iran. This number is considerably lower than what is known for the neighbouring Turkey (i.e., 69 species in seven genera; Danişman et al. 2022) and the Caucasus (i.e., 65 species in seven genera; Otto 2022). The material treated here, although comprising a relatively large number of new species, were collected in a few localities primarily in northern parts of the country (Fig. 35). Considering the small distribution ranges of most dysderids and the presence of several mountainous regions and biodiversity hotspots in Iran (e.g., Alborz and Zagros mountain ranges; Farashi and Shariati 2017), it can be assumed that any new material from this region could potentially comprise further undescribed species. It is possible that the true diversity of Dysderidae in Iran could range between 40 to 60 species, if not higher; interestingly, the widespread and cosmopolitan *D. crocata* has not yet been recorded from this country.

Furthermore, the diversity of Dysderidae in Central Asia is relatively low (i.e., 21 species of three genera; Mikhailov 2022). Most of the species (18) belong to *Dysdera*, and *Dysderella* and *Harpactea* are known only from western Turkmenistan (Dunin 1992; Zamani et al. 2017). The eastern boundary of the family is westernmost Xinjiang, and it appears that their diversity gradually decreases east of the Caucasus (Fomichev and Marusik 2021).

Acknowledgments

We are grateful to Amir Hossein Bakhtiari (Tehran, Iran), Denis Kasatkin (Moscow, Russia), Razieh Rafiei-Jahed (Gorgan, Iran), and Alireza Savoji (Tehran, Iran) for providing us with their collected specimens, Peter J. Schwendinger, and Lionel Monod (MHNG) for arranging a loan of the material deposited in their collection, Ilari E. Sääksjärvi (University of Turku, Finland) for providing funding for publication of this paper, and the editor Gergin Blagoev (University of Guelph, Canada) and the reviewer Christo Deltchev (National Museum of Natural History, Sofia, Bulgaria) for their valuable comments on the manuscript. YM is thankful toward Seppo Koponen (University of Turku, Finland) for arranging the stay in Turku.

References

- Charitonov DE (1956) Obzor paukov semeistva Dysderidae fauny SSSR. Uchenye Zapiski Molotovskogo Gosudarstvennogo Universiteta Imeni A. M. Gor'kogo 10: 17–39.
- Coddington JA (1983) A temporary slide-mount allowing precise manipulation of small structures. Verhandlungen des Naturwissenschaftlichen Vereins in Hamburg 26: 291–292.
- Cooke JAL (1965) Spider genus *Dysdera* (Araneae, Dysderidae). Nature 205(4975): 1027–1028. <https://doi.org/10.1038/2051027b0>
- Danişman T, Kunt KB, Özkütük RS (2022) The Checklist of the Spiders of Turkey. Version 2022. <http://www.spidersofturkey.info>
- Deeleman-Reinhold CL, Deeleman PR (1988) Revision des Dysderinae (Araneae, Dysderidae), les espèces méditerranéennes occidentales exceptées. Tijdschrift voor Entomologie 131: 141–269.
- Dimitrov D (2021) Description of *Dysdera zonsteini* n. sp. (Arachnida: Araneae: Dysderidae) from Turkmenistan. Zootaxa 4938(5): 588–594. <https://doi.org/10.11646/zootaxa.4938.5.6>
- Dunin PM (1982) New data on *Dysdera concinna* L. Koch (Aranei, Dysderidae). Zoologicheskii Zhurnal 61: 605–607. [in Russian]
- Dunin PM (1985) The spider family Dysderidae (Aranei, Haplogynae) in the Soviet Central Asia. Zoologicheskii Zhurnal 139: 114–120.
- Dunin PM (1992) The spider family Dysderidae of the Caucasian fauna (Arachnida Aranei Haplogynae). Arthropoda Selecta 1(3): 35–76.
- Dunin PM, Fet VY (1985) *Dysdera transcaspica* sp. n. (Aranei, Dysderidae) from Turkmenia. Zoologicheskii Zhurnal 64: 298–300.
- Dunlop JA, Penney D, Jekel D (2020) A summary list of fossil spiders and their relatives. World Spider Catalog. Version 20.5. Natural History Museum Bern, Bern. <http://wsc.nmbe.ch> [accessed 6 November 2022]
- Farashi A, Shariati M (2017) Biodiversity hotspots and conservation gaps in Iran. Journal for Nature Conservation 39: 37–57. <https://doi.org/10.1016/j.jnc.2017.06.003>

- Fomichev AA, Marusik YM (2021) Notes on the spider genus *Dysdera* Latreille, 1804 (Araneae: Dysderidae) in Central Asia. *Zootaxa* 5006(1): 73–89. <https://doi.org/10.11646/zootaxa.5006.1.10>
- Forster RR, Platnick NI (1985) A review of the austral spider family Orsolobidae (Arachnida, Araneae), with notes on the superfamily Dysderoidea. *Bulletin of the American Museum of Natural History* 181: 1–230.
- Jocqué R, Dippenaar-Schoeman AS (2006) Spider families of the world. Musée Royal de l'Afrique Central Tervuren, 336 pp.
- Kunt KB, Elverici M, Yağmur EA, Özkütük RS (2019) *Kut* gen. nov., a new troglomorphic spider genus from Turkey (Araneae, Dysderidae). *Subterranean Biology* 32: 95–109. <https://doi.org/10.3897/subtbiol.32.46534>
- Le Peru B (2011) The spiders of Europe, a synthesis of data: Volume 1 Atypidae to Theridiidae. *Mémoires de la Société Linnéenne de Lyon* 2: 1–522.
- Mikhailov KG (2022) Progress in the study of the spider fauna (Aranei) of Russia and neighbouring regions: a 2020 update. *Invertebrate Zoology* 19(3): 295–304. [Supplements 1.01–1.15, 2.01–2.24] <https://doi.org/10.15298/invertzool.19.3.02>
- Otto S (2022) Caucasian Spiders. A faunistic database on the spiders of the Caucasus. Version 02.2022. <https://caucasus-spiders.info/>
- Petrunkévitch AI (1971) Chiapas amber spiders, II. University of California Publications in Entomology 63: 1–44.
- Pocock RI (1889) Arachnida, Chilopoda and Crustacea. In: Aitchison JET (Ed.) *The Zoology of the Afghan Delimitation Commission*. Transactions of the Linnean Society of London (Zoology, 2) 5(3): 110–121. [pl. 13] <https://doi.org/10.1111/j.1096-3642.1889.tb00159.x>
- Roewer CF (1955) Die Araneen der Österreichischen Iran-Expedition 1949/50. *Sitzungsberichte der Österreichischen Akademie der Wissenschaften (I)* 164: 751–782.
- Straus A (1967) Zur Paläontologie des Pliozäns von Willershausen. *Berichte der Naturhistorischen Gesellschaft Hannover* 111: 15–24.
- WSC (2022) World Spider Catalog, Version 23.5. Natural History Museum Bern. <http://wsc.nmbe.ch> [accessed on 22.8.2022]
- Zamani A, Marusik YM, Koponen S (2017) First description of the male of the easternmost *Harpactea* species, *H. parthica* (Araneae: Dysderidae). *Zootaxa* 4238(2): 258–262. <https://doi.org/10.11646/zootaxa.4238.2.6>
- Zamani A, Mirshamsi O, Marusik YM, Moradmand M (2022a) The Checklist of the Spiders of Iran. Version 2022. <http://www.spiders.ir>
- Zamani A, Nadolny AA, Dolejš P (2022b) New data on the spider fauna of Iran (Arachnida: Araneae), Part X. *Arachnology* 19(2): 551–573. <https://doi.org/10.13156/arac.2022.19.2.551>

A new species of the genus *Liotyphlops* Peters, 1881 (Serpentes, Anomalepididae) from Colombia and the synonymization of *Liotyphlops beui* (Amaral, 1924) with *Liotyphlops ternetzii* (Boulenger, 1896)

Fidélis Júnio Marra Santos¹

¹ Pontifícia Universidade Católica do Rio Grande do Sul (PUCRS), Laboratory of Vertebrate Systematics. Av. Ipiranga, 6681 Partenon; 90619-900, Porto Alegre, Rio Grande do Sul, Brazil

Corresponding author: Fidélis Júnio Marra Santos (fidelismarra@gmail.com)

Academic editor: Robert Jadin | Received 8 September 2022 | Accepted 3 January 2023 | Published 7 February 2023

<https://zoobank.org/9F4ADF00-1BE7-4878-9B98-FB23B72B4435>

Citation: Marra Santos FJ (2023) A new species of the genus *Liotyphlops* Peters, 1881 (Serpentes, Anomalepididae) from Colombia and the synonymization of *Liotyphlops beui* (Amaral, 1924) with *Liotyphlops ternetzii* (Boulenger, 1896). ZooKeys 1146: 87–114. <https://doi.org/10.3897/zookeys.1146.94607>

Abstract

A new species of *Liotyphlops* Peters, 1881, *Liotyphlops palauophis* **sp. nov.**, is described from the neighborhoods of Bogota, Colombia from a previous syntype of *L. anops*, and a lectotype is designated for the latter species. The new species is readily distinguished from congeners by having the frontal scale divided (vs single), and a central foramen in the parabasisphenoid (vs foramen absent). High-resolution x-ray computed tomography (HRXCT) was used to study and present data on the skull of the holotype of the new species, the lectotype of *L. anops*, and the holotype of *L. ternetzii*. Additionally, extensive study of skull characters and external morphology failed to find diagnostic characters to differentiate *L. beui* and *L. ternetzii*, and the former is here considered a junior synonym of *L. ternetzii*, which is also redescribed.

Keywords

Biodiversity, *Liotyphlops palauophis* sp. nov., neotropics, reptiles, Scolecophidia, taxonomy

Introduction

The genus *Liotyphlops* Peters, 1881 is a group of small, cryptozoic blindsnakes, distributed in the Neotropics, from Costa Rica to Argentina. *Liotyphlops* is currently composed of 13 species (Santos and Reis 2018; Boundy 2021; Linares-Vargas et al. 2021): *Liotyphlops albirostris* (Peters, 1858); *L. anops* (Cope, 1899); *L. argaleus* Dixon & Kofron, 1984; *L. beui* (Amaral, 1924); *L. bondensis* (Griffin, 1916); *L. caissara* Centeno, Sawaya & Germano, 2010; *L. haadi* Silva-Haad, Franco & Maldonado, 2008; *L. schubarti* Vanzolini, 1948; *L. sousai* Santos & Reis, 2018, *L. taylori* Santos & Reis, 2018, *L. ternetzii* (Boulenger, 1896); *L. trefauti* Freire, Caramaschi & Argôlo, 2007, and *L. wilderi* (Garman, 1883). Brazil has the greatest diversity of *Liotyphlops* snakes, with eight valid species. In recent years, the description of new species of Anomalepididae have been restricted to the genus *Liotyphlops* (Freire et al. 2007; Haad et al. 2008; Centeno et al. 2010; Santos and Reis 2018) and revalidations of supposed synonyms of *L. albirostris* (Linares-Vargas et al. 2021). In the present study, an additional new species of *Liotyphlops* is described from Colombia.

Helminthophis anops was described by Cope (1899) based on two specimens; he wrote: “The collection which furnishes the basis of the investigation presented in the following pages was made in Colombia, near Bogota, for the World’s Exposition of Chicago, where it was exhibited in the department of New Granada. The number of species is fifty-four, of which nine are new to science. I have not been able to ascertain the exact localities at which the specimens were obtained, but most of them, it is believed, were found in the neighborhood of Bogota” (Cope 1899: 3). Subsequently, Dunn (1944) transferred *H. anops* to *Liotyphlops*, also in Anomalepididae. Cope (1899: 10–11) also wrote: “This species has a tendency to subdivision of scales. In one of the two specimens the frontal is divided into two regular scales, and in another the lower extremity of the first labial is cut off on one side”. The holotype of the new species described here (AMNH R-9550) is one of the two syntypes of *H. anops* and distinct from the other syntype (AMNH R-17540) in possessing, among other diagnostic characters, the frontal scale divided (vs single), and a central foramen in the parabasisphenoid (vs foramen absent). The other syntype (AMNH R-17540) is consistent with the species currently identified in Colombia as *L. anops*.

Taxonomic changes over the past century have also included two other species of *Liotyphlops*: *L. beui* and *L. ternetzii*. The original description of *L. ternetzii*, by Boulenger (1896, as *Helminthophis ternetzii*) was based on a single specimen from “Paraguay” (holotype BMNH 1946.1.11.77). Later, Smith and Grant (1958) recognized *Liotyphlops* as a genus distinct from *Helminthophis*, highlighting as a diagnostic character the separation of prefrontal scales in *Liotyphlops*, while in *Helminthophis* the prefrontal scales are widely in contact. They transferred Boulenger’s species to *Liotyphlops*. Boulenger (1896: 584) characterized this species as: “rostral two fifths the width of the head, extending nearly to the level of the eyes, forming a broad, straight suture with the frontal, which is about twice as broad as long; eye scarcely distinguishable through the ocular; two superposed preoculars

and a subocular; four upper labials, first largest, second and third in contact with the lower preocular, third and fourth in contact with the subocular. Diameter of body 52 times in total length; tail nearly twice as long as broad, ending in a spine. 22 scales round the body. Olive above and beneath; head and anal region yellowish. Total length 335 mm.”

Liotyphlops beui was originally described by Amaral (1924), as *Helminthophis beui* from Butantan, São Paulo, Brazil (holotype IB 1806 and paratypes IB 281, IB 282, IB 652, and IB 1041). Amaral (1924: 29) characterized his new species as: “snout acutely rounded; rostral about two fifths the width of the head, not extending posteriorly to the vertical plane of the eyes, rounded posteriorly and forming a narrow suture with the frontal; frontal only about three times as wide as long; one subocular; two preoculars; eye under the suture between the ocular and lower preocular; four upper labials, 1st largest, 2nd and 3rd in contact with the subocular, which separates them from the lower preocular; prefrontal separated from the 2nd labial by the lower preocular, nasal and subocular. Tail more than twice as long as broad, ending in a spine. 22 scale rows around the body. Dark brown to blackish brown; head, as well as anal region and surroundings, light yellow; terminal spine yellowish. Total length, 290 mm; tail, 10 mm.” Only five years after the original description, *H. beui* was placed in the synonymy of *H. ternetzii* by Amaral (1929) himself, but 55 years later Dixon and Kofron (1984) believed the species was valid and removed it from the synonymy of *L. ternetzii* based on the possession of 20 scale rows around the posterior body (22 in *L. ternetzii*) and fewer dorsal scales, 384–455 (vs 463–510 in *L. ternetzii*). Despite some authors maintaining *L. beui* as synonym of *L. ternetzii* (e.g., Peters et al. 1986), most subsequent authors have followed Dixon and Kofron (1984) and treated *L. beui* as a valid species (McDiarmid et al. 1999; Freire et al. 2007; Haad et al. 2008; Centeno et al. 2010; Wallach et al. 2014; Santos and Reis 2018; Boundy 2021; Linares-Vargas et al. 2021).

Here it is important to highlight the research of Dixon and Kofron (1984). They observed that most of the characters utilized for described forms are variable within populations, and occasionally the squamation is different on each side of the head in an individual. Also, according to Dixon and Kofron (1984), the nasal scale is divided and is variously called upper and lower nasals, preseminasals and postseminasals, anterior nasals and postnasals, or just nasals; additionally, the lateral and dorsomedian head scales are variously called subocular(s), preocular(s), ocular, supraocular(s), frontal, and postfrontal(s). They explained that much depends upon one’s concept of the position of the scales as to whether there are two suboculars and one preocular, or two preocular and one subocular, or two supraoculars and one preocular, or two preoculars and one supraocular, etc. Accordingly to Dixon and Kofron (1984) the presence or absence of the division and/or fusion of scales on one side of the head and not on the other has been largely ignored by most describers of *Liotyphlops* species, which has, therefore, resulted in poor species concepts; the only scales that appear to be consistently defined in all writings are the rostral, prefrontal, and frontal scales.

In this paper, the validity of *L. beui* is revisited and *L. ternetzii* is redescribed. A new species of *Liotyphlops* is also described from the neighborhoods of Bogota, Colombia, a lectotype is designated for *L. anops*, and that lectotype is also redescribed. High-resolution x-ray computed tomography (HRXCT) was used to present data on the skull of the holotype of *L. ternetzii* and the holotype of the new species.

Materials and methods

I adopted the definition of the Unified Species Concept (Queiroz 2007), in which species are equated with independently evolving metapopulation lineages. In the absence of autapomorphy for species, consistent morphological difference among separate populations is used as a proxy for lineage independence. The study of external morphology was conducted under a stereomicroscope. The terminology used for the head squamation and scale counts follows Dixon and Kofron (1984) and Santos and Reis (2018). Measurements were taken with digital calipers and are presented as percent of total length (TL), except for subunits of the head, which are presented as percent of head length (HL). The results of morphometric analyzes are presented in the description. Specimens were not sexed and only adult specimens were examined (see Appendix 1). The photographs were obtained using a digital Nikon D5100 camera. For drawing preparation, a Wacom Intuos Draw CTL490DW digital tablet was used with the desktop digital stereomicroscope COSMOS LCD.

For the comparisons of *Liotyphlops ternetzii* and *L. beui*, the holotype of the former and paratypes of the latter were used. In addition, 50 specimens of each of these two species were measured and counted for the comparisons.

The head of the holotype of *L. ternetzii* and paratype of *L. beui* were studied by high-resolution x-ray computed tomography (HRXCT) at the high-resolution x-ray CT facility of the University of Texas at Austin using an Xradia microCT Scanner, and the holotype of the new species of *Liotyphlops* was studied by HRXCT at the high-resolution x-ray CT facility at Pontifícia Universidade Católica do Rio Grande do Sul using a Skyscan 1173 microfocus x-ray CT. The datasets were rendered in three dimensions using CTvox v. 3.2 (Bruker microCT, Inc., Billerica, MA) for Windows.

The terminology used for bones follows Rieppel et al. (2009), Santos and Reis (2018), and Santos and Reis (2019). The locality of the specimens was plotted using Google Earth Pro v. 7.3.2.5495, and the map was built with ArcMap (ArcGis) v. 10.4.1 for desktop using the WGS1984 geodetic datum. Geographical coordinates for historical specimens with imprecise locality records were approximated using the best evidence available and plotted with Google Earth. Only specimens actually examined were used in the map. Institutional abbreviations of specimens examined follow Sabaj (2020), with the addition of CEPB (Centro de Estudos e Pesquisas Biológicas da Pontifícia Universidade Católica de Goiás, Goiânia, Brazil).

Results

Taxonomic account

Liotyphlops palauophis sp. nov.

<https://zoobank.org/0CD30C35-2263-491C-BB62-2494019740C8>

Figs 1–6, Table 1

Helminthophis anops Cope, 1899 (in part). Syntype of *H. anops*.

Type material. *Holotype*. AMNH R-9550, 361 mm TL, Colombia, neighborhood of Bogota, 1899.

Diagnosis. *Liotyphlops palauophis* sp. nov. is distinguished from all other *Liotyphlops* by having the frontal scale divided (vs single) and a central foramen in the parabasisphenoid (vs foramen absent). It is further distinguished from *L. albirostris*, *L. argaleus*, *L. bondensis*, *L. caissara*, *L. haadi*, *L. trefauti*, and *L. wilderi* in having two scales (vs one scale) contacting the posterior edge of the nasal between the second supralabial and prefrontal. It is further distinguished from *L. beui*, *L. schubarti*, *L. taylori*, and *L. ternetzii* by having four (vs three) scales contacting the posterior edge of the prefrontal. It is distinguished from *L. anops* by having 28/26/26 scales around the body and 19 subcaudal scales (vs 26/24/24 scales around the body and 12–14 subcaudal scales), and from *L. sousai* in having 573 dorsal scales and 561 ventral scales (vs 439 dorsal scales and 427 ventral scales).

Description. Meristic data in Table 1. Total length 361.2 mm, head length 5.3 mm (1.5% TL), snout–vent length 353 mm (97.7% TL), tail length 8.2 mm (2.3% TL), head width 3.8 mm (71.7% HL), and head height 3.1 mm (58.5% HL). Body covered with cycloid scales. Rostral scale large, longer than wide, contacting nasals anterolaterally, prefrontals laterally, and divided frontal posteriorly. Pair of triangular prefrontals bordered anterolaterally by rostral, ventrally by large divided nasal, and dorsoposteriorly by frontal. Posterior edge of prefrontals passing posterior edge of rostral. Frontal scale divided. Nasal scale divided and bordered anteriorly by rostral, dorsally by prefrontal, ventrally by first and second supralabials, and posteriorly by two scales that lie between prefrontal and second supralabial. Eye spot not visible. Four scales contacting posterior edge of prefrontal (three cycloid scales + frontal). Two scales contacting posterior edge of nasal between second supralabial and prefrontal. Six scales in first vertical row of dorsal scales. Mental triangular, not divided, wider than long, contacting first infralabials. Supralabials four, infralabials three. Scales around body 28/26/26. Dorsal scales 573, ventral scales 561, and subcaudal scales 19.

Description of skull. High-resolution x-ray computed tomography of skull bones in Figs 3–5. Main body of premaxilla on ventral surface of snout. Maxilla–premaxilla contact widely separated. Lateral maxillary foramina absent. Maxilla alveolar row oriented transversely. Nasal fused. Nasal–frontal boundary convex pos-



Figure 1. Holotype of *Liotyphlops palauophis* sp. nov., AMNH R-9550, 361.2 mm TL, Colombia, neighborhood of Bogota. Scale bar: 5 mm.

Table 1. Meristic characters of species of *Liotyphlops* from the specimens examined in this study, presented as ranges with minimum, maximum, and mode in parentheses. **SPEP** = number of scales contacting posterior edge of prefrontal; **SPEN** = number of scales contacting posterior edge of nasal between second supralabial and prefrontal; **SFVRD** = number of scales in the first vertical row of dorsals; **SL** = number of supralabial scales; **IL** = number of infralabial scales; **ASR** = number of anterior scale rows around body; **MSR** = number of scale rows around the midbody; **PSR** = number of posterior scale rows around body; **DSR** = number of dorsal scale rows; **VSR** = number of ventral scales rows; **SC** = number of subcaudal scales. **n** = number of specimens examined in this study. ^a = number of specimens examined by Santos and Reis (2018). ^b = number of specimens examined by Centeno et al. (2010). ^c = number of specimens examined by Freire et al. (2007). ^d = number of specimens examined by Linares-Vargas et al. (2021).

Species/Count	n	SPEP	SPEN	SFVRD	SL	IL	ASR	MSR	PSR	DSR	VSR	SC
<i>L. albirostris</i> ^a	6	3–3(3)	1–1(1)	5–5(5)	4–4(4)	3–3(3)	24–26(26)	22–22(22)	22–22(22)	432–478	417–453	12–17(12)
<i>L. anops</i> ^a	3	4–4(4)	2–2(2)	5–6(5)	4–4(4)	3–3(3)	26–26(26)	24–24(24)	24–24(24)	562–597	531–572	12–14
<i>L. argaleus</i> ^a	1	4	1	4	4	3	25	23	22	497	472	16
<i>L. beui</i> ^a	50	3–3(3)	2–2(2)	5–6(5)	4–4(4)	3–3(3)	22–26(22)	20–22(22)	20–22(20)	366–532(453)	348–511(364)	11–22(12)
<i>L. bondensis</i> ^d	17	3	1	4	4	3	24	22	22	363–449	347–434	11–17
<i>L. caissara</i> ^b	1	3	1	4	3	3	22	20	20	326	308	10
<i>L. baadi</i> ^a	2	3–3(3)	1–1(1)	4–4(4)	4–4(4)	3–3(3)	20–20(20)	19–20	18–20	333–384	309–348	11–12
<i>L. palauophis</i>	1	4	2	6	4	3	28	26	26	573	561	19
<i>L. schubarti</i> ^a	5	3–3(3)	2–2(2)	5–5(5)	4–4(4)	3–3(3)	22–24(22)	20–22(20)	20–20(20)	417–463	398–451	11–14(13)
<i>L. sousai</i> ^a	1	4	2	6	4	3	24	22	20	439	427	13
<i>L. taylori</i> ^a	1	3	2	5	4	2	22	20	20	455	441	14
<i>L. ternetzii</i> ^a	50	3–3(3)	2–2(2)	5–6(5)	4–4(4)	3–3(3)	22–26(22)	20–23(20)	20–22(20)	353–539(417)	341–514(381)	11–22(15)
<i>L. trefauti</i> ^c	2	4–4(4)	1–1(1)	5–5(5)	4–4(4)	4–4(4)	22–22(22)	22–22(22)	22–22(22)	520–543	499–531	8(8)
<i>L. wilderi</i> ^a	3	3–3(3)	1–1(1)	4–4(4)	4–4(4)	3–3(3)	22–24(22)	22–22(22)	20–21(20)	385–402	371–383	12–19(12)

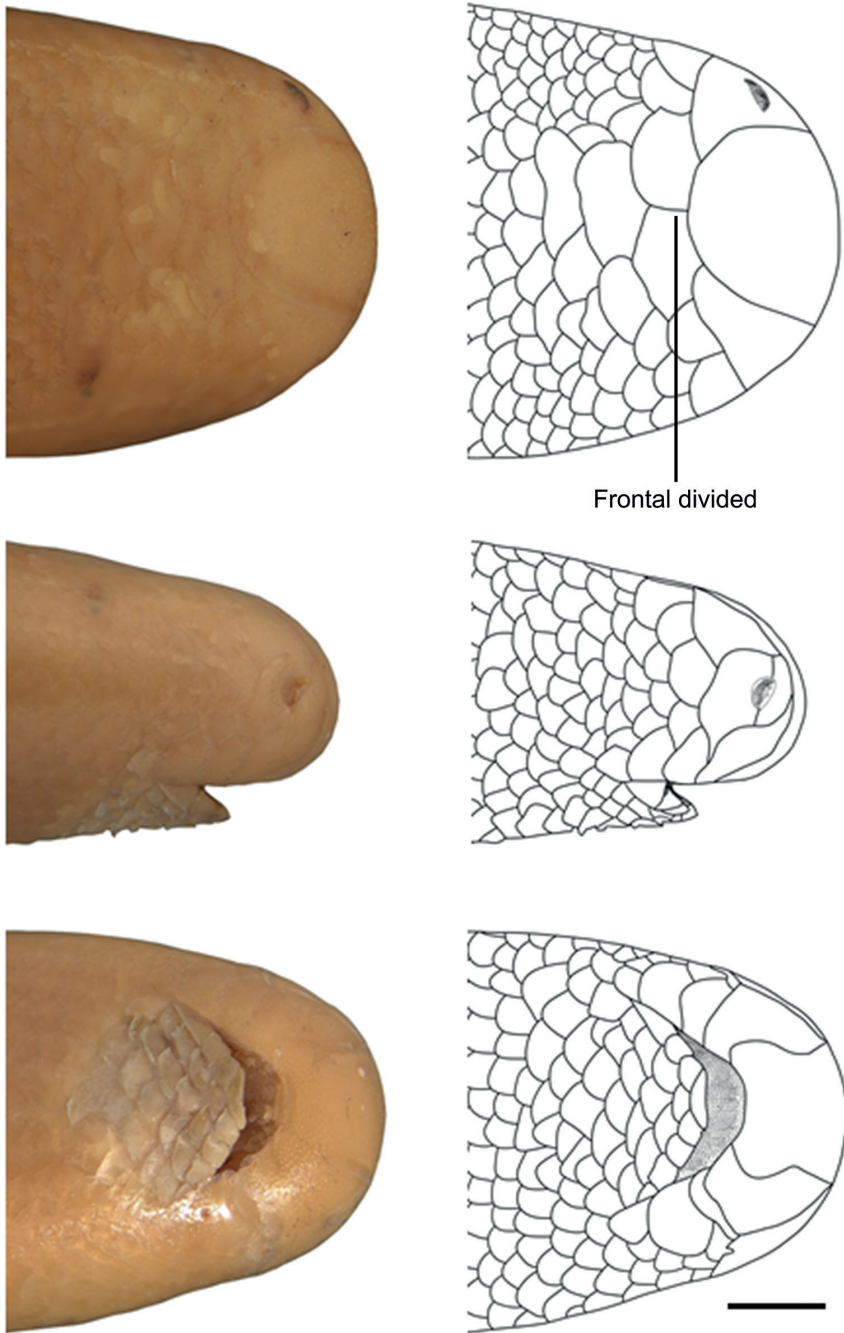


Figure 2. Dorsal (top), lateral (center), and ventral (bottom) views of the head of *Liotyphlops palauophis* sp. nov., AMNH R-9550, holotype. Scale bar: 1 mm.

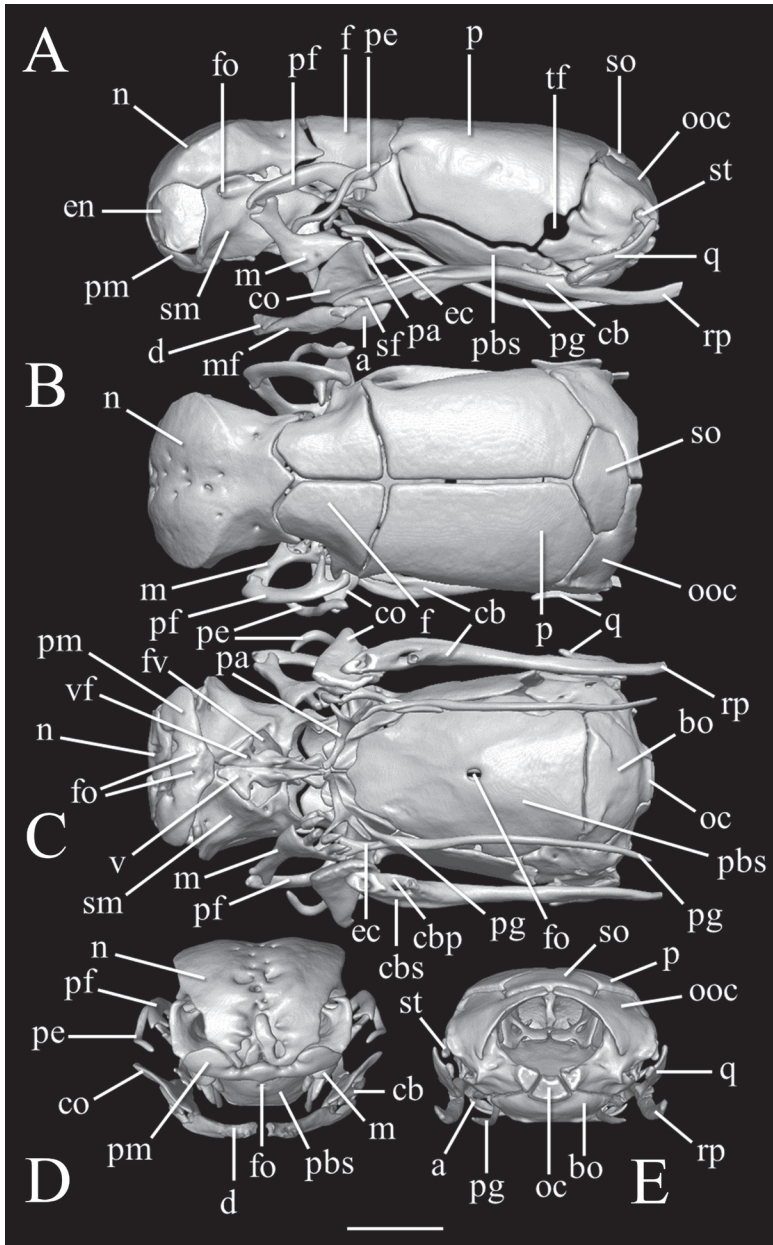


Figure 3. Three-dimensional reconstruction of the skull of *Liotyphlops palauophis* sp. nov., AMNH R-9550, holotype, based on HRXCT data. **A** lateral view **B** dorsal view **C** ventral view with lower jaw partially digitally removed **D** anterior view **E** posterior view. Scale bar: 1 mm. Anatomical abbreviations: **a**: angular; **bo**: basioccipital; **cb**: compound bone; **co**: coronoid; **d**: dentary; **ec**: ectopterygoid; **en**: external naris; **f**: frontal; **fo**: foramen; **fv**: fenestra vomeronasal; **m**: maxilla; **mf**: mental foramen; **n**: nasal; **oc**: occipital condyle; **ooc**: otico-occipital (fused prootic + opisthotic + exoccipital); **p**: parietal; **pa**: palatine; **pbs**: parabasisphenoid; **pe**: postorbital element; **pf**: prefrontal; **pg**: pterygoid; **pm**: premaxilla; **q**: quadrate; **rp**: retroarticular process; **sf**: surangular foramen; **sm**: septomaxilla; **st**: supratemporal; **so**: supraoccipital; **tf**: trigeminal foramen; **v**: vomer; **vf**: vomerine foramen.

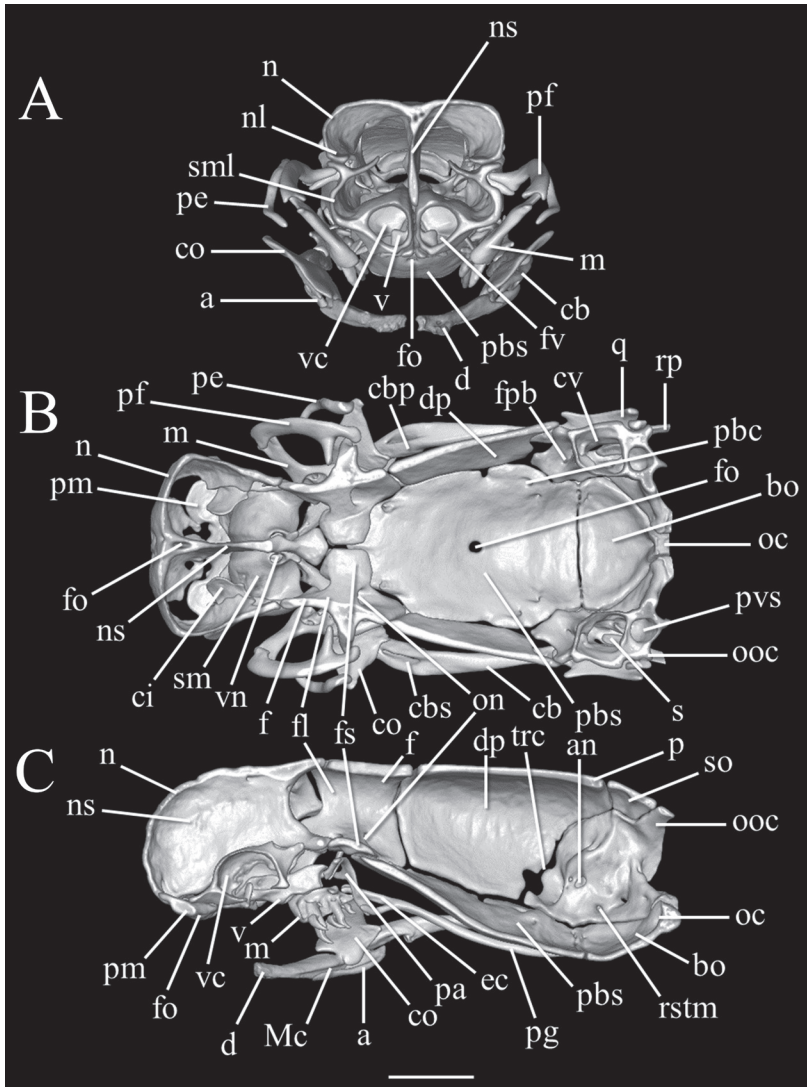


Figure 4. Three-dimensional reconstruction of the skull of *Liotyphlops palauophis* sp. nov., AMNH R-9550, holotype, based on HRXCT data. **A** transversal view **B** frontal view **C** sagittal view. Scale bar: 1 mm. Anatomical abbreviations: **a**: angular; **an**: acoustic nerve foramen; **bo**: basioccipital; **cb**: compound bone; **cbp**: compound bone prearticular component; **cbs**: compound bone surangular component; **ci**: conchal invagination; **co**: coronoid; **cv**: cavum vestibuli; **d**: dentary; **dp**: descensus parietalis; **ec**: ectopterygoid; **en**: external naris; **f**: frontal; **fl**: frontal laterally descending flange; **fo**: foramen; **fpb**: facial nerve palatine branch foramen; **fs**: frontal subolfactory process; **fv**: fenestra vomeronasalis; **m**: maxilla; **Mc**: Meckel's canal; **mf**: mental foramen; **n**: nasal; **nl**: nasal lateral flange; **ns**: medial nasal septum; **oc**: occipital condyle; **on**: optic nerve foramen; **ooc**: otico-occipital (fused prootic + opisthotic + exoccipital); **p**: parietal; **pa**: palatine; **pbc**: parabasal (Vidian) canal; **pbs**: parabasisphenoid; **pe**: postorbital element; **pf**: prefrontal; **pg**: pterygoid; **pm**: premaxilla; **pvs**: posterior vertical semicircular canal; **q**: quadrate; **rp**: retroarticular process; **rstm**: recessus scalae tympani medial aperture; **s**: stapes; **sf**: surangular foramen; **sm**: septomaxilla; **sml**: septomaxilla lateral flange; **st**: supratemporal; **so**: supraoccipital; **tf**: trigeminal foramen; **trc**: trigeminofacialis chamber; **v**: vomer; **vc**: vomeronasal cupola; **vf**: vomerine foramen; **vn**: vomeronasal nerve passage.

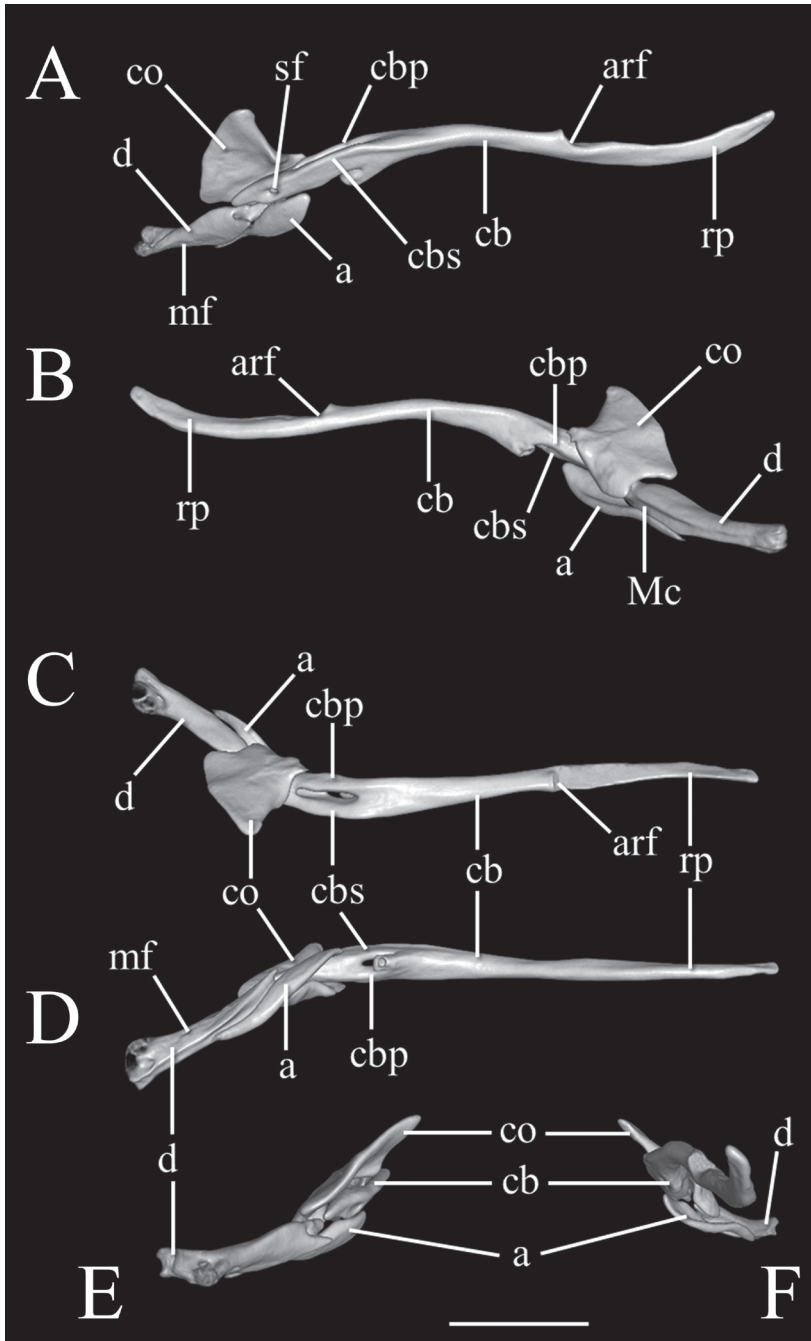


Figure 5. Three-dimensional reconstruction of the lower jaw of *Liotyphlops palauophis* sp. nov., AMNH R-9550, holotype, based on HRXCT data. **A** lateral view **B** medial view **C** dorsal view **D** ventral view **E** anterior view **F** posterior view. Scale bar: 1 mm. Anatomical abbreviations: **a**: angular; **arf**: articular fossa; **cb**: compound bone; **cbp**: compound bone prearticular component; **cbs**: compound bone surangular component; **co**: coronoid; **d**: dentary; **Mc**: Meckel's canal; **mf**: mental foramen; **rp**: retroarticular process; **sf**: surangular foramen.



Figure 6. Location of the holotype of *Liotyphlops palauophis* sp. nov. (black star), lectotype of *Liotyphlops anops* (white dot), and specimens of *L. anops* examined in this study (green dot). ? = lack of detailed information about the type locality of *L. palauophis* sp. nov. and *L. anops*. This locality is based on information provided by Cope (1899).

teriorly in a shallow W-shaped suture. Prefrontal separated from nasal. Prefrontal moveably articulated to frontal. Postorbital element present. Posterior orbital margin incomplete. Frontals gradually tapering anteriorly. Frontal paired. Frontal–parietal contact (dorsal aspect) mostly straight and transverse, median notch in frontals slight at most. Parietal paired. Posterior border of parietal without median projection over supraoccipital. Supratemporal present. Posteromedial flange of septomaxilla short, not contacting frontal. Septomaxilla with lateral flange contributing to posterior border of external naris. Fenestra for duct of Jacobson’s organ posteroventrally positioned. Palatine not in contact with vomer, maxilla, or pterygoid. Central foramen present in parabasisphenoid. Ectopterygoid present. Supraoccipital present and single not partic-

ipating in internal sidewall of neurocranium. External surface (dorsoposterior) of supraoccipital without transverse ridge. Supraoccipital–prootic contact narrow, less than half supraoccipital–parietal contact. Splenial not present as discrete element. Coronoid and angular separated by prearticular portion of compound bone. Retroarticular process long, longer than articular facet. Teeth present in maxilla, but lacking in dentary, premaxilla, palatine, and pterygoid.

Coloration in alcohol. Dorsal and ventral body pale cream with brown pigmentation points along dorsal region of body.

Distribution. Known only from the type locality in the neighborhood of Bogota, Colombia (Fig. 6), according to the information provided by Cope (1899).

Etymology. The species name is in honor of Alfredo Palau Peña (June 10, 1969–August 8, 2020), a Brazilian herpetologist and my friend, who was killed by the COVID-19 virus. A combination of his name *Palau* and the Greek *ophis*, meaning snake.

Liotyphlops anops (Cope, 1899)

Figs 6–10, Table 1

Helminthophis anops Cope, 1899: 10, pl. 4 fig. la–f. Type locality: “New Grenada”, Colombia. According to McDiarmid et al. (1999), Dunn (1944: 48) listed the type locality as “near Bogota”. The latter was the specific locality mentioned on the first page of Cope’s (1899: 3) posthumous publication and the source of much of the material.

Liotyphlops anops Dunn 1944: 48.

Liotyphlops metae–Dunn 1944: 49, figs 3, 4. Holotype: MLS 8. Type locality: “Villavencio, Meta [Colombia], 498 meters”. Placed in synonymy by Dixon and Kofron (1984: 259).

Type material. Lectotype. AMNH R-17540, at least 200 mm TL (estimated from Fig. 7; specimen broken); type locality: Colombia, neighborhood of Bogota. **Lectotype by present designation.**

Diagnosis. *Liotyphlops anops* is distinguished from *L. albirostris*, *L. beui*, *L. bondensis*, *L. caissara*, *L. haadi*, *L. schubarti*, *L. taylori*, *L. ternetzii*, and *L. wilderi* in having four (vs three) scales contacting the posterior edge of the prefrontal. It is further distinguished from *L. argaleus* and *L. trefauti* in having two scales (vs one scale) contacting the posterior edge of the nasal between the second supralabial and the prefrontal. It is distinguished from *L. palauophis* sp. nov. in having the frontal scale single and 26/24/24 scales around the body (vs frontal scale divided and 28/26/26 scales around the body, and from *L. sousai* in having 562–597 dorsal scales and 531–572 ventral scales (vs 439 dorsal scales and 427 ventral scales).

Redescription. Meristic data in Table 1. Total length 186.2–337.7 mm, head length 3.2–4.4 mm (1.3–1.7% TL), snout–vent length 184–332 mm (98.3–98.8% TL), tail length 2.2–5.7 mm (1.2–1.7% TL), head width 2.5–3.7 mm (78.1–85.7% HL), and head height 1.8–2.8 mm (56.2–63.6% HL). Body covered with



Figure 7. Lectotype of *Liotyphlops anops*, AMNH R-17540, approximately 200 mm TL, Colombia, neighborhood of Bogota. Scale bar: 10 mm.

cycloid scales. Rostral large, longer than wide, contacting nasals anterolaterally, prefrontals laterally, and single frontal posteriorly. Pair of triangular prefrontals, bordered anterolaterally by rostral, ventrally by large divided nasal, and dorsoposteriorly by frontal. Posterior edge of prefrontals passing posterior edge of rostral. Divided nasal scale bordered anteriorly by rostral, dorsally by prefrontal, ventrally by first and second supralabials, and posteriorly by two scales that lie between prefrontal and second supralabial. Eye spot poorly visible. Four scales contacting posterior edge of prefrontal (three cycloid scales + frontal). Two scales contacting posterior edge of nasal between second supralabial and prefrontal. Five or six scales in first vertical row of dorsal scales. Mental triangular, not divided, wider than long, contacting first infralabials. Supralabials four, infralabials three. Scales around body 26/24/24. Dorsal scales 562–597, ventral scales 531–572, and subcaudal scales 12–14.

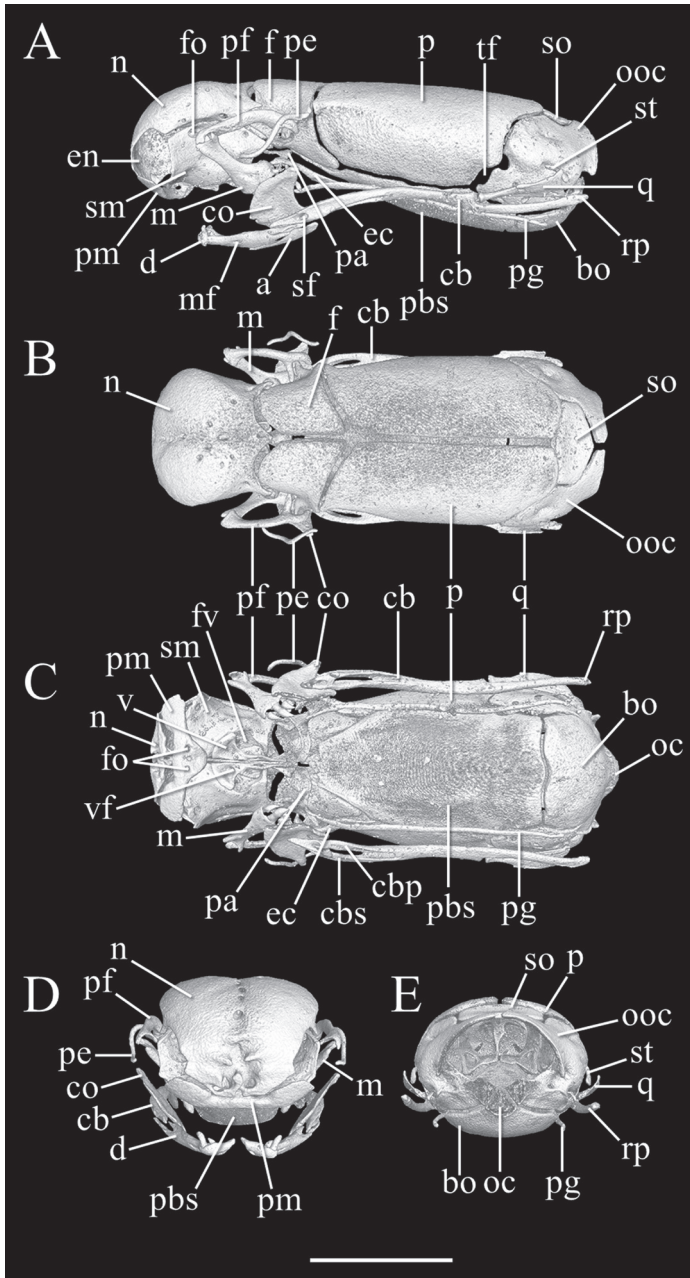


Figure 8. Three-dimensional reconstruction of the skull of *Liotyphlops anops*, MCZ R-67936, based on HRXCT data. **A** lateral view **B** dorsal view **C** ventral view with lower jaw partially digitally removed **D** anterior view **E** posterior view. Scale bar: 1 mm. Anatomical abbreviations: **a**: angular; **bo**: basioccipital; **cb**: compound bone; **co**: coronoid; **d**: dentary; **ec**: ectopterygoid; **en**: external naris; **f**: frontal; **fo**: foramen; **fv**: fenestra vomeronasalis; **m**: maxilla; **mf**: mental foramen; **n**: nasal; **oc**: occipital condyle; **ooc**: otico-occipital (fused prootic + opisthotic + exoccipital); **p**: parietal; **pa**: palatine; **pbs**: parabasisphenoid; **pe**: postorbital element; **pf**: prefrontal; **pg**: pterygoid; **pm**: premaxilla; **q**: quadrate; **rp**: retroarticular process; **sf**: surangular foramen; **sm**: septomaxilla; **st**: supratemporal; **so**: supraoccipital; **tf**: trigeminal foramen; **v**: vomer; **vf**: vomerine foramen.

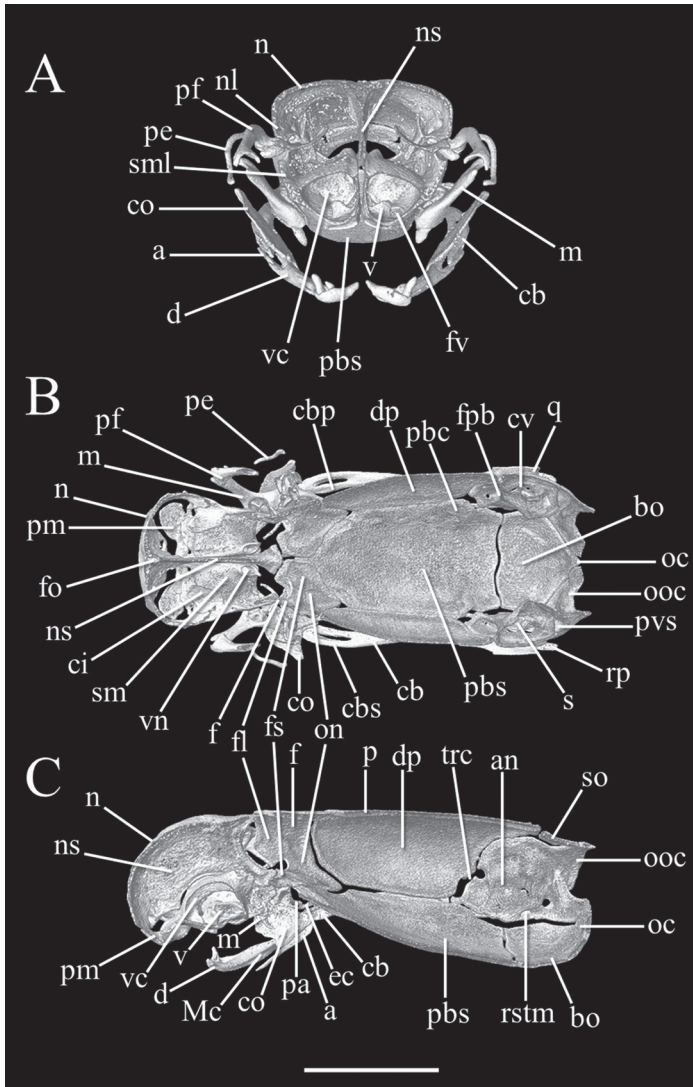


Figure 9. Three-dimensional reconstruction of the skull of *Liotyphlops anops*, MCZ R-67936, based on HRXCT data. **A** transversal view **B** frontal view **C** sagittal view. Scale bar: 1 mm. Anatomical abbreviations: **a**: angular; **an**: acoustic nerve foramen; **bo**: basioccipital; **cb**: compound bone; **cbp**: compound bone prearticular component; **cbs**: compound bone surangular component; **ci**: conchal invagination; **co**: coronoid; **cv**: cavum vestibuli; **d**: dentary; **dp**: descensus parietalis; **ec**: ectopterygoid; **en**: external naris; **f**: frontal; **fl**: frontal laterally descending flange; **fo**: foramen; **fpb**: facial nerve palatine branch foramen; **fs**: frontal subolfactory process; **fv**: fenestra vomeronasalis; **m**: maxilla; **Mc**: Meckel's canal; **mf**: mental foramen; **n**: nasal; **nl**: nasal lateral flange; **ns**: medial nasal septum; **oc**: occipital condyle; **on**: optic nerve foramen; **ooc**: otico-occipital (fused prootic + opisthotic + exoccipital); **p**: parietal; **pa**: palatine; **pbc**: parabasal (Vidian) canal; **pbs**: parabasisphenoid; **pe**: postorbital element; **pf**: prefrontal; **pg**: pterygoid; **pm**: premaxilla; **pvs**: posterior vertical semicircular canal; **q**: quadrate; **rp**: retroarticular process; **rstm**: recessus scallae tympani medial aperture; **s**: stapes; **sf**: surangular foramen; **sm**: septomaxilla; **sml**: septomaxilla lateral flange; **st**: supratemporal; **so**: supraoccipital; **tf**: trigeminal foramen; **trc**: trigeminofacialis chamber; **v**: vomer; **vc**: vomeronasal cupola; **vf**: vomerine foramen; **vn**: vomeronasal nerve passage.

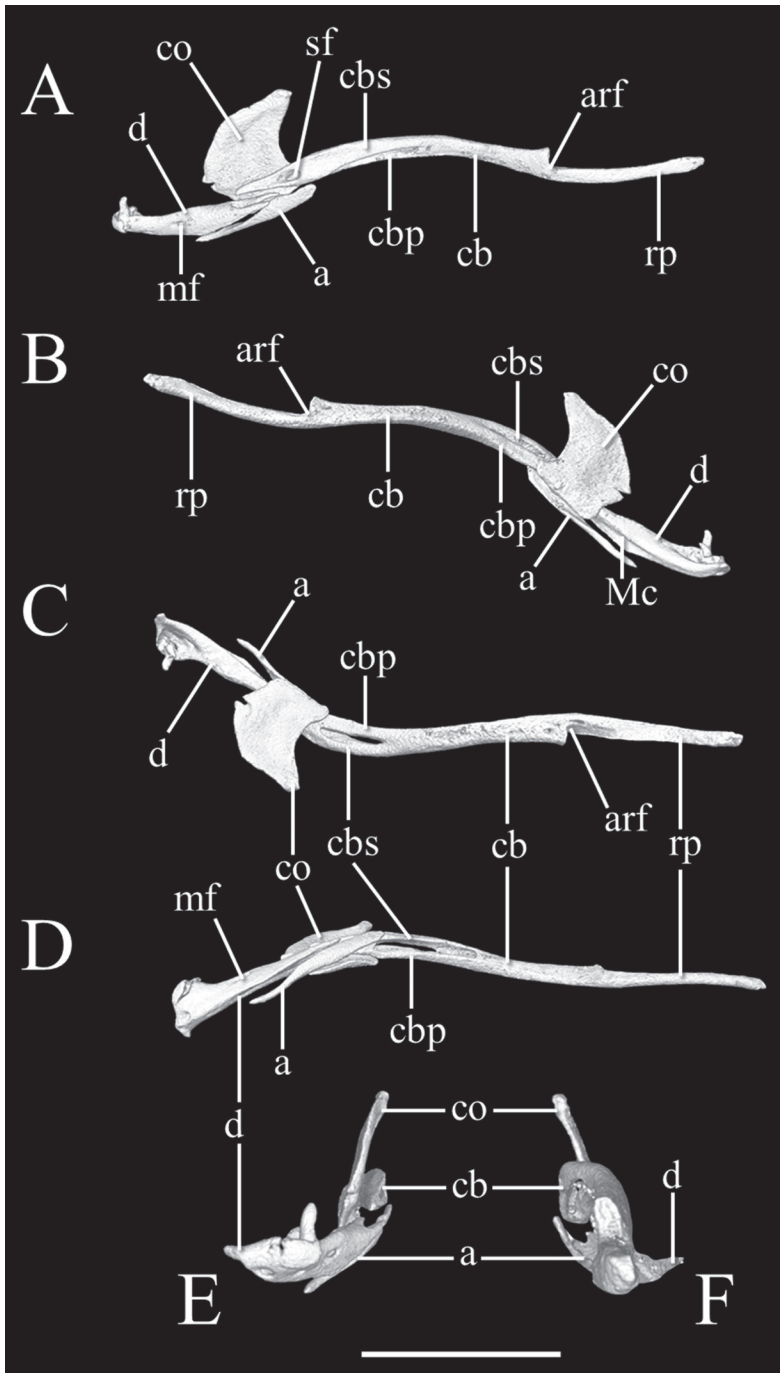


Figure 10. Three-dimensional reconstruction of the lower jaw of *Liotyphlops anops*, MCZ R-67936, based on HRXCT data. **A** lateral view **B** medial view **C** dorsal view **D** ventral view **E** anterior view **F** posterior view. Scale bar: 1 mm. Anatomical abbreviations: **a**: angular; **arf**: articular fossa; **cb**: compound bone; **cbp**: compound bone prearticular component; **cbs**: compound bone surangular component; **co**: coronoid; **d**: dentary; **Mc**: Meckel's canal; **mf**: mental foramen; **rp**: retroarticular process; **sf**: surangular foramen.

Coloration in alcohol. Dorsal and ventral body brown to pale cream. Head pale cream. Scales near opening of cloaca pale cream.

Description of skull. High-resolution x-ray computed tomography of skull bones in Figs 8–10. Main body of premaxilla on ventral surface of snout. Maxilla–premaxilla contact widely separated. Lateral maxillary foramina absent. Maxilla alveolar row oriented transversely. Nasal fused. Nasal–frontal boundary convex posteriorly in shallow W-shaped suture. Prefrontal separated from nasal. Prefrontal moveably articulated to frontal. Postorbital element present. Posterior orbital margin incomplete. Frontals gradually tapering anteriorly. Frontal paired. Frontal–parietal contact (dorsal aspect) anteriorly concave, frontals extending posteriorly into broad median embayment in parietals. Parietal paired. Posterior border of parietal in contact with otico–occipital. Supraoccipital present and fused not participating in internal sidewall of neurocranium. Supratemporal present. Posteromedial flange of septomaxilla short, not contacting frontal. Septomaxilla with lateral flange contributing to posterior border of external naris. Fenestra for duct of Jacobson’s organ posteroventrally positioned. Palatine not in contact with vomer, maxilla, or pterygoid. Ectopterygoid present. Splenial not present as discrete element. Coronoid and angular separated by prearticular portion of compound bone. Retroarticular process long, longer than articular facet. Teeth present in maxilla and dentary, but lacking in premaxilla, palatine, and pterygoid.

Distribution. Central Colombia (neighborhood of Bogota and Villavicencio in the department of Meta) (Fig. 6).

Liotyphlops ternetzii (Boulenger, 1896)

Figs 11–16, Tables 1, 2

Helminthophis ternetzii Boulenger, 1896: 584. Holotype: BMNH 1946.1.11.77. Type locality: Paraguay.

Helminthophis incertus Amaral, 1924: 29. Holotype: MCZ R17846. Type locality: Surinam [Suriname]. Placed in synonymy by Dixon and Kofron (1984 [dated 1983]: 255–256), who also rejected the type locality as Suriname.

Helminthophis beui Amaral, 1924: 25–30. Holotype: IB 1806. Type locality: Butantan, São Paulo, Brazil. syn. nov.

Helminthophis collenettei Parker, 1928: 97. Holotype: BMNH 1946.1.10.73 (formerly BMNH 1928.1.12.1). Type locality: Burity, 2250 ft., 30 miles northeast of Coyaba [Cuiabá], Mato Grosso [Brazil]. Placed in synonymy by Amaral (1954: 192).

[*Liotyphlops*] *incertus*–Vanzolini 1948: 380.

[*Liotyphlops*] *ternetzi*–Smith and Grant 1958: 207.

Liotyphlops ternetzii–Peters and Orejas-Miranda 1970: 183, in part; included *L. beui* in the synonymy.

Liotyphlops ternetzii–McDiarmid et al. 1999: 51–52.

Liotyphlops ternetzii–Wallach et al. 2014: 397–398.

Type material. *Holotype.* BMNH 1946.1.11.77, 325.1 mm TL; type locality: Paraguay.

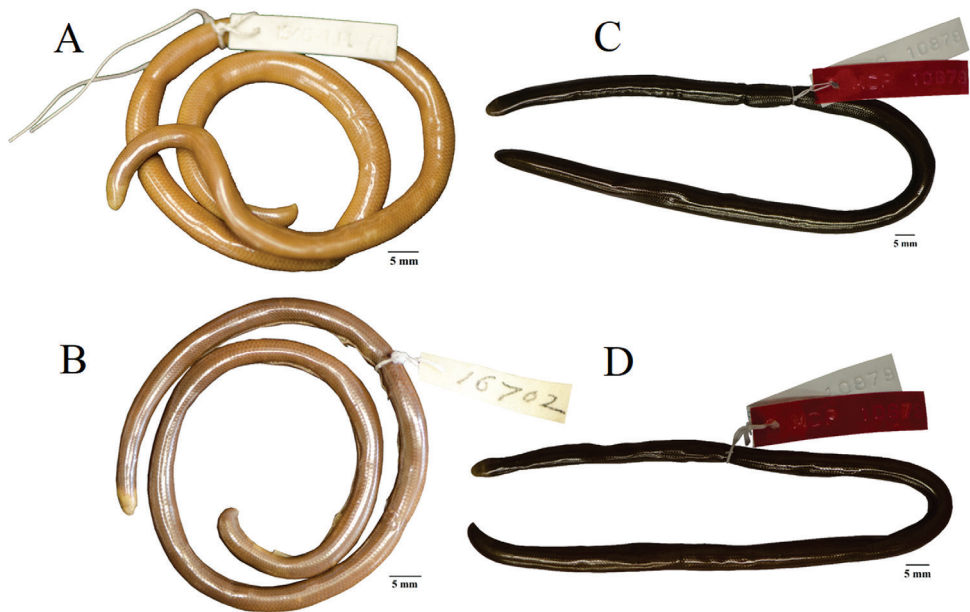


Figure 11. Types of *Liotyphlops ternetzii* and *Liotyphlops beui*. **A** holotype of *L. ternetzii* (BMNH 1946.1.11.77, 325.1 mm TL) from Paraguay **B** paratype of *L. beui* (MCZ 16702, 279.2 mm TL) from Butantan, São Paulo, Brazil **C** specimen of *L. ternetzii* (MCP 10878, 248.9 mm TL) with dark brown coloration **D** specimen of *L. beui* (MCP 10879, 233.9 mm TL) with dark brown coloration.

Diagnosis. *Liotyphlops ternetzii* is distinguished from *L. anops*, *L. argaleus*, *L. sousai*, and *L. trefauti* in having three (vs four) scales contacting the posterior edge of the prefrontal scale. It is distinguished from *L. albirostris*, *L. bondensis*, *L. caissara*, *L. haadi*, and *L. wilderi* in having two scales (vs one scale) contacting the posterior edge of the nasal between the second supralabial and the prefrontal. It is distinguished from *L. taylori* by having three (vs two) infralabial scales, and from *L. palauophis* sp. nov. in having a single frontal scale (vs frontal scale divided). Is distinguished from *L. schubarti* in the pale cream, dark brown, or black coloration (vs light brown).

Redescription. Meristic data in Tables 1, 2. Total length of holotype 325.1 mm, head length 4.8 mm (1.5% TL), snout–vent length 317 mm (97.5% TL), tail length 8.1 mm (2.5% TL), head width 3.6 mm (75% HL), and head height 2.7 mm (56.3% HL). Body covered with cycloid scales. Snout rounded, rostral scale large, longer than wide, contacting nasals anterolaterally, prefrontals laterally, and single frontal posteriorly. Pair of triangular prefrontals, bordered anterolaterally by rostral, ventrally by large divided nasal, and dorsoposteriorly by frontal. Posterior edge of prefrontals passing posterior edge of rostral. Nasal scale divided and bordered anteriorly by rostral, dorsally by prefrontal, ventrally by first and second supralabials, and posteriorly by two scales located between prefrontal and second supralabial. Eye spot poorly visible. Three scales contacting posterior edge of prefrontal (two cycloid scales + frontal). Two scales con-

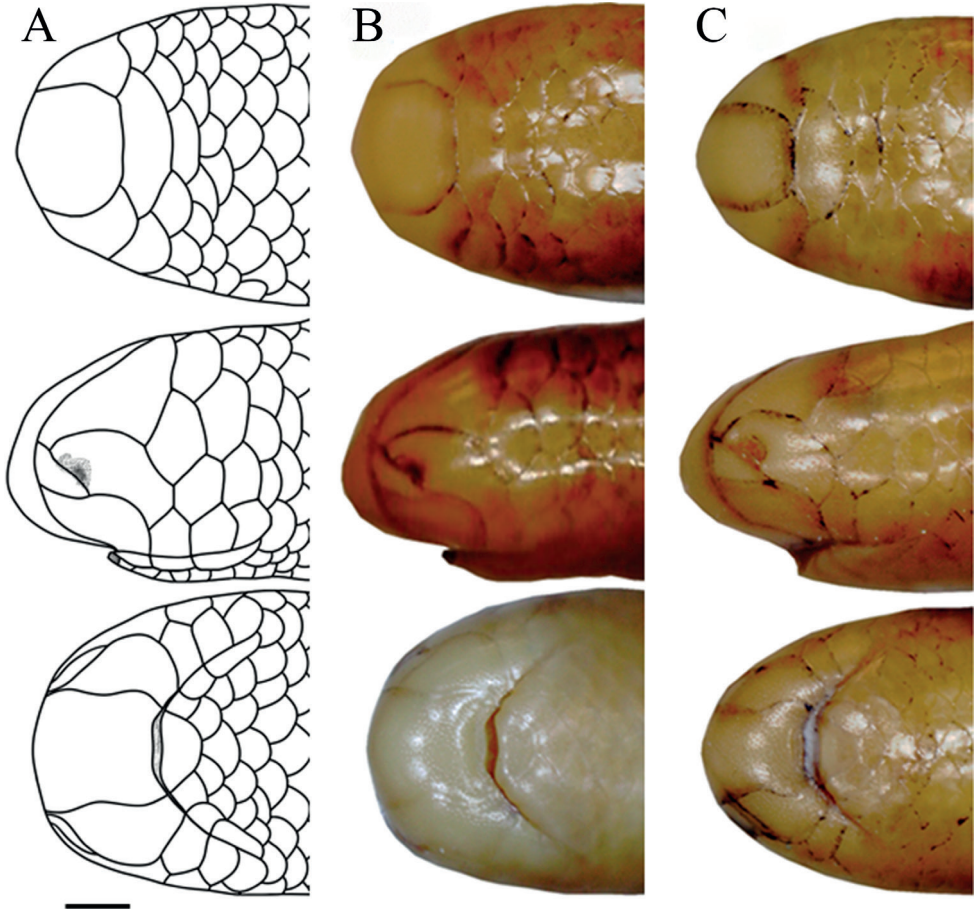


Figure 12. Dorsal, lateral, and ventral views of the head of *Liotyphlops*. **A** *L. ternetzii*, holotype (BMNH 1946.1.11.77), drawing **B** *L. ternetzii*, holotype **C** *L. beui* (MCZ 16702) paratype. Scale bar: 1 mm.

Table 2. Meristic characters of specimens identified as *Liotyphlops beui* and *L. ternetzii*, presented as ranges with minimum, maximum, and mode in parentheses. **SPEP** = number of scales contacting posterior edge of prefrontal; **SPEN** = number of scales contacting posterior edge of nasal between second supralabial and prefrontal; **SFVRD** = number of scales in the first vertical row of dorsals; **SL** = number of supralabial scales; **IL** = number of infralabial scales; **ASR** = number of anterior scale rows around body; **MSR** = number of scale rows around the midbody; **PSR** = number of posterior scale rows around body; **DSR** = number of dorsal scale rows; **VSR** = number of ventral scales rows; **SC** = number of subcaudal scales; **n** = number of specimens examined in this study; **(p)** = *L. beui* paratypes; **(h)** = *L. ternetzii* holotype.

Species/Count	n	SPEP	SPEN	SFVRD	SL	IL	ASR	MSR	PSR	DSR	VSR	SC
<i>L. beui</i>	50	3–3(3)	2–2(2)	5–6(5)	4–4(4)	3–3(3)	22–26(22)	20–22(22)	20–22(20)	366–532(453)	348–511(364)	11–22(12)
<i>L. beui</i> (p)	2	3–3(3)	2–2(2)	5–5(5)	4–4(4)	3–3(3)	22–22(22)	20–20(20)	20–20(20)	462–477	439–452	19–20
<i>L. ternetzii</i>	50	3–3(3)	2–2(2)	5–6(5)	4–4(4)	3–3(3)	22–26(22)	20–23(20)	20–22(20)	353–539(417)	341–514(381)	11–22(15)
<i>L. ternetzii</i> (h)	1	3	2	5	4	3	24	22	21	475	452	20

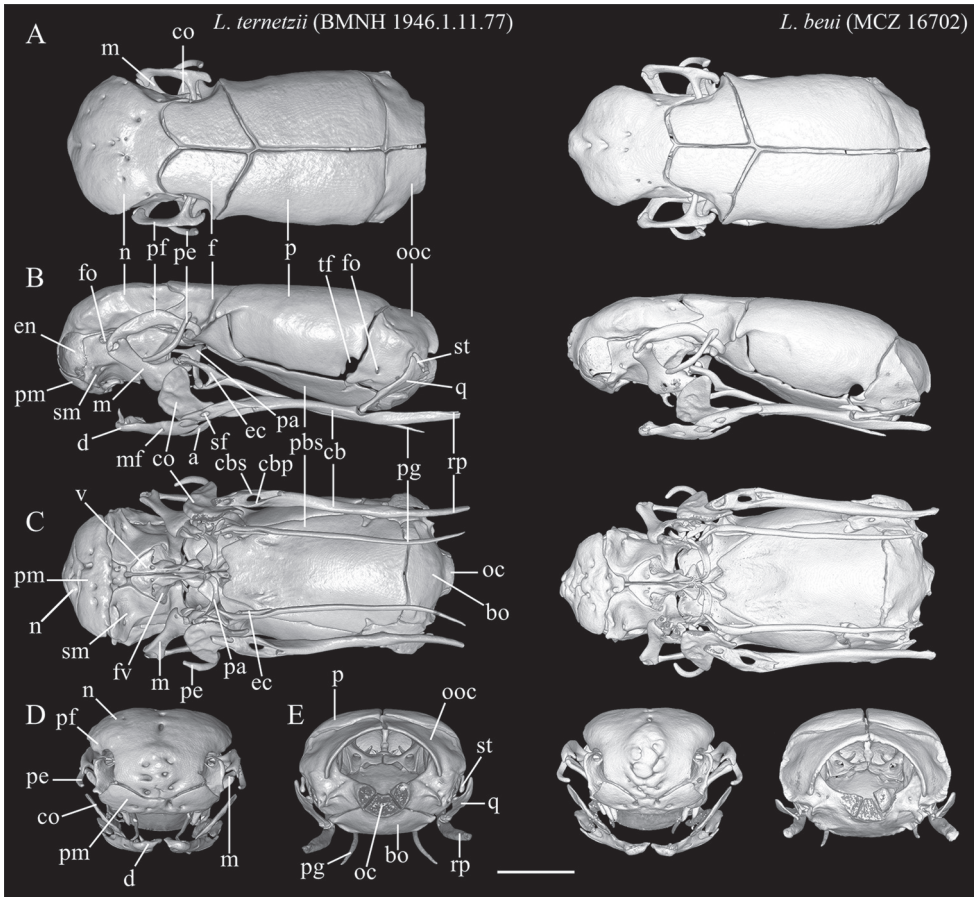


Figure 13. Three-dimensional reconstruction of the skull of holotype *Liotyphlops ternetzii* (BMNH 1946.1.11.77), and of the skull of the paratype *Liotyphlops beui* (MCZ 16702) based on HRXCT data. **A** dorsal view **B** lateral view **C** ventral view **D** anterior view **E** posterior view. Scale bar: 1 mm. Anatomical abbreviations: **a**: angular; **bo**: basioccipital; **cb**: compound bone; **cbp**: compound bone prearticular component; **cbs**: compound bone surangular component; **co**: coronoid; **d**: dentary; **ec**: ectopterygoid; **en**: external naris; **f**: frontal; **fo**: foramen; **m**: maxilla; **mf**: mental foramen; **n**: nasal; **oc**: occipital condyle; **ooc**: otico-occipital (fused prootic + opisthotic + exoccipital); **p**: parietal; **pa**: palatine; **pbs**: parabasisphenoid; **pe**: postorbital element; **pf**: prefrontal; **pg**: pterygoid; **pm**: premaxilla; **q**: quadrate; **rp**: retroarticular process; **sm**: septomaxilla; **sf**: surangular foramen; **st**: supratemporal; **tf**: trigeminal foramen; **v**: vomer.

tacting posterior edge of nasal between second supralabial and prefrontal. Five scales in first vertical row of dorsal scales. Mental triangular, not divided, wider than long, contacting first infralabial. Supralabial scales four, infralabial scales three. Scales around body 24/22/21. Dorsal scales 475, ventral scales 452, and subcaudal scales 20.

Coloration in alcohol. Dorsal and ventral body pale cream. Scales near opening of cloaca and subcaudal scales lighter than rest of body.

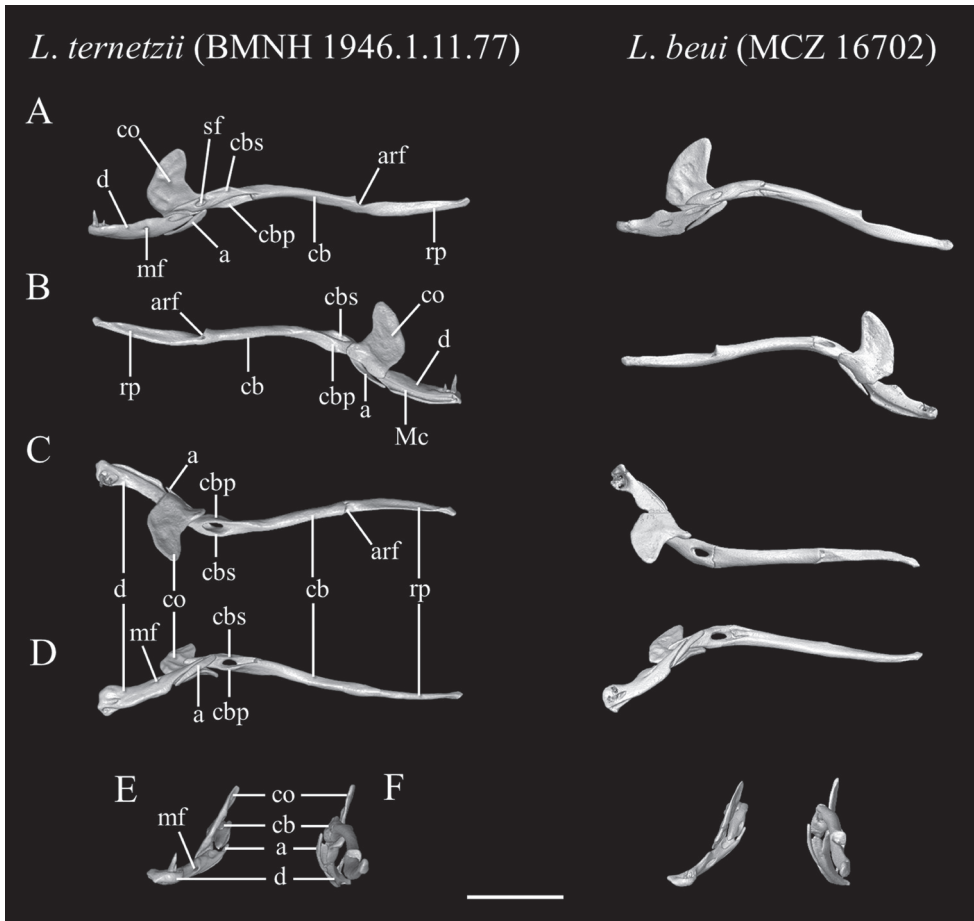


Figure 15. Three-dimensional reconstruction of the lower jaw of *Liotyphlops ternetzii*, BMNH 1946.1.11.77, holotype, and *Liotyphlops beui*, MCZ 16702, paratype, based on HRXCT data. **A** lateral view **B** medial view **C** dorsal view **D** ventral view **E** anterior view **F** posterior view. Scale bar: 1 mm. Anatomical abbreviations: **a**: angular; **arf**: articular fossa; **cb**: compound bone; **cbp**: compound bone prearticular component; **cbs**: compound bone surangular component; **co**: coronoid; **d**: dentary; **Mc**: Meckel's canal; **mf**: mental foramen; **rp**: retroarticular process; **sf**: surangular foramen.

Description of skull. High-resolution x-ray computed tomography of skull bones in Figs 13–15. Main body of premaxilla on ventral surface of snout. Maxilla–premaxilla contact widely separated. Lateral maxillary foramina absent. Maxilla alveolar row oriented transversely. Nasal fused. Nasal–frontal boundary convex posteriorly in shallow W-shaped suture. Prefrontal separated from nasal. Prefrontal moveably articulated to frontal. Postorbital element present. Posterior orbital margin incomplete. Frontals gradually tapering anteriorly. Frontal paired. Frontal–parietal contact (dorsal aspect) anteriorly concave, i.e., frontals extending posteriorly into broad median embayment in parietals. Parietal paired. Posterior border of parietal

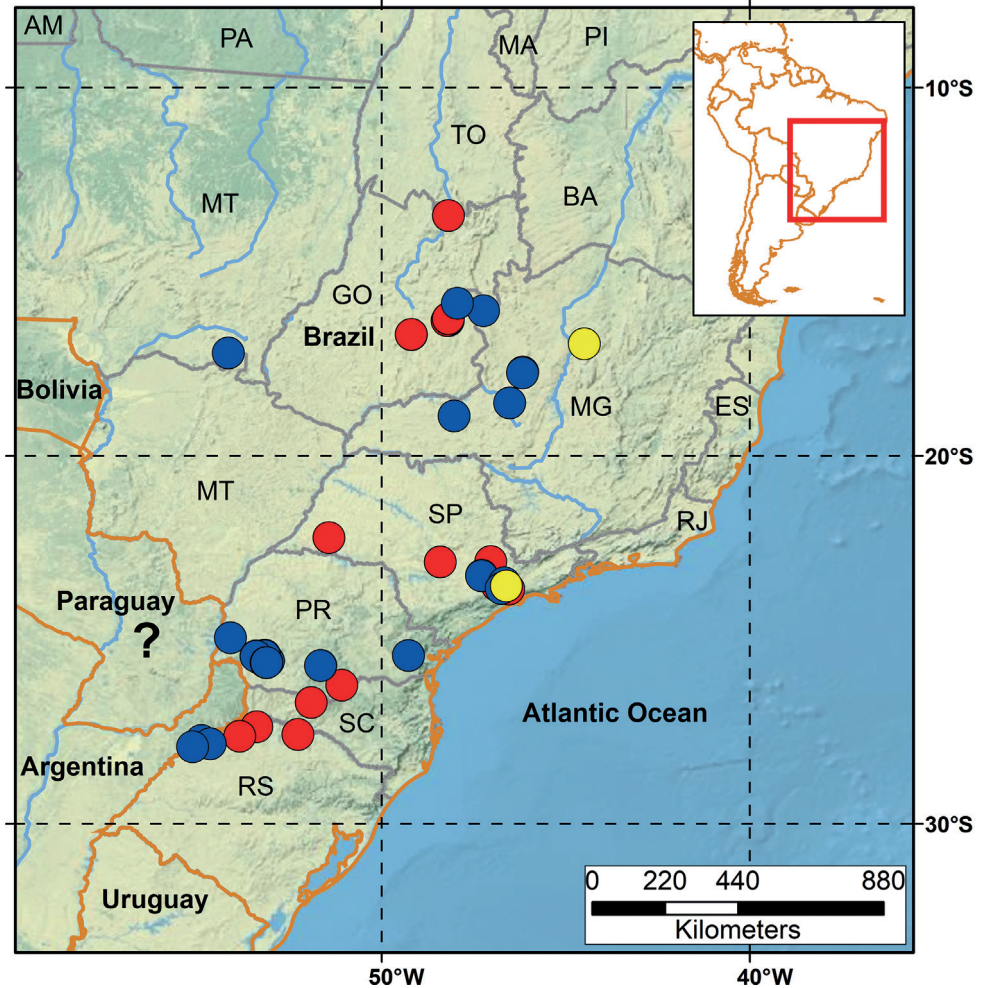


Figure 16. Localities of specimens originally identified as *Liotyphlops ternetzii* (blue dots) and *Liotyphlops beui* (red dots) examined in this study. Paratypes of *L. beui* (yellow dots), and holotype of *L. ternetzii* (? = undetermined type locality).

in contact with otico–occipital. Supraoccipital absent. Supratemporal present. Postero-medial flange of septomaxilla short, not contacting frontal. Septomaxilla with lateral flange contributing to posterior border of external naris. Fenestra for duct of Jacobson’s organ posteroventrally positioned. Palatine not in contact with vomer, maxilla, or pterygoid. Ectopterygoid present. Splenial not present as discrete element. Coronoid and angular separated by prearticular portion of compound bone. Retroarticular process long, longer than articular facet. Teeth present in maxilla and dentary, but lacking in premaxilla, palatine, and pterygoid.

Distribution. Known from Brazil (Mato Grosso, Goiás, Minas Gerais, São Paulo, Paraná, Santa Catarina, and Rio Grande do Sul), Paraguay (Amambay, Caazapá,

Canendiyu, Itapúa, Presidente Hayes), Uruguay (Río Negro, Salto), and Argentina (Corrientes, Entre Ríos, Formosa, Jujuy, Misiones, Salta) (Fig. 16). In the original description, the locality of the holotype is described as Paraguay.

Discussion

The description of new species based on single specimens is generally discouraged due to the obvious limitations, for example, in describing variation and geographical distribution (Santos and Reis 2018). More material will provide data on morphological variation, as well as ecological information that may be useful in conservation efforts. The redescription here of the lectotype of *L. anops* (AMNH R-17540) was based on photographs sent by the curators of the AMNH due to the great fragility of the specimen, making impossible the packing, transport, and the use of invasive techniques. The examination of these photographs of the lectotype was complemented by data obtained by the examination of other specimens of *L. anops*, providing the redescription with data of external morphology and osteology of the skull.

The specimens of *L. beui* (two paratypes and 50 non-types) and *L. ternetzii* (the holotype and 50 non-types) examined (Figs 11–16) showed limited variation in meristic characters (Table 2), which does not warrant the recognition of these taxa as separate species. The number and disposition of head scales do not distinguish the two taxa (Fig. 12): (1) three scales contacting the posterior edge of the prefrontal; (2) two scales contacting the posterior edge of the nasal between the second supralabial and the prefrontal; (3) five or six scales in the first vertical row of dorsal scales; (4) four supralabial scales, and (5) three infralabial scales. The supratemporal bone of anomalepidid snakes is either very reduced or absent (*Anomalepis*), and the high-resolution x-ray tomography showed that the two paratypes of *L. beui* (MCZ R-16702 and MCZ R-17842) lack a supratemporal, which is instead present, although highly reduced, in all other specimens of *L. beui* scanned and examined.

Liotyphlops beui was removed from the synonymy of *L. ternetzii* by Dixon and Kofron (1984) based on two characters: (1) 20 scale rows posteriorly around the body (22 in *L. ternetzii*), and (2) a dorsal scale count of 384–455 (463–510 in *L. ternetzii*). In my sample, however, *L. beui* had 366–532 (mode 453), while *L. ternetzii* had 353–539 (mode 417), with the two ranges completely overlapping; and dorsal scale count in *L. beui* 20–22 (mean 22) and in *L. ternetzii* 20–23 (mean 20), but the holotype of *L. ternetzii* has 22 (Table 2). In addition, all other meristic characters (Table 2), coloration pattern, and an extensive study of skull bone characters showed no significant variation that can be used as diagnostic characters for *L. beui*. After a detailed morphological examination of specimens of *L. beui* and *L. ternetzii*, including the relevant type materials, *L. beui* is considered a junior synonym of *L. ternetzii*.

It is important to highlight that, in view of the limitation of diagnostic phenotypic characters for species of the genus *Liotyphlops* and the lack of knowledge about the

evolutionary relationships of their species, there is a need for fieldwork to collect samples of fresh tissue to obtain genetic material, which will allow studying the systematics and testing the limits of *Liotyphlops* species from a molecular perspective.

Acknowledgements

I am grateful to all curators, collection managers, and their respective institutions for the loan of specimens, and for permission to examining specimens in their care: A. Dias, P. Manzani and K. Rebelo (Museu de Zoologia da UNICAMP, Campinas); C. Spencer and J. McGuire (Museum of Vertebrate Zoology, Berkeley); D. A. Kizirian and L. Vonnahme (American Museum of Natural History, New York); F. Rojas-Runjaic (Museo de Historia Natural La Salle, Caracas); G. Pontes (Museu de Ciências e Tecnologia da Pontifícia Universidade Católica do Rio Grande do Sul, Porto Alegre); H. Silva and B. Bittar (Centro de Estudos e Pesquisas Biológicas da Pontifícia Universidade Católica de Goiás, Goiânia); H. Zaher and A. Carvalho (Museu de Zoologia da Universidade de São Paulo, São Paulo); J. Padial (Carnegie Museum of Natural History, Pittsburgh); J. Rosado (Museum of Comparative Zoology, Cambridge); M. Martins, D. Alvares and V. Caorsi (Universidade Federal do Rio Grande do Sul, Porto Alegre); P. Campbell (Natural History Museum, London); P. Passos (Museu Nacional da Universidade Federal do Rio de Janeiro, Rio de Janeiro); S. Cechin and L. Loebens (Coleção de Répteis da Universidade Federal de Santa Maria, Santa Maria). I thank C. J. Bell, J. Maisano and P. Stafford of The University of Texas at Austin for the support in the acquisition of specimens and CT scanning. I thank A. Augustin of the Pontifícia Universidade Católica do Rio Grande do Sul for help with CT scanning of specimens. I am grateful to J. Romanzini of the MCT-PUCRS for part of the photographs. I thank R. Jadin, R. Forsyth and Z. Zorkova (ZooKeys editors) and the two anonymous reviewers for valuable suggestions during the review process. I thank R. E. Reis by the guidance and support in the development of this research. I thank the Coordenação de Aperfeiçoamento de Pessoal de Nível Superior (CAPES) for a doctoral fellowship.

References

- Amaral A (1924) *Helminthophis*. Proceedings of the New England Zoological Club 9: 25–30.
- Amaral A (1929) Contribuição ao conhecimento dos ophídios do Brasil IV-Lista remissiva dos ophídios do Brasil. Memórias do Instituto Butantan 4: 3–57.
- Amaral A (1954) Contribuição ao conhecimento dos ofídios do Brasil 12. Notas a respeito de *Helminthophis ternetzii* Boulenger, 1896. Memórias do Instituto Butantan 26: 191–195.
- Boulenger GA (1896) Catalogue of the snakes in the British Museum (Natural History). Vol. III, containing the Colubridae (Opisthoglyphae and Proteroglyphae), Amblycephalidae, and Viperidae. British Museum (Natural History), London, 727 pp.

- Boundy J (2021) Snakes of the World: a Supplement. CRC Press, Boca Raton, 273 pp. <https://doi.org/10.1201/9780429461354>
- Centeno FC, Sawaya RJ, Germano VJ (2010) A new species of *Liotyphlops* (Serpentes: Anomalepididae) from the Atlantic Coastal Forest in southeastern Brazil. *Herpetologica* 66(1): 86–91. <https://doi.org/10.1655/08-079.1>
- Cope ED (1899) Contributions to the herpetology of New Granada and Argentina with descriptions of new forms. *The Philadelphia Museums Scientific Bulletin* 1: 3–26. <https://doi.org/10.5962/bhl.title.54674>
- Dixon JR, Kofron CP (1984) The Central and South American anomalepid snakes of the genus *Liotyphlops*. *Amphibia-Reptilia* 4(2):241–264. <https://doi.org/10.1163/156853883X00120>
- Dunn ER (1944) A review of the Colombian snakes of the families Typhlopidae and Leptotyphlopidae. *Caldasia* 3: 47–55.
- Freire EMX, Caramaschi U, Argôlo AJS (2007) A new species of *Liotyphlops* (Serpentes: Anomalepididae) from the Atlantic Rain Forest of northeastern Brazil. *Zootaxa* 1393(1): 19–26. <https://doi.org/10.11646/zootaxa.1393.1.2>
- Haad JJS, Franco FL, Maldonado J (2008) Una nueva especie de *Liotyphlops* Peters, 1881 (Serpentes, Scolecophidia, Anomalepididae) del sur de la Amazonia colombiana. *Biota Colombiana* 9: 295–300.
- Linares-Vargas CA, Bolívar-García W, Herrera-Martínez A, Osorio-Domínguez D, Ospina OE, Thomas R, Daza JD (2021) The status of the anomalepidid snake *Liotyphlops albirostris* and the revalidation of three taxa based on morphology and ecological niche models. *The Anatomical Record* 304(10): 2264–2278. <https://doi.org/10.1002/ar.24730>
- McDiarmid RW, Campbell JA, Touré T (1999) Snake Species of the World. A Taxonomic and Geographic Reference. The Herpetologist's League, Washington DC, [xi +] 511 pp.
- Peters WCH (1881) Einige herpetologische Mittheilungen, 1. Uebersicht der zu den Familien der Typhlopes und Stenostomi gehörigen Gattungen oder Untergattungen. *Sitzungsberichte der Gesellschaft Naturforschender Freunde zu Berlin* 4: 69–71.
- Peters JA, Donoso Barros R, Orejas Miranda B (1986) Catalogue of the Neotropical Squamata (Revised edn.). Part I. Snakes. Washington, D.C., Smithsonian Institution Press. [VIII +] 293 pp.
- Queiroz K (2007) Species concepts and species delimitation. *Systematic Biology* 56(6): 879–886. <https://doi.org/10.1080/10635150701701083>
- Rieppel O, Kley NJ, Maisano JA (2009) Morphology of the skull of the White-Nosed Blind-snake, *Liotyphlops albirostris* (Scolecophidia: Anomalepididae). *Journal of Morphology* 270(5): 536–557. <https://doi.org/10.1002/jmor.10703>
- Sabaj MH (2020) Codes for natural history collections in ichthyology and herpetology. *Copeia* 108(3): 593–669. <https://doi.org/10.1643/ASIHCODONS2020>
- Santos FJM, Reis RE (2018) Two new blind snake species of the genus *Liotyphlops* Peters, 1881 (Serpentes: Anomalepididae), from Central and South Brazil. *Copeia* 106(3): 507–514. <https://doi.org/10.1643/CH-18-081>
- Santos FJM, Reis RE (2019) Redescription of the blind snake *Anomalepis colombia* (Serpentes: Anomalepididae) using high-resolution x-ray computed tomography. *Copeia* 107(2): 239–243. <https://doi.org/10.1643/CH-19-181>

Smith HM, Grant C (1958) New and noteworthy snakes from Panama. *Herpetologica* 14: 207–215.

Wallach V, Williams KL, Boundy J (2014) *Snakes of the World: a Catalogue of Living and Extinct Species*. CRC Press Taylor and Francis Group, New York, [xxvii +] 1209 pp.

Appendix I

Examined specimens

Liotyphlops albirostris: Colombia. Bolívar, Arjona: CM 39565. Panama. Herrera, Santa María: CM 44652. Venezuela. Distrito Capital, road below La Guaira, km 5, East of Caracas: CM 90256. Distrito Capital, Libertador: MHNLS 514. Miranda, Urbanización Altamira: MHNLS 11824. Urbanización Macaracuay: MHNLS 15550.

Liotyphlops anops: Colombia. Neighborhood of Bogota: lectotype AMNH R-17540. Meta, Villavicencio: MCZ R-67936, MCZ R-67937, MZUSP-S 5998.

Liotyphlops argaleus: Colombia. Meta, La Selva: MCZ R-66383 paratype.

Liotyphlops beui: Brazil. Goiás, Goiânia: CEPB 1398, CEPB 1422, CEPB 2491, CEPB 3610. Luziânia: CEPB 6601, CEPB 6602, CEPB 6603, CEPB 6604, CEPB 6900, CEPB 6901, CEPB 6902, CEPB 6903, CEPB 6904, CEPB 6905, CEPB 6642, CEPB 6643, CEPB 6646, CEPB 6651, CEPB 6659, CEPB 6672, CEPB 8849. Minaçu: CEPB 8409. São Paulo, Botucatu: MNRJ 23247. Campinas: MNRJ 8143. Carapicuíba: MCP 16361, MNRJ 10578. Itu: MNRJ 8144. Pirapozinho: MNRJ 22022. São Caetano do Sul: MCP 16365. São Paulo: MCP 16366, MCP 16368, MNRJ 10577, ZUFMS 1569. Instituto Butantan, paratypes MCZ R-16702, MCZ R-17842. Paraná, Boa Vista da Aparecida: MCP 10853, MCP 10855, MCP 10854, MCP 10879. Cruzeiro do Iguaçu: MCP 10880. Curitiba: MCP 16362, MCP 16363. Três Barras do Paraná: MCP 10857, MCP 10858, MCP 10859, MCP 10862, MCP 10864. União da Vitória: MCP 16360. Santa Catarina, Passos Maia: UFRGS 6275. Rio Grande do Sul, Erechim: UFRGS 6494. Frederico Westphalen: MCP 9494. Bom Progresso: MCP 19086.

Liotyphlops haadi: Colombia. Amazonas Department, middle region of the Caquetá River, La Pedrera district: IAvH 5434 holotype. Leticia, Vereda de los Lagos: IAvH 5435 paratype.

***Liotyphlops palauophis* sp. nov.**: Colombia. Neighborhood of Bogota: holotype AMNH R-09550.

Liotyphlops schubarti: Brazil. São Paulo, Campinas: ZUEC REP 2278, ZUEC REP 2279, ZUEC REP 2280, ZUEC REP 2281. Sapucaí: MZUSP-S 4099.

Liotyphlops sousai: Brazil. Santa Catarina, Passos Maia: holotype, UFRGS 6274

Liotyphlops taylori: Brazil. Mato Grosso, Porto Estrela: holotype, MZUSP-S 14975

Liotyphlops ternetzii: Paraguay. holotype, BMNH 1946.1.11.77. Brazil. Mato Grosso, Itiquira: UFRGS 6458. Distrito Federal, Brasília: MCP 18381. Minas Gerais, Cabeceira Grande: MCP 19228. Indianópolis: MNRJ 8147. João Pinheiro:

MNRJ 11329, MNRJ 14957. Patos de Minas: MNRJ 17300. São Paulo, Itu: MCP 10699. São Paulo: MCP 3680, MCP 6986. Taboão da Serra: MCP 7349. Paraná, Boa Vista da Aparecida: MCP 10849, MCP 10869, MCP 10870, MCP 10878, MCP 10850, MCP 10851, MCP 10852. Curitiba: MCP 1943. Cruzeiro do Iguaçu: MCP 10847, MCP 10872, MCP 10873, MCP 10874, MCP 10875, MCP 10876, MCP 10877, MCP 10881, MCP 10882, MCP 10883, MCP 10885, MCP 10886. Diamante D'Oeste: MCP 16364. Pinhão: MCP 7186, MCP 7195, MCP 7196, MCP 7197, MCP 7198, MCP 7199, MCP 7361. Três Barras do Paraná: MCP 10856, MCP 10860, MCP 10861, MCP 10863, MCP 10865, MCP 10866, MCP 10867, MCP 10884. Rio Grande do Sul, Porto Vera Cruz: MCP 11676. Porto Xavier: MCP 11706. Santo Cristo: MCP 11661.

Liotyphlops wilderi: Brazil. Bahia, Itapebi: MNRJ 15657. Minas Gerais, Caeté: MNRJ 20633, MZUSP-S 3842.

Identification and reproductive isolation of *Euborellia* species (Insecta, Dermaptera, Anisolabididae) from East and Southeast Asia

Yoshitaka Kamimura^{1,2}, Chow-Yang Lee^{2,3}, Junsuke Yamasako⁴, Masaru Nishikawa⁵

1 Department of Biology, Keio University, Yokohama 223-8521, Japan **2** Urban Entomology Laboratory, Vector Control Research Unit, School of Biological Sciences, Universiti Sains Malaysia, Minden 11800, Penang, Malaysia **3** Present address: Department of Entomology, University of California, Riverside, CA 92521, USA **4** Institute for Plant Protection, NARO, Kannondai 3-1-3, Tsukuba, Ibaraki 305-8604, Japan **5** Entomological Laboratory, Faculty of Agriculture, Ehime University, Tarumi 3-5-7, Matsuyama 790-8566, Japan

Corresponding author: Yoshitaka Kamimura (kamimura@keio.jp)

Academic editor: Fabian Haas | Received 1 December 2022 | Accepted 11 January 2023 | Published 7 February 2023

<https://zoobank.org/E54EC459-C5BB-4232-91CC-C14E67B27DB6>

Citation: Kamimura Y, Lee C-Y, Yamasako J, Nishikawa M (2023) Identification and reproductive isolation of *Euborellia* species (Insecta, Dermaptera, Anisolabididae) from East and Southeast Asia. ZooKeys 1146: 115–134. <https://doi.org/10.3897/zookeys.1146.98248>

Abstract

Euborellia (Anisolabididae: Anisolabidinae) is one of the most speciose genera of earwigs (Dermaptera), and its species-level classification is difficult. To settle the classification of brachypterous species with abbreviated tegmina recorded from East and Southeast Asia, we examined the morphology and reproductive isolation of three tentative *Euborellia* species, and analyzed the DNA barcoding region of the mitochondrial cytochrome oxidase subunit I (COI) gene. The observed complete reproductive isolation among the three *Euborellia* taxa and considerable differentiation in the COI sequences clearly show that each should be treated as a separate species. Based on morphology, distribution and the DNA sequence, we identify *Euborellia* sp. 1 of Malaysia as *E. annulata* (Fabricius), a circumtropical cosmopolitan with no records of a fully winged form. Samples from Ioto Island (= Iwo-jima Island: Ogasawara Islands, southern Japan) were also identified as this species. *Euborellia* sp. 3, from the main islands of Japan, was generally larger and lacked a Y-shaped pigmented area on the penis lobe, which is characteristic of *Euborellia* sp. 1. We propose reinstating *E. pallipes* (Shiraki) as the oldest name for this taxon. *Euborellia* sp. 2, even the brachypterous form, can be distinguished from these two species by its paler coloration (particularly the femora), ecarinate post-abdomen, and the shape of the male genitalia (parameres). We tentatively identify this species as *E. philippinensis* Srivastava based on the morphology of the brachypterous form, although the macropterous form cannot be distinguished from *E. femoralis* (Dohrn).

Keywords

DNA barcoding, *Euborellia pallipes*, genital morphology, post-copulatory reproductive isolation, reinstatement

Introduction

Euborellia Burr, 1910 (Anisolabididae: Anisolabidinae) is one of the most speciose genera of earwigs. It includes approximately 50 species (Popham and Brindle 1966; Sakai 1982, 1987; Steinmann 1989a, b; Srivastava 1999; Hopkins et al. 2018), in a small order of polyneopteran insects (Insecta: Dermaptera) with more than 2000 described species (Zhang 2013; Hopkins et al. 2018). Like related genera of Anisolabidinae, many *Euborellia* are apterous or brachypterous and are usually dark in color. Due to the scarcity of traits for species diagnoses, classifying this genus is very difficult.

This study examined the relationships among three tentative *Euborellia* species with flap-like vestigial tegmina (= forewings) found in East and Southeast Asia (named *Euborellia* sp. 1, *Euborellia* sp. 2 and *Euborellia* sp. 3 in the rest of the article). *Euborellia* sp. 1 was recorded from Malaysia, and was tentatively identified as *Euborellia annulata* (Fabricius, 1793) in Kamimura et al. (2016). Although the type locality of *E. annulata* is the West Indies, many authors consider this species a senior synonym of *Euborellia stali* (Dohrn, 1864), the type locality of which is Java, which makes it a circumtropical cosmopolitan (Brindle 1981; Sakai 1987; Srivastava 2003). Except for doubtful treatments of this species as a synonym of other *Euborellia* species with fully developed tegmina and wings (see the Results and discussion), both male and female adults of this species are brachypterous. This means that they only have vestigial tegmina as small oval flaps and entirely lack hindwings (Dohrn 1864; Brindle 1981; Sakai 1987; Srivastava 2003; but see Kamimura et al. 2016 for a single aberrant laboratory-raised male with fully developed tegmina but no hindwings). *Euborellia* sp. 2 is known only at the west coast of Penang Island in Malaysia (Kamimura et al. 2016). Although in that study all wild-caught samples were brachypterous, macropterous individuals with fully developed tegmina and wings were found in laboratory-reared populations. Based on the morphology of the brachypterous morph, the previous study tentatively identified the species as *Euborellia philippinensis* Srivastava, 1979, considered endemic to the Philippines (Srivastava 1979, 1999; Sakai 1987; Steinmann 1989a, b). A third possibly distinct species of brachypterous *Euborellia*, tentatively named *Euborellia* sp. 3 here, occurs in the temperate zone of Japan. These three species are inhabiting open lands, including agricultural fields, semi-urban grasslands, sandy seaside or streamside, and can be collected by hand-sorting (Kamimura et al. 2016; Nishikawa 2016).

An apterous species of *Euborellia* was recently discovered as a possible intruder in Europe (Kalaentzis et al. 2021). Based on both morphological and molecular evidence, this species was identified as the apterous form of the Oriental species *Euborellia femoralis* (Dohrn, 1863), which is usually macropterous (Kalaentzis et al. 2021). To resolve the cryptic species diversity of Anisolabidinae in Australia, Stuart et al. (2019)

also demonstrated the effectiveness of an approach incorporating both morphometric and molecular analyses. To settle the classification of *Euborellia* species in Asia, we thus examined reproductive isolation among the three tentative species (*Euborellia* sp. 1, 2, and 3), and their detailed external and genital morphologies. Based on sequences of a mitochondrial cytochrome oxidase subunit I (COI) gene region, which is widely used for DNA barcoding of Dermaptera (Matzke and Kočárek 2015; Stuart et al. 2019; Kalaentzis et al. 2021; Kočárek and Wahab 2021), the genetic divergence and phylogenetic relationships among these and other *Euborellia* species were also examined.

Materials and methods

Reproductive isolation

Two experiments examined pre- and post-copulatory reproductive isolation among the three tentative species. Virgin females were obtained by separating newly emerged adults every three days from laboratory cultures of nymphs (wild-caught or mainly the F_1 generation). For *Euborellia* sp. 1 and *Euborellia* sp. 3, individuals derived from five localities of Malaysia (Batu Ferringi [5.47°N, 100.25°E], Bukit Bendera [5.42°N, 100.26°E], Bayan Indah beach [5.34°N, 100.31°E], and Bayan Lepas [5.33°N, 100.31°E] of Penang Island and Kuantan [3.80°N, 103.34°E], Pahang state; and some of their hybrid F_1) and three localities from Japan (Tokushima city, Tokushima Prefecture [34.12°N, 134.58°E], Yokohama city, Kanagawa Prefecture [35.51°N, 139.57°E], and Komae city, Tokyo Prefecture [35.63°N, 139.57°E]) were used, respectively. All samples of *Euborellia* sp. 2 were derived from a single locality (Sungai Nipah, Penang Island, Malaysia [5.32°N, 100.20°E]), but pairing of a male and a female from the same full-sib family was avoided. For males, wild-caught adults were also used (see Suppl. material 1 for further details). All animals were kept at 26 ± 1 °C (12 h photoperiod) and provided with water and unlimited amounts of commercial cat food.

In the first experiment (Exp. 1), a virgin female (age: 5–68 days after imaginal eclosion: median = 9 days) was paired with a conspecific or heterospecific male in a plastic container (50 × 32 mm, 12 mm high) with plaster of Paris at the base for 21 h ($N = 5$ for each species combination). Then the females were sacrificed by placing them in a freezer (–20 °C) for later examination of their insemination status. The spermatheca was dissected from the females in insect Ringer's solution (0.9 g NaCl, 0.02 g CaCl_2 , 0.02 g KCl, and 0.02 g NaHCO_3 in 100 mL water) under a stereomicroscope (EZ vision, Saxon, Guangzhou, China), and then examined under a light microscope (BX53 or CX21, Olympus, Tokyo; 40–400×). In the second experiment (Exp. 2), a virgin female (age: 3–83 days after imaginal eclosion: median = 6 days) was paired with a conspecific or heterospecific male in a separate plastic vessel (60 mm diameter, 40 mm high) for 72 h ($N = 5$ for each species combination). Then the females were reared separately in the vessel for 30 days after removing the male. Oviposition and hatching of offspring were checked every two or three days. The spermatheca of the females that

produced no hatchlings during the observation period was examined for the presence of sperm, as described above. Females with at least one hatchling or sperm in the spermatheca were scored as “inseminated”.

External and genital morphology

The external morphologies of dried adult materials were examined under a stereomicroscope (S8-APO; Wetzlar, Germany or SZX16; Olympus, Tokyo, Japan) and photographed using an Olympus Pen e-pl1s digital camera (Olympus). “Microscope mode” and “Focus-stacking sub-mode” of a Tough-TG5 digital camera (Olympus) were also used to obtain composite images of the external traits. The male genitalia were extracted from freeze-preserved, dried, or fresh specimens anesthetized with carbon dioxide under a stereomicroscope. After mounting on a glass slide with insect Ringer’s solution, they were observed and photographed under a light microscope (BX53, 100–400 \times ; Olympus) equipped with an Olympus DP80 CCD camera or a differential interference contrast (DIC) microscope (BX53, 100–400 \times ; Olympus) fitted with an Olympus Pen e-pl1s digital camera. Based on photographs taken under the DIC microscope, selected parts of each image in focus were composed using Combine ZP Image Stacking Software (Hadley 2008).

The samples were wild-caught from Penang Island (Bayan Lepas [Penang-1], Batu Ferringi [Penang-2], and Bayan Indah beach [Penang-3]) for *Euborellia* sp. 1. For *Euborellia* sp. 2 and *Euborellia* sp. 3, samples of laboratory stock populations, derived from a female collected from Sungai Nipah, Penang Island, Malaysia (in 2012), and Takasago city, Hyogo Prefecture, Japan [34.75°N, 134.80°E] (in 2018), respectively, were examined. For *Euborellia* sp. 3, wild-caught and mainly F₁-generation offspring were also examined for the following seven localities of Japan: Satsuma-sendai city, Kagoshima Prefecture [31.81°N, 130.31°E: Kagoshima-1], Shimokoshiki Island, Kagoshima Prefecture [31.66°N, 129.72°E: Kagoshima-2], Naruto city, Tokushima Prefecture [34.20°N, 134.60°E], Shizuoka city, Shizuoka Prefecture [35.01°N, 138.39°E: Shizuoka-1], Izunokuni city, Shizuoka Prefecture [35.06°N, 138.95°E: Shizuoka-2], Yokohama city, Kanagawa Prefecture [35.51°N, 139.57°E], and Iwaki city, Fukushima Prefecture [36.88°N, 140.79°E].

For *Euborellia* sp. 1 and 3, which were challenging to discriminate based on their external appearance, three traits were chosen for measurement based on the results of a pilot study: maximum head width (including eyes), maximum pronotum width, and hind tibia length. These traits can usually be measured on dried specimens preserved in museums and can be used for future studies on this group. These traits were measured for dried materials (Suppl. material 2) to the nearest 0.026 mm using a binocular microscope (SZ, Olympus) with an eyepiece. The mean values were used for subsequent analysis for samples in which both the right and left hind tibia lengths were measurable. Otherwise, the measurements of one side were used.

In addition to the samples collected by the authors, two female and one male adult *Euborellia* collected from Ioto Island (= Iwo-jima Island) in the Ogasawara Islands (= Bonin Islands) preserved in the collection of Kanagawa Prefectural Museum of Natural

History (**KPMNH**), Japan were examined: 2♀♀, pond-side at the Northern Airfield site, Ioto Island, Ogasawara, Tokyo, 13–14.XII.2005, Haruki Karube leg.; 1♂, Ioto Island, Ogasawara, Tokyo, 31.XII.2004, Katsumi Sano leg. For comparison, an adult female sample of *E. annulata*, collected from French West Indies: Jarry, Basse-Terre Island, Guadeloupe Archipelago (16.23°N, 61.55°W: 20.XI.2020, Nicolas Moulin leg.) was also observed and measured. Holotype (female) of *Anisolabis pallipes* Shiraki, 1905, in the collection of National Taiwan University (**NTU**), Taipei, Taiwan, was also examined onsite.

DNA barcoding

Total genomic DNA was extracted from fresh, ethanol-preserved, or dried samples of *Euborellia* and other dermapterans (Suppl. material 3), using a DNeasy Blood & Tissue Kit (QIAGEN, Hilden, Germany) according to the manufacturer's instructions. Depending on the size of the specimens, one to three legs on one side were used for DNA extraction. PCR amplification of a mitochondrial cytochrome oxidase subunit I (COI) region (660 base pairs), which is widely used for DNA barcoding of earwigs (Matzke and Kočárek 2015; Stuart et al. 2019; Kalaentzis et al. 2021; Kočárek and Wabab 2021) and other invertebrates (Folmer et al. 1994) was performed using a T100™ thermal cycler (Bio-Rad Laboratories, Hercules, CA, USA) and primers LCO1490 and HCO2198 (Folmer et al. 1994). PCR reactions were conducted in a 20 µL volume containing 1 µL each primer (10 µM), 10 µL 2×PCR buffer, 4 µL dNTPs (2 mM each), 0.4 µL KOD FX Neo DNA polymerase (1.0 unit/µL; Toyobo, Osaka, Japan), and 1 µL genomic DNA. The PCR temperature profile consisted of 2 min at 94 °C, then 35 cycles of 15 sec at 94 °C, 15 sec at 51 °C, and 15 sec at 72 °C, followed by a 6 min final extension at 72 °C. Since the primer set did not work for *Euborellia annulipes* (Lucas, 1847), another set of primers (SKCOI-7 and SKCOI-7) was used to obtain PCR products of this species, which largely overlapping with the LCO1490–HCO2198 region but lacking 44 bases of the 5' end, according to the protocol of Su et al. (2004). Sequencing was done by Eurofins Genomics (Tokyo, Japan) (or FASMACH, Kanagawa, Japan for *E. annulipes*). The chromatograms were checked visually and edited manually where appropriate. After eliminating the primer sequences, the COI sequences have been deposited in DDBJ/ENA/GenBank.

Multiple sequence alignments were conducted with ClustalW (Thompson et al. 2003) implemented in MEGA11 (Tamura et al. 2021) using the default settings. The sequences of other *Euborellia* species and *Apachyus feae* Bormans, 1894 (Apachyidae) available in GenBank were also included in the analysis (Accession numbers: MW703670.1, MW703671.1, MW703672.1, MW703673.1, MW291948.1, and KPO19208.2). The maximum likelihood (ML) analysis and calculation of intraspecific and interspecific *p*-distances were performed with MEGA11. For the ML analysis, the optimal nucleotide substitution model (the general time-reversible model [GTR]+G+I) was determined by MEGA11 using the Bayesian Information Criterion (BIC) and the default search algorithms: a discrete Gamma distribution (+G) with five rate categories and a certain fraction of sites evolutionarily invariable (+I). Because no non-dermapteran samples were added as outgroups, the resultant trees were rooted by a clade of the

Infraorder Protodermaptera. Investigations of the sequence saturations were done plotting the estimated number of base substitutions (transitions and transversions) against the genetic distance (maximum composite likelihood model). The data were obtained for 741 comparisons of 38 sequences (660 bp) obtained in the present study by using MEGA11, and visualized by a personal script written in Python v.3.8.3.

Results and discussion

Reproductive isolation

The crossing experiments revealed that the three tentative *Euborellia* species are strongly isolated (Fig. 1). Interestingly, when the data for 21 h and 72 h pairings were combined, insemination was found to have occurred in all heterospecific pairing combinations (Fig. 1a, b). The insemination success between a female of *Euborellia* sp. 1 and a male of *Euborellia* sp. 2 was very high, 80% in both the 21 h and 72 h pairings (Fig. 1a, b). On average, 73.3% of females paired with a heterospecific male, and 93.3% paired with a conspecific male laid an egg batch (Fig. 1c). All egg batches of females paired with a conspecific male developed normally, resulting in the production of at least one hatchling (Fig. 1d). However, no development was observed in the eggs deposited after heterospecific pairings, with no hatchling success during the 30-day observation period (Fig. 1d).

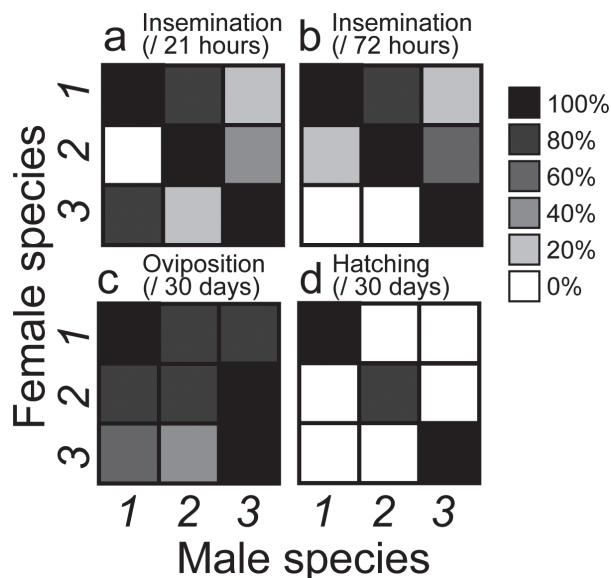


Figure 1. Insemination (a,b), oviposition (c), and hatching success (d) of conspecific and reciprocal heterospecific crosses among the three tentative species of *Euborellia*: *Euborellia* sp. 1 (1), *Euborellia* sp. 2 (2), and *Euborellia* sp. 3 (3). These species are identified as *E. annulata*, *E. philippinensis*, and *E. pallipes*, respectively.

External and male genital morphology

The external morphologies of the three tentative species, particularly those of *Euborellia* sp. 1 and 3, are similar and difficult to distinguish. Except for the fully winged morph of *Euborellia* sp. 2 (Fig. 2d), both male and female adults of these species have the tegmina abbreviated to small oval flaps (Fig. 2a–c). Kamimura et al. (2016) reported one aberrant male with fully developed tegmina but no hindwings for *Euborellia* sp. 1. The coloration of *Euborellia* sp. 2 is generally paler than the other two species, being dark brownish (Fig. 2a–d). In the legs of these species, a black marking develops in the mid part of the femur (indicated by red arrows in Fig. 2h–j) and in the basal half of the tibia (indicated by orange arrows in Fig. 2h–j). In *Euborellia* sp. 1, the former marking is much more conspicuous than the latter, forming an almost complete band (Fig. 2h). By contrast, the tibial marking is more prominent in *Euborellia* sp. 2 (Fig. 2i). These black markings of *Euborellia* sp. 3 develop at almost the same intensity. Still, the femoral band usually does not reach the ventral side (Fig. 2j).

Kalaentzis et al. (2021) reported that the relative lengths of the basal antennomeres are useful for diagnosing *Euborellia* species. However, we found no conspicuous difference in the antennal morphology of the three tentative species: the 1st antennomere is as long as or slightly shorter than the length of the 2nd, 3rd, and 4th combined (Fig. 2e–g). In males of *Euborellia* sp. 1 and 3, the lateral sides of the abdominal segments 6th (in some cases 7th) to 9th are acute-angled posteriorly and carinated (Fig. 2n, p: yellow arrowheads). The corresponding abdominal tergites of *Euborellia* sp. 2 are bent at an almost right angle (Fig. 2o: light blue arrowheads), making the post-abdomen cross-sections rectangular.

The genital morphologies are also quite similar among the *Euborellia* species examined here. The male genitalia are elongated, almost the body length (*Euborellia* sp. 1 and 3) or the abdominal length (*Euborellia* sp. 2). On each penis lobe including a thin virga, two humps of denticulated pads are present (orange and magenta arrowheads in Fig. 2q–s). In addition, a conspicuous Y-shaped area of pigmentation is present only in *Euborellia* sp. 1 (Fig. 2q: black arrowhead). Although previous descriptions of *Euborellia* species lack such a detailed morphology of the penis lobes, judging from the high-resolution images in Kalaentzis et al. (2021), the penises of *E. femoralis* and *E. annulipes* lack the Y-shaped pigmentation. The shape of the parameres is also similar among the species, being weakly emarginated on the inner side. The outer margin is strongly angular in *Euborellia* sp. 2 compared to *Euborellia* sp. 1 and 3 (black arrows in Fig. 2r).

To separate *Euborellia* sp. 1 and 3, three morphological traits, considered measurable in dried specimens from museums, were quantified and compared: the maximum head width, maximum prothorax width, and hind tibia length. Although the sample size is small for *Euborellia* sp. 1, the three traits were generally smaller in *Euborellia* sp. 1 than in *Euborellia* sp. 3, particularly in females (Fig. 3).

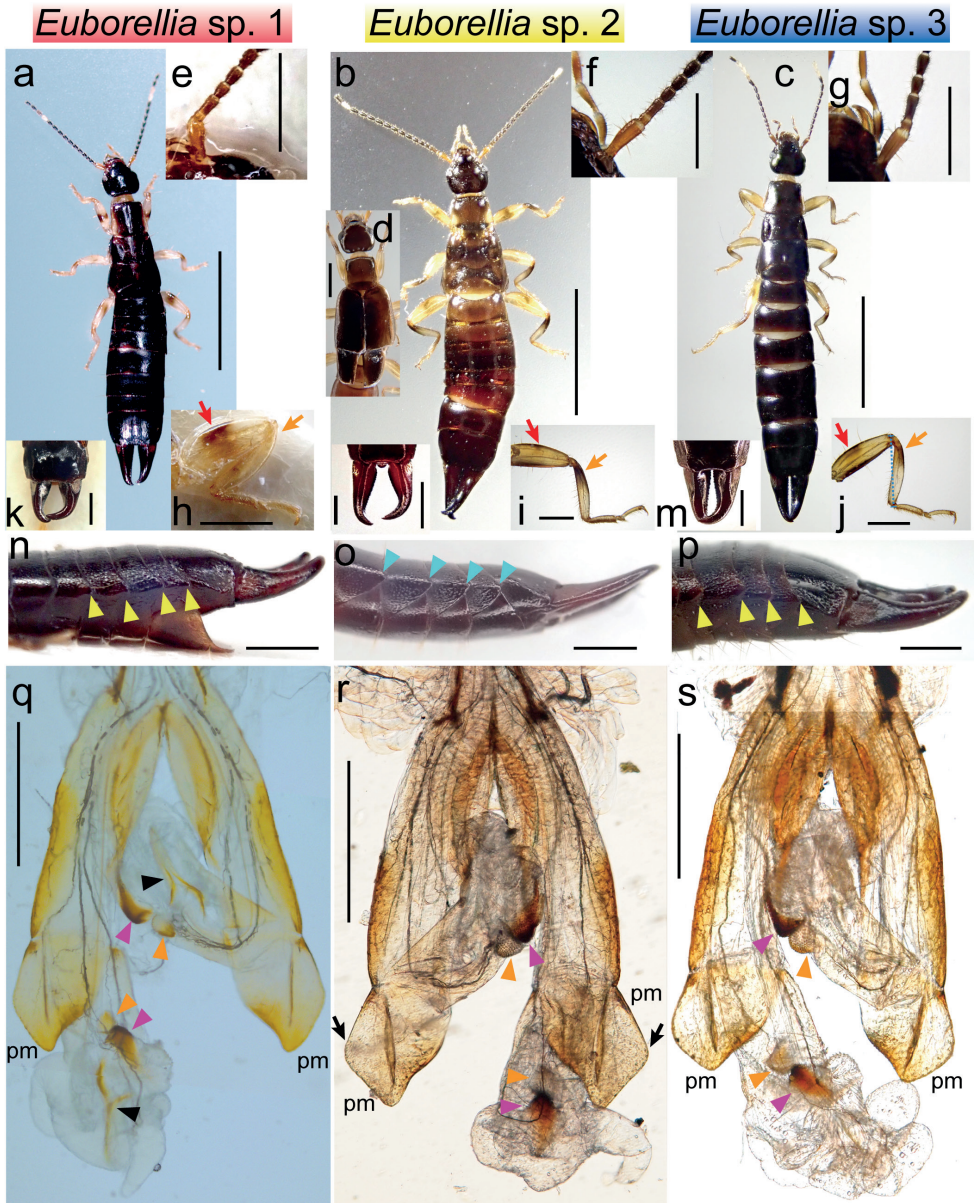


Figure 2. Female habitus (a–c), head and thorax of a fully winged-form male (d), base of female right antenna (e–g), female right hindleg (h–j), male forceps (k–m), left side of male post-abdomen (n–p), and distal part of male genitalia (q–s) of *Euborellia* sp. 1 (identified as *E. annulata*; a, e, h, k, n, q), *Euborellia* sp. 2 (identified as *E. philippinensis*; b, d, f, i, l, o, r), and *Euborellia* sp. 3 (identified as *E. pallipes*; c, g, j, m, p, s). Femoral and tibial black marking are indicated by the red and orange arrows, respectively (h–j). Carination and dorso-lateral angles of the abdominal tergites, the latter forms the lateral ridges, are indicated by the yellow and light blue arrowheads, respectively (n–p). On each penis lobe, a pair of denticulated pads (the orange and magenta arrowheads) and a Y-shaped area of pigmentation (only in *Euborellia* sp. 1: black arrowheads) are present. The external apical angle of the parameres (pm) is acute in *Euborellia* sp. 2 (the black arrow). Scale bars: 5 mm (a–c); 1 mm (d–p); 500 μ m (q–s).

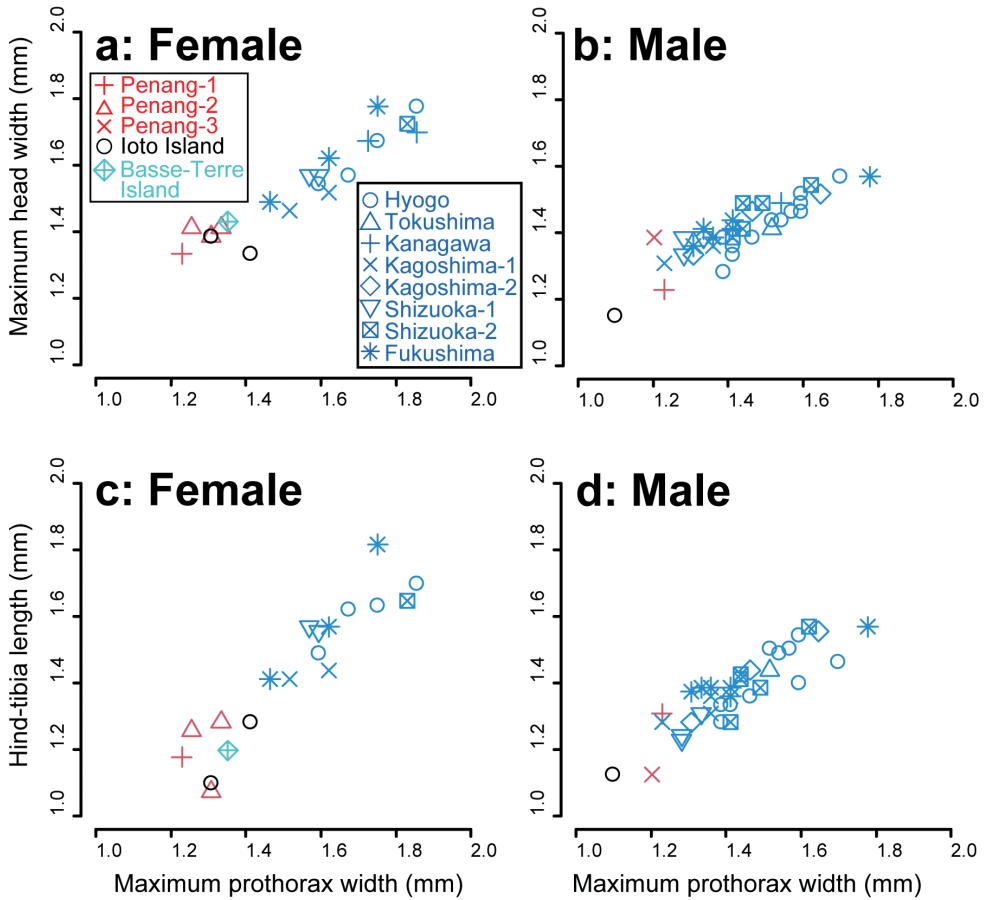


Figure 3. Relationship between the maximum pronotum width and maximum head width (**a, b**), and relationship between the maximum pronotum width and hind tibia length (**c, d**) of female (**a, c**) and male (**b, d**) *Euborellia* species (*Euborellia* sp. 1 and *Euborellia* sp. 3). Red, blue, and black symbols represent samples from Malaysia, the main islands of Japan (Honshu, Shikoku, and Kyushu, and Shimokoshiki Island near Kyushu), or Ioto Island, respectively. The data of a female *E. annulata*, collected from Basse-Terre Island, Guadeloupe Archipelago, is also shown in **a** and **c** (light blue crossed diamonds). Details of the localities are provided in Suppl. material 2.

Examination of additional materials

As additional materials from Japan, two female and one male adult *Euborellia* collected from Ioto Island (= Iwo-jima Island) in the Ogasawara Islands (= Bonin Islands) were examined. The tegmina of these samples are small flaps (Fig. 4a, b) as in the other *Euborellia* samples examined above. In the male specimen, the lateral side of the 6th–9th abdominal tergites protrudes posteriorly and is carinated forming a ridge (Fig. 4c). The conspicuous black band in the femurs (Fig. 4d, e) and the smaller body size compared to *Euborellia* sp. 3 from the main islands of Japan (Fig. 3) indicate that these are identical to *Euborellia* sp. 1. The presence of a Y-shaped area of pigmentation in the male genitalia

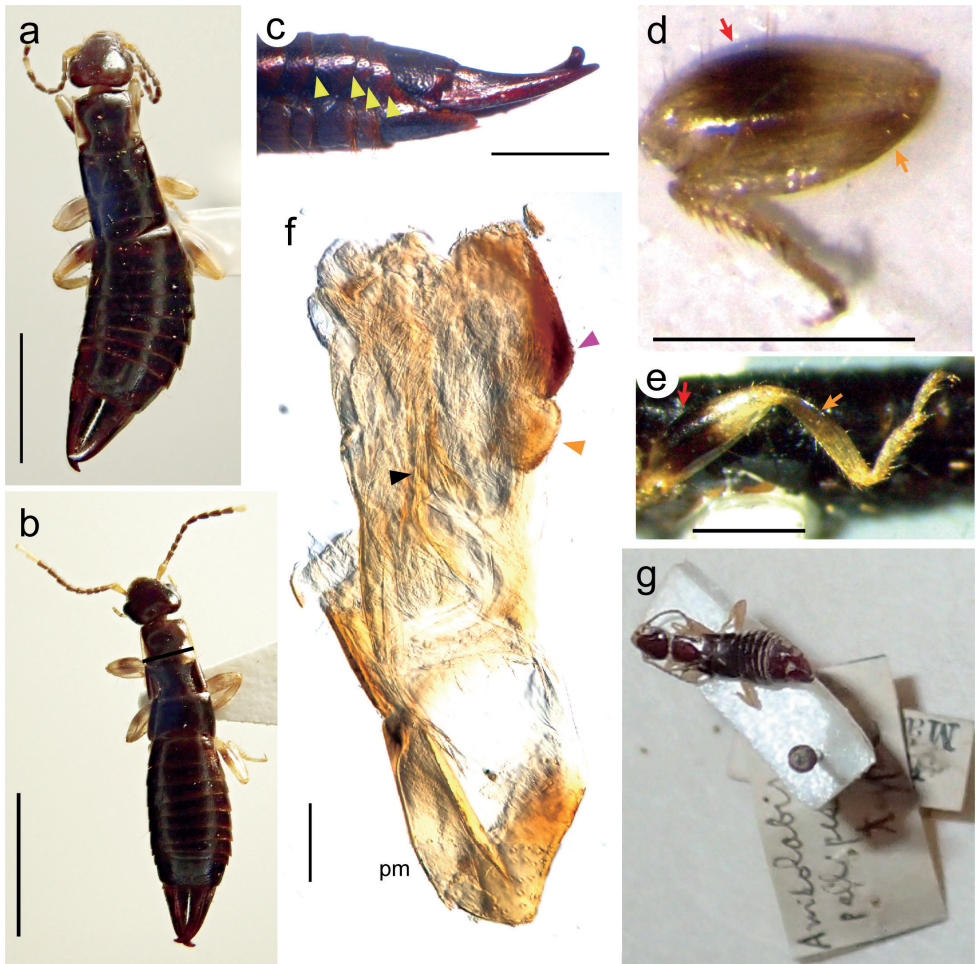


Figure 4. *Euborellia* specimens collected from Ioto Island, Ogasawara Islands, Japan (**a–f**) and the type (holotype) material of *Anisolabis pallipes* Shiraki, 1905, preserved in Insect Museum, National Taiwan University, Taipei, Taiwan (**g**). **a** adult female **b** adult male **c** left lateral view of the male post-abdomen **d** right hindleg of the male **e** left hindleg of the female **f** part of the male genitalia (right paramere [pm] and the penis lobe). For the meanings of the arrows and arrowheads, see the caption of Fig. 2. Scale bars: 3 mm (**a**, **b**); 1 mm (**c–e**); 100 μ m (**f**).

(Fig. 4f) supports this view. A female sample of *E. annulata* from Basse-Terre Island, Guadeloupe Archipelago (French West Indies), near the type locality, was also placed in the cluster of *Euborellia* sp. 1 based on the morphological measurements (Fig. 3a, c).

Based on a brachypterous adult female collected from Takasago, Hyogo Prefecture, Japan, Shiraki (1905) described *Euborellia pallipes* (Shiraki, 1905) as *Anisolabis pallipes* Shiraki, 1905. Although some authors have indicated that the type locality of this species is Taiwan (Formosa) (Burr 1911; Steinmann 1989a, b; Srivastava 2003),

the label of the name-bearing type material (female adult), now in the Insect Museum, National Taiwan University, Taipei, Taiwan (Fig. 4g), indicates that it was collected in Takasago (handwritten, in Japanese), Japan (Digital Archives Project of National Taiwan University 2021). This agrees with the original description (Shiraki 1905) and subsequent examination of the type material by Okuni (1913). Although this material has not been examined in detail and morphological measurements have not been made, its leg coloration with pale markings and locality indicate that the specimen belongs to our *Euborellia* sp. 3.

DNA barcoding and phylogenetic analysis

Although comparable numbers of transversions (Tv) and transitions (Ts) are estimated to occur in the 2nd and 3rd codon positions at the genetic distance larger than ca 0.2 (Fig. 5c, d), in the 1st codon and in total, Ts generally outnumber Tv, both exhibiting a linear relationship with the genetic distance (Fig. 5a, b). Thus, the DNA barcoding region of the Dermaptera is considered to contain phylogenetic information for the diagnoses of species and genera, and relationships among closely related genera.

The percent sequence divergence was lower than 2% within each tentative *Euborellia* species, except for one individual of *Euborellia* sp. 1, which showed about 5% divergence from the other three conspecific samples (Table 1). By contrast, the interspecific divergences were much higher on average: 13.8% between *Euborellia* sp. 1 and 2, 17.0% between *Euborellia* sp. 1 and 3, and 13.7% between *Euborellia* sp. 2 and sp. 3.

Although the support is low (56%), the samples of Anisolabidinae (Anisolabididae) formed a monophyletic clade (Fig. 6). An exception in Anisolabididae is *Platylabia major* Dohrn, 1867 (Platylabiinae: = Palicinae Engel & Haas, 2007; = Palexinae Kočárek, 2010), the phylogenetic placement of which was not resolved in our analysis. In Anisolabidinae, *Euborellia* species, except for *Euborellia arcanum* Matzke & Kočárek, 2015, formed a monophyletic clade (55% support). The DNA barcode region of *E. arcanum*, possibly an introduced species in Europe, is almost identical to that of *Anisolabella ryukyuensis* (Nishikawa, 1969). These species are also similar in the external and genital morphologies (Nishikawa 1969; Matzke and Kočárek 2015), warranting further studies to settle their placements.

In the *Euborellia* clade, multiple samples of each tentative species (*Euborellia* sp. 1, 2, or 3) and *E. femoralis* form monophyletic clades with 100% support. Interestingly, the clade of *Euborellia* sp.1 (from Malaysia) consisted of two subclades, one of which also included *E. annulata* from the West Indies. The sister relationship between *Euborellia* sp. 3 and *E. femoralis* was also supported with high confidence (99%). *Euborellia* sp. (China) and *Euborellia plebeja* (Dohrn, 1863), for which only the fully winged form has been reported (except for records of those treated as *Euborellia* sp. 3 here), form a clade with 91% support, with its sister place being *Euborellia* sp. 2 (95% support). Placement of *E. annulipes* in this genus was not settled.

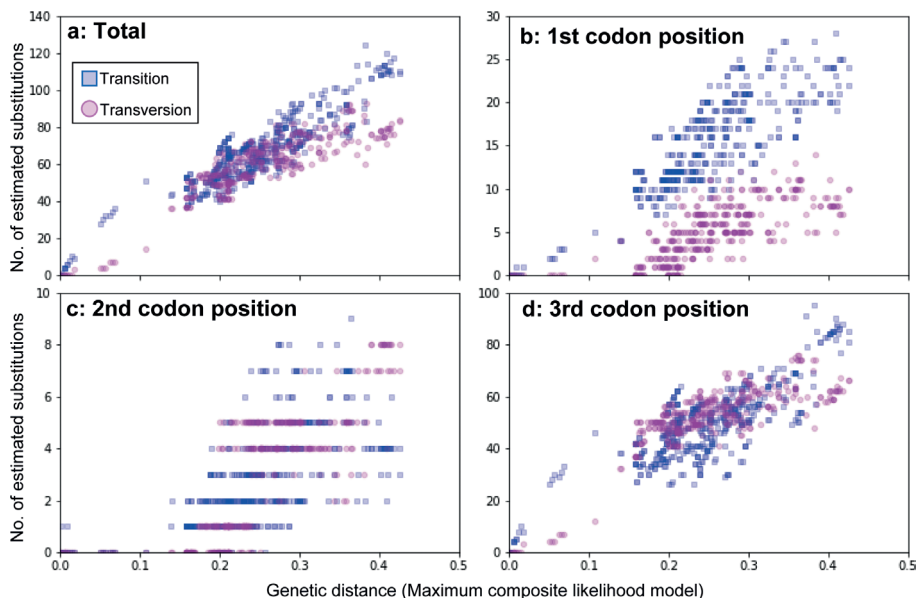


Figure 5. Estimated number of substitutions (transitions and transversions) against the genetic distance (maximum composite likelihood model) in relation to the codon positions.

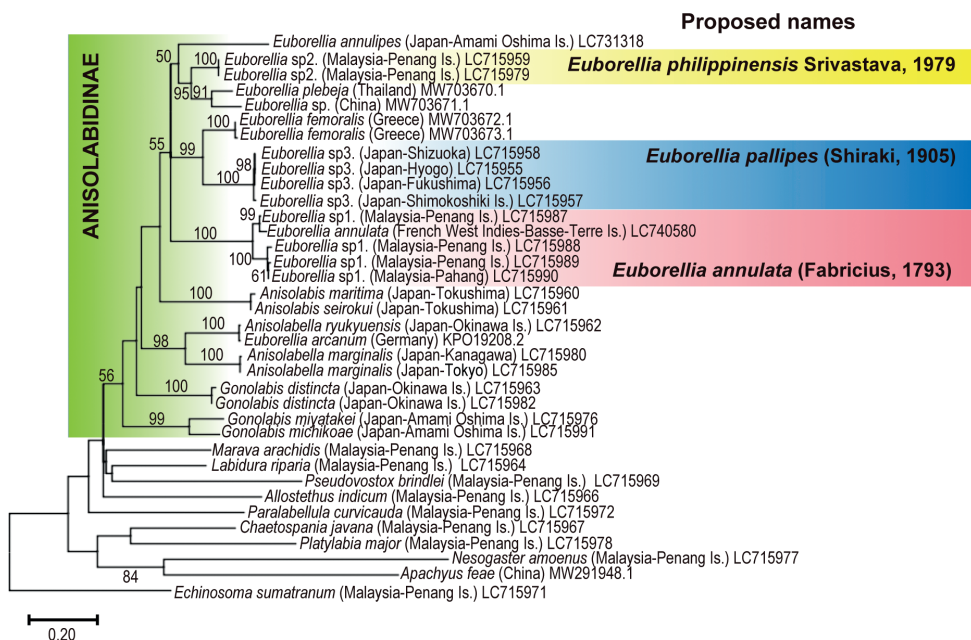


Figure 6. The maximum likelihood phylogenetic tree constructed from COI sequence data. Numbers at the branches indicate bootstrap values (% in 1000 replicates). GenBank accession numbers follow the localities in the parentheses. *Euborellia* sp. 1, *Euborellia* sp. 2, and *Euborellia* sp. 3 are shaded in red, yellow, and blue, respectively, indicating the proposed names. The details of the samples sequenced in the present study (the accession numbers beginning with “LC”), are available in Suppl. material 3 and DDBJ/ENA/GenBank.

Table 1. Percent divergence (p-distance) between the sequences. Intraspecific comparisons are highlighted in a different color for each species.

Species (GenBank Accession No.)	1	2	3	4	5	6	7	8	9	10	11	12	13	14	15	16	17
1 <i>Euborellia</i> sp. 1 (LC715987)*	0.000																
2 <i>Euborellia</i> sp. 1 (LC715988)*	0.055	0.000															
3 <i>Euborellia</i> sp. 1 (LC715989)*	0.052	0.015	0.000														
4 <i>Euborellia</i> sp. 1 (LC715990)*	0.048	0.012	0.006	0.000													
5 <i>Euborellia annulata</i> (LC740580)	0.018	0.065	0.062	0.059	0.000												
6 <i>Euborellia</i> sp. 2 (LC715959)**	0.141	0.139	0.135	0.135	0.142	0.000											
7 <i>Euborellia</i> sp. 2 (LC715979)**	0.141	0.139	0.135	0.135	0.142	0.000	0.000										
8 <i>Euborellia plebeja</i> (MW703670.1)	0.153	0.155	0.152	0.150	0.146	0.097	0.097	0.000									
9 <i>Euborellia</i> sp. (winged species: MW703671.1)	0.144	0.151	0.150	0.150	0.142	0.109	0.109	0.087	0.000								
10 <i>Euborellia</i> sp. 3 (LC715955)***	0.165	0.174	0.167	0.171	0.173	0.136	0.136	0.160	0.153	0.000							
11 <i>Euborellia</i> sp. 3 (LC715956)***	0.165	0.174	0.167	0.171	0.173	0.136	0.136	0.160	0.153	0.000	0.000						
12 <i>Euborellia</i> sp. 3 (LC715957)***	0.165	0.174	0.167	0.171	0.173	0.136	0.136	0.160	0.153	0.000	0.000	0.000					
13 <i>Euborellia</i> sp. 3 (LC715958)***	0.168	0.177	0.170	0.174	0.173	0.139	0.139	0.158	0.154	0.006	0.006	0.006	0.000				
14 <i>Euborellia femoralis</i> (MW703672.1)	0.159	0.152	0.150	0.149	0.155	0.126	0.126	0.150	0.145	0.114	0.114	0.114	0.114	0.000			
15 <i>Euborellia femoralis</i> (MW703673.1)	0.165	0.155	0.152	0.151	0.160	0.124	0.124	0.149	0.147	0.111	0.111	0.111	0.111	0.005	0.000		
16 <i>Euborellia annulipes</i> (LC731318)	0.173	0.174	0.169	0.171	0.171	0.156	0.156	0.152	0.153	0.182	0.182	0.182	0.178	0.166	0.164	0.000	
17 <i>Euborellia arcanum</i> (KP019208.2)	0.171	0.174	0.168	0.168	0.168	0.142	0.142	0.167	0.161	0.188	0.188	0.188	0.192	0.165	0.166	0.179	0.000

* Proposed name: *Euborellia annulata*.** Proposed name: *Euborellia philippinensis*.*** Proposed name: *Euborellia pallipes*.

Identity of the *Euborellia* species

After the description of *Forficula annulata* from “Americae meridionalis” (= southern America) by Fabricius (1793), the taxonomy of *Euborellia* species with flap-like, abbreviated tegmina has long been confused. De Bormans and Krauss (1900) and Burr (1911) listed this species as *Labia annulata* under Spongiphoridae (= Labiidae), and Steinmann (1989b, 1990) followed this view. Brindle (1981), who examined the Fabrician types in the Zoological Museum of Copenhagen University, concluded that the type of *Forficula annulata*, a male collected from the West Indies, is identical to the species known as *Euborellia stali* (Dohrn, 1984) (see also Kevan and Vickery 1997). Accordingly, many subsequent authors treated *E. stali* as a junior synonym of the circumtropical cosmopolitan species *E. annulata*, together with *Anisolabis minuta* Caudell, 1907 (the type locality is Puerto Rico), which Hebard (1923) and Reichardt (1968) proposed to be a junior synonym of *E. stali* (Sakai 1987; Srivastava 2003).

Interestingly, our *Euborellia* sp. 1 made a cluster, both in morphology (Fig. 3) and molecular (Fig. 6) data sets, with the female sample of *E. annulata* collected near its type locality. Thus, we follow the view that *E. annulata* is a circumtropical cosmopolitan, and assign our *Euborellia* sp. 1 to *E. annulata*, as we did in Kamimura et al. (2016). In the present study, we detected the characteristic Y-shaped area of pigmentation on the penis lobe of *Euborellia* sp. 1. Unfortunately, previous descriptions of *Euborellia* species, including those of *E. annulata*, *E. stali*, and *E. minuta*, do not include detailed structures on the penis lobes. Extensive re-examination for this trait is required for the type material and specimens assigned as *E. annulata* from other localities. Our examination of the samples from Ioto Island in the Ogasawara Islands, particularly the detection of a Y-shaped area of pigmentation on the penis lobe of the male specimen, indicates that they are conspecific to our *Euborellia* sp. 1, and thus *E. annulata* (Figs 3, 4a–f). Brindle (1972) reported the occurrence of *E. annulata* (as *E. stali*) in the Pacific, including Chichijima Island in the Ogasawara Islands, which is approximately 200 km north of Ioto Island (see also Nishikawa 2020b).

Interestingly, our molecular analysis detected two sub-clades in *Euborellia annulata*: a female from Bayan Lepas, Penang Island, Malaysia (LC715987) showed only 1.8% divergence from a female from the West Indies (LC740580), while the other Malaysian samples (LC715988–LC715990), including those from other sites of Penang Island, were clustered with 4.8–6.5% differences from the formers (Table 1). We detected no differences in the external morphology between these two subgroups. Considering that some widely-distributed insects show remarkable intraspecific diversity (> 5%) in the CO1 sequences (up to 26.0%: Cognato 2006), we tentatively treat those as a single species *E. annulata*. Future studies should explore for possible isolations among possible sub-lineages of this species.

Kamimura et al. (2016) treated *Euborellia* sp. 2 as *E. philippinensis*, although no fully winged morph had been reported for this species. The external and male genital morphology of the brachypterous form of *Euborellia* sp. 2 agree with the previous descriptions of *E. philippinensis* (Srivastava 1979), including the sharp external apical angle of the parameres (Fig. 2r: black arrows) and the posterior margin and angles of the pronotum broadly rounded (Fig. 2b), compared to those of *E. annulata*.

In addition to *Euborellia* sp. 2, two macropterous *Euborellia* species, *E. plebeja* and *E. femoralis*, have been reported from the Orient (Srivastava 2003). Although the treatment of *E. stali* (with abbreviated tegmina) as a junior synonym of *E. plebeja* by Hebard (1927) caused further confusion and difficulties in the taxonomy of *Euborellia* (Brindle 1972), except for the erroneous treatments of *Euborellia* sp. 3 discussed below, no indisputable example of an apterous or brachypterous form of *E. plebeja* has not been reported. According to Bey-Bienko (1959) and Srivastava (2003), lateral ridges (carina) do not develop in *E. plebeja* (vs. developed in the 6th–9th abdominal tergites of *E. femoralis*) with more prominent external angles of the parameres (vs. external angles convex in *E. femoralis*). Thus, it is difficult to distinguish the macropterous form of *Euborellia* sp. 2, found only in laboratory-reared individuals, from *E. plebeja* (Kamimura et al. 2016). Our phylogenetic analysis also revealed that *Euborellia* sp. 2 is closely related to *E. plebeja* (a Thailand specimen) and *Euborellia* sp. (a Chinese specimen; macropterous), both of which Kalaentzis et al. (2021) sequenced. However, the genetic differentiation in the DNA barcode region is relatively large between *Euborellia* sp. 2 and *E. plebeja* (more than 9.5%: Fig. 6). Kalaentzis et al. (2021) considered that *Euborellia* sp. from China, which is sister to *E. plebeja* with genetic differentiation of about 8.7%, represents another species. Following this view, we tentatively treat *Euborellia* sp. 2 as *E. philippinensis* based on the morphology of the brachypterous form, as we did in Kamimura et al. (2016).

The present results clearly show that *Euborellia* sp. 3 of the main islands of Japan (Honshu, Shikoku, and Kyushu) is a distinct species. After the proposed (and erroneous) synonymy of *E. minuta* and *E. stali* as *E. plebeja* (Hebard 1923, 1927), Hebard (1933) also treated *Anisolabis pallipes* Shiraki, 1905 as a junior synonym of *E. plebeja*. Steinmann (1989a, b) proposed the same synonymy for *A. pallipes*. By contrast, Srivastava (2003) considered *A. pallipes* a junior synonym of *E. annulata* (= *E. stali*). Accordingly, the names *E. plebeja*, *E. stali*, or *E. annulata* have been used for the brachypterous *Euborellia* recorded from the main islands of Japan. However, judging from the type locality and external appearance of the type material bearing this name, we resurrect the name *Euborellia pallipes* (Shiraki, 1905) for our *Euborellia* sp. 3. Thus, though many subsequent authors treated (or suggested treating) this species, which closely resembles our *Euborellia* sp. 1, as a junior synonym of *E. annulata* (Srivastava 2003; Nishikawa 2011, 2016, 2020a), *E. stali* (Nishikawa 1975), or the macropterous species *E. plebeja* (Hincks 1947; Nishikawa 1969; Steinmann 1989a, b; Chen and Ma 2004), we consider that our *Euborellia* sp. 3 is *E. pallipes*, which is distinct from the above-mentioned species. Our identification and diagnoses are summarized in Table 2.

Interestingly, our molecular analysis revealed that this species is sister to *E. femoralis* (Fig. 6), for which only totally apterous or fully winged individuals have been reported (Bey-Bienko 1959; Anisyutkin 1998; Kalaentzis et al. 2021). Although Steinmann (1989a, b) treated the brachypterous species *Anisolabis minuta* Caudell, 1907 (= *E. minuta*) as a junior synonym of *E. femoralis*, this treatment lacks foundation (Srivastava 2003). The identities of *Euborellia* samples with abbreviated tegmina from Taiwan, the Nansei Islands of Japan, Korea, and mainland China, reported under the names *E. annulata* (Nishikawa 2016), *E. pallipes* (Shiraki 1928; Bey-Bienko 1936, 1959; Masaki 1936; Cho 1969; Sakai

Table 2. Diagnostic features of the three brachypterous *Euborellia* species from East and Southeast Asia. Female *E. annulata* and *E. pallipes* are difficult to distinguish, but the former is usually smaller (Fig. 3).

Traits	<i>Euborellia annulata</i> (<i>Euborellia</i> sp. 1)	<i>Euborellia philippinensis</i> (<i>Euborellia</i> sp. 2)	<i>Euborellia pallipes</i> (<i>Euborellia</i> sp. 3)
Black markings of legs	Markings of mid femur are darker than those of basal half of tibia	Markings of mid femur are weaker than those of basal half of tibia	In almost same intensity
Lateral sides of male abdominal segments 6 th (or 7 th) to 9 th	Carinated	Not carinated	Carinated
Outer margin of parameres	Not strongly angular, rounded	Strongly angular	Not strongly angular, rounded
Y-shaped area of pigmentation on penis lobes	Present	Absent	Absent

1970, 1982; Moon and Kim 1983; Kim and Moon 1985), or *E. plebeja* (Moon and Kim 1983, 1991; Kim and Moon 1985; Sakai 1987; Chen and Ma 2004), are not determined at present. Some other brachypterous *Euborellia* species have also been reported from South Asia to the Middle East: *E. abbreviata* Srivastava, 1977 [India], *E. annandalei* (Burr, 1906) [India], *E. manipurensis* Srivastava, 1979 [India], *E. sakaii* Steinmann, 1978 [Afghanistan], and *E. moesta* Gén , 1839 [Iran] (Srivastava 2003; Ko arek 2011a, b), relationships of which to the species studied here are totally unclear. Although the present study shows the effectiveness of DNA barcoding for specific diagnoses of *Euborellia* species, only limited entries are available for the Dermaptera in the sequence data banks. Examinations of molecular and morphological data are required for additional materials, as well as rearing experiments for investigating wing polymorphisms.

Acknowledgements

We thank H.-S. Tee, L.-H. Ang, C.-C. Lee, and X.-Y. Goh for assistance in collecting specimens in the field, and C. Girod and N. Moulin for providing us with important material collected in an inventory for the Conservatoire du Littoral (French coastal protection agency). We also thank W.-J. Wu, C.-C. Scotty Yang, H. Karube, and K. Watanabe for their assistance with examining specimens preserved in NTU and KPMNH. We are grateful also to C. Girod and P. Ko arek for useful comments on a previous version of the manuscript. This study was conducted with the approval of the Economic Planning Unit, Malaysia (Reference No. UPE: 40/200/19/2844). This study was partly supported by Keio Gijuku Academic Development Funds from Keio University (2021 and 2022) to YK, Grants-in-Aid for Scientific Research (KAKENHI) from the Japan Society for the Promotion of Science Nos. 22770058, 15K07133, and 19K06746 to YK, and No. 21H02219 to JY.

References

Anisyutkin LN (1998) To the knowledge of earwigs of the subfamily Anisolabidinae (Dermaptera, Anisolabididae) from SE Asia. *Entomological Review* 78: 627–641.

- Bey-Bienko GY (1936) Nasekomye kochistokrylye (Dermaptera). Fauna SSSR 5. [Earwigs (Dermaptera). Fauna USSR 5]. Izdatelstvo Akademii Nauk USSR, Moskva – Leningrad, 239 pp. <https://djvu.online/file/FUxNgqgCVapfz> [In Russian]
- Bey-Bienko GY (1959) Dermaptera of Sichuan and Yunnan. Results of Chinese-Soviet Zoological and Botanical Expeditions to SW China, 1955–1957. *Entomologicheskoe Obozrenie* 38: 590–672. [In Russian]
- Brindle A (1972) Dermaptera. *Insects of Micronesia* 5: 97–171.
- Brindle A (1981) The types of Dermaptera described by Fabricius. *Entomologist's Record and Journal of Variation* 93: 14–16.
- Burr M (1911) Dermaptera. *Genera Insectorum*, Bruxelles 122: 1–112. <https://doi.org/10.5962/bhl.part.9310>
- Chen Y, Ma W (2004) Dermaptera. *Fauna Sinica* 35: 1–420. [In Chinese]
- Cho PS (1969) Dermaptera. *Illustrated Encyclopedia of Fauna & Flora of Korea* (Vol. 10). Insecta (II), Mun-gyobu, Seoul, 802–816 pp. [pl. 55] [In Korean]
- Cognato AI (2006) Standard percent DNA sequence difference for insects does not predict species boundaries. *Journal of Economic Entomology* 99(4): 1037–1045. <https://doi.org/10.1093/jee/99.4.1037>
- de Bormans A, Krauss H (1900) Forficulidae und Hemimeridae – Das Tierreich 11. Verlag von R. Friedländer und Sohn, Berlin, 142 pp. <https://doi.org/10.5962/bhl.title.69336>
- Digital Archives Project of National Taiwan University (2021) Digital Archives Project of National Taiwan University. <http://www.darc.ntu.edu.tw/newdarc/darc/english/introduction.htm> [Accessed on 2022-7-1]
- Dohrn H (1864) Versuch einer Monographie der Dermapteren. *Stettin entomologische Zeitung* 25: 285–296.
- Engel MS, Haas F (2007) Family-group names for earwigs (Dermaptera). *American Museum Novitates* 3567(1): 1–20. [https://doi.org/10.1206/0003-0082\(2007\)539\[1:FN FED\]2.0.CO;2](https://doi.org/10.1206/0003-0082(2007)539[1:FN FED]2.0.CO;2)
- Fabricius JC (1793) *Entomologia Systematica Emendata et Aucta. Secundum Classes, Ordines, Genera, Species Adjectis Synonymis, Locis, Observationibus, Descriptionibus*. Tome 2. Impensis Christ. Gottl. Proft, Hafniae, 519 pp. <https://doi.org/10.5962/bhl.title.122153>
- Folmer O, Black M, Hoeh W, Lutz R, Vrijenhoek R (1994) DNA primers for amplification of mitochondrial cytochrome c oxidase subunit I from diverse metazoan invertebrates. *Molecular Marine Biology and Biotechnology* 3: 294–299. <https://doi.org/10.1071/ZO9660275>
- Hadley A (2008) Combine ZM imaging software. <https://combinezm.en.lo4d.com/details> [Accessed on 2018-2-10]
- Hebard M (1923) Studies in Indian Dermaptera. *Memoirs of the Department of Agriculture in India, Entomological Series* 7: 195–242.
- Hebard M (1927) Studies in Sumatran Dermaptera. *Proceedings. Academy of Natural Sciences of Philadelphia* 79: 23–48.
- Hebard M (1933) Dermaptera in the collection of the California Academy of Sciences. *The Pan-Pacific Entomologist* 9: 140–144.
- Hincks WD (1947) Preliminary notes on Mauritian earwigs (Dermaptera). *Annals & Magazine of Natural History* 14(116): 517–540. <https://doi.org/10.1080/00222934708654662>
- Hopkins H, Maehr MD, Haas F, Deem LS (2018) Dermaptera Species File. Version 5.0/5.0. [WWW document] <http://Dermaptera.SpeciesFile.org> [Accessed on 2022-7-31]

- Kalaentzis K, Kazilas C, Agapakis G, Kocarek P (2021) Hidden in plain sight: First records of the alien earwig *Euborellia femoralis* (Dohrn, 1863) in Europe. *BioInvasions Records* 10(4): 1022–1031. <https://doi.org/10.3391/bir.2021.10.4.27>
- Kamimura Y, Nishikawa M, Lee C-Y (2016) The earwig fauna (Insecta: Dermaptera) of Penang Island, Malaysia, with descriptions of two new species. *Zootaxa* 4084(2): 233–257. <https://doi.org/10.11646/zootaxa.4084.2.4>
- Kevan DKMcE, Vickery VR (1997) An annotated provisional list of non-saltatorial orthopteroid insects of Micronesia, compiled mainly from the literature. *Micronesia* 30: 269–353.
- Kim CW, Moon TY (1985) A taxonomic revision of Korean Dermaptera. *Entomological Research Bulletin [Korea]* 11: 37–59.
- Kočárek P (2010) Case 3522. Palicinae Burr, 1910 (Dermaptera, Spongiphoridae): Proposed emendation of the current spelling to Paalexinae to remove homonymy with Palicidae Bouvier, 1898 (Crustacea, Decapoda). *Bulletin of Zoological Nomenclature* 67(3): 211–212. <https://doi.org/10.21805/bzn.v67i3.a8>
- Kočárek P (2011a) Dermaptera of Iran with description of *Euborellia angustata* sp. nov. *Acta Entomologica Musei Nationalis Pragae* 51: 381–390.
- Kočárek P (2011b) *Euborellia ornata* sp. nov. from Nepal (Dermaptera: Anisolabididae). *Acta Entomologica Musei Nationalis Pragae* 51: 391–395.
- Kočárek P, Wahab RA (2021) Termitophily documented in earwigs (Dermaptera). *Biology* 10: e1243. <https://doi.org/10.3390/biology10121243>
- Masaki J (1936) On the insect-fauna of various islands of Korea (I). *Kontyû* 10: 251–274. [In Japanese]
- Matzke D, Kočárek P (2015) Description and biology of *Euborellia arcanum* sp. nov., an alien earwig occupying greenhouses in Germany and Austria (Dermaptera: Anisolabididae). *Zootaxa* 3956(1): 131–139. <https://doi.org/10.11646/zootaxa.3956.1.8>
- Moon TY, Kim CW (1983) The systematic study of Korean Dermaptera. I. (Carcinophorinae, Carcinophoridae). *Entomological Research Bulletin [Korea]* 9: 29–42.
- Moon TY, Kim CW (1991) Catalogue of Korean Dermaptera. *Entomological Research Bulletin [Korea]* 17: 67–79.
- Nishikawa M (1969) Notes on the Carcinophorinae of Japan and Ryukyus (Dermaptera: Carcinophoridae). *Kontyû* 37: 41–55.
- Nishikawa M (1975) Dermaptera. In: Ishihara T (Ed.) *Pictorial Encyclopedia of Insect III for Student*. Gakken, Tokyo, 65–66. [(plates) and 187–383 pp.] [In Japanese]
- Nishikawa M (2011) Unidentified earwig (Dermaptera) specimens preserved in the Hiwa Museum for Natural History, Shobara City, Hiroshima, Japan, with a check-list of the earwigs of Hiroshima Prefecture. *Miscellaneous Reports of the Hiwa Museum for Natural History* 52: 1–12. [In Japanese with English abstract]
- Nishikawa M (2016) Dermaptera. In: *Orthopterological Society of Japan (Ed.) The Standard of Polyneoptera in Japan*. Gakken Plus, Tokyo, 170–186. [In Japanese]
- Nishikawa M (2020a) Order Dermaptera. In: *Editorial Committee of Catalogue of the Insects of Japan (Ed.) Catalogue of the Insects of Japan (Vol. 3): Polyneoptera*. Touka Shobo, Fukuoka, Japan, 56–67. [In Japanese]
- Nishikawa M (2020b) Dermaptera of the Bonin Islands, Japan. *Battarigisu* 163: 191–196. [In Japanese]

- Okuni T (1913) Verzeichnis der Japanischen Euplexopteren. Transactions of the Sapporo Natural History Society 4: 182–188. <https://eprints.lib.hokudai.ac.jp/dspace/handle/2115/60865>
- Popham EJ, Brindle A (1966) Genera and species of the Dermaptera. 3. Carcinophorinae and Arixenidae. Entomologist, London 99: 269–278.
- Reichardt H (1968) Catalogue of New World Dermaptera (Insecta). Part II. Labioides, Carcinophoridae. Papéis Avulsos de Zoologia [São Paulo] 22: 35–46.
- Sakai S (1970) Dermapterorum Catalogus Praeliminaris. I. Labiduridae and Carcinophoridae. Daito Bunka University, Tokyo, 49 pp. [and 91 pp.]
- Sakai S (1982) A new proposed classification of the Dermaptera with special reference to the check-list of the Dermaptera of the world. Bulletin of Daito Bunka University 20: 1–108.
- Sakai S (1987) Dermapterorum Catalogus XIX–XX: Iconographia IV–V. Chelisochidae and Anisolabididae. Daito Bunka University, Tokyo, 1567 pp.
- Shiraki T (1905) Neue Forficuliden Japans. Transactions of the Sapporo Natural History Society 1: 91–96. <http://hdl.handle.net/2115/60754>
- Shiraki T (1928) Dermapteren aus dem Kaiserreich Japan. Insecta Matsumurana 3: 1–25. <http://hdl.handle.net/2115/9156>
- Srivastava GK (1979) On a new species of genus *Euborellia* Burr (Dermaptera: Carcinophoridae) from Philippines. Bulletin of the Zoological Survey of India 2: 49–51.
- Srivastava GK (1999) On the higher classification of Anisolabididae (Insecta: Dermaptera) with a check-list of genera and species. Records of the Zoological Survey of India 97(1): 73–100. <https://doi.org/10.26515/rzsi/v97/i1/1999/160257>
- Srivastava GK (2003) Fauna of India and Adjacent Countries, Dermaptera Part II: Anisolaboidea. Zoological Survey of India, Kolkata, India, 235 pp.
- Steinmann H (1989a) Dermaptera. Catadermaptera II. Das Tierreich 105: 1–504. <https://doi.org/10.1515/9783112419687>
- Steinmann H (1989b) World Catalogue of Dermaptera. Kluwer Academic Publishers, Dordrecht, Netherlands, 934 pp.
- Steinmann H (1990) Dermaptera. Eudermaptera I. Das Tierreich 106: 1–558.
- Stuart OP, Binns M, Umina PA, Holloway J, Severtson D, Nash M, Heddle T, van Helden M, Hoffmann AA (2019) Morphological and molecular analysis of Australian earwigs (Dermaptera) points to unique species and regional endemism in the Anisolabididae family. Insects 10(3): 1–25. <https://doi.org/10.3390/insects10030072>
- Su ZH, Imura Y, Okamoto M, Osawa S (2004) Pattern of phylogenetic diversification of the Cychrini ground beetles in the world as deduced mainly from sequence comparisons of the mitochondrial genes. Gene 326: 43–57. <https://doi.org/10.1016/j.gene.2003.10.025>
- Tamura K, Stecher G, Kumar S (2021) MEGA11: Molecular Evolutionary Genetics Analysis version 11. Molecular Biology and Evolution 38(7): 3022–3027. <https://doi.org/10.1093/molbev/msab120>
- Thompson JD, Gibson TJ, Higgins DG (2003) Multiple sequence alignment using ClustalW and ClustalX. Current Protocols in Bioinformatics 00(1): 2–3. <https://doi.org/10.1002/0471250953.bi0203s00>
- Zhang ZQ (2013) Phylum Arthropoda. In: Zhang Z-Q (Ed.) Animal Biodiversity: An outline of higher-level classification and survey of taxonomic richness (Addenda 2013). Zootaxa 3703: 17–26. <https://doi.org/10.11646/zootaxa.3703.1.6>

Supplementary material 1

The samples and results of the crossing experiments

Authors: Yoshitaka Kamimura, Chow-Yang Lee, Junsuke Yamasako, Masaru Nishikawa
Data type: table (Pdf file)

Copyright notice: This dataset is made available under the Open Database License (<http://opendatacommons.org/licenses/odbl/1.0/>). The Open Database License (ODbL) is a license agreement intended to allow users to freely share, modify, and use this Dataset while maintaining this same freedom for others, provided that the original source and author(s) are credited.

Link: <https://doi.org/10.3897/zookeys.1146.98248.suppl1>

Supplementary material 2

The specimens and results of morphological measurements

Authors: Yoshitaka Kamimura, Chow-Yang Lee, Junsuke Yamasako, Masaru Nishikawa
Data type: table (Pdf file)

Copyright notice: This dataset is made available under the Open Database License (<http://opendatacommons.org/licenses/odbl/1.0/>). The Open Database License (ODbL) is a license agreement intended to allow users to freely share, modify, and use this Dataset while maintaining this same freedom for others, provided that the original source and author(s) are credited.

Link: <https://doi.org/10.3897/zookeys.1146.98248.suppl2>

Supplementary material 3

Species and the collection sites of the Dermaptera samples sequenced in this study

Authors: Yoshitaka Kamimura, Chow-Yang Lee, Junsuke Yamasako, Masaru Nishikawa
Data type: table (Pdf file)

Copyright notice: This dataset is made available under the Open Database License (<http://opendatacommons.org/licenses/odbl/1.0/>). The Open Database License (ODbL) is a license agreement intended to allow users to freely share, modify, and use this Dataset while maintaining this same freedom for others, provided that the original source and author(s) are credited.

Link: <https://doi.org/10.3897/zookeys.1146.98248.suppl3>

Three new species in *Tetrastemma* Ehrenberg, 1828 (Nemertea, Monostilifera) from sublittoral to upper bathyal zones of the northwestern Pacific

Natsumi Hookabe¹, Hisanori Kohtsuka²,
Yoshihiro Fujiwara³, Shinji Tsuchida³, Rei Ueshima¹

1 School of Science, The University of Tokyo, 113-0033, Bunkyo, Japan **2** Misaki Marine Biological Station (MMBS), School of Science, The University of Tokyo, 238-0225, Miura, Japan **3** Research Institute for Global Change (RIGC), Japan Agency for Marine–Earth Science and Technology (JAMSTEC), Yokosuka, 237-0061, Kanagawa, Japan

Corresponding author: Natsumi Hookabe (sofeechan312@gmail.com)

Academic editor: J. Norenburg | Received 24 October 2022 | Accepted 4 January 2023 | Published 7 February 2023

<https://zoobank.org/84DB1223-8E0F-4837-BFD2-5616E692DAF1>

Citation: Hookabe N, Kohtsuka H, Fujiwara Y, Tsuchida S, Ueshima R (2023) Three new species in *Tetrastemma* Ehrenberg, 1828 (Nemertea, Monostilifera) from sublittoral to upper bathyal zones of the northwestern Pacific. ZooKeys 1146: 135–146. <https://doi.org/10.3897/zookeys.1146.95004>

Abstract

Monostiliferous nemerteans in the genus *Tetrastemma* Ehrenberg, 1828 are generally characterized as having four eyes, and they occur worldwide, from the intertidal zone to the deep-sea bottom. Recent extensive sampling of *Tetrastemma* has explored the high species diversity, including many undescribed forms, but phylogenetic analysis has revealed non-monophyly of the genus. We herein describe three new species of the genus (*T. album* **sp. nov.**, *T. persona* **sp. nov.**, and *T. shohoense* **sp. nov.**) from northwestern Pacific waters based on specimens collected by dredging or by use of a remotely operated vehicle at depths of 116–455 m. Since anatomical and histological characters traditionally used in systematics of the genus are sometimes interspecifically uniform, a histology-free approach is applied for the species descriptions in this study. To confirm the generic affiliation of the new species, a molecular phylogenetic analysis based on partial sequences of cytochrome *c* oxidase subunit I, 16S rRNA, 18S rRNA, 28S rRNA, and histone H3 genes was performed. Our result shows that all three new species are nested in a subclade formed by species from the North Pacific and American Atlantic, inferring that geographic distribution does not reflect the cladogenesis of *Tetrastemma*. Furthermore, two *Tetrastemma* species with a cylindrical stylet basis, *T. freyae* Chernyshev et al., 2020 from off the coast of India and Hawaii and *T. shohoense* **sp. nov.** from Shoho Seamount, Japan, constitute a clade in the resulting tree.

Keywords

Deep sea, Eumonostilifera, Japan, marine invertebrate, Monostilifera, Nemertea, Pacific, Tetrastemmatidae

Introduction

A histology-free description with DNA barcoding has been progressively introduced to nemertean systematics in the past decade (e.g., Kajihara 2015; Gonzalez-Cueto et al. 2017; Simpson et al. 2017; Kajihara et al. 2018, 2022; Chernyshev et al. 2020; Hookabe et al. 2021a, b; Leiva et al. 2021; Abato et al. 2022). This approach has been applied to two cases, one of which is a description of species with internal characters interspecifically differentiated and observable without histology (e.g., number of proboscis branches in *Gorgonorhynchus* Dakin & Fordham, 1931 [Kajihara 2015; Hookabe et al. 2021a]). In the other case, especially when internal morphology is uniform between most species in a genus, a species description has been performed solely based on characters examined *in-vivo* (shape of head, body coloration and markings, number of eyes, blood color, and stylet apparatus) [e.g., *Baseodiscus* Diesing, 1850 (Kajihara et al. 2022) and *Ototyphlonemertes* Diesing, 1863 (Kajihara et al. 2018)]. Recent descriptions of species in the genus *Tetrastemma* Ehrenberg, 1828, fitting the latter case, have been performed based on characters of living specimens without histological observations (Chernyshev et al. 2020; Hookabe et al. 2021b; Abato et al. 2022).

Tetrastemma is a species-rich genus in Monostilifera (Kajihara 2021), currently encompassing about 110 species from tropical to polar areas (Chernyshev et al. 2021). As the generic name suggests—a composite of the Latin feminine “tetra” (= four) + “stemma” (= simple eyes)—members in the genus are generally characterized by four eyes, but this feature is also found in other genera. Several species in *Tetrastemma* were described based on internal morphology; however, the internal characters were inferred to be almost homogenous within the genus by taxonomic reappraisal based on molecular phylogeny (Chernyshev et al. 2021). Recent examples of a histology-free approach based on characteristics studied *in-vivo* and molecular data are descriptions of *T. freyae* Chernyshev et al., 2020, *T. cupido* Hookabe, Kohtsuka & Kajihara, 2021, and *T. parallelus* Abato, Yoshida & Kajihara, 2022.

Here, we establish three new species based on specimens collected in 2019–2021 from the lower sublittoral to upper bathyal zones of Sagami Bay and the Nishi-Shichito Ridge. The descriptions are histology-free, based on characters of living specimens examined with a light microscope. To test phylogenetic relationships with the congeners, we performed molecular phylogenetic reconstruction using partial sequences of the 16S rRNA (16S), cytochrome *c* oxidase subunit I (COI), 18S rRNA (18S), 28S rRNA (28S), and histone H3 genes (H3).

Materials and methods

Specimens were collected in 2019–2021 by use of a biological dredge in Sagami Bay (116–200 m) or a remotely operated vehicle (ROV) on Shoho Seamount of the Nishi-Shichito Ridge (455 m), northwestern Pacific Ocean. External morphology of the living specimens was documented on the vessel or in the laboratory with a Nikon D5600 digital SLR camera equipped with an AF-S DX Micro-NIKKOR 40mm f/2.8G macro lens (Nikon, Japan). A single specimen collected from Shoho Seamount was further observed

under a compound light microscope by preparing a squeezed specimen with a cover slip and a glass slide. Specimens were anaesthetized with a few drops of bitterns Tenpi Nigari (Amashio, Japan); after the worms were relaxed, the posterior tips were preserved in 99% ethanol for DNA extraction and the rest of the body was fixed in Bouin's fluid for 24–48 hours and later transferred to 70% ethanol. Type specimens have been deposited in the National Museum of Nature and Science, Tsukuba (NSMT), Japan.

DNA extraction, PCR amplification, and sequencing followed Hookabe et al. (2022). DNA sequences determined in the present study have been deposited in DDBJ/EMBL/GenBank (Table 1).

Table 1. List of species included in the phylogenetic analysis and DDBJ/EMBL/GenBank accession numbers for each gene. Country names of each species sampling location are abbreviated as follows: CA = Canada, JP = Japan, RU = Russia, USA = United States of America, and VE = Venezuela.

Species	Sampling location	16S	COI	18S	28S	H3	Source
<i>Tetrastemma 'aequicolor'</i> 24 Qul	Erineyskaya Inlet, RU	MZ231141	MZ216528	MZ231206	MZ231296	MZ216598*	Chernyshev et al. (2021)
<i>Tetrastemma 'aequicolor'</i> 25 Qul	Erineyskaya Inlet, RU	MZ231142	MZ216529	MZ231207	MZ231297	MZ216599*	Chernyshev et al. (2021)
<i>Tetrastemma 'aequicolor'</i> 26 Qul	Erineyskaya Inlet, RU	MZ231143	MZ216530	MZ231208	MZ231298	MZ216600*	Chernyshev et al. (2021)
<i>Tetrastemma album</i> sp. nov.	Sagami Bay, JP	OQ248525	OQ249697	OQ248517	OQ248520	OQ248166	Present study
<i>Tetrastemma cupido</i>	Sagami Bay, JP	OK428649	OK414013	OK428689	OK428648	–	Hookabe et al. (2021b)
<i>Tetrastemma nigrifrons</i>	CA	MZ231144	MZ216531	MZ231209	MZ231299	MZ216601	Chernyshev et al. (2021)
	Oregon, USA	MZ231145	MZ216532	MZ231210	MZ231300	MZ216602	Chernyshev et al. (2021)
	California, USA	MZ231146	MZ216533	MZ231211	MZ231301	MZ216603	Chernyshev et al. (2021)
<i>Tetrastemma stimpsoni</i>	JP	MZ231147	MZ216534	MZ231212	MZ231301	MZ216604	Chernyshev et al. (2021)
	RU	MZ231148	MZ216535	MZ231213	MZ231303	MZ216605	Chernyshev et al. (2021)
	Iturup, RU	MZ231149	MZ216536	MZ231214	MZ231304	MZ216606	Chernyshev et al. (2021)
<i>Tetrastemma elegans</i> B2	York River, USA	MZ231156	MZ216543	MZ231222	MZ231312	MZ216614	Chernyshev et al. (2021)
<i>Tetrastemma elegans</i> C2	USA	MZ231157	MZ216544	MZ231223	MZ231313	MZ216615	Chernyshev et al. (2021)
<i>Tetrastemma elegans</i> D2	York River, USA	MZ231158	–	MZ231224	MZ231314	–	Chernyshev et al. (2021)
<i>Tetrastemma enteroplecta</i> A6	Florida, USA	MZ231159	MZ216546	MZ231225	MZ231314	MZ216616	Chernyshev et al. (2021)
<i>Tetrastemma enteroplecta</i> E3	Florida, USA	MZ231160	–	MZ231226	MZ231316	MZ216618	Chernyshev et al. (2021)
<i>Tetrastemma enteroplecta</i> B7	VE	MZ231161	–	MZ231227	MZ231317	–	Chernyshev et al. (2021)
<i>Tetrastemma freyae</i>	Hawaii, USA	–	MT247877	MZ231229	MZ231319	MT247879	Chernyshev et al. (2020)
<i>Tetrastemma merulum</i> F2	Florida, USA	MZ231163	MZ216550	MZ231231	MZ231321	MZ216622	Chernyshev et al. (2021)
<i>Tetrastemma merulum</i> H5	Florida, USA	MZ231164	MZ216551	MZ231232	MZ231322	MZ216623	Chernyshev et al. (2021)
<i>Tetrastemma persona</i> sp. nov.	Sagami Bay, JP	OQ248526	OQ249698	OQ248518	OQ248521	OQ248167	Present study
<i>Tetrastemma reticulatum</i>	California, USA	MZ231168	MZ216556	MZ231238	MZ231328	MZ216629	Chernyshev et al. (2021)
<i>Tetrastemma shobohense</i> sp. nov.	Shoho Seamount, JP	OQ248524	OQ249700	–	–	–	Present study
<i>Tetrastemma</i> sp. F7	Florida, USA	MZ231173	MZ216564	MZ231246	MZ231336	MZ216637	Chernyshev et al. (2021)
<i>Tetrastemma</i> sp. GM 1	Gulf of Mexico, USA	MZ231175	–	MZ231248	MZ231338	MZ216639	Chernyshev et al. (2021)
<i>Tetrastemma</i> sp. GM 2	Florida, USA	MZ231176	MZ216565	MZ231249	MZ231339	MZ216640	Chernyshev et al. (2021)
<i>Tetrastemma</i> sp. GM 3	Gulf of Mexico, USA	MZ231177	–	MZ231250	MZ231340	MZ216641	Chernyshev et al. (2021)
<i>Tetrastemma</i> sp. I	Iturup, RU	MZ231179	–	MZ231252	MZ231342	MZ216643	Chernyshev et al. (2021)
<i>Tetrastemma</i> sp. IP	Iturup, RU	MZ231180	MZ216567	MZ231253	MZ231343	MZ216644	Chernyshev et al. (2021)
<i>Tetrastemma</i> sp. J 1TjS	Simushir, RU	MZ231182	MZ216570	MZ231256	MZ231346	MZ216647	Chernyshev et al. (2021)
<i>Tetrastemma</i> sp. J 3TjS	Simushir, RU	MZ231183	MZ216571	MZ231257	MZ231347	MZ216648	Chernyshev et al. (2021)
<i>Tetrastemma</i> sp. J 4TjS	Simushir, RU	MZ231184	MZ216572	MZ231258	MZ231348	MZ216649	Chernyshev et al. (2021)
<i>Tetrastemma</i> sp. M1	Urup, RU	–	MZ216573	MZ231259	MZ231349	MZ216650	Chernyshev et al. (2021)
<i>Tetrastemma</i> sp. M2	Urup, RU	–	MZ216574	MZ231260	MZ231350	MZ216651	Chernyshev et al. (2021)
<i>Tetrastemma</i> sp. Ofunato	Off Ofunato, JP	OQ248527	OQ249699	OQ248519	OQ248522	OQ248168	Chernyshev et al. (2021)
<i>Tetrastemma</i> sp. S 1TsS	Simushir, RU	–	MZ216575	MZ231261	MZ231351	MZ216652	Chernyshev et al. (2021)
<i>Tetrastemma</i> sp. S 2TsS	Simushir, RU	–	MZ216576	MZ231262	MZ231352	MZ216653	Chernyshev et al. (2021)
<i>Tetrastemma</i> sp. U 13TsU	Urup, RU	MZ231185	MZ216577	MZ231263	MZ231353	MZ216654	Chernyshev et al. (2021)
<i>Tetrastemma</i> sp. U 18TsU	Urup, RU	MZ231186	MZ216578	MZ231264	MZ231354	MZ216655	Chernyshev et al. (2021)
<i>Tetrastemma</i> sp. UR	Urup, RU	MZ231187	–	MZ231265	MZ231355	MZ216656	Chernyshev et al. (2021)

*Erroneously registered in GenBank under the taxon name *Quasitetrastemma nigrifrons*.

To elucidate phylogenetic positions of specimens examined, we performed phylogenetic analyses based on the maximum-likelihood (ML) method. The newly obtained sequences from four *Tetrastemma* species were aligned using MAFFT v. 7 (Kato and Standley 2013) employing L-INS-i strategy with sequences of other species in the genus, most of which were recently determined by Chernyshev et al. (2021). Ambiguous nucleotide sites in the dataset were removed with Gblocks v. 0.91b (Castresana 2000) using a less stringent option, resulting in 380-bp 16S, 626-bp COI, 1738-bp 18S, 505-bp 28S, and 329-bp H3. The ML analyses were performed with RAxML-NG (Kozlov et al. 2019), for which the best-fit partition scheme and substitution model were selected using PartitionFinder v. 2.1.1 (Lanfear et al. 2017). Nodal support values were derived from 1000 bootstrap pseudoreplicates.

Result

Systematics

Genus *Tetrastemma* Ehrenberg, 1828

Tetrastemma album sp. nov.

<https://zoobank.org/F73378DB-B867-4ABA-A2D7-18CF781D10A7>

Fig. 2A–C

[New Japanese name: misaki-oshiroi-himomushi]

Etymology. The species name is derived from the Latin *album* (white), referring to pure white body of the new species. The Japanese name is named after the white powder foundation traditionally used by Maiko, Geisha, Kabuki actors in Japan.

Material examined. *Holotype:* NMST-NE-H-06, unsectioned complete specimen except for the posterior tip, fixed in Bouin's fluid and later preserved in 70% ethanol, posterior tip preserved in 99% ethanol, collected on March 12, 2021 by NH, biological dredge (R/V *Rinkai-maru*) at depths of 144–200 m, off Jogshima (35°07.41'N, 139°34.11'E–35°07.32'N, 139°33.572'E), Miura, Kanagawa, Japan, NW Pacific.

Description. Head spatulate to rounded in profile (Fig. 2A–C), demarcated by posterior cephalic furrows from body (Fig. 2A). Before anesthetization, body of a live specimen 17 mm long and 1.0–1.2 mm wide. Body uniformly pale colored, without longitudinal or transverse stripe markings (Fig. 2A). Pure white transverse cephalic patch present between anterior and posterior pairs of eyes (Fig. 2B). Head not wider than maximum body width (Fig. 2A–C). A pair of cephalic furrows present; anterior pair not meeting mid-dorsally and ventrally curving anteriorly but not reaching to proboscis pore; posterior pair V-shaped and barely meeting mid-dorsally (Fig. 2B) and running transversely on ventral surface (Fig. 2C). Cerebral ganglia and blood not red and probably uncolored. Internal organs (proboscis, foregut, and intestine) visible as pale regions. Four reddish brown eyes regular in size (Fig. 2B).

Type locality and distribution. The species is only known from the type locality, Sagami Bay, Kanagawa Prefecture, Japan, at depths of 144–200 m (Fig. 1).

Remarks. Having a pure white cephalic patch on a uniformly pale body, *T. album* sp. nov. differs from all the described species. *Tetrastemma coronatum* (Quatrefages, 1846), *T. diadema* Hubrecht, 1879, *T. olgarum* Chernyshev 1998, and *T. pseudocoronatum* Chernyshev 1998 have white cephalic patches but are distinguished from *T. album* sp. nov. in possessing a light brown to dark transverse band on the head. *Tetrastemma albomaculatum* Chernyshev, 2016 also possesses a white cephalic patch but differs from the new species in having a pale-ochre body dorsally spotted with small white dots (Chernyshev 2016).

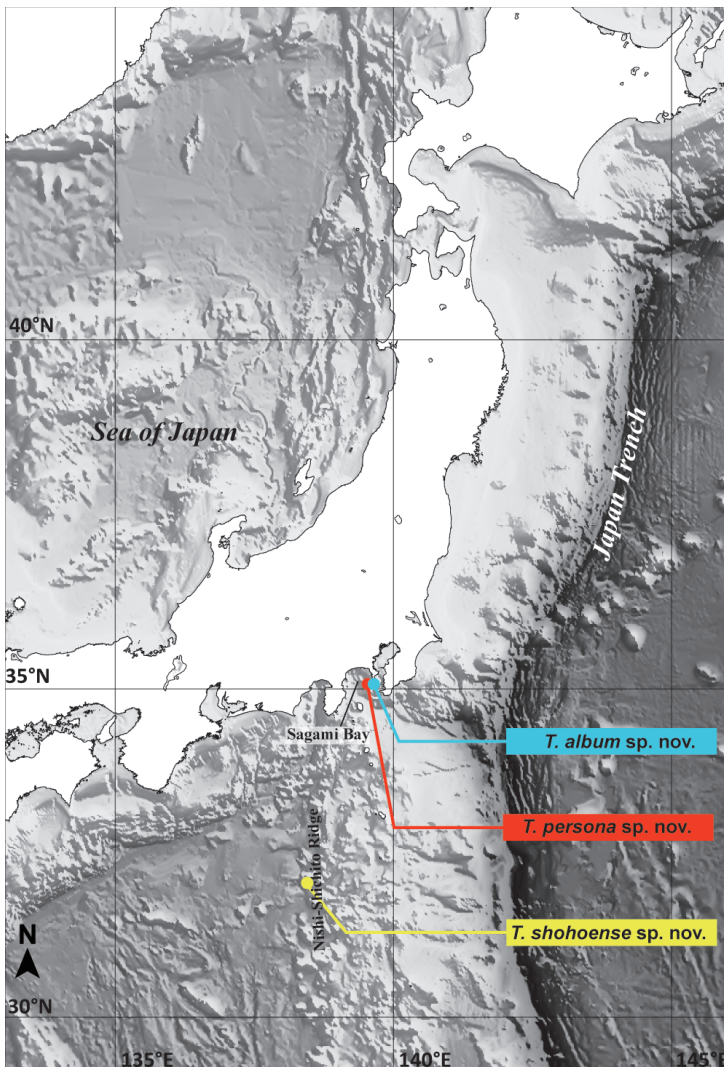


Figure 1. Collection sites of the specimens examined in the present study.

***Tetrastemma persona* sp. nov.**

<https://zoobank.org/E3E48065-E551-477D-9041-89DEE011DEB0>

Fig. 2D

[New Japanese name: misaki-kamen-himomushi]

Etymology. The species name is derived from the Latin *persōna* (mask), referring to a broad cephalic patch of the new species masking eyes and internal organs in head region. The Japanese name “kamen” means a mask in Japanese.

Material examined. Holotype: NMST-NE-H-07, unsectioned complete specimen except for the posterior tip, fixed in Bouin’s fluid and later preserved in 70% ethanol, posterior tip preserved in 99% ethanol, collected on July 31 2020 by NH, biological dredge (R/V *Rinkai-maru*) at depths of 116–211 m, off Jogshima (35°08.32'N, 139°32.857'E–35°08.40'N, 139°32.504'E), Miura, Kanagawa, Japan, NW Pacific. **Paratype:** NMST-NE-P-08, unsectioned complete specimen fixed in Bouin’s fluid and later preserved in 70% ethanol, collected on the same date and locality as the holotype.

Description. Head slightly narrower than middle part of body and weakly demarcated from trunk (Fig. 2D). Before anesthetization, body of a live specimen 7.0–10 mm long and 0.8–1.0 mm wide. Body uniformly pale to yellow colored without longitudinal or transverse stripe markings (Fig. 2D). Vermilion-red cephalic patch spade-shaped (Fig. 2D), covering both anterior and posterior pairs of eyes (Fig. 2D) but not posteriorly reaching to anterior pair of cephalic furrows; eyes regular in sizes. A posterior pair of cephalic furrows not well distinguished probably due to the small body size. Cerebral ganglia and blood not red and probably uncolored. Internal organs (proboscis, foregut, and intestine) not well visible through body wall. Rhynchocoel visible as whitish region through body wall, extending about 1/2–2/3 of the body length.

Type locality and distribution. The species is only known from the type locality, Sagami Bay, Kanagawa Prefecture, Japan, at depths of 116–211 m (Fig. 1, Table 1).

Remarks. *Tetrastemma persona* sp. nov. has atypically short rhynchocoel in the genus and most resembles *T. roseocephalum* (Yamaoka, 1947) and *T. yamaokai* Iwata, 1954 in having a pale body without any markings and a red cephalic patch. Pattern variation of a cephalic patch (shield shape or horse-shoe shape) was reported in both *T. roseocephalum* and *T. yamaokai*; referring to the original description of *T. yamaokai*, the name may be a junior synonym of *T. roseocephalum*, as suggested by Kajihara (2007). The external morphology of *T. persona* sp. nov. is similar to a form with a shield-shaped cephalic patch of *T. roseocephalum* (Iwata 1954).

The subtle difference in the shape of cephalic patch between *T. persona* sp. nov. (spade-shaped) and *T. roseocephalum* (shield-shaped) was supported by our molecular analysis. The new species did not constitute a clade with *T. roseocephalum* but with *T. album* sp. nov. (Fig. 3); *T. roseocephalum* belongs to Clade C of Chernyshev et al. (2021).

An uncorrected genetic distance based on 657 bp of COI was 16% between *T. album* sp. nov. and *T. persona* sp. nov., comparable with interspecific values observed among Monostilifera (e.g., Sundberg et al. 2016; Hookabe et al. 2022).

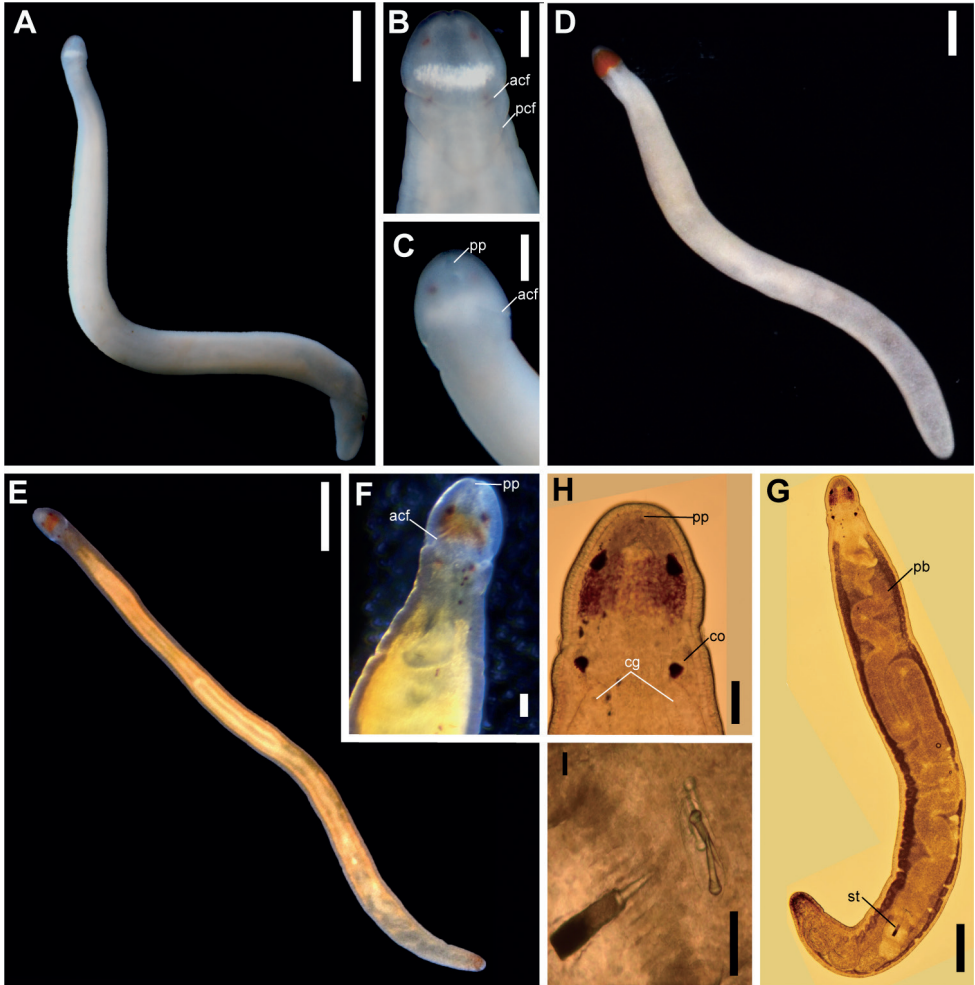


Figure 2. Holotype specimens of new *Tetrastemma* species; photographs were taken in life by NH **A–C** *T. album* sp. nov. **A** complete body, dorsal view **B** head, dorsal view **C** head, ventral view **D** *T. persona* sp. nov., complete body, dorsal view **E–I** *T. shohoense* sp. nov. **E** complete body **F** head, ventral view **G** squeezed specimen under a cover slip, complete body, dorsal view **H** head, dorsal view **I** stylet apparatus. Abbreviations: acf, anterior cephalic furrow; pcf, posterior cephalic furrow; cg, cerebral ganglia; co, cerebral organ; pb, proboscis; pp, proboscis pore. Scale bars: 2 mm (**A**); 500 μ m (**B**, **C**, **G**); 1 mm (**D**, **E**); 100 μ m (**F**, **H**); 50 μ m (**I**).

***Tetrastemma shohoense* sp. nov.**

<https://zoobank.org/9D1CD900-900F-4114-8853-16C480FDD75D>

Fig. 2E–I

[New Japanese name: shoho-kakubari-himomushi]

Etymology. The species is named after the type locality, Shoho Seamount of the Nishi-Shichito Ridge, Japan.

Material examined. *Holotype*: NMST-Nem-H-05, unsectioned complete specimen except for the posterior tip, fixed in Bouin's fluid, posterior tip preserved in 99% ethanol, collected on November 29 2020 by NH, by use of ROV *KM-ROV* (dive #123) during KM20-10C cruise of R/V *Kaimei*, at a depth of 455 m, near the summit of Shoho Seamount of the Nishi-Shichito Ridge (32°19.39'N, 138°44.48'E), Japan, NW Pacific.

Description. Head spatulate in profile (Fig. 2E–H), not well demarcated from body by anterior cephalic furrows (Fig. 2E). Before anesthetization, body of a live specimen 5.5 mm long and 0.3 mm wide. Background body color generally white, tinged with bright yellow to orange, and almost transparent (Fig. 2E). Head with a red rectangle cephalic patch without extending behind a posterior pair of eyes (Fig. 2E, H). Anterior pair of cephalic furrows present (Fig. 2F) but posterior one not well distinguished. Cerebral ganglia and blood uncolored (Fig. 2G, H). Alimentary canals visible as bright yellow organs through body wall (Fig. 2E). Proboscis pale, extending about 3/4 of the body length (Fig. 2E). Four brown eyes present; anterior pair slightly larger than posterior ones (Fig. 2H).

Stylet basis cylindrical, 55.0 μm in length and 25.0 μm in maximum width; central stylet smooth, 47.0 μm in length; (stylet length) / (basis length) ratio 0.85 (Fig. 2I). Two accessory stylet pouches present, each containing two stylets (Fig. 2I).

Type locality and distribution. The species is only known from the type locality, Shoho Seamount of the Nishi-Shichito Ridge, Japan, at a depth of 455 m (Fig. 1), among the sandy sediments on rocky substrates.

Remarks. Having a dark cephalic patch and cylindrical stylet basis and lacking a longitudinal line on the dorsal surface of the body, *T. shohoense* sp. nov. resembles *T. freyae* Chernyshev et al., 2020 originally described based on Hawaiian and Indian specimens. The new species is differentiated from *T. freyae* in the color of the cephalic patch as well as the non-flared posterior margin of the cylindrical stylet basis.

A genetic distance based on COI between *T. shohoense* sp. nov. and *T. freyae* (specimens from Hawaii (MT247877) and India (MT247878) was 12.6%; the value is comparable with interspecific values observed among Monostilifera (e.g., Sundberg et al. 2016; Hookabe et al. 2022).

Molecular phylogeny

The sequence data set for molecular phylogenetic analyses in the present study is primarily based on Chernyshev et al. (2021). Since we confirmed that our new species are nested in *Tetrastemma* Clade B of Chernyshev et al. (2021), we used three species in Clade A (*Tetrastemma* sp. GM1 Gulf of Mexico, *Tetrastemma* sp. GM2 USA FL, and *Tetrastemma* sp. GM3 Gulf of Mexico) as outgroup taxa (Fig. 3). Clade B was subdivided into two clades with a full support value, one of which was a clade formed by *T. freyae* and *T. shohoense* sp. nov. The two species are characterized by having a cylindrical stylet basis in the proboscis. In the other subclade in Clade B, *T. album* sp. nov. and *T. persona* sp. nov. were included (Fig. 3). A clade constituted by newly described

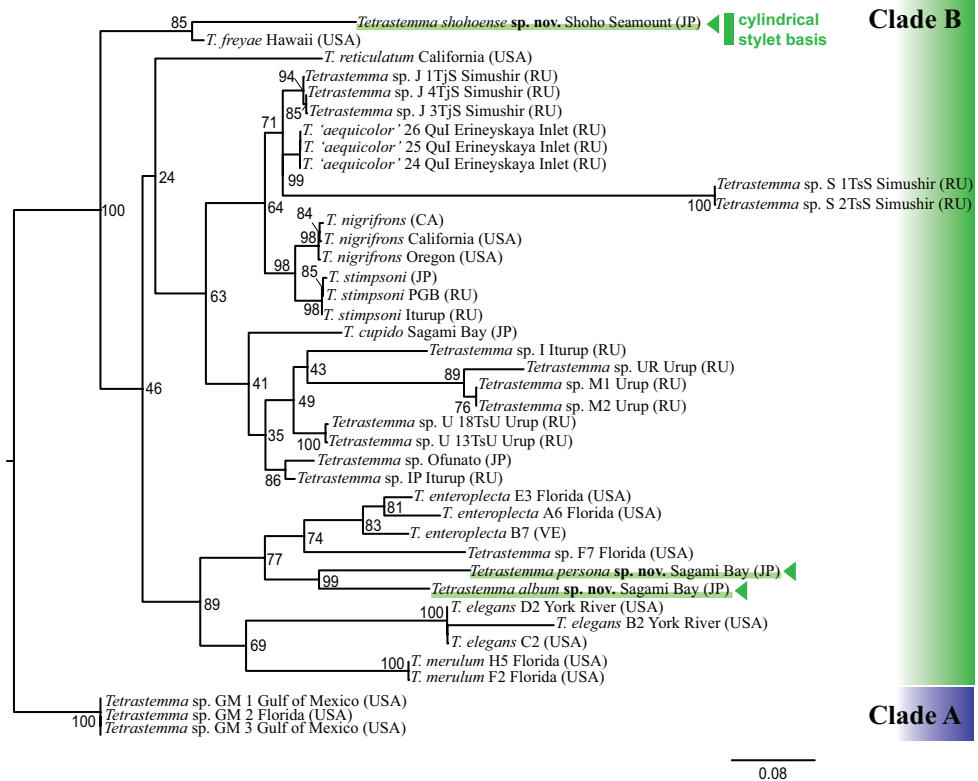


Figure 3. A maximum-likelihood (ML) tree based on concatenated sequences of two mitochondrial [16S rRNA (16S; 380 bp) and cytochrome *c* oxidase subunit I (COI; 626 bp)] and three nuclear gene markers [18S rRNA (18S; 1738 bp), 28S rRNA (28S; 505 bp), and histone H3 (H3; 329 bp)]. Numbers near each node are support values generated by a separate partitioned ML bootstrap analysis with 1000 replicates. Country names of each species sampling location are abbreviated as follows: CA = Canada, JP = Japan, RU = Russia, USA = United States of America, and VE = Venezuela.

species, *T. album* sp. nov. and *T. personae* sp. nov., from Sagami Bay (Japan) with 99% of BS, was nested in the American Atlantic clade formed by *T. elegans* (Girard, 1852) (Virginia), *T. enteroplecta* (Corrêa, 1954) (Florida and Venezuela), *T. merulum* (Corrêa, 1954) (Florida), and *Tetrastemma* sp. F7 (Florida). The clade formed by *T. album* sp. nov. and *T. personae* sp. nov. was sister-related to a clade formed by *T. enteroplecta* (Florida and Venezuela) and *Tetrastemma* sp. F7 (Florida) with 77% of BS (Fig. 3).

Discussion

Three species herein described (*T. album* sp. nov., *T. personae* sp. nov., and *T. shohoense* sp. nov.) fell within a clade referred to as *Tetrastemma* Clade B of Chernyshev et al. (2021) (Fig. 3). One of the findings from the tree is that two species with cylindrical

stylet basis, *T. freyae* and *T. shohoense* sp. nov., formed a clade regardless of the differences in habitat and collection depths of these two species; *T. freyae* was described based on specimens collected from live corals and mussel beds at depths shallower than 3 m in Hawaii and India (Chernyshev et al. 2020), while *T. shohoense* sp. nov. was found from sandy sediments in bathyal zone in Japan. A cylindrical stylet basis is likely to be acquired independently at least twice in Clade B (*T. freyae* and *T. shohoense* sp. nov.) and Clade C (*T. albomaculatum* and *T. parallelos*).

The other thing we can see on the phylogenetic tree is that *T. album* sp. nov. and *T. persona* sp. nov. are nested in a clade formed by several American Atlantic species, *T. enteroplecta*, *T. elegans*, *T. merulum*, and *Tetrastemma* sp. F7 (Chernyshev et al. 2021) (Fig. 3). A previous molecular analysis has inferred that *Tetrastema* clade B is subdivided into geographically distinct structures: North Pacific and American Atlantic subclades (Chernyshev et al. 2021). To obtain a more accurate picture of *Tetrastemma* phylogeny and speciation, again, further sampling of taxa, without bias toward shallow-water species, is needed for future phylogenetic analyses.

Acknowledgements

We thank Masanori Okanishi (Hiroshima Shudo University), Mamoru Sekifuji, and Michiyo Kawabata (MMBS) for their support in collecting specimens in Sagami Bay. NH thanks Toru Miura (MMBS) for providing NH with facilities for studying at MMBS. We are grateful to Katsunori Fujikura and Tetsuji Maki (JAMSTEC), the captain, the crew, the ROV operation team, and all the other participants in the research project Development of Biodiversity Monitoring Methods for the Management of Deep-sea Marine Protected Areas during KM20-10C cruise. NH also thanks Hiroshi Kajihara (Hokkaido University) for kindly sharing the relevant taxonomic literature with NH. This research was performed by the Environment Research and Technology Development Fund (JPMEERF20S20700) of the Environmental Restoration and Conservation Agency Provided by the Ministry of Environment of Japan and financially supported by JSPS KAKENHI (No. 21J14807 for NH) from Japan Society for the Promotion of Science. Finally, we thank the handling editor, Jon Norenburg and the three referees, Alexei V. Chernyshev, Hiroshi Kajihara, and Christina I. Ellison for the careful and insightful review of our manuscript.

References

- Abato J, Yoshida R, Kajihara H (2022) Histology-free description and phylogenetics of *Tetrastemma parallelos* sp. nov. (Nemertea: Eumonostilifera) from Japan. *Journal of Natural History* 56(29–32): 1265–1277. <https://doi.org/10.1080/00222933.2022.2118642>
- Castresana J (2000) Selection of conserved blocks from multiple alignments for their use in phylogenetic analysis. *Molecular Biology and Evolution* 17(4): 540–552. <https://doi.org/10.1093/oxfordjournals.molbev.a026334>

- Chernyshev AV (1998) Nemerteans of the genus *Tetrastemma* (Enopla, Monostilifera) from the Far East seas of Russia. *Zoologicheskii Zhurnal* [Зоологический журнал] 77: 995–1002.
- Chernyshev AV (2016) Nemerteans of the coastal waters of Vietnam. In: Adrianov AV, Lutaeenko KA (Eds) Biodiversity of the Western Part of the South China Sea. *Dal'nauka*, Vladivostok, 279–314.
- Chernyshev AV, Polyakova NE, Vignesh MS, Jain RP, Sanjeevi P, Norenburg JL, Rajesh RP (2020) A histology-free description of a new species of the genus *Tetrastemma* (Nemertea: Hoplonemertea: Monostilifera) from Hawaii and India. *Zootaxa* 4808(2): 379–383. <https://doi.org/10.11646/zootaxa.4808.2.10>
- Chernyshev AV, Polyakova NE, Norenburg JL, Kajihara H (2021) A molecular phylogeny of *Tetrastemma* and its allies (Nemertea, Monostilifera). *Zoologica Scripta* 50(6): 824–836. <https://doi.org/10.1111/zsc.12511>
- Corrêa DD (1954) Nemertinos do litoral Brasileiro. *Boletim da Faculdade de Filosofia, Ciências e Letras, Universidade de São Paulo* 19: 1–90. <https://doi.org/10.11606/issn.2526-3382.bffclzoologia.1954.120084>
- Dakin WJ, Fordham MGC (1931) A new and peculiar marine nemertean from the Australian coast. *Nature* 128(3236): e796. <https://doi.org/10.1038/128796b0>
- de Quatrefages A (1846) Étude sur les types inférieurs de l'embranchement des annelés. *Annales des Sciences Naturelles, Zoologie, Série* 3(6): 173–303.
- Diesing CM (1850) *Systema Helminthum* (Vol. I). W Braumuller, Vindobonae.
- Diesing KM (1863) Nachträge zur Revision der Turbellarien. *Sitzungsberichte der Kaiserlichen Akademie der Wissenschaften. Mathematisch-Naturwissenschaftliche Classe* 46: 173–188.
- Ehrenberg CG (1828–1831) Phytozoa turbellaria Africana et Asiatica in *Phytozoorum Tabula IV et V delineata*. In: Hemprich FG, Ehrenberg CG (Eds) *Symbolae Physicae, seu Icones et Descriptiones Corporum Naturalium Novorum aut Minus Cognitorum Quae ex Itineribus per Libyam, Aegyptium, Nubiam, Dongalam, Syriam, Arabiam et Habessiniam, pars zoologica II, animalia evertebrata exclusis insectis*. *Officina Academica, Berlin*, 53–67. [pls IV, V] <https://doi.org/10.5962/bhl.title.107403>
- Girard C (1852) Descriptions of two new genera and two species of Nemertes. *Proceedings of the Boston Society of Natural History* 4: 185–186.
- Gonzalez-Cueto J, Castro LR, Quiroga S (2017) *Nipponnemertes incainca* sp. n. Adoption of the new taxonomic proposal for nemerteans (Nemertea, Cratenemertidae). *ZooKeys* 693: 1–15. <https://doi.org/10.3897/zookeys.693.12015>
- Hookabe N, Xu CM, Tsuyuki A, Jimi N, Sun SC, Kajihara H (2021a) A new nemertean with a branched proboscis, *Gorgonorhynchus citrinus* sp. nov. (Nemertea: Pilidiophora), with molecular systematics of the genus. *Invertebrate Systematics* 35: 350–359. <https://doi.org/10.1071/IS20057>
- Hookabe N, Kohtsuka H, Kajihara H (2021b) A histology-free description of *Tetrastemma cupido* sp. nov. (Nemertea: Eumonostilifera) from Sagami Bay, Japan. *Marine Biology Research* 17(5–6): 467–474. <https://doi.org/10.1080/17451000.2021.1979236>
- Hookabe N, Kajihara H, Chernyshev AV, Jimi N, Hasegawa N, Kohtsuka H, Okanishi M, Tani K, Fujiwara Y, Tsuchida S, Ueshima R (2022) Molecular phylogeny of the genus *Nipponnemertes* (Nemertea: Monostilifera: Cratenemertidae) and descriptions of 10 new

- species, with notes on small body size in a newly discovered clade. *Frontiers in Marine Science* 9: e906383. <https://doi.org/10.3389/fmars.2022.906383>
- Hubrecht AAW (1879) The genera of European nemerteans critically revised, with description of several new species. *Note from the Leyden Museum* 1: 193–232.
- Iwata F (1954) The fauna of Akkeshi Bay. XX. Nemertini in Hokkaido (revised report). *Journal of the Faculty of Science, Hokkaido University. Series 6, Zoology* 12: 1–39.
- Kajihara H (2007) A taxonomic catalogue of Japanese nemerteans (phylum Nemertea). *Zoological Science* 24(4): 287–326. <https://doi.org/10.2108/zsj.24.287>
- Kajihara H (2015) A histology-free description of the branched-proboscis ribbonworm *Gorgonorhynchus albocinctus* sp. nov. (Nemertea: Heteronemertea). *Publications of the Seto Marine Biological Laboratory* 43: 92–102. <https://doi.org/10.5134/199852>
- Kajihara H (2021) Higher classification of the Monostilifera (Nemertea: Hoplonemertea). *Zootaxa* 4920(2): 151–199. <https://doi.org/10.11646/zootaxa.4920.2.1>
- Kajihara H, Tamura K, Tomioka S (2018) Histology-free descriptions for seven species of interstitial ribbon worms in the genus *Ototyphlonemertes* (Nemertea: Monostilifera) from Vietnam. *Species Diversity* 23(1): 13–37. <https://doi.org/10.12782/specdiv.23.13>
- Kajihara H, Abukawa S, Chernyshev AV (2022) Exploring the basal topology of the heteronemertean tree of life: establishment of a new family, along with turbotaxonomy of Valenciiniidae (Nemertea: Pilidiophora: Heteronemertea). *Zoological Journal of the Linnean Society* 196(1): 503–548. <https://doi.org/10.1093/zoolinnean/zlac015>
- Katoh K, Standley DM (2013) MAFFT multiple sequence alignment software version 7: Improvements in performance and usability. *Molecular Biology and Evolution* 30(4): 772–780. <https://doi.org/10.1093/molbev/mst010>
- Kozlov AM, Darriba D, Flouri T, Morel B, Stamatakis A (2019) RAxML-NG: A fast, scalable and user-friendly tool for maximum likelihood phylogenetic inference. *Bioinformatics* 35(21): 4453–4455. <https://doi.org/10.1093/bioinformatics/btz305>
- Lanfear R, Frandsen PB, Wright AM, Senfeld T, Calcott B (2017) PartitionFinder 2: New methods for selecting partitioned models of evolution for molecular and morphological phylogenetic analyses. *Molecular Biology and Evolution* 34: 772–773. <https://doi.org/10.1093/molbev/msw260>
- Leiva NV, Nacarí L, Baeza JA, González MT (2021) First report of an egg-predator nemertean worm in crabs from the south-eastern Pacific coast: *Carcinonemertes camanchaco* sp. nov. *Scientific Reports* 11(1): 1–13. <https://doi.org/10.1038/s41598-021-98650-0>
- Simpson LA, Ambrosio LJ, Baeza JA (2017) A new species of *Carcinonemertes*, *Carcinonemertes conanobrieni* sp. nov. (Nemertea: Carcinonemertidae), an egg predator of the Caribbean spiny lobster, *Panulirus argus*. *PLoS ONE* 12(5): e0177021. <https://doi.org/10.1371/journal.pone.0177021>
- Sundberg P, Kvist S, Strand M (2016) Evaluating the utility of single-locus DNA barcoding for the identification of ribbon worms (phylum Nemertea). *PLoS ONE* 11(5): e0155541. <https://doi.org/10.1371/journal.pone.0155541>
- Yamaoka T (1947) *Prostoma roseocephalum* Yamaoka, as submitted by S. Okuda. In: Uchida S (Ed.) Revised Edition Illustrated Encyclopedia of the Fauna of Japan (Exclusive of Insects). Hokuryukan, Tokyo, 1469 pp. [In Japanese]

A remarkable new species of the flat bug genus *Nesoproxius* (Hemiptera, Aradidae), the first Oceanian representative with brachyptery

Shusuke Shimamoto¹, Seidai Nagashima², Hiroshi Nagano³, Tadashi Ishikawa¹

1 Laboratory of Entomology, Faculty of Agriculture, Tokyo University of Agriculture, 1737 Funako, Atsugi-shi, Kanagawa, 243-0034, Japan **2** Itami City Museum of Insects, 3-1 Koyaike, Itami-shi, Hyogo, 664-0015, Japan **3** Japan Wildlife Research Center, 3-3-7, Kotobashi, Sumida-ku, 130-8606, Tokyo, Japan

Corresponding author: Shusuke Shimamoto (1202shusuke@gmail.com)

Academic editor: J. Oliveira | Received 6 October 2022 | Accepted 20 January 2023 | Published 7 February 2023

<https://zoobank.org/CC56DFBE-33D4-4B22-85EE-598A612759EC>

Citation: Shimamoto S, Nagashima S, Nagano H, Ishikawa T (2023) A remarkable new species of the flat bug genus *Nesoproxius* (Hemiptera, Aradidae), the first Oceanian representative with brachyptery. ZooKeys 1146: 147–163. <https://doi.org/10.3897/zookeys.1146.96029>

Abstract

A new flat bug species, *Nesoproxius kishimotoi* **sp. nov.**, from the Oceanian region (Ogasawara Islands, Japan) is described. It is the first brachypterous representative in the genus *Nesoproxius*. The sexual dimorphism, nymph, and habitat are also described for the first time in this genus. A key to the species of *Nesoproxius* is also provided.

Keywords

Carventinae, nymph, oceanic island, taxonomy, the Ogasawara (Bonin) Islands

Introduction

The Ogasawara (Bonin) Islands, in the northernmost part of Micronesia, are among the Pacific islands that make up the Oceanian biogeographic region. These subtropical oceanic islands belonging to Japan are registered as a UNESCO World Natural Heritage site because of abundant endemic species with unique evolutionary patterns (UNESCO World Heritage Centre 1992; Government of Japan 2010a). The insect

fauna of the Ogasawara Islands is also characterized by a high number of endemic species, accounting for approximately a quarter of the total species of insects on the islands (Government of Japan 2010a). However, many of these endemic species are endangered (Ministry of the Environment 2015) because of the various threats they face, such as damage caused by the invasive green anole (*Anolis carolinensis* Voight, 1832) and adverse climatic conditions, including a drying trend and severe drought (Yoshida and Iijima 2009; Karube 2014; Karube et al. 2019).

Many undetermined species have recently been discovered, with some of them having been described as new endemic species (Ishikawa 2009; Ishikawa and Karube 2020; Souma and Kamitani 2020; Polhemus and Yasunaga 2021; Souma 2022), implying that the insect fauna of the Ogasawara Islands is insufficiently known. Two undetermined flat bug (Aradidae) species have been found to date (Government of Japan 2010b), and one of them, *Carventus* sp., has only been found so far in Chichijima Island. However, we have confirmed that the undetermined species belongs to the genus *Nesoproxius*, and not *Carventus* (unpublished).

Nesoproxius Usinger & Matsuda, 1959, a genus within the flat bug subfamily Carventinae, was originally established as a subgenus of *Proxius* Stål, 1873 and then upgraded to its current rank by Kormilev and Froeschner (1987). At present, nine species have been described from the Philippines to New Guinea, and an unidentified species has been recorded from the Ryukyu Islands, Japan (Kormilev 1983; Kormilev and Froeschner 1987; Nagashima and Shono 2012; Ishikawa 2016), thereby indicating that all known species are distributed in the Oriental and Australian regions. Additionally, all species in the genus exhibit macropterous features, which are rare among the genera in the subfamily Carventinae, as most of its members show apterous characteristics. However, all specimens from the undetermined species in the Ogasawara Islands showed brachypterous features, which helped us arrive to the conclusion that it is an undescribed species with brachypterous wings. Therefore, we describe *Nesoproxius kishimotoi* sp. nov. as the first brachypterous and Oceanian species belonging to *Nesoproxius*. We also provide a description of the nymphs and information on the habitat of this new species, as well as an identification key to species to facilitate identification.

Materials and methods

Most of the data were obtained from field surveys conducted by the first author in three of the Ogasawara Islands (Chichijima, Anijima, and Ototojima islands) during 2021 and 2022. These surveys which were part of a biodiversity monitoring program in a series of green anole control projects executed by the Ministry of the Environment in Japan. The remaining analyzed specimens were provided by our collaborators. Dried specimens were used for morphological observations, which were performed using a stereoscopic microscope (Olympus SZX7 and Leica M165C). All measurements were performed using a micrometer eyepiece and provided in millimeters. Illustrations were made using a stereoscopic microscope (Leica M165C) with the aid of a drawing tube (Figs 5, 6, 8).

Photographs of the specimens were taken using a digital camera (Canon EOS 5D Mark IV) with a Canon MP-E 65 mm *f*/2.8 1–5× macro lens (Figs 1, 3, 7), and photographs of habitats and living individuals were taken using either of two cameras: a Canon EOS 90D with a Laowa 100 mm F2.8 2× Ultra Macro APO lens or an Olympus EM-1 Mark II with a M. Zuiko digital ED 12–200 mm F3.5–6.3 lens (Figs 4, 9). Photographs of the specimens were focus-stacked using Helicon Focus 7 (Helicon Soft Ltd), and all illustrations, photographs, and images were edited using Adobe Photoshop CC (Adobe Inc.). The distribution map was created and modified by the authors with the aid of SimpleMappr (Shorthouse 2010) (Fig. 10A) and using GSI maps (Fig. 10B). Finally, the terminology used here follows that of Usinger and Matsuda (1959) and Kormilev (1968), and scientific names of plants are based on Yonekura and Kajita (2003). The specimens studied here were deposited at the Laboratory of Entomology, Tokyo University of Agriculture, Atsugi, Japan (TUA) and Kanagawa Prefectural Museum of Natural History, Odawara, Japan (KPMNH).

Taxonomy

Genus *Nesoproxius* Usinger & Matsuda, 1959

Nesoproxius Usinger & Matsuda, 1959: 113 (as subgenus of *Proxius*); upgraded to the generic rank by Kormilev and Froeschner (1987). Type species by original designation: *Proxius* (*Nesoproxius*) *minutus* Usinger & Matsuda, 1959.

Remarks. *Nesoproxius* was previously diagnosed as a macropterous genus (Usinger and Matsuda 1959; Kormilev 1968, 1970, 1978). A brachypterous morph was found in this genus for the first time in the new species described below.

Nesoproxius kishimotoi Shimamoto & Nagashima, sp. nov.

<https://zoobank.org/D2E26489-AF11-4034-B75E-F8CC78CBFAB7>

Figs 1–9

Japanese name: Ogasawara-shiro-hiratakamemushi

Carventus sp.—Government of Japan 2010b: 208.

Type series. Holotype: ♂, “JAPAN, Ogasawara Islands, Ototojima Island, southwest of Ainosawa, 27.1587°N, 142.1894°E, alt. ca 160 m, 11.VII.2021, Shusuke Shimamoto” (TUA).

Paratypes (5 ♂ 12 ♀): **JAPAN, Ogasawara Islands: Chichijima Island:** 1 ♀, Renju-dani, 7.III.1999, Toshio Kishimoto (TUA); 2 ♂ 3 ♀, Renju-dani, 3.III.2022, Shusuke Shimamoto (KPMNH); 1 ♂, Nishi-kaigan, 20.VI.1999, Toshio Kishimoto (TUA). **Ototojima Island:** 2♀, same data as holotype (TUA); 1 ♂ 3 ♀, southwest of

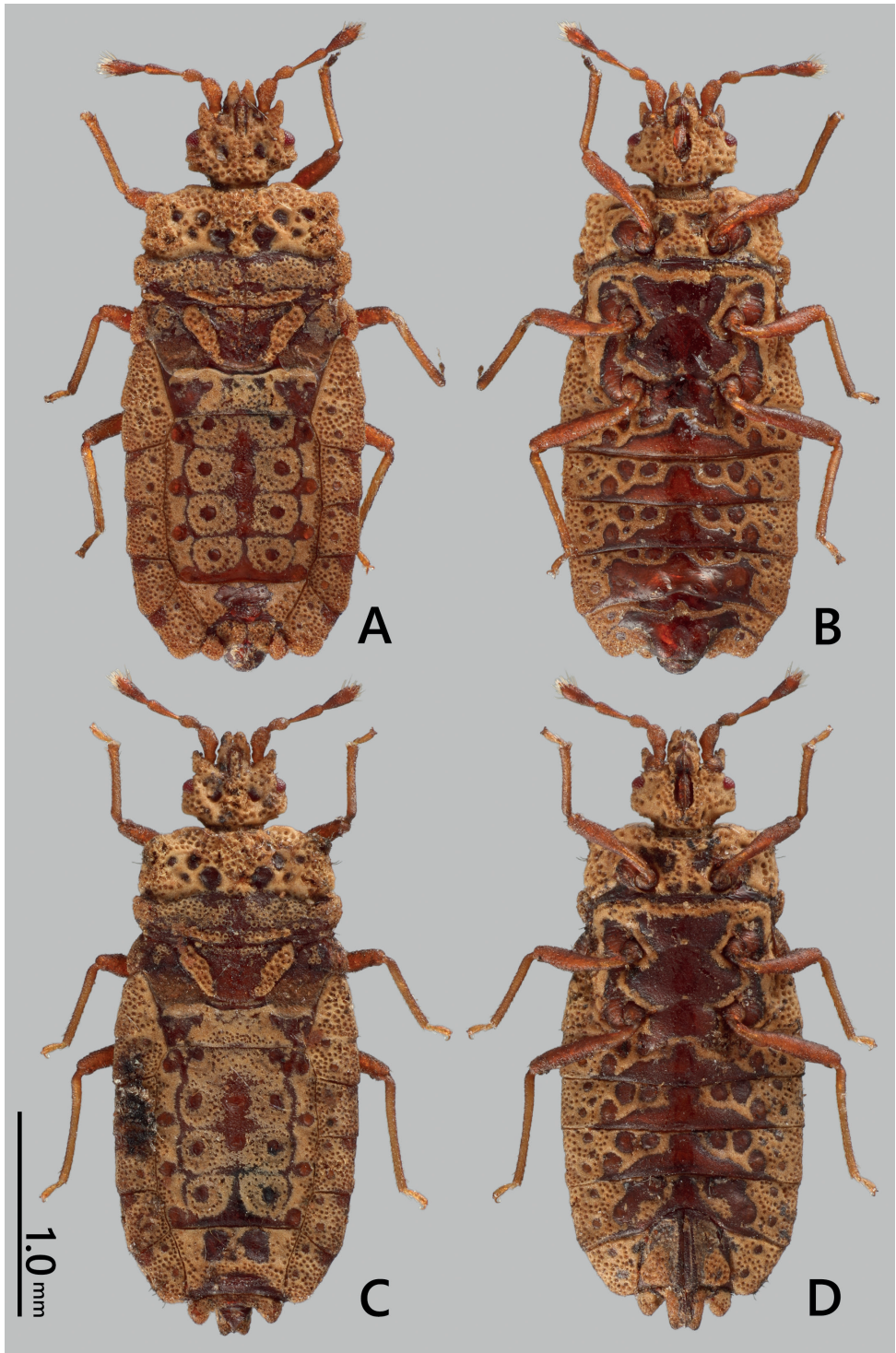


Figure 1. *Nesoproxius kishimotoi* sp. nov. **A, B** male holotype **C, D** female paratype **A, C** dorsal view **B, D** ventral view.

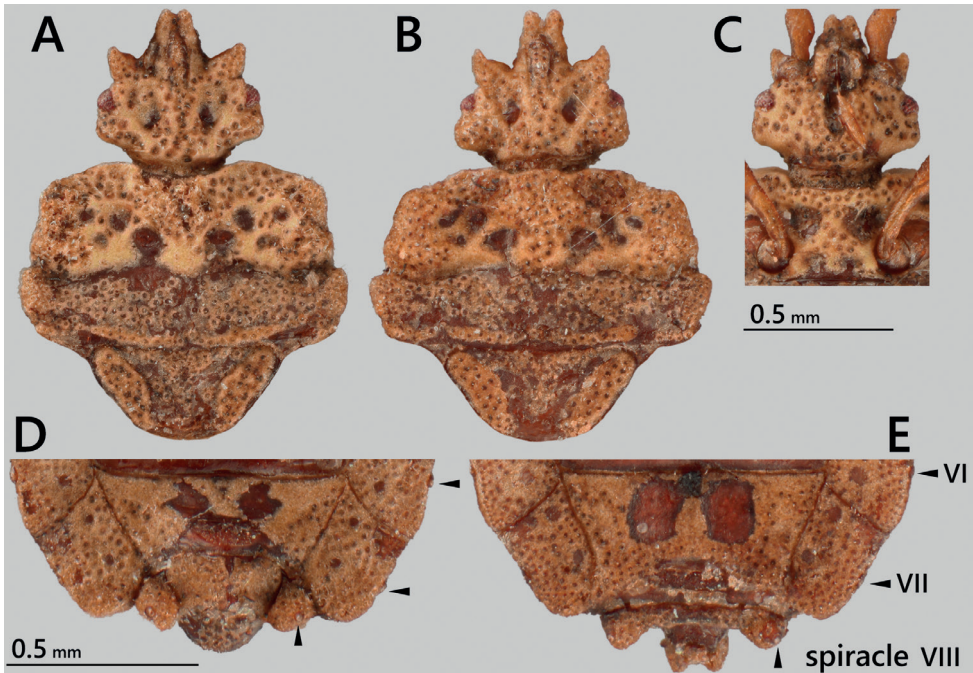


Figure 2. *Nesoproxius kishimotoi* sp. nov., paratypes **A, B** head, pronotum, and scutellum, dorsal view **A** male **B** female **C** ventral view of head and pronotum **D, E** apical part of abdomen, dorsal view **D** male **E** female.

Ainosawa, 27.1591°N, 142.1899°E, alt. ca 160 m, 17.VII.2021, Shusuke Shimamoto (TUA); 1 ♂ 3 ♀, southwest of Ainosawa, 27.1591°N, 142.1899°E, alt. ca 160 m, 18.VII.2021, Shusuke Shimamoto (TUA).

Additional specimens examined. Nymphs (2 spec.): **JAPAN, Ogasawara Islands: Ototojima Island:** 1 spec. (fourth instar), same data as holotype (TUA); 1 spec. (fifth instar), southwest of Ainosawa, 27.1591°N, 142.1899°E, alt. ca 160 m, 18.VII.2021, Shusuke Shimamoto (TUA).

Diagnosis. This new species is the only brachypterous species in this genus, and it can be distinguished from all other *Nesoproxius* species by a combination of the following characters: body length approximately 3.0–3.5 mm; incrustation of body surface ocher; head vertex only slightly longitudinally raised; pronotum with only a slightly convex median ridge; scutellum trapezoidal without a median ridge; and abdomen with a relatively smooth margin.

Description. Male (holotype) (Figs 1A, B, 5A, B). Body reddish brown, mostly covered with punctured ocher incrustations; brachypterous. Head slightly shorter than width across eyes; genae produced over tip of clypeus, slightly shorter than antennal segment I, contiguous to each other in front of clypeus; antenniferous lobes bluntly produced at apex, with parallel outer margins; postocular margins subparallel; posterolateral angles subangular, reaching level of outermost point of eye in dorsal view; vertex slightly raised longitudinally. Labium not reaching level of posterior margin of head in

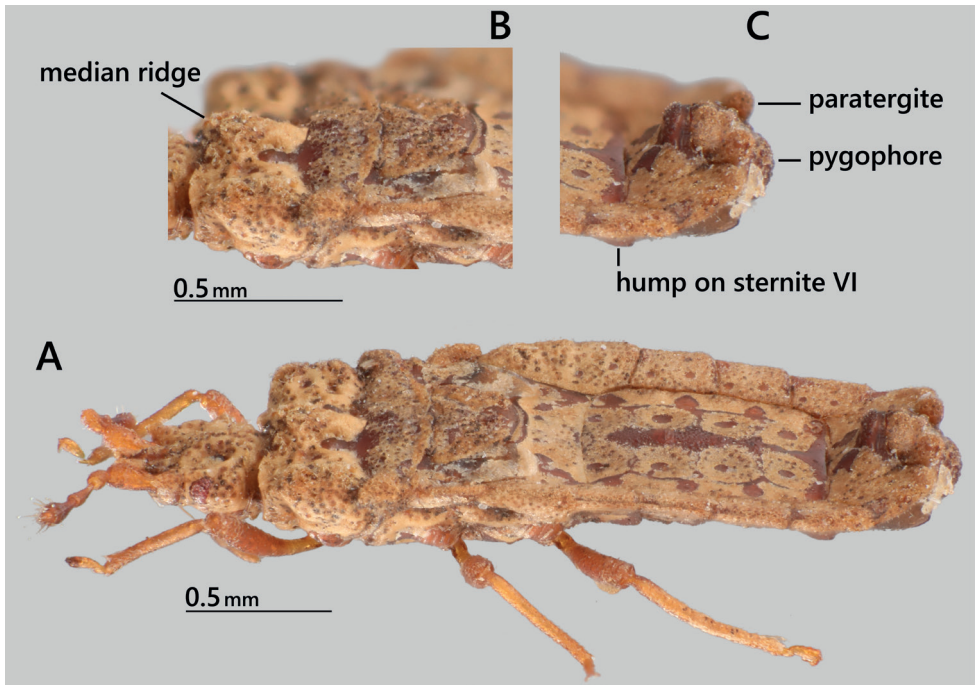


Figure 3. *Nesoproxius kishimotoi* sp. nov., male paratype, dorsolateral view **A** habitus **B** pronotum and scutellum **C** apical part of abdomen.

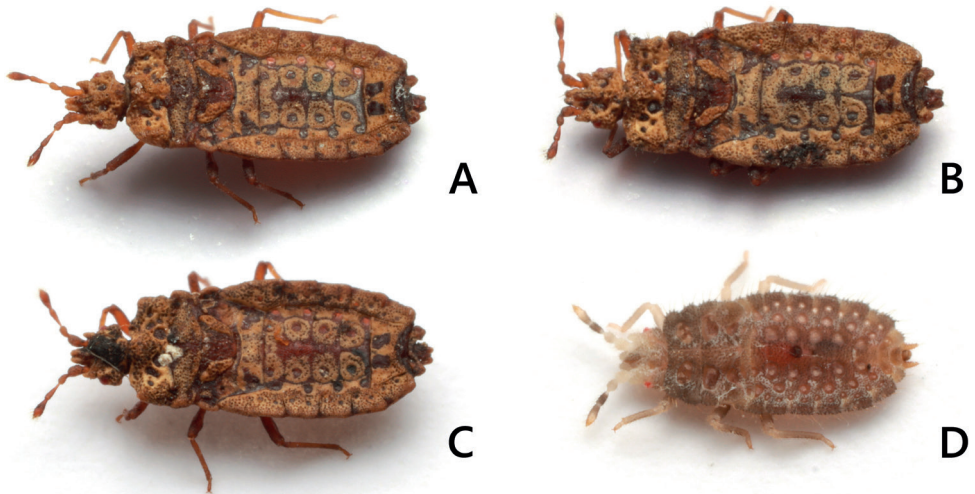


Figure 4. Living individuals of *Nesoproxius kishimotoi* sp. nov. **A, B** adult female **C** same, feigning death **D** fourth instar nymph.

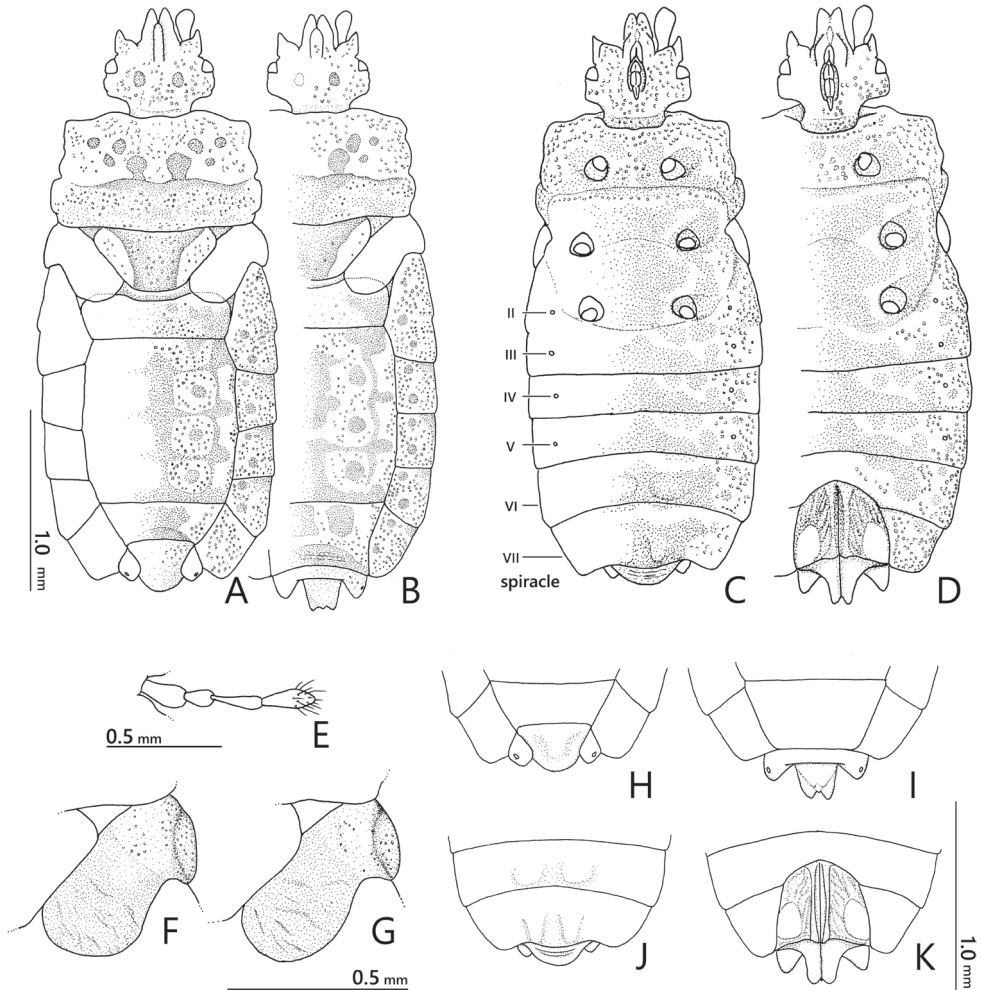


Figure 5. *Nesoproxius kishimotoi* sp. nov., paratypes **A, B** habitus, dorsal view **A** male **B** female **C, D** habitus, ventral view **C** male **D** female **E** left antenna, male **F, G** hemelytra, dorsal view **F** male **G** female **H, I** apical part of abdomen, dorsal view **H** male **I** female **J, K** apical part of abdomen, ventral view **J** male **K** female.

ventral view. Antennae 1.3 times as long as width across eyes; approximate proportion of segments I–IV 1.0: 0.7: 1.0: 1.1.

Pronotum 1.9 times as wide as its length on midline, 1.3 times as long as head (excluding neck) on midline; anterior lobe strongly incrustated, with median ridge weakly inflated and slightly projected anteriorly, and with four pairs of ovate smooth depressions; anterior margin slightly arched forward beyond collar at lateral one-third; anterolateral angles rounded, not projected beyond collar; lateral margins of anterior lobe convex and sinuate; posterior lobe weakly incrustated; lateral margins of posterior lobe

convex anteriorly, then posteriorly concave; posterior margin weakly projected posteriorly. Scutellum trapezoidal, 0.4 times as long as its basal width, widely incrustated and elevated along lateral margins, with lateral margins straight and apex slightly rounded; median ridge thinly incrustated, slightly elevated basally; lateral incrustated fields isosceles triangular. Metanotum slightly visible behind apex of scutellum in dorsal view. Hemelytron reaching basal part of mediotergite I+II; corium reaching basal half of scutellum, projected laterally beyond lateral margin of metanotum, with posterolateral angle reflexed; hemelytral membrane rugose.

Abdomen 1.4 times as long as its maximum width, with subparallel lateral margins. Mediotergite I+II mostly covered with incrustation, provided with a pair of smooth depressions laterally; mediotergites III–VI fused, weakly elevated longitudinally on midline, mostly covered with four inner pairs and three outer pairs of incrustations; inner paired incrustations each with a round smooth depression, and outer paired incrustations reaching lateral margins of respective mediotergites; mediotergite VII covered with incrustations anteriorly and laterally. Dorsal laterotergites mostly covered with incrustations, each with two round callous spots and callous outer anterolateral angle; dorsal laterotergite II+III slightly protruding at middle (posterolateral angle of original dorsal laterotergite II) and at posterolateral angle; posterolateral angles of dorsal laterotergites IV–VI not protruding; outer margin of dorsal laterotergite VI slightly angulated posteriorly; dorsal laterotergite VII posteriorly protruding and subangular, reaching level of tip of paratergite VIII in dorsal view, not reaching level of tip of pygophore. Sternite I+II covered with incrustation; sternites III–VI reticulately incrustated with small to large callosities; sternite VI with a pair of circular humps medially; sternite VII less incrustated, elevated posteromedially, with a pair of subtriangular humps medially. Paratergite VIII rhomboid, angulated posteriorly, reaching level of basal two-thirds of pygophore. Spiracles II–V ventral, spiracles VI and VII lateral, visible in dorsal view, spiracle VIII dorsolateral, visible in dorsal view.

Pygophore (Figs 2D, 5H) acorn-shaped, slightly shorter than its width, incrustated in basal half, scabrous in apical half.

Female (Figs 1C, D, 2B, E, 5B, D, G, I, K). Generally similar to male, larger than male in general; anterolateral angles of pronotum less projected; abdomen with relatively rounded lateral margins; tergite VIII subangular, nearly reaching level of basal two-thirds of paratergite IX; paratergite IX rectangular, posteriorly tricuspidate.

Variation (Fig. 6). The extent of incrustations on the body surface varies among individuals as follows: posterior lobe of pronotum not incrustated (Fig. 6C, G) to completely incrustated (Fig. 6D); median part of scutellum not incrustated (Fig. 6C, F, G) to mostly incrustated (Fig. 6D); incrustations of mediotergites I+II and III–VI reduced (Fig. 6D, E) to highly developed (Fig. 6A–C, F–H); glabrous callosities of mediotergite VII commonly fused into one large smooth area (Fig. 6B, C) or rarely separated (Fig. 6A) in male, and commonly separated (Fig. 6D, E, G, H) or rarely fused (Fig. 6F) in female.

Measurements [in mm, ♂ (holotype and paratypes; $n = 5$), holotype in parentheses / ♀ (paratypes; $n = 5$)]. Body length 2.85–3.06 (2.88) / 3.06–3.47; head length

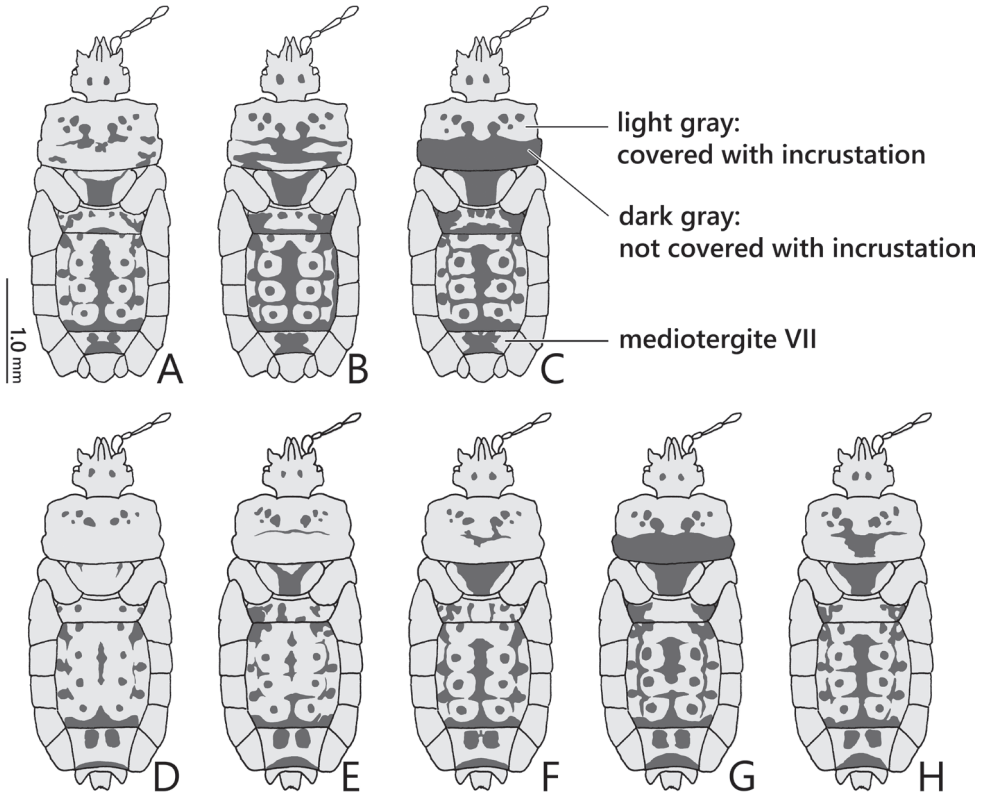


Figure 6. *Nesoproxius kishimotoi* sp. nov., paratypes, variation of incrustation on head, pronotum, scutellum, and mediotergites, dorsal view **A–C** male **D–H** female.

0.48 (0.48) / 0.48–0.57, width across eyes 0.55–0.57 (0.57) / 0.50–0.61; length of antennae 0.69–0.72 (0.72) / 0.70–0.80; pronotum length 0.61–0.64 (0.64) / 0.61–0.70, width 1.07–1.16 (1.11) / 1.11–1.20; scutellum length 0.32–0.36 (0.32) / 0.30–0.55, width 0.61–0.80 (0.80) / 0.68–0.93; abdomen length 1.55–1.64 (1.64) / 1.55–1.84, width 1.18–1.30 (1.27) / 1.30–1.41; pygophore length 0.23–0.25 (0.23), width 0.32–0.34 (0.32).

Nymph (Figs 7, 8). **Fifth instar.** Body generally beige; clypeus, vertex and posterolateral angles of head, lateral margin of thorax and abdominal segments, and center of tergites IX and X greyish beige; body length 3.3 mm; dorsum with continuously granules bearing a pubescence on apex; margin of body with larger granules bearing a longer and more erect seta on apex; head 0.6 times as long as its width on midline; antennal segment IV longest; pronotum provided with a pair of depressions, each depression with five small pits; mesonotum with a pair of smooth depressions, wing pad rounded at apex, reaching basal half of metanotum; metanotum with a pair of smooth depressions; abdominal tergites II–VI mostly not segmented; tergites I–VIII each with 1–4 pairs of round or ring-shaped depressions; two dorsal scent gland openings prominent on midline of tergum, anterior opening conspicuous and located on segment IV,

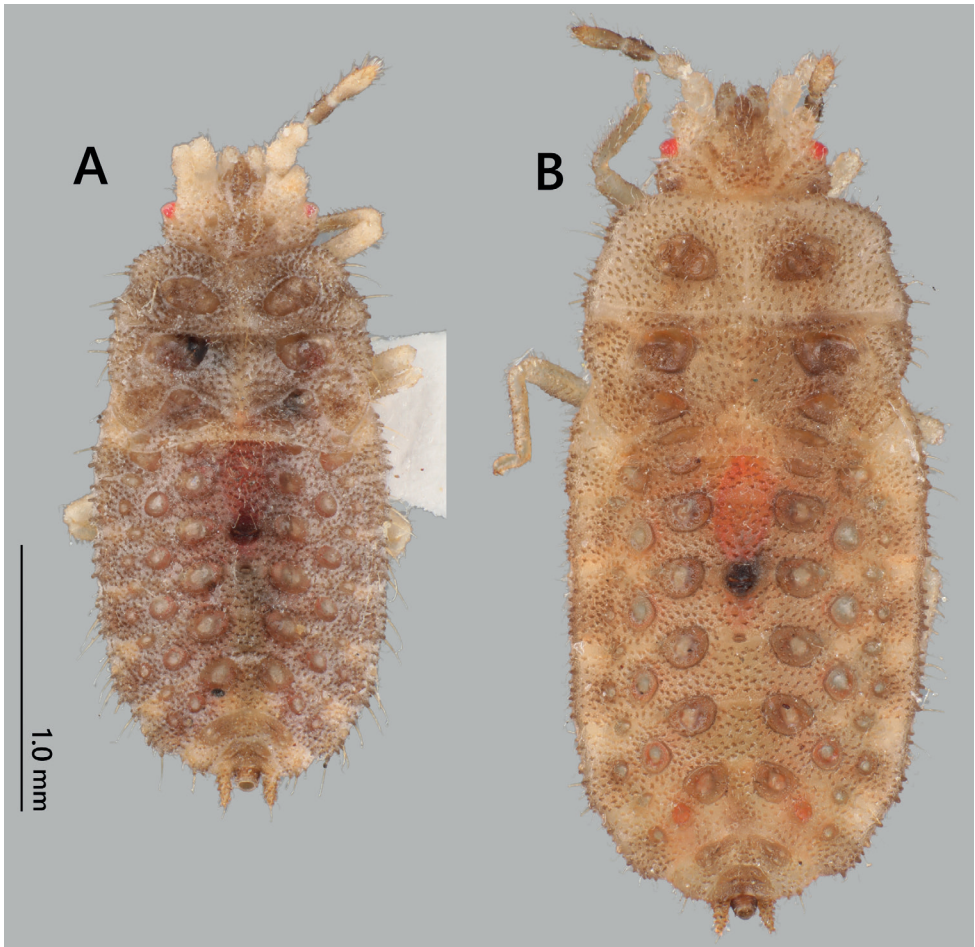


Figure 7. Nymphs of *Nesoproxius kishimotoi* sp. nov. **A** fourth instar, dorsal view **B** fifth instar, dorsal view.

posterior opening more reduced than anterior opening and located on segment V; segment IX with a pair of posteriorly elongated processes; segment X tube-shaped.

Fourth instar. Generally similar to fifth instar but body generally dark gray, both sides of head beige; body length smaller, 2.6 mm; setae arising from margin of body relatively longer than fifth instar.

Remarks. This new species is the first one to exhibit a brachypterous condition in *Nesoproxius*; all specimens examined showed brachypterous features, and none exhibited an apterous or macropterous condition. Even excluding the characteristics of brachypterous wings, this new species can be easily distinguished from other *Nesoproxius* species by the relatively low development of the median ridges on the pronotum and scutellum, as well as the relatively smooth abdominal margin. The unique characteristics of this new species may have been acquired through the long-term isolation in the Ogasawara Islands, which are far from New Guinea, the center of the geographic distribution of the genus.

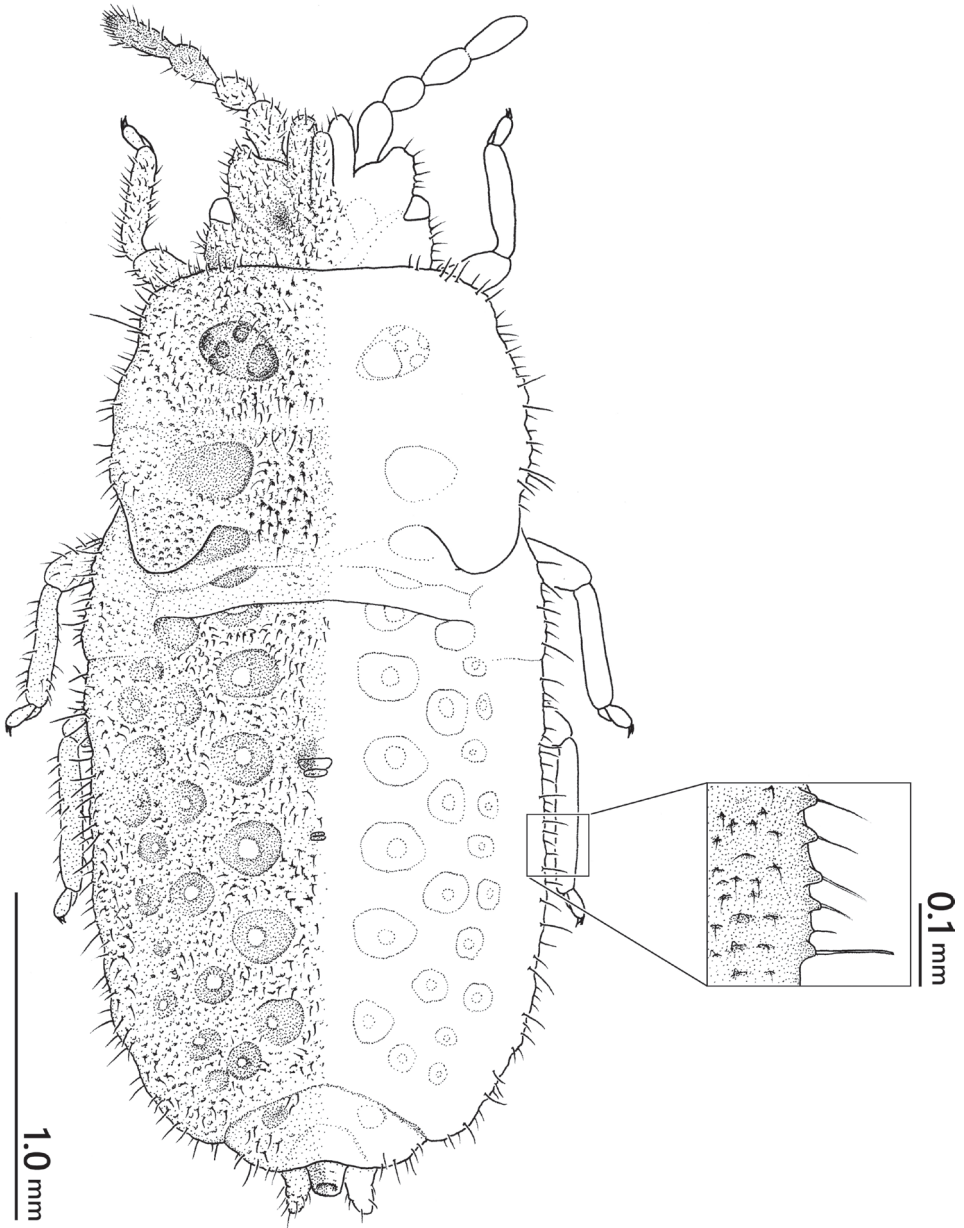


Figure 8. Fifth instar nymph of *Nesoproxius kishimotoi* sp. nov., dorsal view.

In this study, we also clarified for the first time that sexual dimorphism in this *Nesoproxius* species is manifested in the pattern of incrustations, particularly those on mediotergite VII. Previous studies have described and illustrated this characteristic; however, all known species have been described based on one or two individuals, most

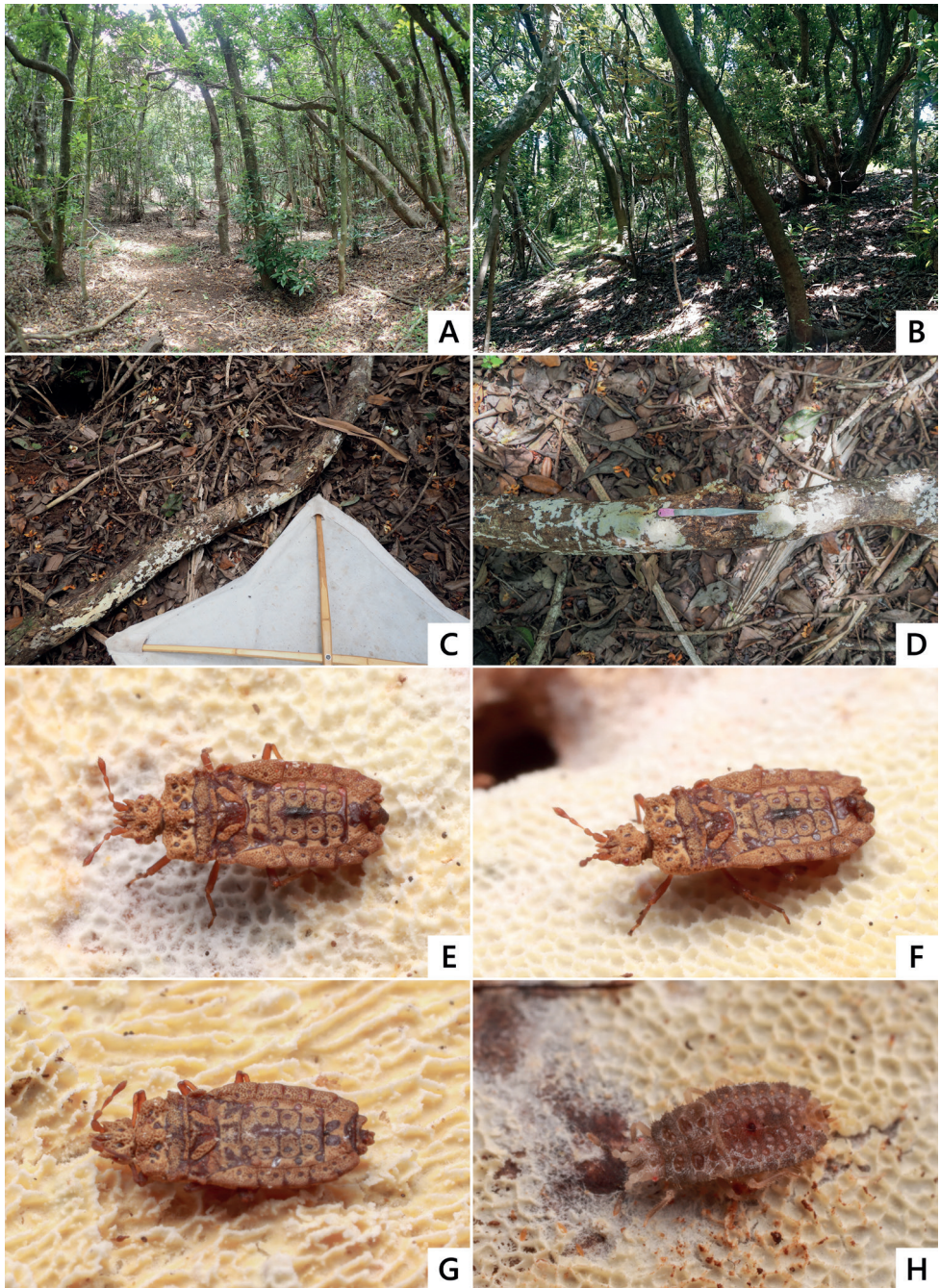


Figure 9. Habitats and living individuals of *Nesoproxius kishimotoi* sp. nov. **A, B** Habitat in Ototojima Island **C, D** decayed fallen branches of *Schima wallichii mertensiana*, of which the type specimens were collected **E** adult male, dorsal view **F** ditto, dorsolateral view **G** adult female, feigning death **H** fourth instar nymph, dorsolateral view.

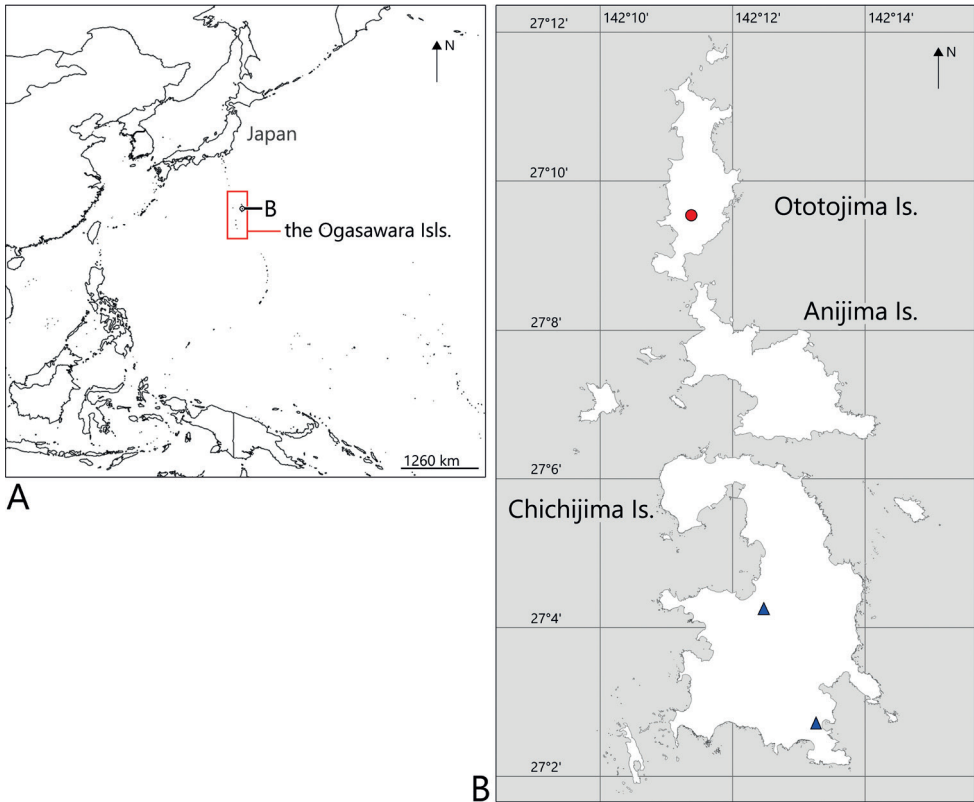


Figure 10. Distribution map of *Nesoproxius kishimotoi* sp. nov. **A** location of the Ogasawara Islands **B** detail distribution in the Ogasawara Islands, red circle = holotype locality; blue triangles = paratype localities.

of which were females (Usinger and Matsuda 1959; Kormilev 1968, 1970, 1978); therefore, identifying and describing species of this genus are necessary considering the existence of incrustations that might be the indicators of sexual dimorphism.

Moreover, this is the first time that nymphal stages have been described for *Nesoproxius* species. The body of the nymph is covered with sparse pubescence on the dorsal surface; however, it does not show the incrustations found in adults. In addition, as setae on the body margin are longer in 4th instar than in 5th instar nymphs, they possibly are relatively longer in younger instars.

Etymology. The specific name is after Toshio Kishimoto, the first collector of this species.

Distribution (Fig. 10). Japan: the Ogasawara Islands (Chichijima and Ototojima islands).

This new species, endemic to the Ogasawara Islands, represents the northernmost occurrence reported for *Nesoproxius*, which is far from the distribution of its congeners, and it is the first representative in this genus from the Oceanian region.

Habitats and biology (Figs 4, 9). The new species inhabits the relatively humid forest floor of forests with tall trees, dominated by *Schima wallichii mertensiana* (Siebold & Zucc.) Bloemb. (Theaceae). However, despite our repeated field surveys, this flat bug was not found in Anijima Island, located between Chichijima and Ototojima islands (where the species inhabits), likely because, unlike the other two islands, it is entirely covered by sclerophyllous shrubs and has a dry forest floor. Therefore, it seems likely that a dry environment such as found Anijima Island is not suitable for the *N. kishimotoi* sp. nov. For this species to persist, maintaining the good condition of the ecosystems on Chichijima and Ototojima islands is necessary; however, frequent droughts in recent years may pose a challenge by negatively impacting the habitat of this species.

Nesoproxius kishimotoi sp. nov. was collected from the undersurface of decayed fallen branches of *Schima wallichii mertensiana* on the forest floor. Both adults and nymphs moved very slowly and frequently feigned death with folded legs and antennae. As the adults and nymphs were found together on the same branches, they all seem to inhabit the same cluster; however, their habitat range seems to be limited and scattered. The reason for this is not clear; however, it is possible that the severe damages to the soil ecosystem caused by predation by alien nemertines in the Ogasawara islands (Shinobe et al. 2017) reduce flat bug populations. Lastly, and as mentioned previously, to conserve this evolutionarily important and unique flat bug species in the Ogasawara Islands, preventing droughts and eliminating predatory alien species are necessary.

Key to species of the genus *Nesoproxius* (based on Kormilev 1968, 1970, 1978, 1983)

- 1 Small species, less than 3.5 mm.....2
- Larger species, over 4.0 mm5
- 2 Median ridge of scutellum clearly elevated as a T-shape.....3
- Median ridge of scutellum slightly elevated basally or clearly elevated longitudinally.....4
- 3 Median ridge of scutellum contiguous with lateral incrustated fields posteriorly ..
.....*N. constrictus* Kormilev, 1978
- Median ridge of scutellum not contiguous with lateral incrustated fields posteriorly *N. gracilis* Kormilev, 1968
- 4 Anterior margin of pronotum straight; anterior angles of pronotum not projected; scutellum triangular, with median ridge clearly elevated along midline wholly..... *N. minutus* Usinger & Matsuda, 1959
- Anterior margin of pronotum sinuate; anterior angles of pronotum projected beyond collar; scutellum trapezoidal, with median ridge slightly elevated mediobasally.....*N. kishimotoi* sp. nov.
- 5 Median ridge of pronotum strongly inflated, overlapping with base of head.....6
- Median ridge of pronotum slightly inflated, not overlapping with base of head 8

- 6 Spiracle VIII lateral *N. malayensis* Kormilev, 1983
 – Spiracle VIII dorsal 7
 7 Median ridge of vertex subtriangular; median ridge of pronotum truncate posteriorly *N. vietnamensis* Kormilev, 1968
 – Median ridge of vertex ovate; median ridge of pronotum angulate posteriorly...
 *N. yoshimotoi* Kormilev, 1970
 8 Pronotum hexagonal; posterior angle of abdominal segment VII of female not reaching tip of paratergite *N. hexagonalis* Kormilev, 1968
 – Pronotum subrectangular or trapezoidal; posterior angle of abdominal segment VII of female reaching or exceeding tip of paratergite 9
 9 Pronotum subrectangular, without a projection on lateral margin; posterior angle of abdominal segment VII of female not produced into a long spine
 *N. punctulatus* Kormilev, 1968
 – Pronotum trapezoidal, with a projection on lateral margin slightly before middle; posterior angle of abdominal segment VII of female produced into a long spine *N. angulatus* Kormilev, 1968

Acknowledgements

We are very thankful to Jader Oliveira (University of São Paulo, São Paulo, Brazil), Ernst Heiss (Tiroler Landesmuseum, Innsbruck, Austria), Hécio Gil-Santana (Instituto Oswaldo Cruz, Rio de Janeiro, Brazil), and an anonymous reviewer for the critical reading of the manuscript and for giving valuable comments. We are grateful to the Kanto Regional Environment Office, Ministry of the Environment, Japan (Saitama, Japan) for allowing us to use the specimens collected from the Ogasawara Islands by the project of the Ministry of the Environment in Japan. We sincerely thank Toshinobu Matsumoto (Japan Wildlife Research Center, Tokyo, Japan), Toshio Kishimoto (Museum of Natural and Environmental History, Shizuoka, Japan), and Hiroaki Kojima (TUA) for providing valuable comments and suggestions and supporting our fieldwork. We also thank to Mitsuhiko Toda, Yusuke Oyamada, Emi Kinoshita, Yuki Murakami (Japan Wildlife Research Center, Tokyo, Japan), Haruki Karube, Reiko Kaga (KPMNH), and Hitoshi Ishikawa (Shizuoka, Japan) for providing opportunities to conduct this study. This study was partly supported by Sasakawa Scientific Research Grant from the Japan Science Society (2021–5021) and grant from the Nodai Research Institute (464073322) to the first author. We would like to thank Editage (www.editage.jp) for the English language editing.

References

- Government of Japan (2010a) Nomination of the Ogasawara Islands for Inscription on the World Heritage List. Government of Japan, Tokyo, 229 pp.

- Government of Japan (2010b) Species list. In: Government of Japan, Appendix of Nomination of the Ogasawara Islands for Inscription on the World Heritage List. Government of Japan, Tokyo, 147–242.
- Ishikawa H (2009) Occurrence of a new grasshopper, *Boninoxya anijimensis* gen. et sp. nov. (Orthoptera, Acrididae, Oxyinae) in the Ogasawara Islands, Japan. Japanese Journal of Systematic Entomology 17(1): 115–120.
- Ishikawa H, Karube H (2020) A new species of the genus *Hexacentrus* (Orthoptera: Tettigoniidae) from Hahajima, the Ogasawara Islands, south Japan. Japanese Journal of Systematic Entomology 26(2): 333–335.
- Ishikawa T (2016) Family Aradidae. In: Hayashi M, Tomokuni M, Yoshizawa K, Ishikawa T (Eds) Catalogue of the Insects of Japan (Vol. 4), Paraneoptera. Entomological Society of Japan and Touka-shobo, Fukuoka, 452–457. [in Japanese]
- Karube H (2014) The peculiar beetle and alien species problem of Ogasawara Islands. The Nature and Insects 49(9): 8–11. [in Japanese]
- Karube H, Takeda S, Tsutsui H, Nagano H, Oyamada Y, Toda M (2019) Impacts of the severe drought of 2016–2017 on endemic insects in the Ogasawara Islands, based on monitoring data of endemic dragonflies, endemic beetles, and endemic hemipterans. Ogasawara Yearly Research Bulletin 42: 31–43. [in Japanese]
- Kormilev NA (1968) Aradidae in the Bishop Museum, Honolulu, III (Hemiptera: Heteroptera). Pacific Insects 10: 575–597.
- Kormilev NA (1970) Aradidae in the Bishop Museum, Honolulu, V. (Supplement) (Hemiptera-Heteroptera). Pacific Insects 12: 701–722.
- Kormilev NA (1978) Aradidae in the Bishop Museum, Honolulu, VII (Hemiptera: Heteroptera). Pacific Insects 18: 53–60.
- Kormilev NA (1983) New oriental aradid bugs in the collection of the British Museum (Natural History) (Insecta: Hemiptera). Journal of Natural History 17(3): 437–469. <https://doi.org/10.1080/00222938300770291>
- Kormilev NA, Froeschner RC (1987) Flat bugs of the world. A synonymic list (Heteroptera: Aradidae). Entomography 5: 1–246.
- Ministry of the Environment (2015) Red Data Book 2014. Threatened Wildlife of Japan (Vol. 5), Insecta. Gyosei, Tokyo, 509 pp. [in Japanese]
- Nagashima S, Shono Y (2012) Family Aradidae Brullé, 1836. Flat bugs, bark bugs. In: Ishikawa T, Takai M, Yasunaga T (Eds) A Field Guide to Japanese Bugs. Terrestrial Heteropterans III. Zenkoku Noson Kyoiku Kyokai, Tokyo, 289–314. [pls 52–66] [in Japanese]
- Polhemus AD, Yasunaga T (2021) A new species of the plant bug genus *Pilophorus* Hahn from the Ogasawara (Bonin) Islands, Japan (Hemiptera: Heteroptera: Miridae: Phylinae). Zootaxa 5060(3): 447–450. <https://doi.org/10.11646/zootaxa.5060.3.10>
- Shinobe S, Uchida S, Mori H, Okochi I, Chiba S (2017) Declining soil Crustacea in a World Heritage Site caused by land nemertean. Scientific Reports 7(1): e12400. <https://doi.org/10.1038/s41598-017-12653-4>
- Shorthouse DP (2010) SimpleMappr, an online tool to produce publication-quality point maps. <http://www.simplemappr.net> [accessed on 01.10.2022]

- Souma J (2022) Two new species of the genus *Omoplax* (Hemiptera: Heteroptera: Tingidae) from Mukojima Island, with new records of lace bugs endemic to the Ogasawara Islands, Japan. *Acta Entomologica Musei Nationalis Pragae* 62(1): 117–127. <https://doi.org/10.37520/aemnp.2022.008>
- Souma J, Kamitani S (2020) Taxonomic review of the lace bug genus *Omoplax* (Hemiptera: Heteroptera: Tingidae) endemic to “Oriental Galapagos” (the Ogasawara Islands, Japan) with the description of its new allied genus and species. *Entomological Science* 24(1): 3–11. <https://doi.org/10.1111/ens.12445>
- Stål C (1873) *Enumeratio hemipterorum. Bidrag till en forteckning ofver alla hittills kända Hemiptera, jemte systematiska meddelanden af C. Stal, 3. Kungliga Svenska Vetenskapsakademiens Handlingar* 11(2): 1–163.
- UNESCO World Heritage Centre (1992) Ogasawara Islands. <https://whc.unesco.org/en/list/1362/> [accessed on 01.10.2022]
- Usinger RL, Matsuda R (1959) *Classification of the Aradidae*. British Museum, London, 410 pp.
- Yonekura K, Kajita T (2003) BG Plants Wamei-Gakumei Index (YList). <http://ylist.info> [accessed on 01.10.2022] [in Japanese]
- Yoshida K, Iijima Y (2009) Hydroclimatic conditions during the last decade in the Ogasawara (Bonin) Islands. *Japanese Journal of Limnology* 70(1): 13–20. [in Japanese] <https://doi.org/10.3739/rikusui.70.13>

Redescription of *Periplaneta arabica* (Bey-Bienko, 1938) (Blattodea, Blattidae), with a comparative analysis of three species of *Periplaneta* Burmeister, 1838 (*sensu stricto*)

Xin-Xing Luo¹, Qian-Qian Li¹, Alireza Zamani², Yan-Li Che¹, Zong-Qing Wang¹

1 Institute of Entomology, College of Plant Protection, Southwest University, Beibei, Chongqing 400716, China **2** Zoological Museum, Biodiversity Unit, FI-20014 University of Turku, Turku, Finland

Corresponding author: Zong-Qing Wang (zqwang2006@126.com)

Academic editor: Frédéric Legendre | Received 26 July 2022 | Accepted 18 January 2023 | Published 9 February 2023

<https://zoobank.org/D382AF5A-64EC-4AFF-B5AB-1B2B7A976E5B>

Citation: Luo X-X, Li Q-Q, Zamani A, Che Y-L, Wang Z-Q (2023) Redescription of *Periplaneta arabica* (Bey-Bienko, 1938) (Blattodea, Blattidae), with a comparative analysis of three species of *Periplaneta* Burmeister, 1838 (*sensu stricto*). ZooKeys 1146: 165–183. <https://doi.org/10.3897/zookeys.1146.90817>

Abstract

The blattid cockroach *Periplaneta arabica* (Bey-Bienko, 1938) has been poorly understood since its original description. In this study, male and female (including nymph) of *P. arabica* are paired using DNA barcoding, and their morphological characters (including both external characteristics and genitalia) are described. A detailed comparative morphological study of this species and the closely related *Periplaneta americana* (Linnaeus, 1758) and *Periplaneta lateralis* Walker, 1868 was carried out to explore phylogenetically relevant characters.

Keywords

Blattid cockroach, DNA barcoding, female genitalia, habitat adaptation, male genitalia, sexual dimorphism, *Shelfordella*, taxonomy

Introduction

According to Beccaloni (2014), the Blattinae genus *Shelfordella* Adelung, 1910 comprised three species before it was synonymized with *Periplaneta* (Deng et al. 2023). The taxonomic status of *Shelfordella* remains unclear even though several revisions were carried out by Princis (1954) and Bohn (1985) based on the external morphological characters. In addition, many molecular phylogenetic studies (Legendre et al. 2015; Bourguignon et al. 2018; Arab et al. 2020; Liao et al. 2021; Djernæs and Murienne 2022; Li et al. 2022; Deng et al. 2023) have shown that *Periplaneta americana* (Linnaeus, 1758), the type species of *Periplaneta* Burmeister, 1838, is the sister species to *Sh. lateralis* (Walker, 1868). Considering both molecular data and morphological characters of male genitalia of *P. americana* and *Sh. lateralis*, *Shelfordella* was considered as a synonym of *Periplaneta* (Deng et al. 2023), resulting in the restoration of *Periplaneta lateralis* Walker, 1868 and *Periplaneta monochroma* Walker, 1871, and the transference of *Shelfordella arabica* Bey-Bienko, 1938 to *Periplaneta*. *Periplaneta arabica* was originally described with a female specimen as its type, and the male has not been described.

DNA barcoding has been confirmed to be a helpful tool in discovery of new species, matching nymphs with adults, and revealing sexual dimorphism and cryptic species in cockroaches (Evangelista et al. 2013; Che et al. 2017; Yang et al. 2019; Li et al. 2022; Zhu et al. 2022). Herein, we use DNA barcoding to pair male, female and nymphs of *P. arabica*, allowing a comprehensive redescription of this species. We also take the opportunity to compare the morphological characters of *P. arabica*, *P. americana* and *P. lateralis*, to show the structural complexity and diversity of species of *Periplaneta s.s.*, as well as to provide detailed information useful for future phylogenetic studies on the genus.

Material and methods

Morphological study

Specimens (stored in absolute ethanol at -20 °C) examined are deposited in the Institute of Entomology, College of Plant Protection, Southwest University, Chongqing, China (SWU). Abdominal segments were soaked in 10% NaOH solution at 70 °C for 10 minutes. They were cleaned in distilled water, dissected in glycerol under a Motic K400 stereomicroscope, then stored in glycerol. Photographs were taken using a Canon M5 plus a Laowa 65 mm F2.8 CA-Dreamer Macro 2X Macro lens attached to a Leica M205A stereomicroscope. All figures were modified in Adobe Photoshop CC 2019. The morphological terminology used in this paper mainly follows Roth (2003). The terminology of veins follows Li et al. (2018), and those of the sclerites of male and female genitalia mainly follows Klass (1997) and McKittrick (1964), respectively. Measurements were obtained by Vernier Caliper.

Abbreviations used are as follows:

Cu	cubitus
CuA	cubitus anterior
CuP	cubitus posterior
hlap	process (p) of hook of L3
M	media
Pcu	postcubitus
R	radius
RA	radius anterior
RP	radius posterior
ScP	subcostal posterior
V, V[1], V[s]	vannal veins
L1, L2, L3, L4C, L4D, L4E L4G	sclerites of the left phallomere
R1G, R1H, R1F, R2, R3	sclerites of the right phallomere

DNA extraction, amplification and sequencing

Total DNA extraction was obtained from muscle tissue using the Hipure Tissue DNA Mini Kit, and the remaining specimens were stored in 95% ethanol. The primers used to amplify the 658 bp cytochrome c oxidase subunit I (COI) fragment were COI-F2 (5'-CAACAAATCATAAAGATATTGGAAC-3') and COI-R2 (5'-TAAACTTCTG-GATGACCAAAAAATCA-3') or COI-F3 (5'-CAACYAATCATAAAGANATTG-GAAC-3') and COI-R3 (5'-TAAACTTCAGGGTGACCAAAAAATCA-3') (Yang et al. 2019). The amplification reaction was in according to the protocols in Wang et al. (2021). The cycling conditions were as follows: initial denaturation at 98 °C for 2 min, followed by 35 cycles of 98 °C for 10 s, 49–51 °C for 10 s, 72 °C for 10 s, and a final extension at 72 °C for 10 min. The PCR products were then sequenced by BGI Technology Solutions Co. Ltd (BGI-Tech) (Beijing, China).

Sequence processing and molecular analysis

A total of 25 COI sequences were analyzed, of which, 17 sequences were from three *Periplaneta* species (i.e., six sequences of *P. arabica*, five sequences of *P. americana* and six sequences of *P. lateralis*) (Table 1). Sequences were aligned by MAFFT ver. 7 (<https://mafft.cbrc.jp/alignment/server/>) with the G-INS-i strategy (Katoh et al. 2019), and manually adjusted using MEGA ver. 7.0.26 (Kumar et al. 2007). The intra- and interspecific genetic distances were quantified in MEGA based on the Kimura 2-parameter (K2P) distance model (Kimura 1980) (Suppl. materials 1, 2). The maximum likelihood (ML) tree was constructed in IQ-TREE ver. 1.6.8 (Nguyen et al. 2015) with 10,000 ultrafast bootstrap replicates; the partition scheme and best-fitting substitution models (COI_pos 1, TRN+I+G; COI_pos 2, TVM+I; COI_pos 3, HKY+I+G) were selected in PartitionFinder ver. 2.1.1 (Lanfear et al. 2017) by the corrected Akaike Information Criterion (AICc).

Table 1. Samples used in ML analyses with localities, voucher numbers, and accession numbers (bold represent the new sequences). Abbreviations: young nymph (YN); late nymph (LN).

Species	Voucher number	Locality/References	Accession Number
<i>Periplaneta arabica</i>	1213(YN), 1208(♀), YL1(♂), SYL(♂), Shelarab1211(LN), YL2(♀)	Dehloran, Ilam, Iran	OP727639 to OP727640 and OP727649 to OP727652
<i>Periplaneta americana</i>	1416(♂), 1124(♂), 1417(♀), 1415(♀)	Bahamas: Exuma, Staniel (Pringle et al. 2019) Yuanjiang, Yunnan, China Mt Diaoluo, Hainan, China Meizhou Island, Fujian, China	MK936745 OP727642 OP727638 and OP727643 OP727641
<i>Periplaneta lateralis</i>	2401(♂), 2430(♀), 2433(♀), 2435(♀), 2440(♀)	Laboratory Rearing (online shopping)	OP727644 and OP727648
<i>Blatta orientalis</i>	–	Breeds of Kyle Kandilian (Bourguignon et al. 2018)	MG882183
<i>Periplaneta brunnea</i>	–	Bourguignon et al. (2018)	MG882174
<i>Periplaneta fuliginosa</i>	–	Bourguignon et al. (2018)	MG882182
<i>Periplaneta australasiae</i>	–	Ma et al. (2019)	MF149696
<i>Cryptocercus meridianus</i>	–	Ma et al. (2019)	MH184379
<i>Tryonicus mackerrasae</i>	–	Li et al. (2017)	MG518617
<i>Hebardina concinna</i>	–	Bourguignon et al. (2018)	MG882205
<i>Mantis religiosa</i>	–	Deng et al. (2023)	ON645482
		Ye et al. (2016)	NC030265

Results

Molecular analysis

In this study, we used six COI sequences of *P. arabica*, five COI sequences of *P. americana* and six COI sequences of *P. lateralis*. All new sequences were deposited in GenBank with accession numbers OP727638 to OP727652. Intraspecific COI genetic divergence (K2P) of *P. arabica* and *P. lateralis* is 0%, but for *P. americana*, the intraspecific COI genetic divergence ranged from 0.00% to 2.30%. Interspecific COI genetic divergence ranged from 9.9% (*P. arabica* and *P. americana*) to 13.1% (*P. americana* and *P. lateralis*).

In our ML analyses, samples including adults and nymphs from the same morphospecies are clustered together with high support values (Fig. 1). *Periplaneta arabica* was recovered as the sister to *P. americana* on the basis of COI data but with a rather low support (bootstrap support (BS) = 79). These three species (i.e., *P. arabica*, *P. lateralis* and *P. americana*) formed a monophyletic group with *Blatta orientalis* as the sister (BS = 79 and 60, respectively).

Taxonomy

Genus *Periplaneta* Burmeister, 1838

Periplaneta Burmeister, 1838: 502. Type species: *Periplaneta americana* (Linnaeus, 1758). Shelford 1910: 17; Bey-Bienko 1950: 116; Princis 1966: 404; Asahina 1980: 103; Roth 1999: 168.

Cacerlaca Saussure, 1864: 71; Princis 1966: 405.

Paramethana Shelford, 1909: 309; Princis 1966: 473.

Shelfordella Adelung, 1910: 329; Princis 1966: 507; Bohn 1985: 39.

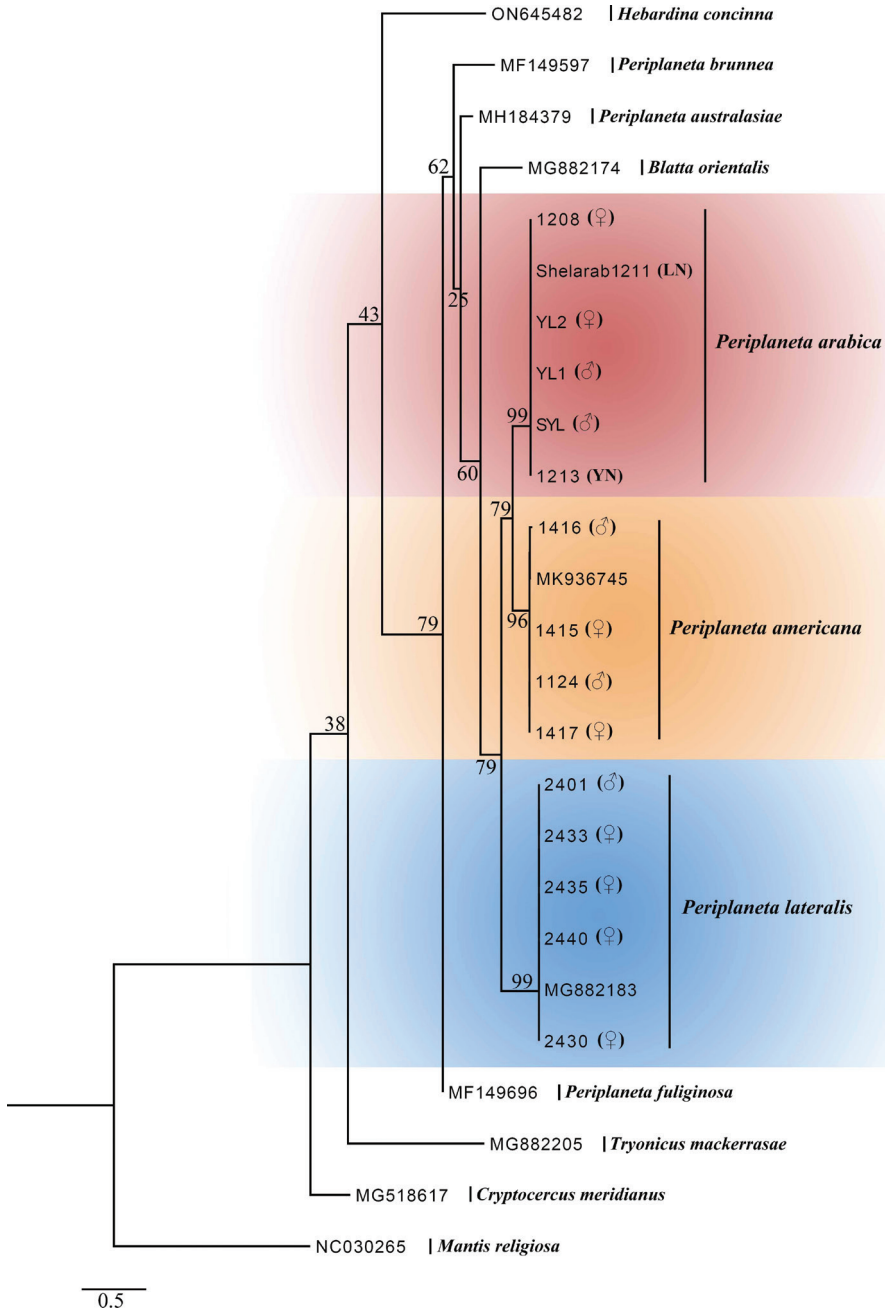


Figure 1. Maximum likelihood (ML) tree derived from COI sequences with 10,000 ultrafast bootstrap replicates.

Diagnosis (based on species covered in this paper; *Periplaneta s.s.*). Sexual dimorphism indistinct or distinct. Pronotum subelliptical in male, subelliptical or campaniform in female. Tegmina and wings well developed in male, developed or reduced in

female. Legs slightly slender. Abdomen with the first tergite unspecialized in male. Hind margin of supra-anal plate hyaline and concave in the middle; cerci long, apically tapering. Hind margin of subgenital plate slightly convex. **Genitalia of male:** L1 weakly sclerotized with pubescence; hind margin of L4C nearly truncated; the caudal part of L2 with a long spine toward right; L3 with hlap weakly developed; the basal part of L4G constrict. R1H with two long spines at apex; the caudal part of R1G with a long and curved spine toward right. **Genitalia of female:** Anterior arch (a.a.) with two symmetrical foot-shaped projections; spermathecal plate (sp.pl) nearly crescent-shaped; the enlarged part of spermatheca (sp.) curved, subelliptical or irregular; basivalvulae (bsv.) subelliptical; laterosternal shelf (ltst.sh.) with postero-lateral angle extended towards outer margin.

***Periplaneta arabica* (Bey-Bienko, 1938)**

Figs 2, 3, 4 (in part), 5 (in part), 6

Shelfordella arabica Bey-Bienko, 1938: 235 (Type locality: Mecca, Saudi Arabia); Bohn 2007: 87.

Blatta (*Shelfordella*) *arabica*: Princis 1966: 509.

Material examined (all deposited in SWU). 6 males, 2 females and 7 nymphs; IRAN; Ilam Province: Dehloran county, near the border with Iraq, surroundings of Changuleh [33°0'49.37"N, 46°36'38.63"E, approximate coordinates], unnamed cave, II. 2020, A.H. Aghaei leg.

Diagnosis. Combining the following characteristics, this species is easily distinguished from its congeners: 1) interocular space slightly wider than the interocellar space and less than interantennal space in male, interocular space wider than interantennal space in female; 2) tegmina of female reduced and nearly square; 3) legs slender, pulvilli and arolia absent; 4) hind margin not extending outward and slightly concave in the middle, forming an obtuse angle in supra-anal plate of male; 5) caudal part of L2 with a well sclerotized spine; 6) hlap weakly developed, but larger than that of the other two species; 7) distal part of R1H with two long spines and no serration.

Redescription. Measurements (mm). Male. Body length including tegmen: 30.6–36.4; body length: 24.2–27.3; pronotum length × width: 6.7–7.7 × 7.2–7.7; tegmen length × width: 24.9–29.2 × 4.6–5.4. **Female.** Body length: 23.5–25.5; pronotum length × width: 6.4–6.8 × 6.6–7.2; tegmen length × width: 4.4–6.4 × 6.6–7.3.

Coloration. Body brown or reddish brown, eyes black, ocelli white; tegmina and wings yellowish brown.

Male (Fig. 2). Head and thorax. Vertex exposed. Interocular space slightly wider than the interocellar space, less than interantennal space. Antenna longer than the body (Fig. 2C). Pronotum subelliptical, with surface sparsely pubescent, the central part of anterior margin depressed, and hind margin slightly convex, the widest point approximately in the middle (Fig. 2D). Tegmina and wings well developed, exceeding the end

of abdomen by about 5.3–7.7 mm. Tegmina with ScP strong, the distal part fusing with anterior branches of R; anterior branches of R with 2–4 bifurcations, posterior branches reaching the outer margin; the base of M distinct with 2–4 bifurcations; CuA slender with a few branches; V indistinct (Fig. 2J). Wings with ScP slender, the distal part of RA indistinct, RP slightly strong and distinct; M with 2–3 bifurcations at the end; CuA strong; V distinct (Fig. 2K). Legs (Fig. 2E–I) slender. Front femur type A₂ (Fig. 2E). Hind metatarsus longer than the remaining segments combined (Fig. 2H). Pulvilli and arolia reduced; claws symmetrical (Fig. 2I). **Abdomen.** First tergite unspecialized. Supra-anal plate transversely broad, the lateral margins curved, and the hind margin slightly concave in the middle; the distal part less sclerotized and hyaline (Fig. 2L). Paraprocts (pp.) long strip-shaped and symmetrical. Cerci long, apically tapering. Subgenital plate nearly square, the hind margin slightly convex (Fig. 2M). Styli long, slender. **Genitalia** (Fig. 2N, O). L1 weakly sclerotized with pubescence. L4C with microspines on the lateral margin; the distal part expanded, hind margin nearly truncated. L2 curved and extended to left, the caudal part with a long spine toward right. L4D small (Fig. 2O). L4E flat. L3 unciform and well sclerotized; the base wide, downwardly tapering; the distal part bifurcated, hlap weakly developed. L4G elliptical with the basal part constricted. R1H flaky, with two long spines at the apex. The basal part of R1G broad, the distal with a long and curved narrow process toward right. R1F irregular and its outer margin thickened. R2 with a ridge-like projection in dorsal view. R3 located at the upper right, triangular and weakly sclerotized.

Female (Fig. 3). Head and thorax. Interocular space wider than interantennal space (Fig. 3B). Pronotum campaniform; anterior margin straight and hind margin convex, the widest point after the middle (Fig. 3A). Tegmina square, reduced and not reaching the first tergite of abdomen; lateral margins of tegmina truncated, forming nearly right angle with the anterior margin; R parallel to the anterior margin (Fig. 3I). Hind wings small lobe-like (Fig. 3J). **Abdomen** (Fig. 3K, L). Hind margin of tergum X (TX) with median invagination, and with a membranous line inside. Paraprocts (pp.) wide, nearly triangular. Subgenital plate divided; median with intersternal fold (inst.f.). **Genitalia** (Fig. 3K, L). First valve (v.I) sclerotized with dense punctures; the distal part hyaline, and the base fused with first valvifer (vlf.I). First valvifer short, parallel to paratergites (pt.) and laterosternite IX (ltst.IX). Paratergites slender and laterosternite IX irregular. Valvifer II (p.I.) annular. Second valve (v.II) small and flaky, the base fused, connecting with third valve (v.III) by membrane. Third valve (v.III) large and less sclerotized. Anterior arch (a.a.) wide and its central part with two symmetrical foot-shaped projections, surface with microtrichia. Spermathecal plate (sp.pl) well sclerotized and nearly crescent-shaped. Spermathecal opening (sp.o.) located at anterior margin of spermathecal plate. Spermatheca (sp.) divided into two branches, one branch with the distal part enlarged. Basivalvulae (bsv.) subelliptical with punctures. Postero-lateral angle of laterosternal shelf (ltst.sh.) extended towards outer margin. Vestibular sclerite (vst.s.) strip-shaped.

Nymph. Early instars are yellowish brown with ocelli and eyes small; in older nymphs, the body turns brown or reddish brown (Fig. 3E–H).

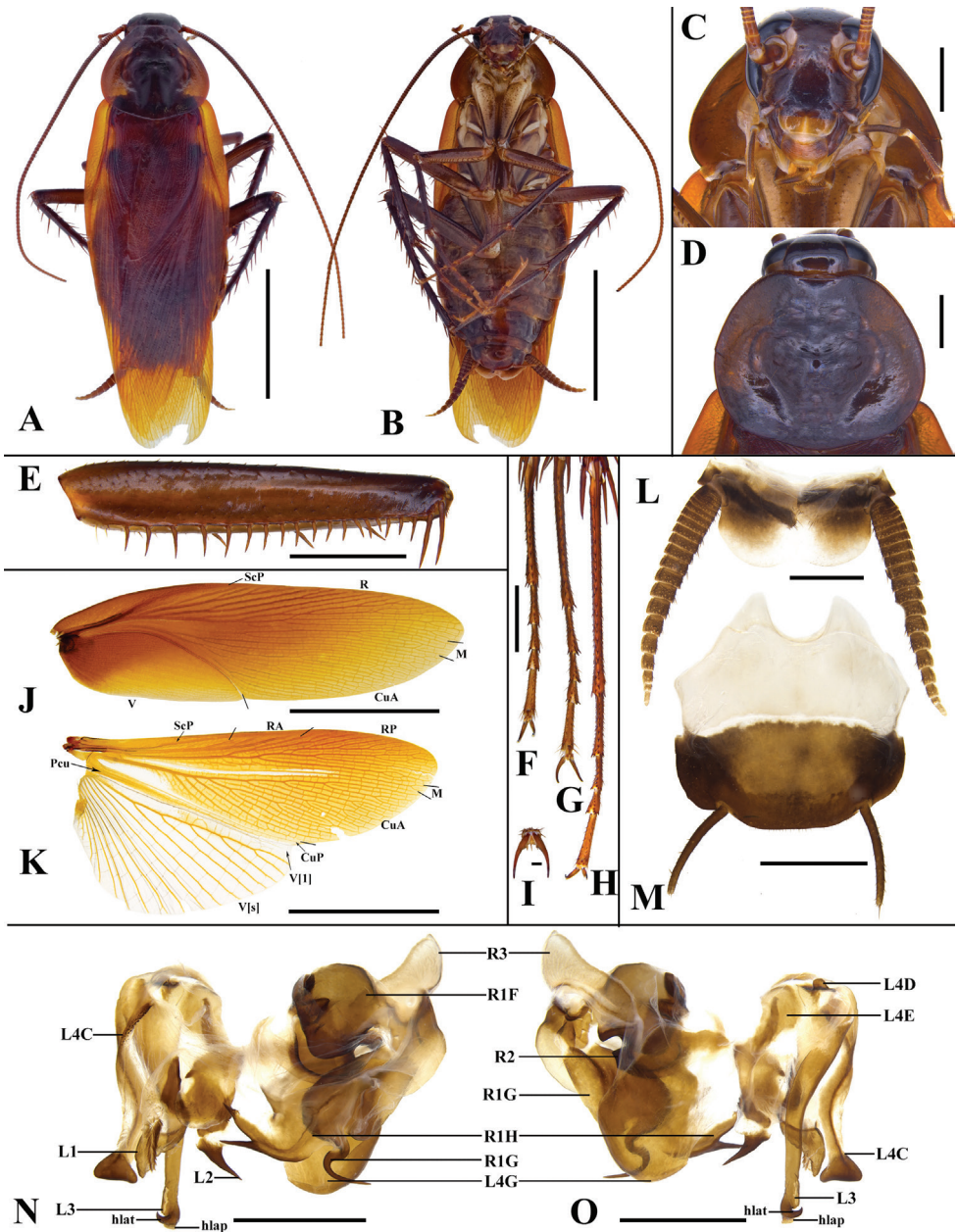


Figure 2. Male of *Periplaneta arabica* (Bey-Bienko, 1938) **A** habitus, dorsal view **B** habitus, ventral view **C** head **D** pronotum **E** front femur **F–H** tarsi (front, middle, hind) **I** arolium of hind leg **J** tegmen **K** hind wing **L** supra-anal plate **M** subgenital plate **N** phallomere, dorsal view **O** phallomere, ventral view. Scale bars: 10.0 mm (**A**, **B**, **J**, **K**); 2.0 mm (**C**, **D**, **E**, **F**, **G**, **H**, **L**, **M**, **N**, **O**); 0.5 mm (**I**).

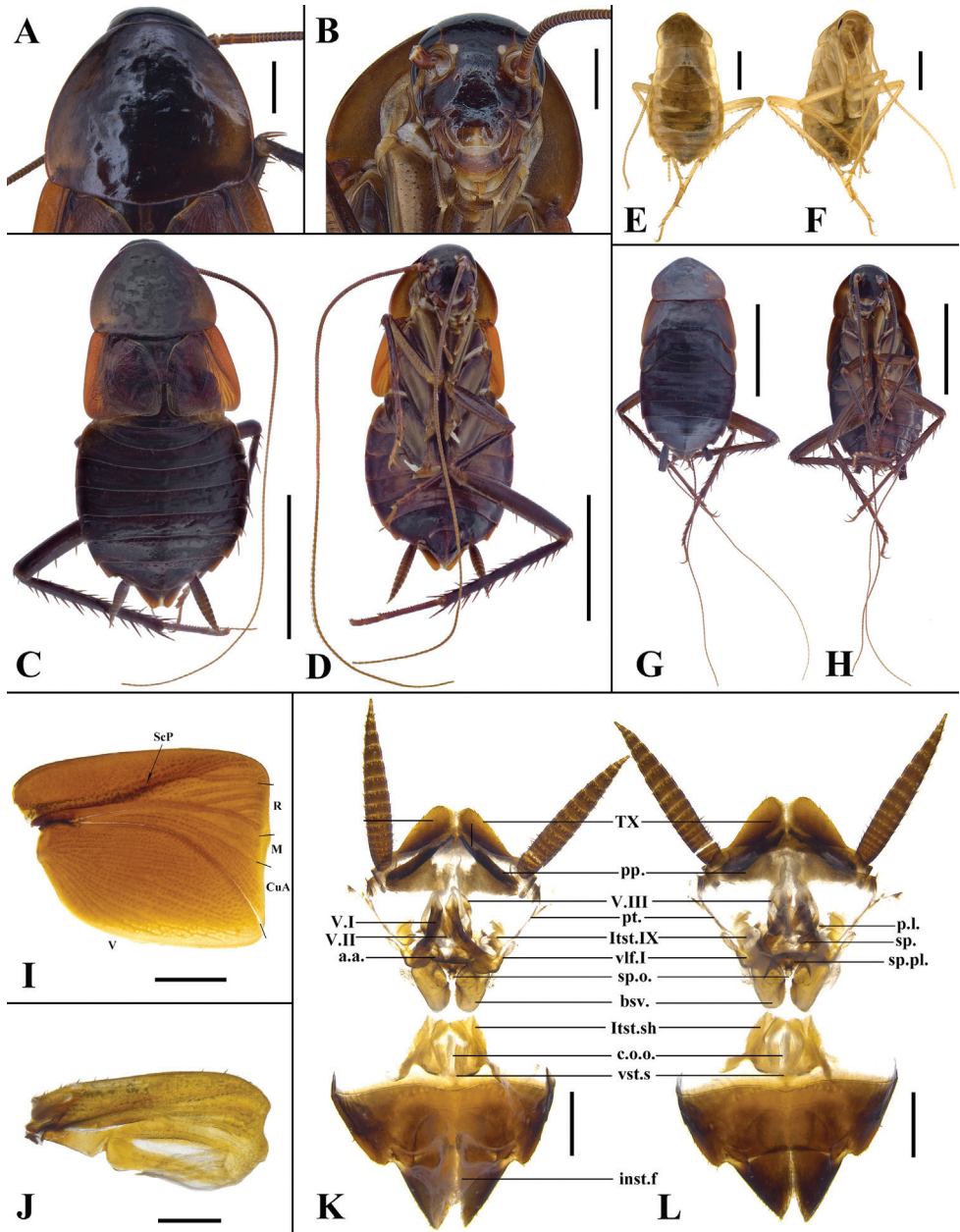


Figure 3. Female and nymph of *Periplaneta arabica* (Bey-Bienko, 1938) **A–D, I–L** female **A** pronotum **B** head **C** habitus, dorsal view **D** habitus, ventral view **I** tegmen **J** hind wing **K** genitalia, dorsal view **L** genitalia, ventral view **E–H** habitus of nymph, dorsal and ventral views. Scale bars: 10.0 mm (**C, D, G, H**); 2.0 mm (**A, B, E, F, I, K, L**); 1 mm (**J**).

Distribution. Saudi Arabia (Mecca); Yemen; United Arab Emirates; Oman; Iran (Ilam Province; new country record).

Remarks. Bey-Bienko (1938) first documented and described this species based on a female specimen from Mecca, Saudi Arabia. Bohn (2007) provided some morphological characteristics of the male in the key to genera and species occurring in the United Arab Emirates. After checking the original description by Bey-Bienko (1938) and Bohn (2007) and the images of the type specimens, we consider *P. arabica* to be characterized by: 1) interocular space slightly wider than the interocellar space in female; 2) pronotum anterior margin straight and hind margin convex in female; 3) tegmina nearly square in female; 4) hind margin slightly concave in the middle to form an obtuse angle in supra-anal plate of male; these characteristics are present in our specimens as well. Therefore, we concluded that our material collected from western Iran should belong to *P. arabica*. Matching of individuals of different sexes and life stages was possible with DNA barcoding.

Comparative morphology of *P. americana*, *P. arabica* and *P. lateralis*

A detailed morphological comparison of *P. americana*, *P. arabica* and *P. lateralis* was performed in this study. The following intraspecific variations were found in all three species: 1) the number of veins branches of wings; 2) the marks on disc of pronotum in male and female of *P. americana*; and 3) the color of the pronotum and abdominal tergite of female of *P. lateralis*.

External morphological characters

The external morphological characteristics of *P. americana*, *P. arabica* and *P. lateralis* (Fig. 4) are compared in Table 2. Males of the three species have similar shapes of pronotum, wings, and supra-anal and subgenital plates, and lack tergite gland. Interocular space and interantennal space of females were both wider than the single eye spacing. The main differences among these three species are as follows: body size (i.e., *P. americana* > *P. arabica* > *P. lateralis*), tegmina and wings of females, and the presence or absence of arolia and pulvilli.

Genitalia of male and female

As depicted in Fig. 5, the genitalia of *P. americana*, *P. arabica* and *P. lateralis* are highly similar in appearance but differ in the degree of development of the sclerites. In males (see *P. arabica* for detailed description), the results ranked in descending order are as follows: *P. lateralis* > *P. arabica* > *P. americana* for the pubescence density in L1, *P. arabica* > *P. americana* > *P. lateralis* for the sclerotization degree of spine in L2, and *P. arabica* > *P. lateralis* > *P. americana* for the development degree of the hlap in L3. In addition, there are certain differences in other aspects, for example, the basal margin of L4C in *P. americana* and *P. arabica* bears a row of microspines that is absent in *P. lateralis*, and a row of serration at the margin of R1H is present in *P. americana*

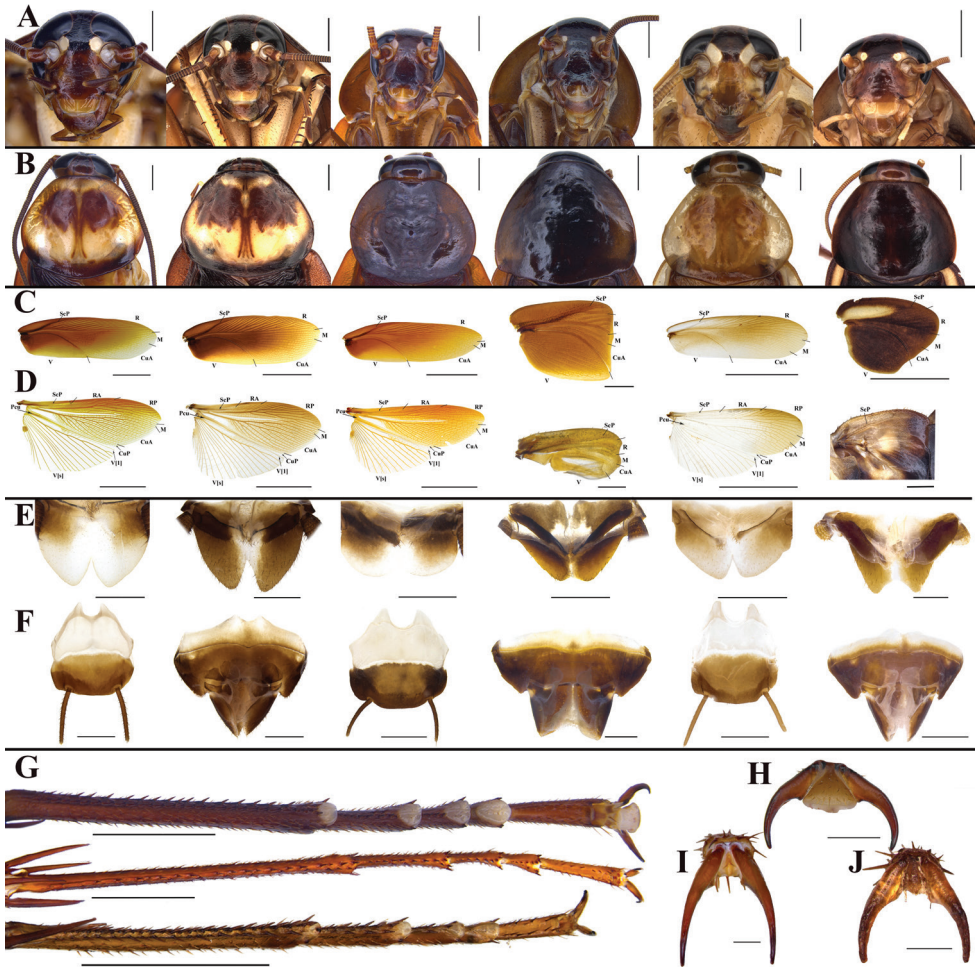


Figure 4. A–F In order from left to right, male of *P. americana*, female of *P. americana*, male of *P. arabica*, female of *P. arabica*, male of *P. lateralis*, female of *P. lateralis* **A** heads **B** pronota **C** tegmina **D** hind wings **E** supra-anal plates **F** subgenital plates **G** hind tarsi (in order from top to bottom: *P. americana*, *P. arabica*, *P. lateralis*) **H–J** arolia of hind legs (in order: *P. americana*, *P. arabica*, *P. lateralis*). Scale bars: 10.0 mm (**C, D** *P. americana*, males of *P. arabica* and *P. lateralis*); 2.0 mm (**A, B, E–G**, and females of *P. arabica* and *P. lateralis* in **C**); 1.0 mm (**D** females of *P. arabica* and *P. lateralis*); 0.5 mm (**H–J**).

but absent in *P. arabica* and *P. lateralis*. In females (see *P. arabica* for detailed description), the degree of development of some sclerites (i.e., valvifer II, laterosternite IX, basalvalvulae and laterosternal shelf) is ranked as *P. americana* > *P. arabica* > *P. lateralis*. *Periplaneta americana* differs from *P. lateralis* and *P. arabica* in the following characters: hind margin of basalvalvulae (bsv.) with two symmetrical protrusions in the former, which is lacking in the latter two; furthermore, the enlargement of spermathecae (sp.) in *P. americana* is longer and curved (the degree of curvature varies among samples), but usually irregular in *P. arabica* and subelliptical in *P. lateralis*.

Table 2. Comparison of external morphological characters of males and females of three species of *Periplaneta* s.s. Dimensions are in mm: mean±SEM (standard error of the mean). Abbreviations: Interocular space (IS); ocelli distance (OD); antennal sockets distance (ASD).

Species	<i>P. americana</i>		<i>P. arabica</i>		<i>P. lateralis</i>	
	male	female	male	female	male	female
Measured specimens (N)	23	15	6	2	17	13
Body length include tegmen (mm)	37.239±0.5960	33.327±0.3514	32.917±0.8388	–	24.206±0.2286	–
Body length	31.539±0.7966	30.113±0.6298	26.025±0.6537	24.500±1.0000	19.806±0.2397	20.715±0.3665
Distance comparison of IS, OD and ASD	IS ≤ OD < ASD	OD ≤ IS < ASD	OD < IS ≤ ASD	OD < ASD < IS	OD < IS < ASD	OD < IS ≤ ASD
Ocelli size	Medium	Medium	Medium	Small	Large	Medium
Pronotum shape	Subelliptical	Subelliptical	Subelliptical	Campaniform	Subelliptical	Campaniform
Tegmina	Well developed	Well developed	Well developed	Reduced and nearly square	Well developed	Reduced and nearly triangular
Hind wings	Well developed	Well developed	Well developed	Reduced and small lobed	Well developed	Reduced and fused to metanotum
Legs	Slightly slender	Slightly slender	Slender	Slender	Slightly slender	Slightly slender
Front femora	Type A2	Type A2	Type A2	Type A2	Type A2	Type A2
Pulvilli	Present	Present	Absent	Absent	Present	Present
Arolia	Medium	Medium	Absent	Absent	Minute	Minute
First tergite of abdomen	No tergite gland	–	No tergite gland	–	No tergite gland	–
Supra-anal plate's shape	Hind margin extending outward and concave in the middle to form a sharp angle	Middle of hind margin deeply concave, forming one acute angle	Middle of hind margin concave and not extending	Hind margin not extending outward and slightly concave in the middle to form an obtuse angle	Hind margin extending outward and slightly concave in the middle to form an acute angle	Middle of hind margin forming an obtuse angle
Supra-anal plate's sclerotization degree	The distal part less sclerotized and hyaline	Less sclerotized in the middle	The distal part less sclerotized and hyaline	Less sclerotized in the middle	The distal part less sclerotized and hyaline	Less sclerotized in the middle
Subgenital plate's shape	Hind margin slightly convex	–	Hind margin slightly convex	–	Hind margin slightly convex	–

Discussion

In recent years, molecular phylogenetic analyses have shown that *P. americana* has phylogenetic affinity with *P. lateralis* (Legendre et al. 2015; Bourguignon et al. 2018; Arab et al. 2020; Liao et al. 2021; Djernæs and Murienne 2022; Li et al. 2022; Deng et al. 2023), whereas *P. australasiae*+*P. fuliginosa*+*P. brunnea* would be the sister group to *Homalosilpha* (Liao et al. 2021; Djernæs and Murienne 2022; Deng et al. 2023). Deng et al. (2023) also included *P. japonica* and *P. karnyi*, neither of which clustered with *P. americana*. This inevitably raised doubts about the characteristics used in the past to distinguish *Periplaneta* and *Shelfordella*. Until recently, the development of tegmina and wings, pulvilli and arolia were usually considered the main diagnostic characters between these two genera (Adelung 1910; Bey-Bienko 1938; Bohn 1985). But, based on the phylogenetic results and some genital characteristics, Deng et al. (2023) considered *Shelfordella* as a synonym of *Periplaneta*. Considering the results of the current study, we also confirmed that *P. americana* differs significantly from *P. arabica* and *P. lateralis*

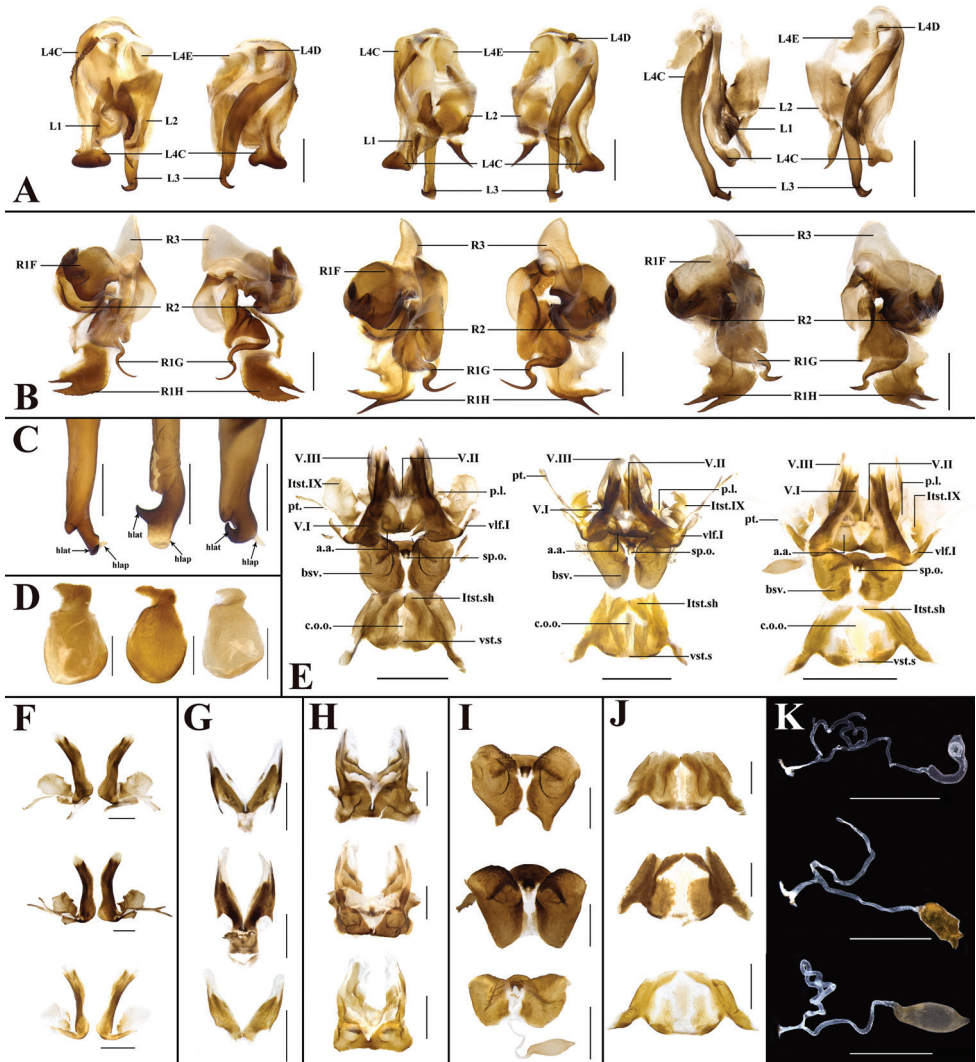


Figure 5. In order from left to right and top to bottom: *P. americana*, *P. arabica*, *P. lateralis* **A** left phallosome, dorsal and ventral views **B** right phallosome, dorsal view **C** L3 **D** L4G **E** overall female genitalia **F** first valve (v.I), first valvifer (vlf.I) and laterosternite IX (Istst.IX) **G** second valve (v.II) **H** third valve (v.III) and anterior arch (a.a.) **I** basalvalvulae (bsv.) and spermathecal opening (sp.o.) **J** laterosternal shelf (Istst.sh.) **K** spermathecae (sp.). Scale bars: 2.0 mm (**E**); 1.0 mm (**A**, **B**, **D**, **F**, **G**, **H**, **I**, **J**, **K**); 0.5 mm (**C**).

in these characteristics. Our DNA-based analyses provided favorable evidence in the matching of females and males in all three species, as well as the pairing of adults and nymphs in *P. arabica*. Therefore, we had the possibility to compare males of these species and found that genitalia of both sexes of these three species were extremely similar, with differences in the developmental degree of sclerites. After a comparative morphological study on the genitalia of Blaberidae, Roth (1970, 1972, 1973) concluded that genital



Figure 6. Male of *P. arabica* from a cave in Ilam, Iran. Photographed by Alireza Zamani.

characters could be used as diagnostic characters for tribes, genera and groups. Until now, no such detailed genital comparison has been done in Blattidae, and our study might be helpful to solve the polyphyly of *Periplaneta* (Djernæs and Murienne 2022; Deng et al. 2023). In addition, considering the close relationship of *P. americana* and *P. lateralis* and the fact that both *P. arabica* and *P. lateralis* originated from West Asia (Beccaloni 2014), we speculate that *P. americana* might have originated in this region as well, and later dispersed naturally or was introduced by humans to other parts of the world, before gradually becoming a notorious indoor pest.

Before the extensive usage of molecular data in cockroach systematics, most genera of Blattinae were established mainly on the basis of external morphological characters. As a matter of fact, the wings, pulvilli and arolia of cockroaches are heavily influenced by the environment and lifestyle (Arnold 1974; Bell et al. 2007). In deserts, a cave-dwelling lifestyle is a survival strategy for cockroaches (Roth and Willis 1960). Material of *P. arabica* reported in this study were sampled from a natural cave in western Iran (Fig. 6), which has a subtropical desert climate (Burstyn et al. 2019). Morphologically, slender antennae and legs, absent pulvilli and arolia, lighter body and very small ocelli of early instars are consistent with the convergent evolution of cave-dwelling species (Bell et al. 2007; Lucañas and Lit 2016). In contrast, *P. americana* has well-developed tegmina and wings, and developed pulvilli and arolia in both sexes, which could be favorable to facilitate its dispersal and climbing ability (Clemente and Federle 2008), and also beneficial for this species to

colonize other environments (e.g., human settlements, tree trunks in the wild, landfills, and shallow caves with abundant guano; Lucañas et al. 2022) in search for food. Therefore, influenced by their environment and lifestyle, these three species have maintained a high similarity in genitalia, but greatly diverged in external morphology.

Acknowledgements

We are deeply thankful to Amir Hossein Aghaei for collecting the specimens of *P. arabica*. We are especially grateful to Wenbo Deng and Yishu Wang for their professional suggestions. We also sincerely thank Dr. Frédéric Legendre, Dr. Leonid Anisyutkin, and two anonymous reviewers for their valuable suggestions on our manuscript. This study was funded by the National Natural Science Foundation of China (No. 32170458, 31872506, 31772506).

References

- Adelung Nv (1910) Ueber einige bemerkenswerte Orthopteren aus dem palacarktischen Asien. *Horae Societatis Entomologicae Rossicae* 39: 328–358.
- Arab DA, Bourguignon T, Wang ZQ, Ho SYW, Lo N (2020) Evolutionary rates are correlated between cockroach symbionts and mitochondrial genomes. *Biology Letters* 16(1): 20190702. <https://doi.org/10.1098/rsbl.2019.0702>
- Arnold JW (1974) Adaptive features on the tarsi of cockroaches (Insecta: Dictyoptera). *International Journal of Insect Morphology & Embryology* 3(3–4): 317–334. [https://doi.org/10.1016/0020-7322\(74\)90026-9](https://doi.org/10.1016/0020-7322(74)90026-9)
- Asahina S (1980) Taxonomic notes on non-domiciliary *Periplaneta* species from the Ryukyus, Taiwan, Hong Kong and Thailand. *Japanese Journal of Sanitary Zoology* 31(2): 103–115. <https://doi.org/10.7601/mez.31.103>
- Beccaloni GW (2014) Cockroach Species File Online. Version 5.0/5.0. World Wide Web electronic publication. <http://Cockroach.SpeciesFile.org> [accessed 20 May 2022]
- Bell WJ, Roth LM, Nalepa CA (2007) *Cockroaches: ecology, behavior, and natural history*. JHU Press, 247 pp.
- Bey-Bienko GY (1938) On some new or interesting Asiatic Blattodea. *Annals & Magazine of Natural History* 11(2): 230–238. <https://doi.org/10.1080/00222933808526759>
- Bey-Bienko GY (1950) Fauna of the USSR. Insects: Blattodea. Institute of Zoology. Academy of Sciences of the URSS Moscow 40: 116. [ns]
- Bohn H (1985) *Blatta furcata* (Karny), the nearest relative of the Oriental cockroach (*Blatta orientalis* L.) (Insecta: Blattodea: Blattidae). *Israel Journal of Zoology* 33: 39–50.
- Bohn H (2007) Order Blattoptera. *Arthropod fauna of the UAE* 1: 84–103.
- Bourguignon T, Tang Q, Ho SYW, Juna F, Wang ZQ, Arab DA, Cameron SL, Walker J, Rentz D, Evans TA, Lo N (2018) Transoceanic dispersal and plate tectonics shaped global cockroach distributions: Evidence from mitochondrial phylogenomics. *Molecular Biology and Evolution* 35(4): 970–983. <https://doi.org/10.1093/molbev/msy013>

- Burmeister H (1838) Handbuch der Entomologie. Reimer II(2): 397–756.
- Burstyn Y, Martrat B, Lopez JF, Iriarte E, Jacobson MJ, Lone MA, Deininger M (2019) Speleothems from the Middle East: An example of water limited environments in the SISAL Database. *Quaternary* 2(2): 16. <https://doi.org/10.3390/quat2020016>
- Che YL, Gui SH, Lo N, Ritchie A, Wang ZQ (2017) Species delimitation and phylogenetic relationships in ectobiid cockroaches (Dictyoptera, Blattodea) from China. *PLoS ONE* 12(1): e0169006. <https://doi.org/10.1371/journal.pone.0169006>
- Clemente CJ, Federle W (2008) Pushing versus pulling: Division of labour between tarsal attachment pads in cockroaches. *Proceedings of the Royal Society B, Biological Sciences* 275(1640): 1329–1336. <https://doi.org/10.1098/rspb.2007.1660>
- Deng WB, Luo XX, Liao SR, Wang ZQ, Che YL (2023) Inclusion of rare taxa from Blattidae and Anaplectidae improves phylogenetic resolution in the cockroach superfamily Blattodea. *Systematic Entomology* 48(1): 23–39. <https://doi.org/10.1111/syen.12560>
- Djernæs M, Muriene J (2022) Phylogeny of Blattoidea (Dictyoptera: Blattodea) with a revised classification of Blattidae. *Arthropod Systematics & Phylogeny* 80: 209–228. <https://doi.org/10.3897/asp.80.e75819>
- Evangelista D, Buss L, Ware JL (2013) Using DNA barcodes to confirm the presence of a new invasive cockroach pest in New York City. *Journal of Economic Entomology* 106(6): 2275–2279. <https://doi.org/10.1603/EC13402>
- Katoh K, Rozewicki J, Yamada KD (2019) MAFFT online service: Multiple sequence alignment, interactive sequence choice and visualization. *Briefings in Bioinformatics* 4(20): 1160–1166. <https://doi.org/10.1093/bib/bbx108>
- Kimura M (1980) A simple method for estimating evolutionary rates of base substitutions through comparative studies of nucleotide sequences. *Journal of Molecular Evolution* 16(2): 111–120. <https://doi.org/10.1007/BF01731581>
- Klass KD (1997) The external male genitalia and the phylogeny of Blattaria and Mantodea. *Bonner Zoologische Monographien* 42: 1–341.
- Kumar NP, Rajavel AR, Natarajan R, Jambulingam P (2007) DNA barcodes can distinguish species of Indian mosquitoes (Diptera: Culicidae). *Journal of Medical Entomology* 44(1): 1–7. <https://doi.org/10.1093/jmedent/41.5.01>
- Lanfear R, Frandsen PB, Wright AM, Senfeld T, Calcott B (2017) PartitionFinder 2: New methods for selecting partitioned models of evolution for molecular and morphological phylogenetic analyses. *Molecular Biology and Evolution* 34: 772–773. <https://doi.org/10.1093/molbev/msw260>
- Legendre F, Nel A, Svenson GJ, Robillard T, Pellens R, Grandcolas P (2015) Phylogeny of Dictyoptera: Dating the origin of cockroaches, praying mantises and termites with molecular data and controlled fossil evidence. *PLoS ONE* 10(7): e0130127. <https://doi.org/10.1371/journal.pone.0130127>
- Li WJ, Wang ZQ, Che YL (2017) The complete mitogenome of the wood-feeding cockroach *Cryptocercus meridianus* (Blattodea: Cryptocercidae) and its phylogenetic relationship among cockroach families. *International Journal of Molecular Sciences* 18(11): 2397. <https://doi.org/10.3390/ijms18112397>

- Li XR, Zheng YH, Wang CC, Wang ZQ (2018) Old method not old-fashioned: Parallelism between wing venation and wing-pad tracheation of cockroaches and a revision of terminology. *Zoomorphology* 137(4): 519–533. <https://doi.org/10.1007/s00435-018-0419-6>
- Li Y, Luo XX, Zhang JW, Wang ZQ, Che YL (2022) A new species of *Bundoksia* Lucañas, 2021 with comments on its subfamilial placement, based on morphological and molecular data. *ZooKeys* 1085: 145–163. <https://doi.org/10.3897/zookeys.1085.72927>
- Liao SR, Wang YS, Jin DT, Chen R, Wang ZQ, Che YL (2021) Exploring the relationship of *Homalosilpha* and *Mimosilpha* (Blattodea, Blattidae, Blattinae) from a morphological and molecular perspective, including a description of four new species. *PeerJ* 9: e10618. <https://doi.org/10.7717/peerj.10618>
- Linnaeus C (1758) *Systema naturæ* 1, Editio Decima. Sweden: Holmiæ, 1–824.
- Lucañas CC, Lit Jr IL (2016) Cockroaches (Insecta, Blattodea) from caves of Polillo Island (Philippines), with description of a new species. *Subterranean Biology* 19: 51–64. <https://doi.org/10.3897/subtbiol.19.9804>
- Lucañas CC, Lit Jr IL, Quibod MNRM, Bicaldo PRD, Laroná AR (2022) Cockroaches from caves in Samal Island, Philippines, with notes on the invasive *Periplaneta americana* (L.) (Blattodea: Blattidae). *Philippine Entomologist* 36(1): 15–24.
- Ma JN, Liu JH, Shen YM, Fan ZX, Yue BS, Zhang XY (2019) Population genetic structure and intraspecific genetic distance of *Periplaneta americana* (Blattodea: Blattidae) based on mitochondrial and nuclear DNA markers. *Ecology and Evolution* 9(22): 12928–12939. <https://doi.org/10.1002/ece3.5777>
- McKittrick FA (1964) Evolutionary studies of cockroaches. Cornell University Agricultural Experiment Station 389: 1–197.
- Nguyen LT, Schmidt HA, von Haeseler A, Minh BQ (2015) IQ-TREE: A fast and effective stochastic algorithm for estimating maximum-likelihood phylogenies. *Molecular Biology and Evolution* 32(1): 268–274. <https://doi.org/10.1093/molbev/msu300>
- Princis K (1954) Wo ist die Urheimat von *Blatta orientalis* L. zu suchen? *Opuscula Entomologica* 19: 202–204.
- Princis K (1966) Blattariae: Suborbo Blattoidea Fam.: Blattidae, Nocticolidae. *Orthopterorum Catalogus* 8: 404–509.
- Pringle RM, Kartzinel TR, Palmer TM, Thurman TJ, Fox-Dobbs K, Xu CCY, Hutchinson MC, Coverdale TC, Daskin JH, Evangelista DA, Gotanda KM, A. Man in 't Veld N, Wegener JE, Kolbe JJ, Schoener TW, Spiller DA, Losos JB, Barrett RDH (2019) Predator-induced collapse of niche structure and species coexistence. *Nature* 570: 58–64. <https://doi.org/10.1038/s41586-019-1264-6>
- Roth LM (1970) The male genitalia of Blattaria. 2. *Poeciloderrhis* spp. (Blaberidae: Epilamprinae). *Psyche* 77(1): 104–119. <https://doi.org/10.1155/1970/37214>
- Roth LM (1972) The male genitalia of Blattaria. 9. Blaberidae, *Gyna* spp. (Perisphaeriinae) *Phoraspis*, *Thorax*, and *Phlebonotus* (Epilamprinae). *Transactions of the American Entomological Society* 98: 185–217.
- Roth LM (1973) The male genitalia of Blattaria. 11. Perisphaeriinae. *Psyche* 80: 305–348. <https://doi.org/10.1155/1973/48938>

- Roth LM (1999) Descriptions of new taxa, redescriptions, and records of cockroaches, mostly from Malaysia and Indonesia (Dictyoptera: Blattaria). *Oriental Insects* 33(1): 168. <https://doi.org/10.1080/00305316.1999.10433789>
- Roth LM (2003) Systematics and phylogeny of cockroaches (Dictyoptera: Blattaria). *Oriental Insects* 37(1): 1–186. <https://doi.org/10.1080/00305316.2003.10417344>
- Roth LM, Willis ER (1960) The biotic associations of cockroaches. *Smithsonian Miscellaneous Collections* 141: 1–440. <https://doi.org/10.1002/jps.2600500438>
- Saussure (1864) Mémoires pour servir a l’Histoire Naturelle du Mexique des Antilles et des Etats-Unis. Orthoptères de l’Amérique Moyenne 18(3–4): 71.
- Shelford R (1909) Transactions of the entomological society of London. Royal Entomological Society of London, 309 pp.
- Shelford R (1910) Orthoptera fam. Blattidae subfam. Blattinae (= Periplanetinae). In: Wytzman P (Ed.) *Genera Insectorum. Belgique*, 17 pp.
- Walker F (1868) Catalogue of the specimens of Blattarie in the collection of the British Museum. Printed for the Trustees of the British Museum, 1–239. <https://doi.org/10.5962/bhl.title.8495>
- Walker (1871) Catalogue of the specimens of Dermaptera Saltatoria in the collection of the British Museum. Part V. Supplement to the catalogue of Blattariae. Printed for the Trustees of the British Museum, 1–43.
- Wang YS, Chen R, Jin DT, Che YL, Wang ZQ (2021) New record of *Cyrtototula* Uvarov, 1939 (Blaberidae, Epilamprinae) from China, with three new species based on morphological and COI data. *ZooKeys* 1021: 127–143. <https://doi.org/10.3897/zookeys.1021.59526>
- Yang R, Wang ZQ, Zhou YH, Wang ZQ, Che YL (2019) Establishment of six new *Rhabdoblattea* species (Blattodea, Blaberidae, Epilamprinae) from China. *ZooKeys* 851: 27–69. <https://doi.org/10.3897/zookeys.851.31403>
- Ye F, Lan XE, Zhu WB, You P (2016) Mitochondrial genomes of praying mantises (Dictyoptera, Mantodea): Rearrangement, duplication, and reassignment of tRNA genes. *Scientific Reports* 6(1): 25634. <https://doi.org/10.1038/srep25634>
- Zhu J, Zhang JW, Luo XX, Wang ZQ, Che YL (2022) Three cryptic *Anaplecta* (Blattodea, Blattoidea, Anaplectidae) species revealed by female genitalia, plus seven new species from China. *ZooKeys* 1080: 53–97. <https://doi.org/10.3897/zookeys.1080.74286>

Supplementary material I

Genetic divergence of distances calculated by K2P model method using cytochrome c oxidase subunit I (COI) gene sequences in MEGA

Authors: Xin-Xing Luo, Qian-Qian Li, Alireza Zamani, Yan-Li Che, Zong-Qing Wang
Data type: table (excel file)

Copyright notice: This dataset is made available under the Open Database License (<http://opendatacommons.org/licenses/odbl/1.0/>). The Open Database License (ODbL) is a license agreement intended to allow users to freely share, modify, and use this Dataset while maintaining this same freedom for others, provided that the original source and author(s) are credited.

Link: <https://doi.org/10.3897/zookeys.1146.90817.suppl1>

Supplementary material 2

Interspecific genetic divergence of distances calculated by K2P model method using cytochrome c oxidase subunit I (COI) gene sequences in MEGA

Authors: Xin-Xing Luo, Qian-Qian Li, Alireza Zamani, Yan-Li Che, Zong-Qing Wang

Data type: table (excel file)

Copyright notice: This dataset is made available under the Open Database License (<http://opendatacommons.org/licenses/odbl/1.0/>). The Open Database License (ODbL) is a license agreement intended to allow users to freely share, modify, and use this Dataset while maintaining this same freedom for others, provided that the original source and author(s) are credited.

Link: <https://doi.org/10.3897/zookeys.1146.90817.suppl2>

Identification and distribution of leafrollers (Lepidoptera, Tortricidae) associated with berries (Rosaceae) cultivated in Mexico

Isabel Ruiz-Galván¹, Néstor Bautista-Martínez¹, Lauro Soto-Rojas¹,
Samuel Pineda-Guillermo², Jesús Romero-Nápoles¹

1 *Colegio de Postgraduados Campus Montecillo, Instituto de Entomología y Acarología, km. 36.5 Carretera México-Texcoco, Montecillo, C.P. 56230, Texcoco, Estado de México* **2** *Instituto de Investigaciones Agropecuarias y Forestales, Universidad Michoacana de San Nicolás de Hidalgo, Morelia, Michoacán, Mexico*

Corresponding author: Néstor Bautista-Martínez (nestor@colpos.mx)

Academic editor: Christian Schmidt | Received 5 February 2022 | Accepted 6 January 2023 | Published 9 February 2023

<https://zoobank.org/3A0FF9F8-526A-43FC-9AC3-D29898CB885A>

Citation: Ruiz-Galván I, Bautista-Martínez N, Soto-Rojas L, Pineda-Guillermo S, Romero-Nápoles J (2023) Identification and distribution of leafrollers (Lepidoptera, Tortricidae) associated with berries (Rosaceae) cultivated in Mexico. ZooKeys 1146: 185–196. <https://doi.org/10.3897/zookeys.1146.81734>

Abstract

Berries are agricultural products of great economic interest for Mexico, and their production has increased in recent years; however, crops are affected by tortricid leafrollers. From August 2019 to April 2021 in Michoacán and Guanajuato, Mexico, a study was conducted to determine the species of tortricids associated with blackberries (*Rubus* spp. L.), raspberries (*Rubus idaeus* L.) and strawberries (*Fragaria* × *ananassa* Duch.), as well as their altitudinal distribution. In 12 orchards located in these states, shoots, leaves and flowers infested by larvae were collected. The species were identified by male genitalia and were determined taxonomically as *Amorbia cuneana* (Walsingham, 1879), *Argyrotaenia montezumae* (Walsingham, 1914) and *Platynota* sp. Walker, 1859, found at elevations from 1290 to 2372 m. The most abundant species were *A. cuneana* and *A. montezumae*. Generally, these tortricids prefer to feed on tender vegetative parts of the plant, but the economic impact they have is not known. It is worth mentioning that the number of species found is lower than those reported in other countries, but it is necessary to broaden the study area to other berry-producing regions to determine whether their distribution is wider.

Keywords

Altitude, blackberry, damage, genitalia, raspberry, strawberry, tortricids

Introduction

The small fruits (berries) of the family Rosaceae include blackberries (*Rubus* spp. L.), raspberries (*Rubus idaeus* L.) and strawberries (*Fragaria* × *ananassa* Duch.). The family is widely distributed although is better adapted to temperate climates (Rzedowski 2021). The Mexican states where production of these berries is concentrated are mainly Michoacán, Jalisco, Baja California, and Guanajuato (SIAP 2021). According to data from FAO-FAOSTAT (2021), Mexico is situated among the first five berry-producing countries of the world, and production has increased in the last 15 years. In 2020, Mexico exported more than US\$1989 million in berries (SIAVI 2021).

As in other crops, this group of berries is affected by pests that limit production. The family Tortricidae (microlepidoptera) is one of the most diverse of Lepidoptera. It is divided into three subfamilies, Tortricinae, Olethreutinae, and Chlidanotinae (Gilligan and Epstein 2014), that together include approximately 11,500 species and 1787 genera (Gilligan et al. 2018; Gilligan et al. 2020). The number of tortricid agricultural pests worldwide is estimated at 700 species (Gilligan and Epstein 2014), although there are undescribed species. The distribution of the family is cosmopolitan, although it is better adapted to temperate, subtropical, and tropical climates (Meijerman and Ulenberg 2000). In general, species of Tortricinae have a polyphagous habit, while most Olethreutinae are oligophagous. They feed on approximately 12,000 species, including vegetable, fruit, ornamental and forest crops (Hill 1987; Brown et al. 2008). Tortricids, are commonly known as leaf rollers because the larvae feed often on foliage, produce silk, and shelter in rolled leaves while they feed. They have also been found defoliating or boring into shoots, flowers and fruits of diverse plant species (Brown et al. 2008).

Some species of microlepidoptera are of major economic importance and may cause total production loss (Akbarzadeh 2012). Gilligan et al. (2020) argue that, of the total number of Lepidoptera introduced into North America, 23% to 30% are tortricids. The compilation by Brown et al. (2008) presents 97 species of tortricids associated with *Rubus* spp. and 52 species associated with *Fragaria* spp. worldwide. Among reported leaf roller hosts are species of Rosaceae, such as the genera *Rubus* and *Fragaria* sp. (McQuillan 1992; Brown et al. 2014, 2019) with records of their association in regions of Australia, Asia, Europe and North America (Brown et al. 2008).

Knowledge of diversity is fundamental in fauna research (Luis-Martínez et al. 2020), including determination of a species geographic distribution, its association with its hosts, and its ecological biogeography (Arita and Rodríguez 2001). Monteagudo-Sabaté et al. (2001) consider altitude to be one of the most important components in species determination. Sanders (2002) stated that greater species diversity occurs at low altitudes. In contrast, the studies of McCoy (1990) suggest that greater richness occurs at middle altitudes.

Despite the diversity of tortricids reported in berries in other regions of the world and the economic importance of berries, knowledge of the interaction of this group of insects and plants is scarce. Only López et al. (2014), Martínez et al. (2014), and Juárez-Gutiérrez et al. (2015) have reported *Argyrotaenia montezumae* (Walsingham, 1914) and *Amorbia cuneana* (Walsingham, 1879) in blackberries (*Rubus idaeus* L.),

while Tejeda-Reyes et al. (2020) reported *A. montezumae* in strawberries (*Fragaria × ananassa*). Worldwide, ecosystems are transforming at an accelerated pace, and for this reason, determining species in unexplored areas is a priority.

Therefore, the objective of this study was to identify the species of tortricids that feed on berries of Rosaceae along an altitudinal gradient from 1290 to 2337 m in Michoacán and Guanajuato, Mexico.

Material and methods

Sampling sites and collection of plant material

The study was conducted from August 2019 to April 2021 in Michoacán and Guanajuato, Mexico (Table 1). The commercial crops sampled were (*Rubus* spp.) varieties ‘Tupy’ and ‘brazos’, raspberry (*Rubus idaeus* L.) variety ‘Meerker’, and strawberry (*Fragaria × ananassa* Duch.) variety ‘Camino real’. The orchards were located at elevations from 1290 to 2337 m, with average annual temperature of 21 °C, and a warm temperate climate (García 1998). In each orchard, 1 ha of the crop was sampled in linear rows. Shoots and leaves with evidence of leafroller larvae were collected. Three to 12 plant parts were collected on each sampling date, depending on the abundance of larvae. The phenological phases of the crops were vegetative development, flowering, and fruit set.

Infested plant organs were cut into lengths of 10 to 15 cm. Each plant part was conditioned individually in a Num. 4 plastic cup (Reyma, Mexico) with water and sponge. A “plastic cage” constructed with two 1-L plastic cups joined at the edges was later introduced. The upper cup had organza fabric (Parisina, Mexico) on the bottom. Each sample was labeled with collection data. The collected material was transported to the Entomology Laboratory of the Colegio de Postgraduados, Campus Montecillo, Texcoco, State of Mexico, where they were kept at a temperature of 25±2 °C, 60 ± 20% relative humidity and photoperiod of 12:12 h (light/dark) until adult emergence.

Species identification

Adults were separated by sex and morphotypes, mounted and labeled. The specimens were identified by comparing male genitalia, with illustrations, literature, and taxonomic keys of Obratzsov (1961), Mackay (1962), Phillips-Rodríguez and Powell (2007), Razowski et al. (2008), Trematerra and Brown (2004), Brown (2013), Gilligan and Epstein (2014) and Gilligan et al. (2018). In addition, identification was corroborated by taxonomists specialized in Tortricidae, Dr John W. Brown (National Museum of Natural History, Washington D.C. USA) and Dr Jason Dombroskie (Insect collection of Cornell University, Ithaca, NY, USA). The genitalia were photographed with a Photomicroscope III Carl Zeiss (Carl Zeiss, Germany). Larva and adult specimens of the species found are located in the Entomological Collection of the Institute of Plant Health (CEAM), Colegio de Postgraduados, Campus Montecillo, Texcoco, State of Mexico, Mexico.

Results

We collected 255 plant parts with larvae; of these 85% were blackberry, 10% raspberry and 5% strawberry. We identified three species of tortricids: *Argyrotaenia montezumae* (Tortricinae: Archipini), and *Amorbia cuneana* and *Platynota* sp. (Tortricinae: Sparganothini). *Amorbia cuneana* was the most abundant species in the three crops, accounting for more than 60% of all the species found during the study period. The different species were distributed over all the altitudes studied, from 1290 to 2337 m. Nevertheless, we observed that *A. montezumae* preferred higher altitudes. Table 1 presents the number of emerged adults at each site and their host.

Table 1. Tortricids identified in blackberry, raspberry, and strawberry orchards in Guanajuato and Michoacán, Mexico. Number of emerged adults in parentheses.

State	Municipality	Crop	Altitude (m)	Coordinates	Species	Plant part attacked	Sampling date
Michoacán	Los Reyes	Blackberry	1290	19.5944, -102.4885	<i>Platynota</i> sp. (1♂)	Leaf bud	9-IX-2019 02-X-2019
					<i>Amorbia cuneana</i> (6♂, 5♀)	Leaf bud	15-X-2019
	Peribán	Blackberry	1372	19.5510, -102.4609	<i>Amorbia cuneana</i> (3♂)	Leaf bud	02-X-2019 16-X-2019
					<i>Argyrotaenia montezumae</i> (1♂)	Leaves	20-XI-2019
	Tangancícuaro	Blackberry	1702	19.8986, -102.1939	<i>Amorbia cuneana</i> (2♂)	Leaf bud	02-IX-2019 01-X-2019
					<i>Argyrotaenia montezumae</i> (2♂)	Leaves	15-X-2019 18-XI-2019
					<i>Amorbia cuneana</i> (3♂, 3♀)	Leaf bud	09-IX-2019 01-X-2019
					<i>Argyrotaenia montezumae</i> (2♂)	Leaves	15-X-2019 18-XI-2019
					<i>Argyrotaenia montezumae</i> (2♂)	Leaves	15-X-2019 18-XI-2019
	Maravatío	Raspberry	1707	19.8903, -102.1794	<i>Argyrotaenia montezumae</i> (2♂)	Leaf bud	15-X-2019 18-XI-2019
		Blackberry	2030	19.8911, -100.3578	-----*	Leaf bud	18-X-2019 22-XI-2019 04-XII-2019
	Villa Madero	Raspberry	2031	19.8920, -100.3564	<i>Amorbia cuneana</i> (1♂, 1♀)	Leaf bud	18-X-2019 22-XI-2019
					<i>Argyrotaenia montezumae</i> (1♀, 3♂)	Leaves	04-XII-2019
			1650	19.4160, -101.2307	<i>Argyrotaenia montezumae</i> (1♂)	Leaves	17-X-2019 22-XI-2019 02-XII-2019
					<i>Amorbia cuneana</i> (2♀, 2♂)	Leaf bud	17-X-2019 22-XI-2019
Guanajuato	Jaral del Progreso	Raspberry	1723	20.4199, -101.0595	<i>Argyrotaenia montezumae</i> (3♀, 2♂)	Leaves	02-XII-2019
					<i>Amorbia cuneana</i> (2♀)	Leaf bud	30 IX-2020
					<i>Argyrotaenia montezumae</i> (2♀)	Leaf bud	14-IV-2021
	Victoria de Cortázar	Raspberry	1729	20.3421, -101.0287	<i>Amorbia cuneana</i> (2♀, 3♂)	Leaf bud	30-IX-2020
					<i>Argyrotaenia montezumae</i> (2♀)	Leaf bud	14-IV-2021
	Jaral del Progreso	Strawberry	1724	20.3756, -101.0501	<i>Amorbia cuneana</i> (1♀)	Leaves	30-IX-2020
					<i>Argyrotaenia montezumae</i> (2♀, 1♂)	Leaves	14-IV-2021

*Collected larvae that did not complete development to adult stage.

Damage

The leafrollers *A. cuneana* and *A. montezumae* oviposit in flattened oval masses of more than 100 eggs on the face of the leaves and near the central vein. *Amorbia cuneana* covers the egg mass with a white secretion that extends beyond the mass (Fig. 1A), while *A. montezumae* oviposits the eggs superimposed and uncovered. When the eggs hatch, the larvae disperse, actively searching for a feeding site. Cannibalism among *A. cuneana* larvae is evident since they are found isolated on the same plant in the crop and it was observed in the field and laboratory (Espino-Herrera et al. 2012).

Larvae of both species feed on tender developing leaves (Fig. 1B). They join the lateral edges of the leaves with silk (Fig. 1C) and form a shelter of joined leaves where small perforations can be observed (Fig. 1D, E) or a leaf rolled into a “turnover” shape (Fig. 1F). Only one larva is found in each shelter where it feeds, protects itself and pupates.

Discussion

Brown et al. (2008) presents 97 species of tortricids that are associated with the genus *Rubus* spp. and 52 species with *Fragaria* spp. worldwide. Therefore, the three species found in blackberry, raspberry and strawberry at altitudes between 1290 and 2337 m constitute only 2% of the species richness of Tortricidae in these hosts in Mexico. These three species are only a small fraction of the 25 and 24 species of microlepidoptera reported on the American continent associated with *Rubus* and *Fragaria*, respectively (Hill 1987; Brown et al. 2008).

Records of *Amorbia* spp., *Argyrotaenia* spp. and *Platynota* spp. in crops are scarce in Mexico. Juárez-Gutiérrez et al. (2015) registered the presence of *A. cuneana* in blackberry (*Rubus* sp.) in Michoacán, while Urías-López and Salazar-García (2008) registered this same species in avocado (*Persea americana* Miller) in Nayarit. Rosas and Villegas (2008) reported that *Argyrotaenia* sp. feeds on avocado foliage and fruits in Nayarit and Michoacán. *Argyrotaenia montezumae* has also been reported in blackberries (López et al. 2014; Martínez et al. 2014; Barreto et al. 2016), in strawberries (Tejeda-Reyes et al. 2020), and hawthorn (*Crataegus mexicana* Moc. & Sessé ex DC.) (Tejeda-Reyes et al. 2021). Varela-Fuentes et al. (2009) identified *Platynota rostrana* Walker (1863) feeding on Valencia orange (*Citrus sinensis* L. Osbeck) and lemon (*Citrus limon* (Linnaeus) N.L. Burman) in Tamaulipas, while Bautista et al. (2014) argue that *Platynota* sp. feeds on *Opuntia* spp. in the state of Mexico.

Adult *Amorbia* are one of the largest tortricid moths in North America. They are generally distinguished by a diffuse pattern on their forewings (Powell and Brown 2012) and by the fenestra on the dorsal abdominal segments (Phillips-Rodríguez and Powell 2007): in segments 2 to 6 for *A. emigratella* and only one in segment 2 for *A. cuneana* (Gilligan and Epstein 2014). However, it is essential to look at more specific structures for their identification. The masculine genitalia of *A. cuneana* and *A. emigratella* are similar, but traits such as the less pronounced basal expansion of the

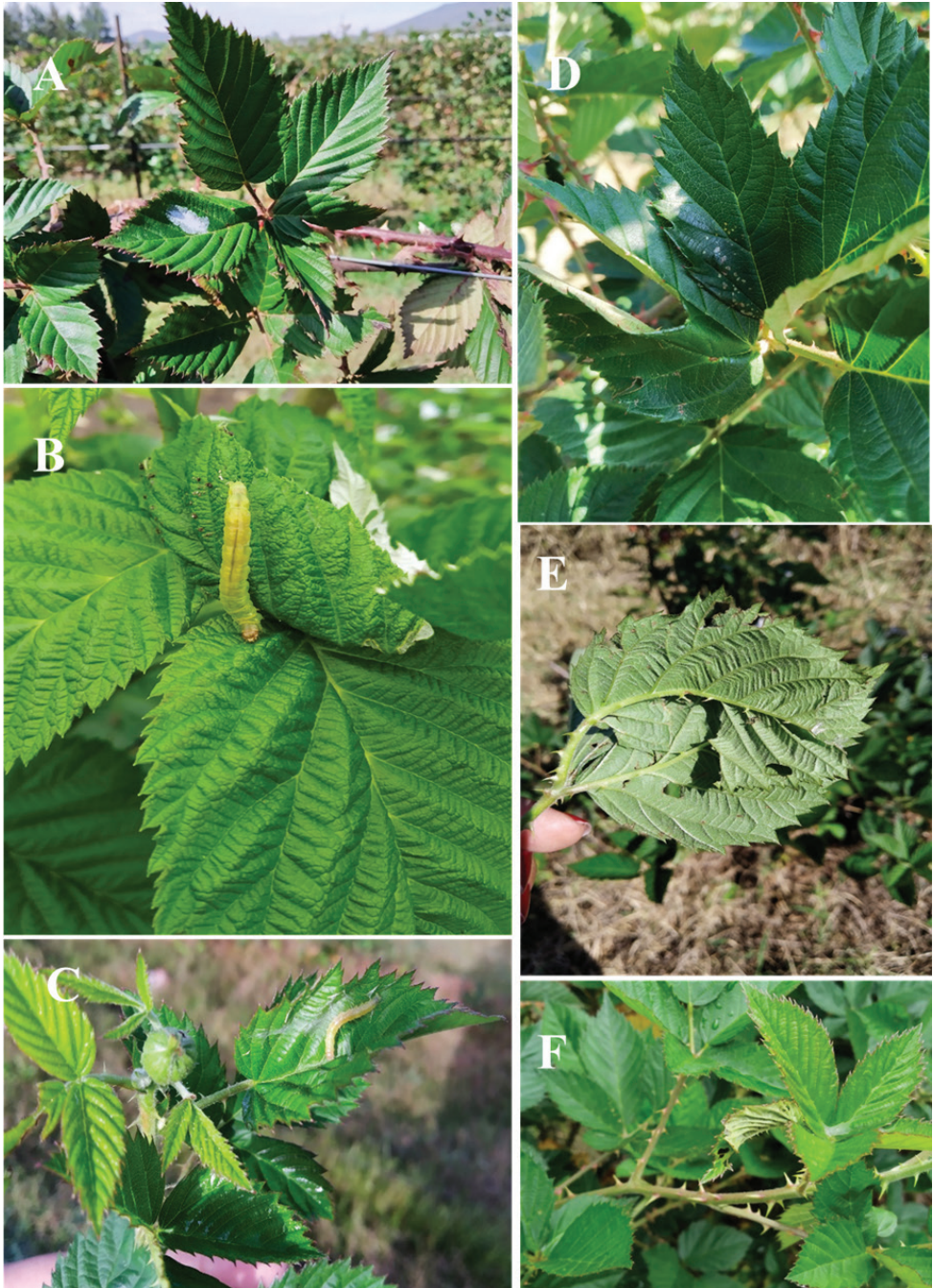


Figure 1. Damage caused by leafrollers in berries **A** *A. cuneana* egg mass in blackberry **B** *A. montezumae* in a raspberry shoot **C** silk produced by a larva on a leaf **D** and **E** folded leaves with a larva inside **F** leaf rolled toward the face.

uncus in *A. emigratella* and the slightly narrower distal half of the valva, and the different articulation of the base of the uncus with the dorsal of the tegumen in *A. cuneana* (Fig. 2B), are highly useful for separating these two species (Powell and Brown 2012).

In our study, *A. cuneana* was found feeding on raspberry and blackberry leaf buds and on strawberry leaves in 10 of the 12 sampled orchards at elevations of 1290 to 2337 m, coinciding with Juárez-Gutiérrez et al. (2015) who reported *A. cuneana* feeding on blackberry leaves and with Powell and Brown (2012) who report this genus at altitudes of 2500 m in California. The highest species richness of the *Amorbia* species is reported at elevations of 500–1500 m (Phillips-Rodríguez and Powell 2007). Gilligan and Epstein (2014) highlight that this tortricid has been registered feeding on 34 genera of plants belonging to 25 families, including *Rubus* spp. as economically important crops. Moreover, the compilation of Brown et al. (2008) reveals that *Fragaria* spp. has not been registered as a host to any species of *Amorbia*. This has been ratified by Powell and Brown (2012) and Gilligan and Epstein (2014). Therefore, this is the first report of association between strawberry (*F. × ananassa*) and *A. cuneana*, whose larvae were found rolling young strawberry leaves in Jaral del Progreso, Guanajuato. Nevertheless, several studies show that insects can adapt and incorporate new plants as food, although initially populations are low (Gassmann et al. 2006; Zhang et al. 2015; Messina et al. 2020). We suggest increasing the study area and sampling periodicity in strawberry-producing regions to study the association.

The genus *Argyrotaenia* Stephens includes around 116 species described worldwide (Powell 1983; Powell et al. 1995; Razowski 1996); of these, 115 species occupy habitats from Canada to Argentina (Obratzsov 1961; Brown 1999), the region of greatest species richness. Identification of *Argyrotaenia* is based mostly on external traits and genitalia. *Argyrotaenia montezumae* shows an aedeagus slightly capitated, cornuti with thick tips, and a dilated coecum penis curved slightly downward (Fig. 2C, D) (Obratzsov 1961). Our finding concerning *A. montezumae* coincides with López et al. (2014) who report this species in blackberry crops (*Rubus* sp.) at elevations of 1350 m in Zamora, Michoacán. We also ratify that *A. montezumae* feeds on strawberry leaves (*F. × ananassa*), as indicated by Tejeda-Reyes et al. (2020). In our study area, *A. montezumae* is present in 83% of the studied orchards found at altitudes of up to 2337 m in blackberry, raspberry and strawberry fields. Therefore, it is undoubtable that this species is found in berry-producing areas of Mexico.

Finally, the genus *Platynota* includes 33 polyphagous species described and distributed on the American continent (Powell and Brown 2012). In our study, from a rolled blackberry leaf with a larva inside, an adult *Platynota* sp. emerged (Fig. 2E, F), thus corroborating that the genus *Rubus* is host to *Platynota*, as indicated by Gilligan and Epstein (2014), although it is necessary to extend the study area. Because of the small number of emerged specimens, it is difficult to assert which species we are dealing with. For this reason, we report it at the genus level. It is important to underline that several species of the genus have not been described despite its abundance in Central America (Brown 2013).

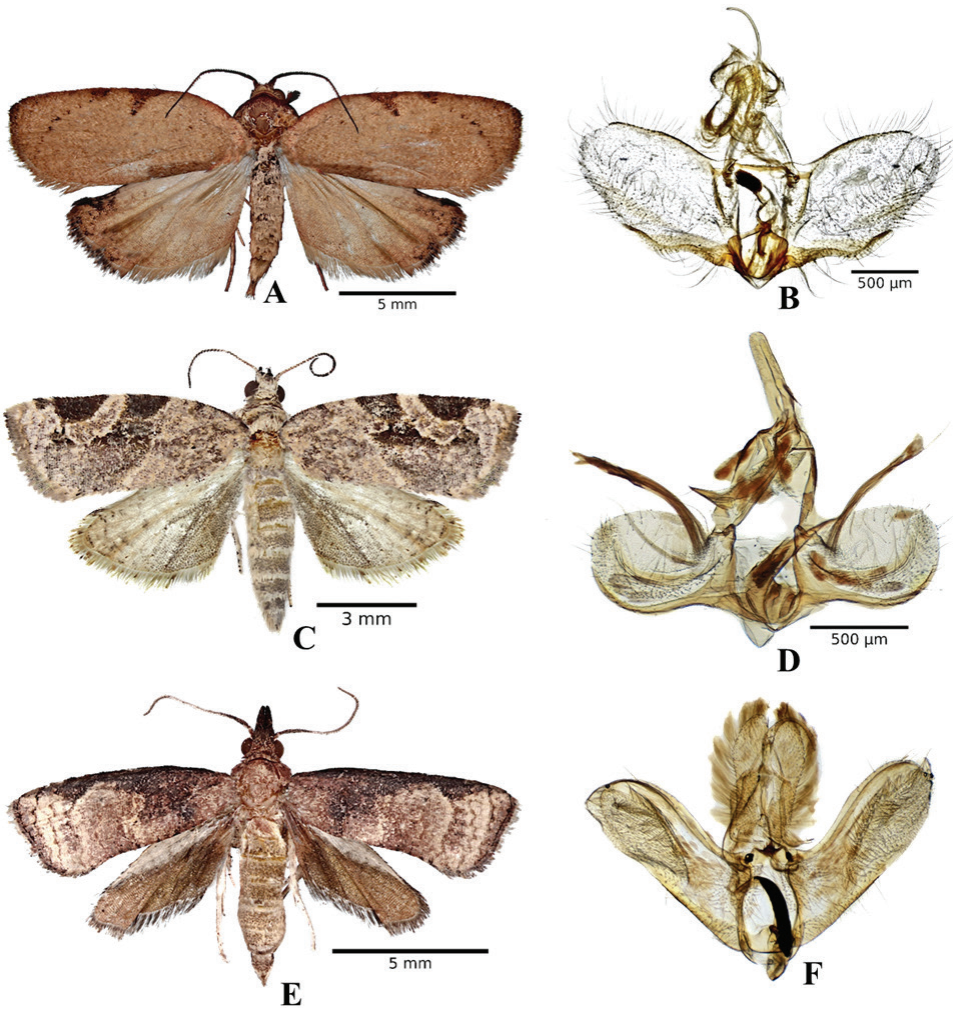


Figure 2. **A** and **B** *Amorbia cuneana*, Tangancicuaro, Michoacán **C** and **D** *Argyrotaenia montezumae*, Peribán, Michoacán **E** and **F** *Platynota* sp., Los Reyes, Michoacán.

Our results extend the distribution of *A. cuneana* and *A. montezumae* to an elevation of 2337 m, without ruling out the possibility of finding them at lower or higher altitudes, wherever there are host plants since tortricids adapt better to temperate, subtropical and tropical climates (Meijerman and Ulenberg 2000), climates that coincide with the berry-growing regions of the country. Moreover, we can speculate that there may exist other tortricid species associated with berries, such as *Apotoforma* sp., which was found feeding on blackberry vegetative buds, flowers, and young fruits in Coatepec, Veracruz, Mexico (Ruiz 2019). However, in our study we did not find this species even though the elevation of this locality coincides with the lowest studied altitude. Morón and Terrón (1988) estimated that in Mexico there may exist 1500 species of tortricids, most have not been described.

Conclusions

Three species of tortricids, *A. cuneana*, *A. montezumae* and *Platynota* sp., were identified associated with strawberries, raspberries, and blackberries in the producer regions of Michoacán and Guanajuato, Mexico, at altitudes from 1290 to 2337 m. The first two species were more abundant in the three crops, while *Platynota* sp. was observed only in blackberries. The three species belong to the subfamily Tortricinae, whose main characteristics are their behavior as leafrollers and their polyphagous feeding habit. In the three species of cultivated plants, both species were associated only with tender shoots and leaves. In our study, we did not quantify losses and damage from feeding. In later studies, measures for managing this group of insects should be designed, and the economic losses they cause to berry production in Mexico should be determined.

Acknowledgements

We thank Dr John W. Brown and Dr Jason Dombroskie for their support in corroborating identification of the species. We also thank the growers who allowed us to sample their orchards and Romualdo Ochoa for his support during sampling, as well as Rodolfo Raya, José Luis García, and José Lara for their help in locating the orchards where we collected the samples.

References

- Akbarzadeh SGH (2012) Population abundance of grape berry moth, *Lobesia botrana* (Denis et Schiffermuller) (Lep., Tortricidae) and its related crop damage in Orumieh vineyards. *Journal of Entomological Research* [summer] 4 (14): 91–102.
- Arita H, Rodríguez P (2001) *Ecología Geográfica y Macroecología*. In: Llorente Bousquets J, Morrone JJ (Eds) *Introducción a la biogeografía en Latinoamérica: teorías, conceptos, métodos & aplicaciones*. UNAM, Ciudad de México, México, 63–0.
- Barreto O, Martínez AM, Vinuela E, Figueroa JI, Rebollar A, Chavarrieta JM, Valdez JM, Lobit P, Pineda S (2016) Biological Parameters of *Argyrotaenia montezumae* (Lepidoptera: Tortricidae) and Influence of the Oviposition Substrate Color on Fecundity. *Annals of the Entomological Society of America* 109(5): 671–677. <https://doi.org/10.1093/aesa/saw040>
- Bautista MN, Vargas MH, Ramirez AS, Perez PR (2014) First Report of the *Platynota* n. sp. (Lepidoptera: Tortricidae) Genus in Prickly Pear (*Opuntia* spp.) in the Municipality of Villa Milpa Alta, Mexico DF, Mexico. *Southwestern Entomologist* 39(2): 379–381. <https://doi.org/10.3958/059.039.0215>
- Brown JW (1999) Five new species of *Argyrotaenia* (Tortricidae: Archipini) from Mexico and the Southwestern United States. *Journal of the Lepidopterists' Society* 53(3): 114–125.
- Brown JM (2013) Two new neotropical species of *Platynota* with comments on *Platynota stultana* Walsingham and *Platynota xylophaea* (Meyrick) (Lepidoptera: Tortricidae).

- Proceedings of the Entomological Society of Washington 115(2): 128–139. <https://doi.org/10.4289/0013-8797.115.2.128>
- Brown JW, Robinson G, Powell JA (2008) Food plant database of the leafrollers of the world (Lepidoptera: Tortricidae) (Version 1.0). <http://www.tortricid.net/foodplants.asp> [Accessed on: 2021-07 30]
- Brown JW, Copeland RS, Aarvik L, Miller SE, Rosati ME, Luke Q (2014) Host records for fruit-feeding Afrotropical Tortricidae (Lepidoptera). *African Entomology* 22(2): 343–376. <https://doi.org/10.4001/003.022.0225>
- Brown JW, Dyer LA, Villamarín-Cortez S, Salcido D (2019) New larval host records for Tortricidae (Lepidoptera) from an Ecuadorian Andean cloud forest. *Insecta Mundi* 720: 1–12.
- Espino-Herrera AM, Chavarrieta-Yáñez JM, Martínez-Castillo AM, Figueroa-De la Rosa JI, Rodríguez-Enríquez CL, Rebollar-Alviter Á, Pineda-Guillermo S (2012) Canibalismo de larvas de *Amorbia* sp. expuestas a la parasitación por *Apanteles* sp. y supervivencia de este parasitoide. In: Sansinenea R, Zumaquero RJL, Del Rincón CMC (Eds) XXXV Congreso Nacional de Control Biológico, Puebla (Puebla), noviembre de 2012. Benemérita Universidad Autónoma de Puebla, 106–110.
- FAO-FAOSTAT (2021) Crop statistics. <http://www.fao.org/faostat/en/#data/QC> [Accessed on: 2021-07-29]
- García E (1998) Modificaciones al sistema de clasificación climática de Köppen. Offset Larios, México, 217 pp.
- Gassmann AJ, Levy A, Tran T, Futuyama DJ (2006) Adaptations of an insect to a novel host plant: A phylogenetic approach. *Functional Ecology* 20(3): 478–485. <https://doi.org/10.1111/j.1365-2435.2006.01118.x>
- Gilligan TM, Epstein EM (2014) Tortricids of Agricultural Importance. Interactive Keys developed in Lucid 3.5. <http://idtools.org/id/leps/tortai/tortricidae.html> [Accessed on: 2021-06 26]
- Gilligan TM, Baixeras J, Brown JW (2018) T@RTS: Online World Catalogue of the Tortricidae (Ver. 4.0). <http://www.tortricid.net/catalogue.asp> [Accessed on: 2021-06 26]
- Gilligan TM, Brown JW, Baixeras J (2020) Immigrant Tortricidae: Holarctic versus Introduced Species in North America. *Insects* 11(9): 594. <https://doi.org/10.3390/insects11090594>
- Hill DS (1987) *Agricultural Insect Pests of Temperate Regions and Their Control*. CUP Archive, Cambridge University Press, Reino Unido, 659 pp.
- Juárez-Gutiérrez AC, Martínez AM, Figueroa JI, Rebollar AA, Aguilera PMM, Pineda S (2015) Registro del enrollador de las hojas, *Amorbia cuneana* (Walsingham) (Lepidoptera: Tortricidae), en zarzamora en Rancho Huatarillo, Peribán, Michoacán. *Acta Zoológica Mexicana* (n. s.) 31(2): 341–343. <https://doi.org/10.21829/azm.2015.312998>
- López I, Pineda S, Figueroa JI, Sánchez JA, Martínez AM, Williams RN, Rebollar AA (2014) Identification, Parasitoids, and Population Dynamics of a Blackberry Leafroller (Lepidoptera: Tortricidae) from Michoacan, Mexico. *Southwestern Entomologist* 39(3): 503–510. <https://doi.org/10.3958/059.039.0311>
- Luis-Martínez A, Sánchez GA, Ávalos-Hernández O, Salinas-Gutiérrez JL, Trujano-Ortega M, Arellano-Covarrubias A, LLorente-Bousquets J (2020) Distribución y diversidad de Papilionidae y Pieridae (Lepidoptera: Papilionoidea) en la Región Loxicha, Oaxaca, México. *Revista de Biología Tropical* 68(1): 139–155. <https://doi.org/10.15517/rbt.v68i1.37587>

- Mackay MR (1962) Larvae of the North American Tortricinae (Lepidoptera: Tortricidae). Entomology Research Institute Research Branch, Canada Department of Agriculture Ottawa. Ontario. The Canadian Entomologist, 182 pp. <https://doi.org/10.4039/entm9428fv>
- Martínez AM, Barreto-Barriga O, Pineda S, Rebollar AA, Chavarrieta JM, Figueroa JI (2014) Parasitoides asociados a los enrolladores de hojas de zarzamora *Argyrotaenia montezumae* Walsingham y *Amorbia* sp. (Lepidoptera: Tortricidae), en Michoacán, México. Acta Zoológica Mexicana 30(3): 553–563. <https://doi.org/10.21829/azm.2014.30377> [nueva serie]
- McCoy E (1990) The Distribution of Insects along Elevational Gradients. Oikos 58(3): 313–322. <https://doi.org/10.2307/3545222>
- McQuillan PB (1992) A checklist of the Tasmanian tortricid moths (Lepidoptera: Tortricidae) and their host-plant relationships. Papers and Proceedings of the Royal Society of Tasmania 126: 77–89. <https://doi.org/10.26749/rstpp.126.77>
- Meijerman L, Ulenberg SA (2000) Arthropods of Economic Importance: Eurasian Tortricidae. https://eurasian-tortricidae.linnaeus.naturalis.nl/linnaeus_ng/app/views/introduction/topic.php?id=3386&epi=164 [Accessed on: 2021-06 26]
- Messina FJ, Lish MA, Springer A, Gompert Z (2020) Colonization of Marginal Host Plants by Seed Beetles (Coleoptera: Chrysomelidae): Effects of Geographic Source and Genetic Admixture. Environmental Entomology 49(4): 938–946. <https://doi.org/10.1093/ee/nvaa065>
- Monteagudo-Sabaté D, Luis-Martínez A, Vargas-Fernández I, Llorente-Bousquets J (2001) Patrones altitudinales de diversidad de mariposas en la Sierra Madre del Sur (México) (Lepidoptera: Papilionoidea). SHILAP Revista lepidopterológica 29(115): 2007–237.
- Morón MA, Terrón RA (1988) Entomología Práctica. Instituto de Ecología AC. Sociedad Mexicana de Entomología. México, D.F, 393 pp.
- Obraztsov NS (1961) Descriptions of and Notes on North and Central American Species of *Argyrotaenia*, with the Description of a New Genus (Lepidoptera, Tortricidae). American museum of natural history central park west at 79th street, New York, N.Y, 42 pp.
- Phillips-Rodríguez E, Powell JA (2007) Phylogenetic relationships, systematics, and biology of the species of *Amorbia* Clemens (Lepidoptera: Tortricidae: Sparganothini). Zootaxa 1670(1): 1–109.
- Powell JA (1983) Tortricoidea. In: Hodges RW (Ed.) Check list of the lepidoptera of America north of Mexico. E. W. Classey, Ltd., and Wedge Entomological Research Foundation, London, 31–42.
- Powell JA, Brown JW (2012) Tortricoidea, Tortricidae (part): Tortricinae (part): Sparganothini and Atteriini. The Wedge Entomological Research Foundation, Washington, DC, 230 pp.
- Powell JA, Razowski J, Brown JW (1995) Tortricidae: Tortricinae. In: Heppner JB (Ed.) Atlas of Neotropical Lepidoptera, checklist: part 2, Hyblaeoidea-Pyraloidea-Tortricoidea. Association for Tropical Lepidoptera. Scientific Publishers, Gainesville, Florida, 138–150.
- Razowski J (1996) Tortricidae. In: Karsholt O, Razowski J (Eds) The Lepidoptera of Europe. A distributional checklist. Apollo Books, Stenstrup, 130–157.
- Razowski J, Landry B, Roque-Albelo L (2008) The Tortricidae (Lepidoptera) of the Galapagos Islands, Ecuador. Revue Suisse de Zoologie 115(1): 185–220. <https://doi.org/10.5962/bhl.part.80425>

- Rosas GNM, Villegas MJM (2008) Bionomics of a novel species of *Argyrotaenia* (Lepidoptera: Tortricidae) presents in mexican avocado orchards. *Acta Zoológica Mexicana* (n.s.) 24(1): 129–137. <https://doi.org/10.21829/azm.2008.241627>
- Ruiz MC (2019) Enrollador de hojas de zarzamora *Apotoforma* sp., y sus agentes de control en Coatepec, Veracruz, México. *Southwestern Entomologist* 44(3): 689–694. <https://doi.org/10.3958/059.044.0314>
- Rzedowski J (2021) La familia Rosaceae en México. *Polibotánica* 51: 1–16. <https://doi.org/10.18387/polibotanica.51.1>
- Sanders N (2002) Elevational Gradients in Ant Species Richness: Area, Geometry, and Rapoport's rule. *Ecography* 25(1): 25–32. <https://doi.org/10.1034/j.1600-0587.2002.250104.x>
- SIAP [Servicio de Información Agroalimentaria y Pesquera] (2021) Anuario Estadístico de la Producción Agrícola. <https://nube.siap.gob.mx/cierreagricola/> [Accessed on: 2021-06 26]
- SIAMI [Sistema de Información Arancelaria Vía Internet] (2021) Sistema de Información Arancelaria Vía Internet. <http://www.economia-snci.gob.mx/> [Accessed on: 2021-09 20]
- Tejeda-Reyes MA, Rebollar-Alviter A, Valdez-Carrasco JM, Lomelí-Flores JR, González-Hernández H (2020) First report of *Argyrotaenia montezumae* in strawberry, in Zamora, Michoacan, Mexico. *Southwestern Entomologist* 45(3): 831–833. <https://doi.org/10.3958/059.045.0326>
- Tejeda-Reyes MA, Valdez-Carrasco JM, González-Hernández H (2021) First report of *Argyrotaenia montezumae* y *Templemania millistriata* in hawthorn (*Crataegus mexicana*) in Chiautzingo, Puebla, Mexico. *Southwestern entomologist* 46(1): 291–294. <https://doi.org/10.3958/059.046.0133>
- Trematerra P, Brown JW (2004) Argentine *Argyrotaenia* (Lepidoptera: Tortricidae): Synopsis and descriptions of two new species. *Zootaxa* 574(1): 1–12. <https://doi.org/10.11646/zootaxa.574.1.1>
- Urías-López MA, Salazar-García S (2008) Poblaciones del gusano telarañero y barrenador de ramas en huertos de aguacate “Hass” de Nayarit, México. *Agricultura Técnica en México* 34(4): 431–441.
- Varela-Fuentes S, Brown JW, Silva-Aguirre G (2009) Registro de *Platynota rostrana* (Walker, 1863) (Lepidoptera: Tortricidae) en cítricos de México. *Acta Zoológica Mexicana* (n.s.) 25(3): 651–654. <https://doi.org/10.21829/azm.2009.253666>
- Zhang B, Segraves KA, Xue HJ, Nie RE, Li WZ, Yan XK (2015) Adaptation to different host plant ages facilitates insect divergence without a host shift. *Proceedings of the Royal Society B: Biological Sciences* 282(1815): 20151649. <https://doi.org/10.1098/rspb.2015.1649>